Several new methods for the development of latent and blood fingerprints

A thesis
submitted in partial fulfilment for the degree
of
Doctorate of Philosophy in Chemistry
at the
University of Waikato

by

Jonathan Paul Caldwell

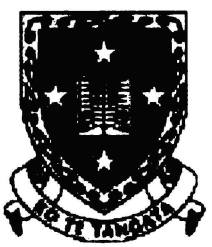

The
University
of Waikato
Te Whare Wānanga
o Waikato

1999

Abstract

Several new methods for the development of latent and blood fingerprints have been investigated as well as a preliminary appraisal of a technique for the estimation of post–mortem interval and age of blood stains.

The utilisation of coordinatively–unsaturated (six–coordinate) europium and terbium complexes as reactive reagents for the direct visualisation of latent fingerprints on porous and non–porous surfaces has been investigated. The main complex investigated in this study was tris(6,6,7,7,8,8,8-heptafluoro-2,2-dimethyl-3,5-octanedionato) europium(III) [$Eu(fod)_3$] and was the only one which proved to be effective in the fluorescent visualisation of latent fingerprints using a one step process. $Eu(fod)_3$ was found to work for fingerprints on porous paper and to a limited extent on aluminium drink cans and galvanized iron.

The use of the two and three ringed analogues of *ortho*–phthalaldehyde (OPA) for the fluorescent enhancement of latent fingerprints was also investigated. Solution trials proved that the reaction products of 2,3-naphthalenedicarboxaldehyde (NDA) and 2,3-anthracenedicarboxaldehyde (ADA) with analine produce favourable "red–shifts" in emission wavelengths which would make them stand out from the blue background emissions commonly obtained from paper. However, poor results were obtained when NDA and ADA were trailed on latent fingerprints on paper.

2,2'-azino-di-[3-ethylbenzthiazolinesulfonate(6)] diammonium salt (ABTS), *ortho*-phenylenediamine (OPD), and *para*-phenylenediamine (PPD) have been found to be successful reagents in the visual enhancement of blood fingerprints. Colours obtained from the oxidised products are green, orange, and purple respectively. A comparison with the commonly–used and hazardous 3,3'-diaminobenzidine (DAB) has proved all three reagents to be effective, safer alternatives with the added bonus of ABTS being (as far as is known) non–toxic.

A preliminary appraisal has indicated that fluorescein diacetate (FDA) may be useful in estimating the post–mortem interval or age of blood stains and blood prints.

Of the range of techniques and processes investigated with the aim of improving fingerprint visualisation, some proved unsuccessful, yet provided some useful information. These included attempts to improve the colloidal gold technique of latent fingerprint visualisation, increase the chemiluminescence from luminol–treated blood fingerprints in the presence of bromide ions, increase the colour development of ABTS–treated blood fingerprints using an albumin antibody conjugated to peroxidase, an attempt to force fluorescein into the lipid component of a latent fingerprint by acidification of an alkaline solution of fluorescein, and an attempt to stain blood fingerprints with a fluorescent protein stain called SYPRO™ Orange.

Acknowledgments

The completion of this thesis would not have been possible without the help of several people whose help whether it be direct or otherwise was greatly appreciated. Their expertise, advice, encouragement and enthusiasm helped me to achieve the finished product you now have before you.

Firstly a big thank you to my chief supervisor Dr. Nick Kim. Thanks Nick for the wisdom, advice, and continual encouragement you provided along with your humorous and genial manner.

Thanks also to my other two supervisors, Dr. Bill Henderson for his ESMS advice and for the initial suggestion of using NMR shift reagents and to Dr. Tony Cartner for his advice on use of the laser.

I am also grateful to Dr. Peter Molan for his original suggestion of ABTS and to Wendy Jackson for her help with the ESMS. Thank you to Murray Ashby from Ruakura Research Station and the nurses at the campus medical centre for the supplying or extracting of blood. My two *"partners in crime"* Karen Murphy and Stefan Hill also deserve a thank you for their helpful advice which was always much appreciated. I am also very grateful to the Fingerprint Section of the Waikato Police Department for allowing me the use of their Polilight® and video camera.

Many thanks to my girlfriend Rachel for being so supportive and providing me with continual encouragement. Thank you also to Rachel's family who provided me with such a relaxing environment in Tauranga whilst I was writing up.

Finally thank you to my parents David and Susan and to my late grandmother Jessie whose support, encouragement and continual interest in my work was greatly appreciated.

Table of Contents

List of Figures

List of Tables

List of Abbreviations

ABTS	2,2′-azino-di-[3-ethylbenzthiazolinesulfonate(6)]
ADA	2,3-anthracenedicarboxaldehyde
DAB	3,3′-diaminobenzidine
DCM	dichloromethane
DFO	1,8 diazafluoren-9-one
DMF	dimethylformamide
DNA	deoxyribonucleic acid
dpm	tris(2,2,6,6-tetramethyl-3,5-heptane-dionato)
DSMO	dimethyl sulfoxide
DTPA-pAS	diethylenetriamine pentaacetic acid-4-aminosalicylic acid
EDTA	ethylenediaminetetraacetic acid
ELISA	enzyme-linked immunosorbent assay
ESMS	electrospray mass spectrometry
ESR:Forensic	Environmental Science Research (Forensic section)
FDA	fluorescein diacetate
fod	tris(6,6,7,7,8,8,8-heptafluoro-2,2-dimethyl-3,5-octanedionato)
MEK	methyl ethyl ketone
NDA	2,3-naphthalenedicarboxaldehyde
NMR	nuclear magnetic resonance
OPA	*ortho*-phthalaldehyde
OPD	*ortho*-phenylenediamine
PMI	post-mortem interval
POD	peroxidase
PPD	*para*-phenylenediamine
SBW	spectral band width
SEM	scanning electron microscopy
TEC	thenoyl europium chelate
THF	tetrahydrofuran
UV	ultra violet
UV/Vis	ultra violet/visible
WHO	World Health Organisation
XRD	X-ray diffraction

Chapter One
Introduction

1.1 *Background*

Identification of an individual by comparison of fingerprints has been well established since the beginning of the century. The first scientific appraisal of fingerprint patterns was carried out by Henry Galton (1822–1911). Galton's book *Fingerprints* was published in 1892, and laid the groundwork for a fingerprint classification system with categories of arches, loops and whorls. Edward Henry, the English Inspector General of Police in Bengal, developed Galton's classification system further and published his book *Classification and use of Fingerprints* in 1900. In 1904, another classification system, based on arches, whorls and left and right loops, was published by Vucetich in Argentina. Although there are a number of fingerprint classification systems in use today, most are derived in some way from these early works (Odell, 1982).

The current *Henry system* assigns a numerical expression to each fingerprint, and is based on four groups of ridge patterns: arches (which can be plain or tented), loops, whorls and composites (Odell, 1982).

Fingerprints still remain the single most important piece of forensic evidence, accounting for over 80% of successful clearances of violent crime (Burridge, 1996). Their high evidential value lies in the fact that fingerprint patterns are unique to each individual (including identical twins, which share the same DNA). In criminal cases their presence therefore represent an unequivocal link between the individual who left them and the scene of the crime. In addition, fingerprint evidence is well established and highly regarded in the justice system (by contrast, the newer technique of DNA "fingerprinting" is still often the subject of legal challenge). Fingerprint evidence is likely to retain its importance and is not likely to be superseded by DNA typing or related genetic techniques. Rather the two areas are complimentary (Kim, 1998).

Characteristic patterns on each finger are formed during the foetal stage of life and remain unchanged throughout life providing no serious injury occurs (Odell, 1982).

1.2 *Types of fingerprints left at a crime scene*

A fingerprint can be left on an object in one of the following three ways (Pounds, 1988):

- A **plastic print** is the term given to a negative impression of the ridge pattern produced when the finger presses against a soft pliable surface, such as fresh paint, glue on an envelope or stamp, soap, wax, flour, thick dust, tar, resin, clay, putty etc.
- A **visible print** is a positive visible image of a print left when a finger coated with a foreign substance (blood, paint, ink, grease, oils, face powders, soot etc.) presses against a clean surface.
- The **term latent print** refers to the normally invisible fingerprint pattern composed of natural skin gland secretions which were present on the finger at the time it touched the surface.

Most (>90%) fingerprints deposited at crime scenes fall into the third category. Latent prints are therefore very important, but their usually invisible nature means that some form of visualisation process is required for their detection. Such processes are usually chemical reactions, and therefore the composition of latent prints is of fundamental significance to the visualisation process which might be applied.

1.3 *Composition of fingerprints*

There are three types of glands associated with the skin whose secretions contribute to a latent fingerprint deposit (Pounds, 1988).

Sudoriferous glands are also known as sweat glands. Sweat functions to help maintain body temperature and eliminate wastes. The two principal types of sudoriferous glands are:

- **Eccrine** glands, which are distributed throughout the skin except for a few small areas such as the lip margins, eardrums, and nail beds of the fingers and toes. Eccrine glands are most

numerous in the skin of the palms of the hands (where their density reaches about 500 per cm^2) and the soles of the feet.

- **Apocrine** glands, which are more limited in distribution to the skin of the armpits, pubic region and mammary areolae. Apocrine sweat glands begin to function at puberty.

Sebaceous glands secrete an oily substance called sebum, and are also known as oil glands. Most sebaceous glands are associated with the hair follicles. Sebum forms a protective film that protects the hair from drying and becoming brittle, prevents excessive evaporation of water from the skin, and works to keep the skin soft and pliable.

Ceruminous glands are present in the external auditory canal, and secrete cerumen, otherwise know as earwax.

Secretions most likely to be found on the fingers are those associated with the eccrine glands, and to a lesser extent the sebaceous glands. Secretions from the sebaceous glands are transferred to the hands by touching the face and head.

Apart from its water content, eccrine sweat contains up to 1% of other substances the main constituents of which are presented in Table 1.1 (Knowles, 1978).

Table 1.1
Major constituents of eccrine sweat.

Inorganic constituents		Organic constituents
Cations	Anions	
Ammonium	Chloride	Amino acids
Metal ions (particularly Na^+)	Hydroxide	Ascorbic acid
	Phosphate	Choline
	Sulfate	Creatinine
		Lactic acid
		Sugars
		Urea
		Uric acid

The main constituents excreted from the sebaceous glands are presented in Table 1.2 (Powe, 1972).

Table 1.2
Major constituents of the sebaceous glands.

Compound	Relative amount present
Glycerides (mono, di and tri)	35-60%
Free fatty acids	15-30%
Wax esters	12-16%
Squalene	10-12%
Sterol esters	1-3%
Sterols	1-3%
Hydrocarbons	1-3%

The amount of material secreted from the glands varies between individuals and is influenced by a range of internal stimuli (such as mental and emotional disposition, and physiological state), and external stimuli (such as sensory inputs of temperature and humidity) (Kim, 1998).

1.4 *Common visualisation methods for latent fingerprints*

1.4.1 General

Many of the reagents for visualisation of latent fingerprints work by reacting with specific components of latent fingerprints which are themselves derived from eccrine and sebaceous secretions (Tables 1.1 and 1.2). The scope of this study includes the visualisation of latent and blood fingerprints and therefore the reagents tested were targeted at either constituents of latent fingerprints, or constituents of blood. For a detailed, comprehensive review of common methods for latent prints the reader is referred to Menzel (1999).

1.4.2 Ninhydrin

Ninhydrin (2,2-dihydroxy-1,3-indanedione) was first prepared by Ruhemann (1910). It reacts with amino acids to form a purple product which is referred to as "Ruhemanns Purple" (Fig. 1.1). Ninhydrin is most commonly used as a colourmetric reagent for the detection of amino acids in thin layer and paper chromatography.

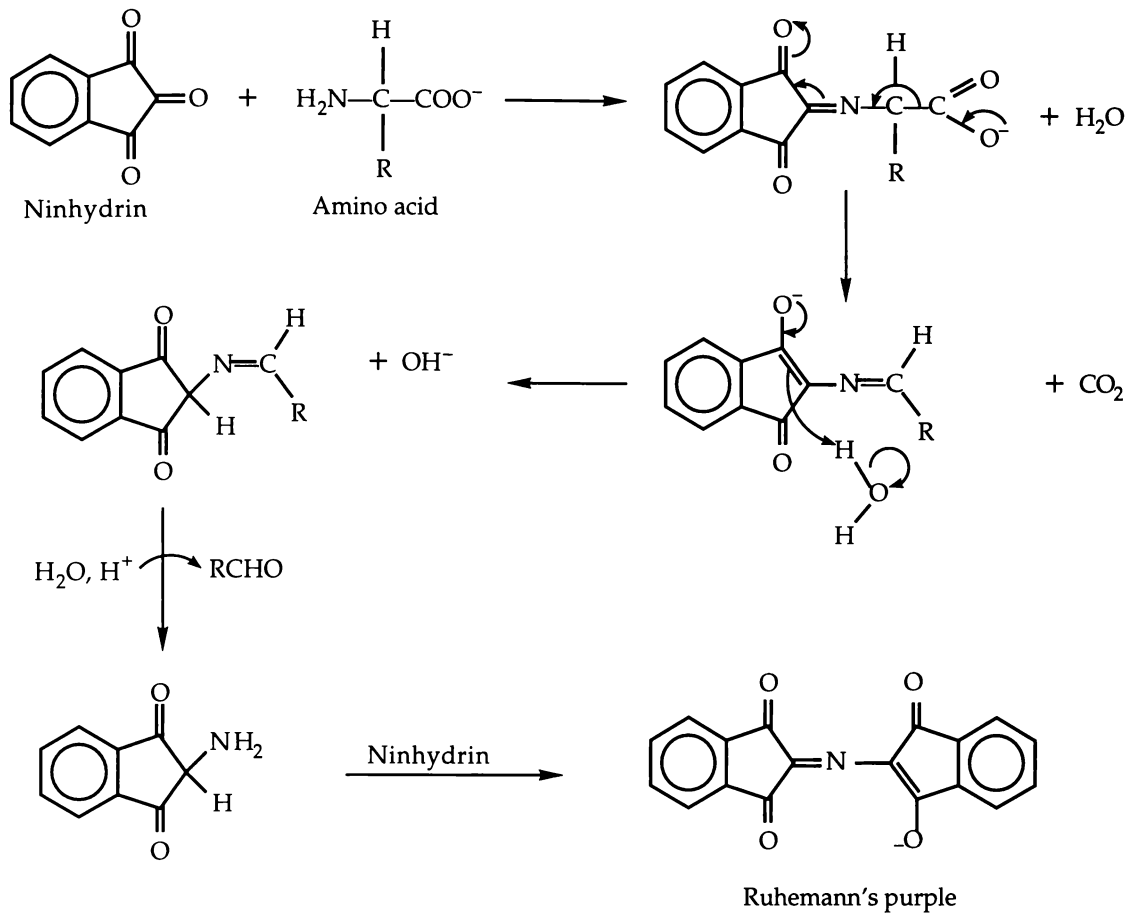

Fig. 1.1
Reaction of ninhydrin with an amino acid (Bottom et al., 1978).

The use of ninhydrin for the detection of latent fingerprints was first suggested by Oden and von Hofsten (1954) after noting that purple coloured fingerprints were revealed on paper chromatograms that had been handled. It has since been commonly employed for revealing latent fingerprints on paper and porous surfaces where it reacts with the amino acid fraction of fingerprint deposits which originate from the eccrine sweat glands.

For detection of latent fingerprints, documents are usually soaked or sprayed with a solution of ninhydrin (0.2-1.0%). The type of solvent used depends on whether or not it is likely to cause the ink on the document to run. Solvent choices include acetone, acetone/water, acetone/acetic acid, ethanol, methanol and freon/ethanol/acetic acid (Pounds, 1988). Development conditions used also vary between laboratories from simple air curing to drying at precisely specified temperatures and humidity (Pounds, 1988).

1.4.3 Fluorescent reagents

High intensity light sources such as lasers have been commonly used to induce fluorescence in natural or contaminated fingerprint deposits or where fluorescent derivatives have been prepared. The basic principles and applications have been well reviewed by Menzel (1980).

Ideally, for a reagent to be successful in producing fluorescent products by reaction with components of fingerprints it should fulfil the following criteria (Pounds, 1988):

- The reagent itself should not be fluorescent.
- The fluorescence of the final product should be significantly different from any background fluorescence e.g. optical brightners in paper.
- The reagent should react specifically with components of the fingerprint rather than with compounds in the background material.

A number of organic reagents have been produced for this purpose, most of which target the amino acid component of fingerprints. Many of these reagents tend to deviate from the ideal characteristics listed above. Four examples are presented in Fig. 1.2 to 1.5 (Pounds, 1989; Pounds et al., 1990).

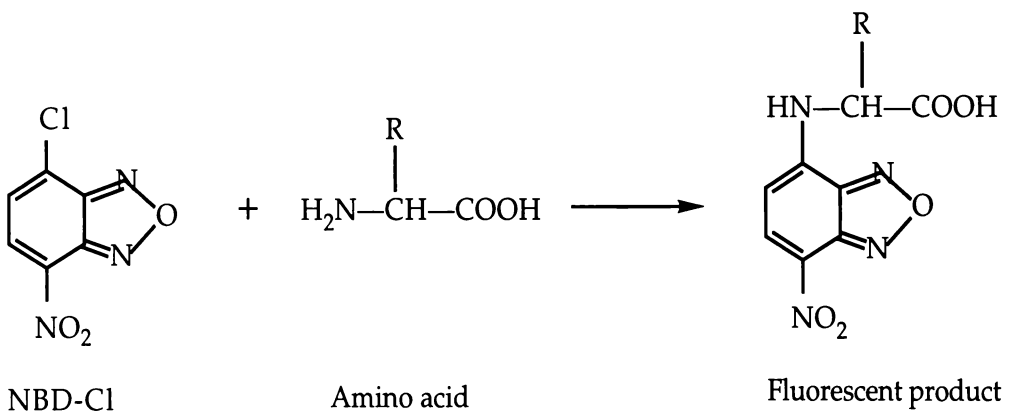

Fig. 1.2
Reaction of 7-chloro-4-nitrobenzo-2-oxa-1,3-diazole (NBD-Cl) with an amino acid.

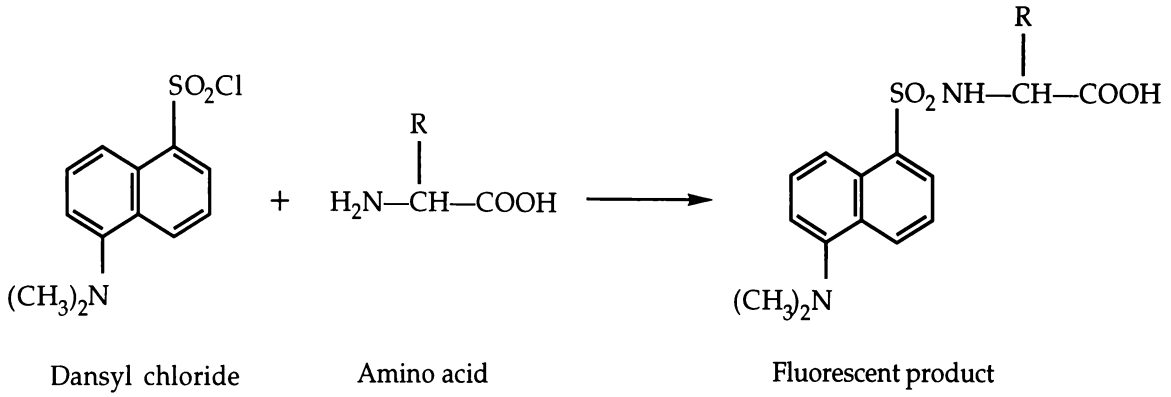

Fig. 1.3
Reaction of 1-dimethylaminonaphthalene-5-sulfonyl chloride (Dansyl chloride) with an amino acid.

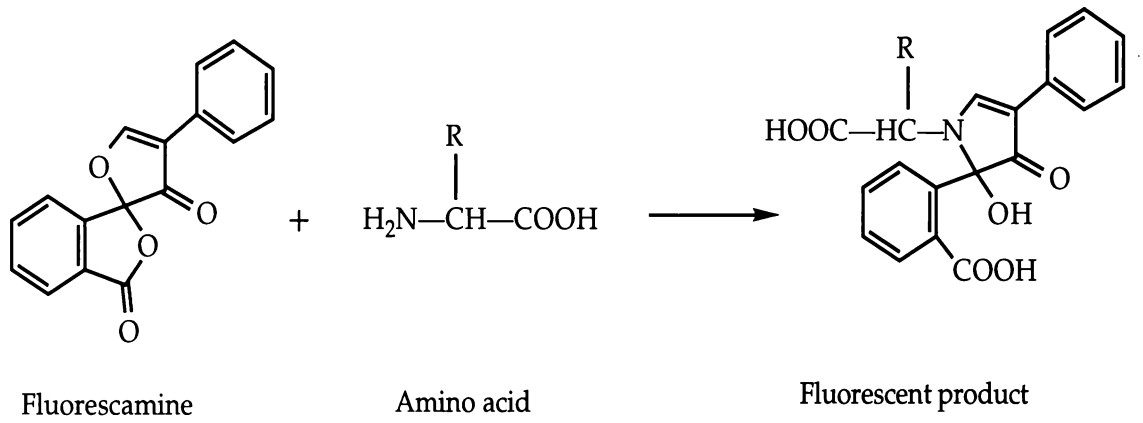

Fig. 1.4
Reaction of 4-phenylspiro(furan-2-(3H), 1'-phthalan)-3,3'-dione (Fluorescamine) with an amino acid.

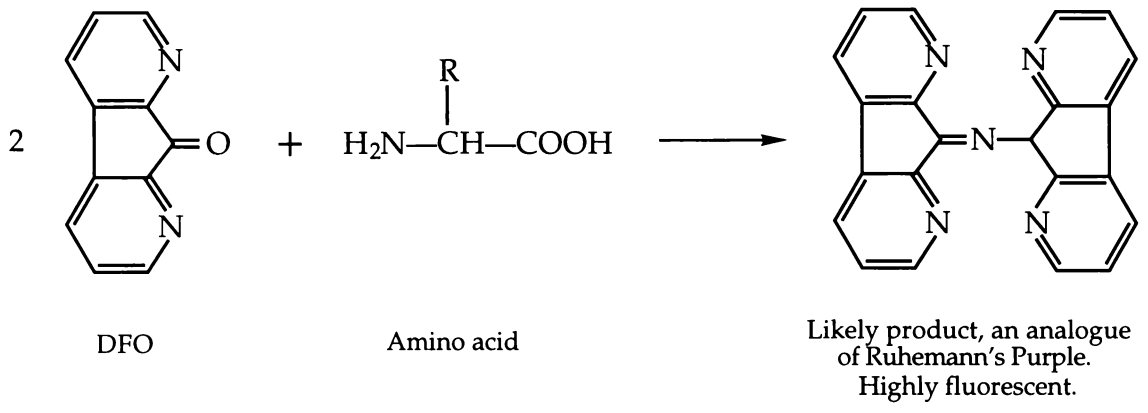

Fig. 1.5
Reaction of 1,8 diazafluoren-9-one (DFO) with an amino acid.

DFO is not as good as ninhydrin/$ZnCl_2$ under normal illumination, but gives far superior fluorescence under laser excitation (514 nm). It was first synthesised by Druey and Schmidt (1950), but it was not until 1989 that its potential as a fingerprint visualisation reagent was realised (Pounds et al., 1990). Toxic and potential carcinogenic properties of DFO were undetermined as at 1990.

1.4.4 Cyanoacrylate esters (Super Glues™)

Ethyl, methyl or butyl cyanoacrylate ester monomers (Fig. 1.6) are used in *Super Glues™* with the addition of a suitable stabiliser.

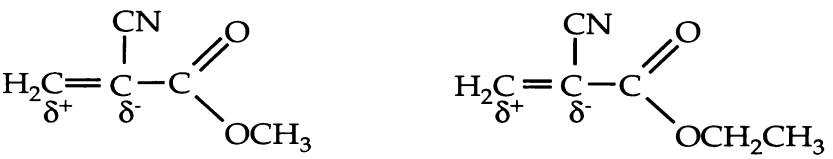

Fig. 1.6
Two monomers of cyanocrylate ester.

A weak base such as water is sufficient to initiate a rapid anionic polymerisation to form a very strong (but brittle) adhesive (Fig. 1.7).

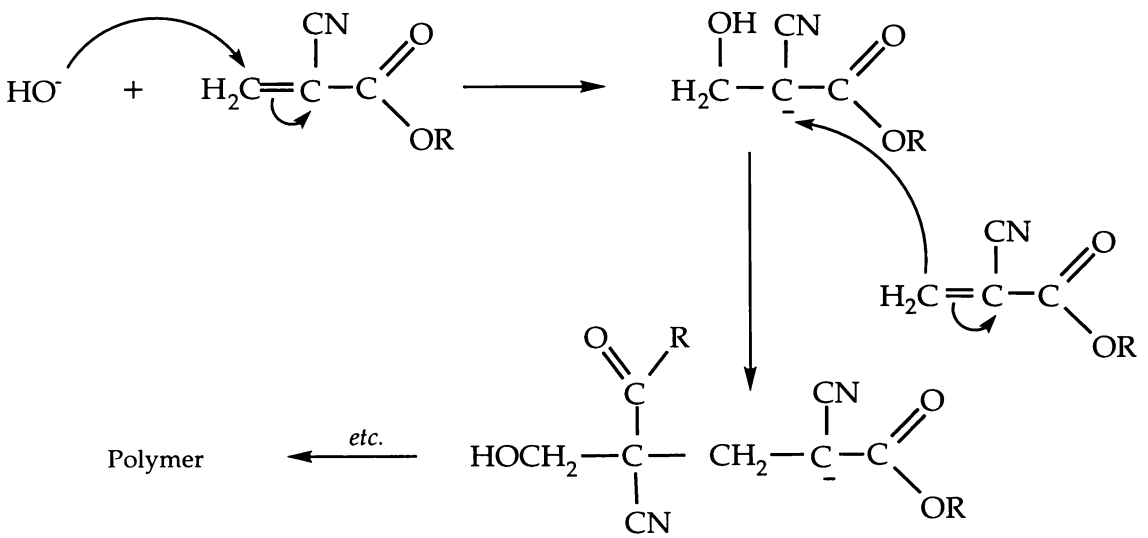

Fig. 1.7
Polymerisation of cyanocrylate ester (Kim, 1998).

In 1980, it was discovered that *Super Glue™* fumes could be used to successfully 'develop' latent fingerprints on a wide range of surfaces such as polythene bags, plastics, glass, rubber gloves, electrical tape, leather, metals and firearms (Pounds, 1988). Presumably this occurs as a result of the weak base (water and ammonium hydroxide) content of the prints causing the initiation of a high number of polymerisation nucleation sites. Under these conditions, the product is a white polymer which deposits along the ridges of the print.

1.4.5 Iodine

Exposure to iodine vapour is one of the oldest techniques in latent fingerprint visualisation, with a description of its use being given as early as 1891 (Forgeot, 1891). In this method, the fingerprints take on the characteristic purplish-brown colour of iodine. A wide range of methods have been used to deliver iodine vapour to the sample, among them:

- Simple exposure to I_2 gas by putting the exhibit and a dish of iodine crystals in an enclosed cabinet.
- Use of a pipe to draw and blow the I_2 gas over the sample. In this case the iodine crystals are usually held in a conical flask, which is warmed in a water bath.
- Use of a chemical reaction to form $I_2(g)$, which is directed over the sample.
- Dusting of the prints with finely-ground iodine crystals.

Two possible mechanisms by which iodine vapour reveals latent fingerprints have been proposed. The first is a physical process which involves the absorption of iodine into lipid material in the prints (both I_2 and lipids are non-polar). The second mechanism is a chemical process which involves the iodination of unsaturated lipids (*e.g.* oleic acid and linoleic acid in Fig. 1.8) in the prints.

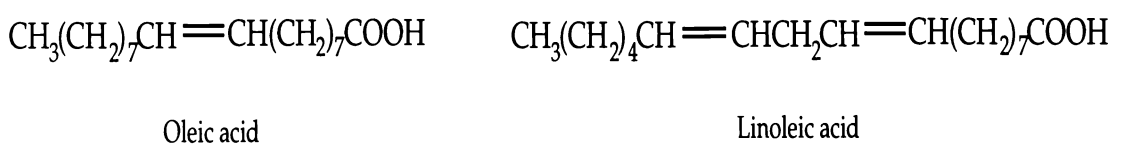

Oleic acid Linoleic acid

Fig. 1.8
Unsaturated lipids (oleic acid and linoleic acid) in latent prints.

It is now assumed that in terms of colour-formation the first process—simple absorption—is dominant (among other things, the iodination of lipids will as frequently as not produce colourless compounds).

After the source of $I_{2(g)}$ is removed, visualised prints fade fairly rapidly. This behaviour is attributed to both diffusion of the iodine back out of the prints, and progressive reaction of iodine with the unsaturated lipids in the prints.

In order to overcome this problem, the prints are 'fixed' before being photographed. Chemical fixers work by reaction with the iodine in the prints to form a stable product. An example is 7,8-benzoflavone (also used as an anti-cancer agent) which reacts with the iodine to form a stable dark purple product. Two routes for the addition of iodine to 7,8-benzoflavone are presented in Fig. 1.9.

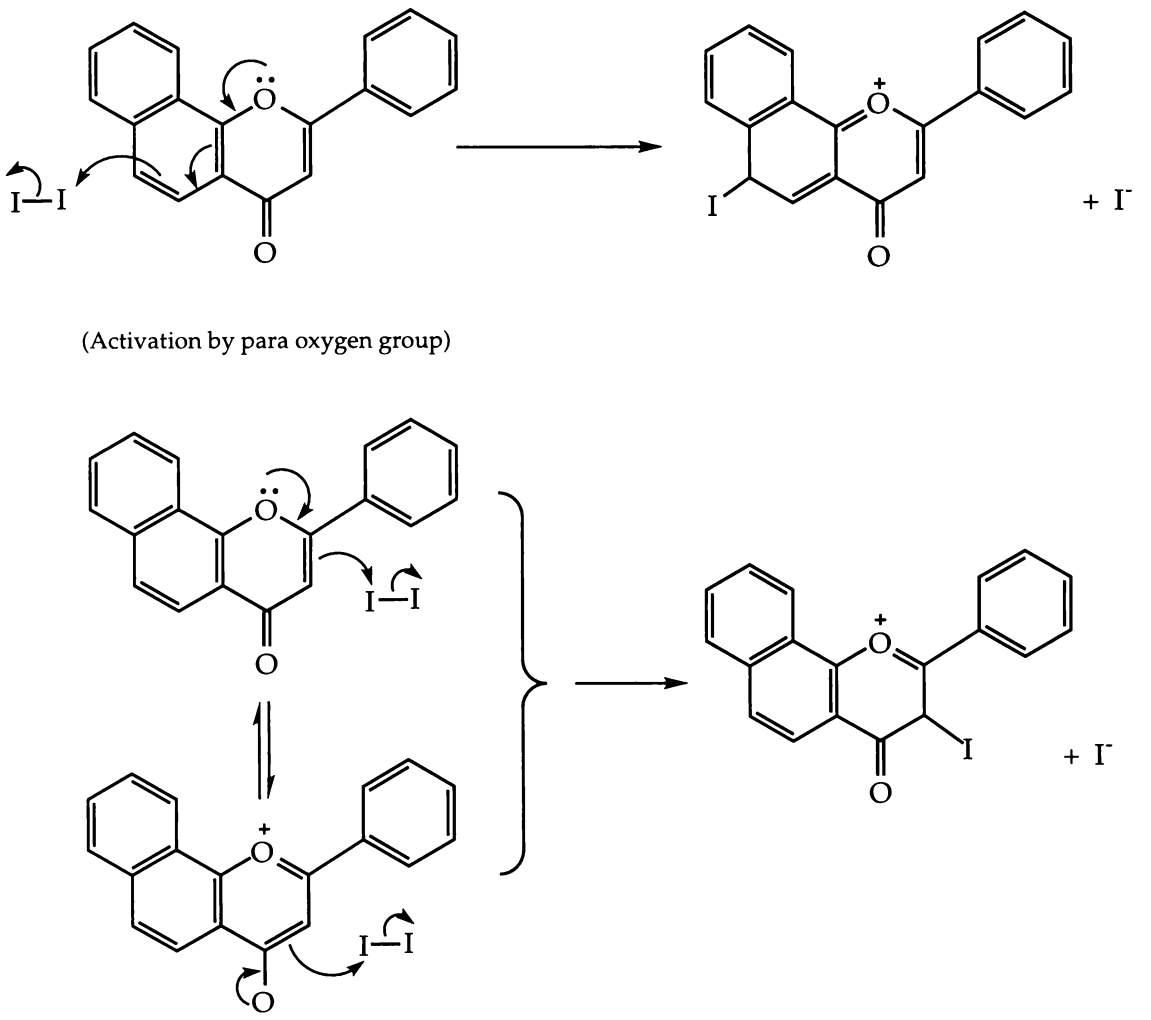

Fig. 1.9
Reaction of 7,8-benzoflavone with iodine via two routes (Kim, 1998).

1.5 Common visualisation methods for finger–prints in blood

Violence is a common occurrence in present-day society. Even New Zealand can expect to average almost one murder per week (Jones, 1997). Crimes of violence often not only involve close contact between the victim and the criminal but also the shedding of blood. It is therefore likely that a fingerprint examiner may observe fingerprints in blood at the scene or on an exhibit.

Depending on the thickness of the blood however, the bloodied fingerprint may only be partially visible to the eye. Added to this is the problem that the colour of different surfaces may also interfere with the visibility of the bloodied fingerprint. Various treatment or enhancement procedures are available for revealing invisible parts and or improving the contrast of bloodied fingerprints.
Techniques used for bloodied fingerprints can depend on such things as the sensitivity or toxicity of the chemicals being used and also the type of surface which the print is on.

The reaction between 3,3'-diaminobenzidine (DAB) and hydrogen peroxide is catalysed by the peroxidase activity of blood to give a dark brown insoluble product. As the reaction is specific for blood, it produces little background colouration and no destaining is necessary (Jones, 1997). A more detailed discussion on DAB is provided in section 2.1.1 in Chapter 2.

The protein stain Amido Black (naphthalene Black 12B) has been, until quite recently, the recommended treatment for bloodied prints on both porous and non-porous surfaces. The treated prints are visible as blue/black ridges against a light blue or colourless background. Superior results can be obtained however, using DAB (Jones, 1997).

Although 1,8-diazafluoren-9-one (DFO) is more commonly used for the detection of latent fingerprints (section 1.3.3 on fluorescent reagents) it has been found to be effective for the treatment of bloodied fingerprints on porous surfaces such as paper. DFO however, has been found to only work on faint blood prints on

porous or semi-porous surfaces. The result is a photoluminescent blood stain rather than a coloured one (Jones, 1997).

1.6 *The need for new reagents and methods*

Although various methods for the detection of fingerprints exist, there is still considerable scope for development in this area. In a meeting in late 1995 between researchers from the University of Waikato's Chemistry Department, with senior members of both the NZ Police and New Zealand Crown Research Institute, *ESR:Forensic* a number of specific areas were identified in which research in chemistry could significantly contribute to success or otherwise of visualising latent fingerprints. To a large extent, the scope of this research was originally based on the most practical of these areas. As the project progressed, the scope was extended to cover certain additional areas which might show particular promise.

New methods are constantly being required to meet the ever changing demands of criminal detection. Although 3,3'-diaminobenzidine (DAB) is one of the best reagents (Olsen, 1985) for the detection of fingerprints in blood the unnecessary health risks (Holland et al., 1974) associated with its use make it less desirable than it might otherwise be (refer to section 2.1.1 in Chapter 2 for a more detailed discussion on the risks of DAB). Better methods and new reagents which result in different coloured products and fluorescent emissions are also required for various surfaces due to background interference's. For example, bank notes in New Zealand pose problems with visualisation of fingerprints not only because of the interference from background fluorescence (due to optical brightners, calcite and TiO_2) but also because of the non-porous type of material (rag) they are made from (Fisher, 1999). Another reason for the development of new methods and reagents is the necessity for more user-friendly procedures for less skilled examiners and more easily executed procedures for "in the field" applications.

The primary aim of this study was to develop new reagents and techniques for the visualisation of both latent and blood fingerprints. For this reason the thesis is divided into various sections or chapters for each type of reagent or technique developed or appraised. Because each section or chapter is a complete topic in itself

each chapter includes its own introduction, methodology, results and summary. In Chapters 2 and 3, the suitability of three reagents (ABTS, OPD and PPD) for the enhancement of blood fingerprints is assessed and discussed. The utilisation of a coordinatively-unsaturated (six-coordinate) europium complex as a reactive reagent for the direct visualisation of latent fingerprints on porous and non-porous surfaces is discussed in Chapter 4. An investigation of o-phthalaldehyde and its analogues is discussed in Chapter 5. A preliminary appraisal of a possible method which could be used for the estimation of post-mortem interval (PMI) and the age of blood stains and blood prints is given in Chapter 6. Chapter 7 includes various unsuccessful attempts at producing new reagents and methods. A summary of the various methods investigated in this thesis is given in Chapter 8. A breakdown of the approach according to the targeted constituent and its placement in the thesis is provided in Table 1.3.

Table 1.3
Summary of reagents or techniques developed or appraised and their placement in the thesis.

Print type and/or constituent targeted	Reagent	Purpose	Chapter
blood	ABTS	print visualisation	2
blood	OPD & PPD	print visualisation	3
blood	fluorescein diacetate	blood ageing	6
latent - amino acids	OPA, NDA & ADA	print visualisation	5
- various[a]	$Eu(fod)_3$	print visualisation	4
latent & blood	several	print visualisation	7

[a]Mainly water-soluble constituents.

1.7 *References*

Bottom C.B., Hana S.S., and Siehr D.J. (1978). *Biochem. Ed.*, **6**, 4.

Burridge P. (1996). Personal communication from chief fingerprint officer, Auckland Police Department, Auckland, New Zealand.

Druey J. and Schmidt P. (1950). Phenanthrolinchinone and diazafluorene. *Helvetica Chimica Act.*, **50**, 1080-1087.

Fisher, T.H.W. (1999). *Aspects of forensic chemistry of trace evidence: Explosive residue analysis, and detection of fingerprints on banknotes.* Masters thesis, University of Waikato, Hamilton, New Zealand.

Forgeot R. (1891). *Arch. d'Anthropol. Crim.*, **6**, 387.

Holland V.R., Saunders A.L., Rose F.L., Walpole A.L. (1974). A safer substitute for diaminobenzidine in the detection of blood. *Tetrahedron*, **30**, 3299-3302.

Jones K. (1997). *A Review of blood enhancement techniques.* Report prepared for the New Zealand Police, Royal New Zealand Police College.

Kim N.D. (1998). Course notes for: *Environmental, Forensic and Toxicological Chemistry*, Waikato University, Hamilton, New Zealand.

Knowles A.M. (1978). *J. Phys. E: Sci Instrum.*, **11**, 713.

Menzel E.R. (1980). *Fingerprint Detection with Lasers.* Marcell Dekker, New York, USA.

Powe W.C. (1972). *Detergency, Theory and Test Methods.* Dekker, New York, USA.

Pounds C.A. (1988). Developments in fingerprint visualisation. *Forensic Science Progress*,Vol. 3. Springer-Verlag, Berlin, 91-119.

Pounds C.A., Grigg R. (1989). Personal communication.

Odell R. (1982). Fingerprints. In: *Science against.* Marshall Cavendish, London.

Oden S., and von Hofsten B. (1954). *Nature*, **173**, 449.

Olsen R.D., Sensitivity comparison of blood enhancement techniques. *Identification, News*, (August 1985) 10-14.

Ruhemann S. (1910). *J. Chem. Soc.*, **97**, 1438 & 2025.

Pounds C.A., Grigg R., and Mongkolaussavaratana T. (1990). The use of 1,8 diazafluoren-9-one (DFO) for the fluorescent detection of latent fingerprints on paper. A preliminary evaluation. *J. Forens. Sci.*, **35**(1), 169-175.

Menzel E.R. (1999). *Fingerprint Detection with Lasers.* 2nd edition. Marcel Dekker, Inc., New York.

Chapter Two

Comparison of a new method for enhancement of blood fingerprints using ABTS with the currently used DAB method

2.1 *Introduction*

2.1.1 Background to this work

A blood fingerprint is produced when a finger touches blood that has not dried and then deposits a print on a surface. The resulting blood fingerprint may be composed mainly of serum, mainly of red cells, or of both (Jones, 1997). Blood fingerprints often tend to appear blotchy or smeared with some areas of little material deposition, and other areas in which furrows between ridges are filled in because of very heavy blood deposition. Thus, ridge detail is often obliterated in some areas and is all together absent in other areas. Since blood is a highly coloured substance, relatively tiny amounts are visible to the unaided eye. Only a few blood prints that are not readily visible to the unaided eye will have sufficient material deposited to be detected by the methods currently available (Jones, 1997).

Tests used for the forensic examination of suspected bloodstains can often be applied to the enhancement of fingerprints in blood. In the case of fingerprints, an additional constraint is that the ridge detail must be left intact by the test.

A group of methods called "catalytic tests" make use of the peroxidase activity of the iron-containing components of red blood cells. They are useful for indicating likely areas for further testing but are not specific for blood. Specificity however, is not as important in the enhancement of blood fingerprints, since it is visualisation of the stain pattern rather than identification of the stain's components which is important.

Some of the more commonly-used reagents for the examination of blood stains which involve the peroxidase activity of blood are 3,3'-diaminobenzidine (DAB), luminol, *ortho*-tolidine, leucomalachite green, phenolphthalein and

tetramethyldiaminobenzidine. Of those currently in use, 3,3'-diaminobenzidine (DAB) provides the best results in visualising fingerprint impressions made in blood (Olsen, 1985).

The enhancement of blood fingerprints using DAB involves an oxidation reaction in which the oxidant, hydrogen peroxide, oxidises DAB (hydrogen donor) to a dark brown product. The heme group of hemoglobin in blood exhibits a peroxidase-like activity which catalyses the breakdown of hydrogen peroxide (Saferstein, 1988). The peroxidase reaction consists of two successive steps each involving one electron. A general equation for peroxidase catalysed reactions cannot be formulated because the course of the reaction depends on the type of substrate. In the simplest case the same molecule acts as the hydrogen donor for both steps. The equation of the overall reaction where AH_2 is a hydrogen donor (DAB) and A is its oxidised form is usually:

$$AH_2 + H_2O_2 \longrightarrow 2\,H_2O + A$$

The intermediate AH is in many cases detectable (Lück, 1965).

Hemoglobin, which is contained in red blood cells, serves as the oxygen carrier in blood and also plays a vital role in the transport of carbon dioxide and hydrogen ion (Stryer, 1988). The capacity of hemoglobin to bind oxygen depends on the presence of a nonpolypeptide unit called a *heme group* (Stryer, 1988). The heme consists of an organic part and an iron atom. The organic part, *protoporphyrin*, is made up of four pyrrole rings, which are linked by methene bridges to form a tetrapyrrole ring. Four methyl, two vinyl, and two propionate side chains are attached to the tetrapyrrole ring. These substituents can be arranged in fifteen different ways. Only one of these isomers, called protoporphyrin IX, is present in biological systems (Stryer, 1988). The iron atom in heme binds to the four nitrogens in the centre of the protoporphyrin ring. Protoporphyrin IX and a heme group are illustrated in Fig. 2.1. The iron can form two additional bonds, one on either side of the heme plane, and these bonding sites are termed the fifth and sixth coordination positions. The iron atom can be converted between the ferrous

(+2) and the ferric (+3) oxidation states; only the ferrous form is capable of binding oxygen (Stryer, 1988).

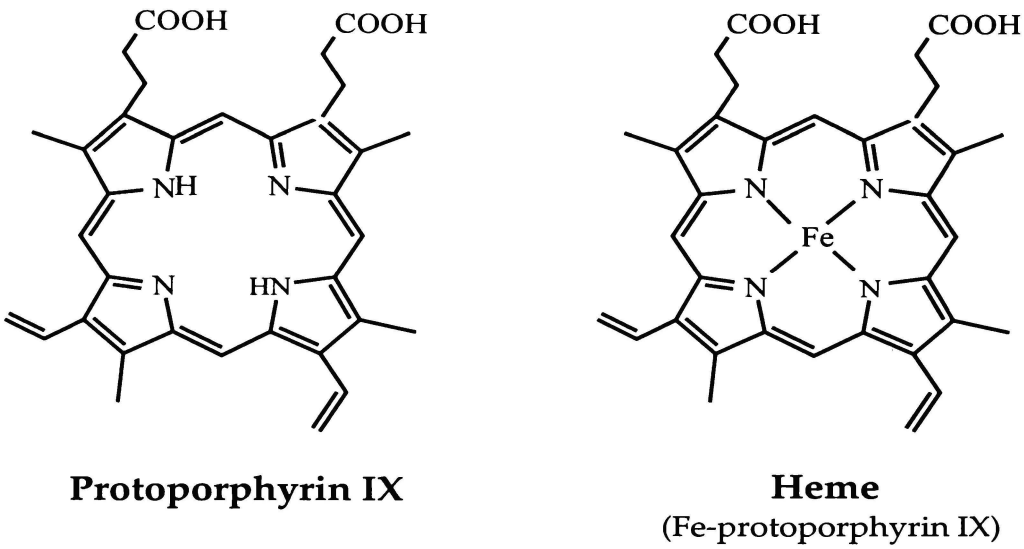

Fig. 2.1
Structures of protoporphyrin IX and the heme group, which acts as a pseudo-peroxidase centre in catalytic blood tests.

The reaction of the heme group with hydrogen peroxide has been studied by Kremer (1989). The overall reaction of hemin was found to proceed at 100 times below the rate of catalase (a peroxidase) and about 10 times greater than the rate of ferric ion. This peroxidase activity is enhanced at alkaline pH by the addition of imidazoles which bind to the hemin. Hydroxide ion seems to be necessary for peroxidase activity. Excess imidazoles will inhibit the reaction. At acidic pH, coordination of the nitrogen bases is enhanced (Uno et al., 1995).

The reactions of hydrogen peroxide with peroxidases and catalase result in heterolytic cleavage of the oxygen-oxygen bond to produce a two-electron-oxidised "oxene" species, which has recently been identified by using hemin compounds. Crystal structures of cytochrome *c* peroxidase and catalase (which also contain heme groups) reveal a general-acid/general-base mechanism to assist the hydroxide leaving group, proposed to occur as shown in Fig. 2.2 (Traylor and Xu, 1990) (Im represents covalently attached imidazole; B represents added buffers).

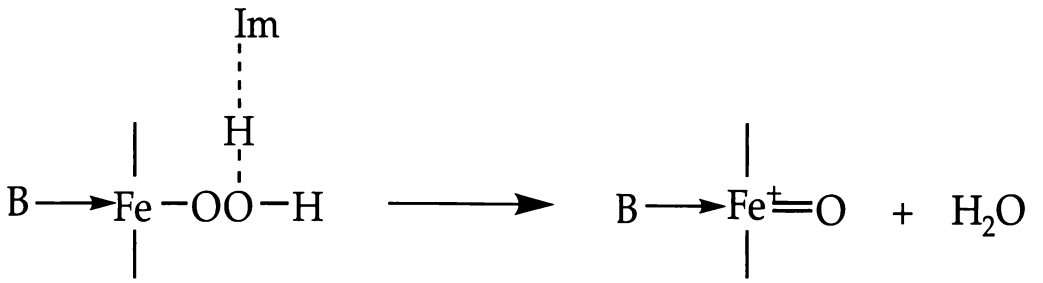

Fig. 2.2
Proposed mechanism for heterolytic cleavage of the oxygen-oxygen bond in hydrogen peroxide at a cytochrome c peroxidase or catalase centre.

In the process Fe(III) is reduced to Fe(II). In the case of the reaction of DAB and peroxide at a heme centre, DAB is oxidised to the brown coloured product shown in Fig. 2.3 (Saferstein, 1988).

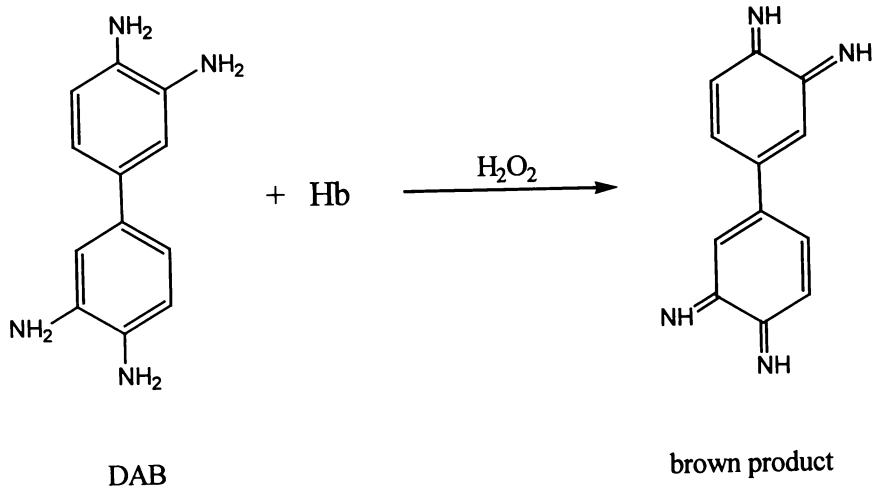

Fig. 2.3
Oxidation of 3,3'-diaminobenzidine (DAB) at a heme centre (Hb) in the presence of H_2O_2.

Unfortunately, 3,3'-diaminobenzidine (DAB) is considered to be toxic. DAB, an odourless, white to slightly reddish-white crystalline organic compound, has been identified at 30 hazardous waste sites in the United States. In the past, US. industries used large quantities of DAB to produce dyes for paper, clothes, and leather. Since the ban on its production in the US in the 1970s, this compound is imported only for speciality uses. People living near hazardous waste sites might be exposed to diaminobenzidine by drinking contaminated water, by inhaling contaminated air, or by swallowing or touching contaminated dust. People can also

be exposed through use of DAB dyes on paper, clothes, and other materials. Human occupational data and studies of laboratory animals suggest that people exposed to DAB may develop adverse systemic health effects of cancer, and the compound has been classified as a carcinogen by four health and environment organisations including the World Health Organisation (WHO). Urinary bladder cancer is the most common form of cancer caused by exposure to DAB (Choudhary, 1996).

The book, *Hazards in the Chemical Laboratory* (Bretherick, 1986) lists the use of diaminobenzidine and its salts as being now prohibited in the United Kingdom under The Carcinogenic Substances Regulations 1967. Sigma-Aldrich Pty., LTD's data sheet on DAB lists it as "toxic: may cause cancer; harmful by inhalation, in contact with skin and if swallowed; possible risk of irreversible effects; possible mutagen."

The sensitivity and specificity of the diaminobenzidine test are both well-attested by the fact that in spite of the hazards associated with exposure to this compound, there has been a marked reluctance to abandon its use for any substitute hitherto found. However, the incidence of cancer among workers exposed to DAB has rendered the search for a satisfactory alternative of paramount importance (Holland et al., 1974). Because of the dangers inherent in the use of DAB (Searle, 1970; Miller et al., 1966; Holland et al., 1974) it was decided that a new non-toxic and specific method for the detection of fingerprints in blood would be investigated.

2,2'-azino-di-[3-ethylbenzthiazolinesulfonate(6)] diammonium salt (ABTS)*, the chemical structure of which is shown in Fig. 2.4, has been used previously as a chromogen for the determination of plasma or serum hemoglobin and has proven sensitive and accurate (Marklund, 1978; Takayanagi and Yashiro, 1984). ABTS, although structurally unrelated to DAB, also undergoes oxidation to a coloured form (green) in the presence of H_2O_2 and hemoglobin. Marklund (1978) and Rey et al. (1970) consider ABTS to be non-toxic and safe to use.

---

* ABTS is usually commercially obtained as the diammonium salt. Throughout this chapter the abbreviation ABTS will stand for the diammonium salt.

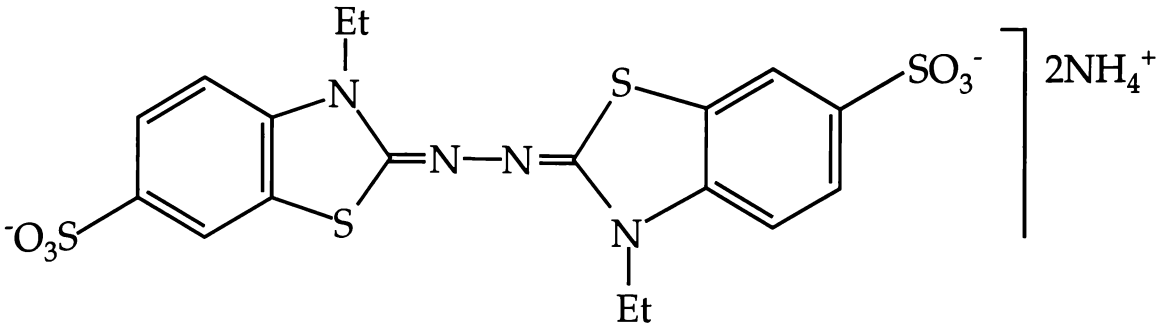

Fig. 2.4
Chemical structure of ABTS diammonium salt.

A German patent from 1970 describes the use of ABTS and its various analogues for the "Colorimetric determination of hydroperoxides". The compounds are reported as being completely stable and nontoxic (Rey et. al, 1970).

In a Japanese study on the testing of reagents for preliminary screening of blood stains, Yatomi (1981) found the sensitivity of ABTS comparable to that of DAB. In another study on the colorimetry of hemoglobin in plasma with ABTS, it was found that the minimum detectable hemoglobin concentration is 20 mg/L. The absorbance was measured at 410 nm (Takayanagi and Yashiro, 1984).

Most recently, ABTS has been used to estimate the plasma total antioxidant capacity in a Chinese population with a lower incidence of cardiovascular disease compared with Caucasian populations, in relation to dietary intake, age, sex and presence of cardiovascular diseases (Jean et al., 1997).

2.1.2 Crystal structure of ABTS

Introduction

Crystals of ABTS were accidentally grown by the author after a concentrated solution of ABTS was left in the fridge. At the time (1997) no published literature on the crystal structure existed so it was felt prudent that a crystal structure should be obtained. However, by the time a crystal structure had been obtained, a published crystal structure of ABTS had appeared in the literature (Mousty et al.,

1997). The following is a brief summary of the XRD results obtained by the author which compare favourably with those obtained by Mousty et al. (1997).

Blue/green irregular crystals of dimensions 0.56 x 0.13 x 0.07 mm were grown from an aqueous solution (0.1 *M*) of ABTS-$(NH_4)_2$. Intensity data and accurate cell parameters were collected at the University of Auckland on a Siemens SMART CCD system diffractometer with monochromated Mo-Kα X-rays (λ = 0.71073 Å). The data collection nominally covered over a hemisphere of reciprocal space, by a combination of three sets of exposures; each set had a different *f* angle for the crystal and each exposure covered 0.3° in *w*. The crystal to detector distance was 5.0 cm. The data sets were corrected empirically for absorption using SADABS.

Crystal data

Formula: $C_{18}H_{28}N_6O_8S_4$

Mr = 584.70

Crystal class = monoclinic

Space group = $P2_1/c$

Unit cell dimensions: a = 8.7066 (2) Å, b = 36.7362 (9) Å, c = 8.2111 (2) Å

β = 97.103 (1)°

U = 2606.1 (1) $Å^3$

Z = 4

F(000) = 1224

μ(Mo-Kα) = 0.419 mm^{-1}

D(calc) = 1.490 g cm^{-3}

Transmission factors: 1.000, 0.913

A total of 15080 reflections at 2θ = 53° were collected at 203(2) K, of which 5272 were independent [R(int) = 0.0321].

Solution and refinement

The structure was solved by direct methods and routinely developed. The asymmetric unit consists of two independent halves of two centrosymmetric molecules (Fig. 2.5). All non-hydrogen atoms were anisotropic, the aryl and ethyl

protons were included in calculated positions but the NH_4^+ and H_2O protons were located from difference maps and included in the refinement without constraint.

The refinement based on F^2 (SHELXL-97) converged with R_1 = 0.0425 for 4198 data with $I > 2\sigma(I)$, 0.0612 for all data; wR_2 = 0.0933 and GooF = 1.099. After the final least-squares refinement the final difference map showed no peaks or troughs greater than ± 0.34 eÅ^{-3}. Refer to Appendix 2.1 for bond lengths, angles, atomic coordinates and equivalent isotropic displacement parameters.

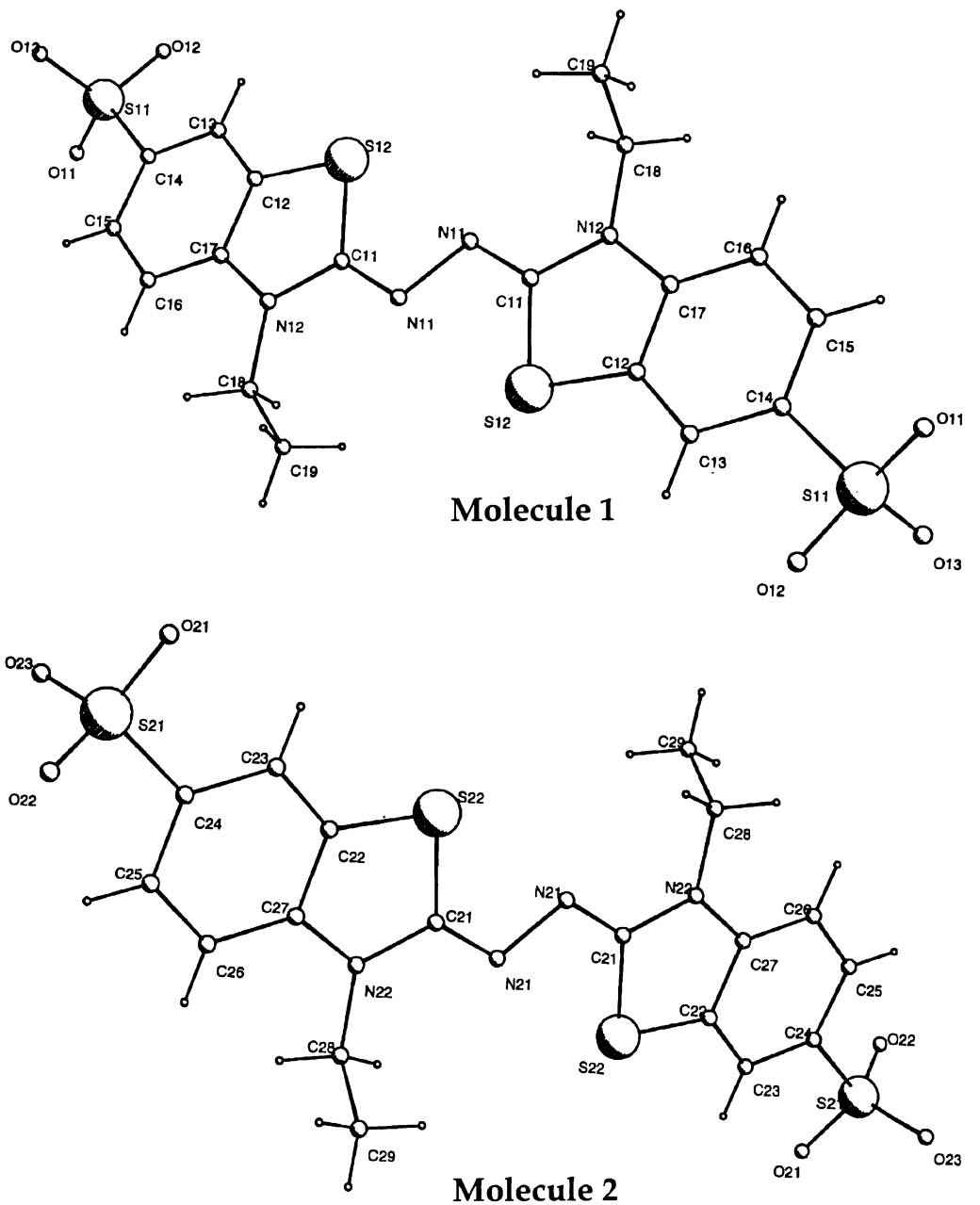

Fig. 2.5
Crystal structure of 2,2'-azino-di-[3-ethylbenzthiazolinesulfonate(6)] diammonium salt (ABTS).

2.1.2 Scope and layout of this chapter

In order to assess the potential of ABTS as an alternative to DAB for the enhancement of fingerprints in blood a comparison with DAB was carried out. This process involved the following steps:

a) Determination of the optimal conditions for colour development in the ABTS-blood reaction in solution. Methodology, results and discussion of this work are outlined in section 2.3.
b) Determination of the optimal conditions for the similar DAB-blood reaction in solution in order to ensure the comparison with ABTS was a valid one. Methodology, results and discussion of this work are outlined in section 2.4.
c) Assessment of the effectiveness of ABTS for visualisation of blood fingerprints deposited on surfaces (as distinct from blood dissolved in solution). Optimal conditions determined by solution tests (outlined in the earlier sections) were used as a starting point in these trials, and results were compared with those obtainable using DAB. Methodology and results of ABTS and DAB trials on actual blood fingerprints are detailed in section 2.5.
d) Assessment of the sensitivity of ABTS compared with DAB for visualisation of blood. Methodology, results and discussion of this work are outlined in section 2.6.
e) Concurrent work carried out at a nearby institution on the effect of ABTS and DAB treatment on subsequent DNA analysis is discussed in section 2.7, with a price comparison of the two different treatments being given in section 2.8.
f) A summary of this chapter is provided in section 2.9.

2.2 *Materials and instrumentation*

Chemicals used in this research were purchased from the following sources:

- ABTS®-$(NH_4)_2$, was purchased from Boehringer Mannheim (BM) Laboratories.
- 3,3′ diaminobenzidine was purchased from Aldrich Chemical Company.
- 5-sulfosalicylic acid and $NaH_2PO_4.2H_2O$ were purchased from M&B Laboratory Chemicals.
- $Na_2HPO_4.12H_2O$ (AR) was purchased from BDH.
- Citric acid was purchased from Ajax Chemicals (Univar).
- Hydrogen peroxide (27%) was purchased from Andrew Chemicals Division.

Other materials used in this research were obtained from the following sources:

- Blood was collected freshly from one of two sources: sheep's blood which was gifted from Ruakura Research Centre, Hamilton, New Zealand, where it had been extracted from the jugular vein of a live sheep in a standard procedure; and human blood which was extracted

from the arm of the author at the University of Waikato Medical Centre, Hamilton. In both cases blood was collected straight into a 5 or 10 mL vaccutainer containing EDTA as an anti-coagulant. 500 μL of the sheep's blood was then diluted with water to a final volume of 250 mL in a volumetric flask (500 times dilution) for optimisation of pH and H_2O_2 concentrations. The remainder of the sheep's blood was used to lay down bloody fingerprints on paper for later use along with human blood from the author.

- Paper (A4, 80 gsm) was obtained from Copyright (Australian Paper, Ltd.) and glass slides from Marienfeld.

The following instrumentation was used in this research:

- A Varian Cary 1 UV-Visible Spectrophotometer (SBW = 0.2 nm, signal averaging time = 0.100 sec) was used for solution trials.
- A Meterlab™ pH meter (model PHM240) was used for confirming the pH values of buffer solutions.

2.3 *ABTS solution optimisation trials*

2.3.1 Preliminary trials

The following results obtained from preliminary trials on the use of ABTS on blood fingerprints led on to the need to develop a methodology for a systematic investigation of optimal ABTS solution conditions.

An ABTS working "solution" was prepared by dissolving 100 mg ABTS in 20 mL distilled water.

1. A few drops of this solution were dripped over a fingerprint in ovine blood (on white paper) followed by a few drops of 2.7% freshly prepared H_2O_2. The fingerprint had been previously fixed with sulfosalicylic acid according to the procedure employed by Lavis (1994). Fingerprint ridges became green in a matter of seconds. The print was left for approximately 20 seconds before rinsing off the ABTS solution in distilled water. The enhancement was good but there was some background staining.
2. One half of a fingerprint in ovine blood was treated with ABTS solution and H_2O_2 for 30 seconds before rinsing in water. The other half was treated in the same way for 2 minutes before rinsing. The half treated for 2 minutes had better enhancement.
3. One half of a fingerprint was treated as above for 2 minutes. The other half was immersed in 10 mL of the above ABTS solution with a few drops of freshly prepared 2.7% H_2O_2 solution for 2 minutes. The immersion method resulted in much better enhancement.

4. One half of a fingerprint was immersed in ABTS/H_2O_2 solution for 2 minutes. The other half was immersed for 5 minutes. Both immersion times resulted in similar enhancement.
5. One half of a fingerprint was immersed in an ABTS solution prepared in phosphate buffer (pH 7.4). The other half was immersed in the ABTS solution prepared in water. The half immersed in the buffered solution had no background staining and the ridge detail of the print was less smudgy.

Lück, 1965 states that the pH optimum for peroxidase catalysis varies depending on the hydrogen donor, in this case ABTS. Based on this and from the preliminary results above it was decided that before further work with ABTS could be carried out the optimum ABTS to H_2O_2 concentration ratio and pH conditions needed to be established. A UV/Vis spectroscopy study of solutions containing ABTS and blood was needed.

2.3.2 Methodology

Optimisation of pH and H_2O_2 concentrations

The optimal pH and H_2O_2 concentrations favouring best colour development of ABTS in a solution containing small amounts of blood in a 10 mm quartz cuvette were firstly determined by UV/Vis spectroscopy on a Varian Cary 1 UV–Visible Spectrophotometer (SBW = 0.2 nm, signal averaging time = 0.100 sec). For oxidised ABTS the peak maximum occurs at 415 nm.

All solutions prepared contained 100 µL of ABTS stock solution, 750 µL of the 1:500 blood solution, a specified volume of 2.7% H_2O_2, and a sufficient volume of buffer solution to give a final volume of 11.8 mL. Changes in the absorbance of these solutions with time at 415 nm were then determined on the UV/Vis Spectrophotometer against a blank containing 750 µL of the 1:500 blood solution, the same volume of 2.7% H_2O_2 as in the sample, and a sufficient volume of buffer solution to give a final volume of 11.8 mL. The H_2O_2 was always added last, with the time of the subsequent reaction being recorded from that point.

Experiments to determine the optimal concentration of H_2O_2 were initially carried out at a pH value of 7.4 (using a phosphate buffer). Volumes of H_2O_2 added were varied from 5 to 100 µL. Experiments to determine the optimal pH were then

performed using a set volume of 10 μL 2.7% H_2O_2 and varying the pH from 4.4 to 8.0. Further experiments to determine the optimal concentration of H_2O_2 at a pH value of 5.4 (citric acid/phosphate buffer) were carried out with H_2O_2 volumes ranging from 1 to 1000 μL. All buffer solutions used were 0.1–0.2 *M* in strength.

An ABTS stock solution was prepared by dissolving 125 mg ABTS in 50 mL distilled water (2.5 g/L) This stock solution was used for the optimisation of pH and H_2O_2 concentrations. A 1:500 diluted blood solution was also used in the optimisation studies. Buffer solutions were prepared according to the directions presented in Table 2.1 (Dawson et al., 1986).

Table 2.1
Buffer solutions used for determination of optimum pH.

pH	Volume (mL)			
	H_2O	Na_2HPO_4 (0.2 *M*)	NaH_2PO_4 (0.2 *M*)	Citric Acid (0.1 *M*)
4.4	—	44.1	—	55.9
5.0	—	51.5	—	48.5
5.4	—	55.75	—	44.25
5.8	50	4	46	—
6.8	50	24.5	25.5	—
7.4	50	40.5	9.5	—
8.0	50	47.35	2.65	—

Determination of a suitable blood and ABTS concentration

Before solution based trials to determine the optimum pH and H_2O_2 concentrations could begin however, suitable blood and ABTS concentrations had to be established so that UV/Vis absorbance data was on scale. Spectra of blood and ABTS were obtained and a check on the proper subtraction of the blank from the sample absorbances was carried out.

A spectrum of blood was firstly obtained using ovine blood. A 10 mL sample which had been collected from the jugular vein of a live sheep into a vaccutainer was immediately diluted up to 500 mL with distilled water to give a 50 times dilution (collection was carried out by a technician of AgResearch in accordance with their standard ethics protocols). This dilution was carried out to avoid clotting. This solution was then diluted further to give a final dilution of 1000

times and run against a blank of water on a UV/Vis spectrophotometer (SBW = 0.2 nm, signal averaging time = 0.100 sec).

The 1000 times diluted blood solution was run against a blank of itself to check for complete subtraction of the blank from the test solution.

A spectrum of ABTS was then obtained by adding 100 µL of ABTS stock solution (2.5 g/L) to 10 mL of phosphate buffer (pH 7.4) and running it against a blank of just phosphate buffer (pH 7.4).

Next an ABTS solution containing 1 mL ABTS stock solution (2.5 g/L), 0.75 mL of the 50 times diluted blood solution, 50 µL H_2O_2 (2.7%) and 9.95 mL phosphate buffer (pH 7.4) was prepared. The solution was then scanned on the UV/Vis spectrophotometer between 300 to 650 nm against a blank containing, 0.75 mL of the 50 times diluted blood solution and 11 mL phosphate buffer (pH 7.4). Scans were carried out 1 and 4 minutes after adding the H_2O_2 to the test solution.

An investigation into the effect of H_2O_2 on the absorbance of blood was then carried out using a fresh sample of ovine blood. A sample was collected via vaccutainer, 500 µL of which was diluted up to 250 mL in a volumetric flask (giving a dilution factor of 500). A 0.75 mL aliquot of this solution was then added to 11 mL of phosphate buffer (pH 7.4). A spectrum was run with a blank of phosphate buffer (pH 7.4) and the absorbance values for the 412 and 208 nm wavelength peaks recorded (major peaks for blood). A 50 µL aliquot of H_2O_2 (2.7%) was then added to the buffered blood solution and the absorbance values recorded at the 412 and 208 nm peaks 7.5, 15.5 and 20 minutes after the H_2O_2 was added.

The experiment was then repeated but with the UV/Vis scan centred on the 412 nm peak and scans being taken before the H_2O_2 was added and 2 and 25 minutes after the H_2O_2 was added.

A spectrum of an ABTS solution showing the oxidation of ABTS with time was obtained. The solution was prepared with 100 µL ABTS stock solution, 0.75 mL of the 500 times diluted blood solution, 50 µL H_2O_2 (2.7%) and 10.9 mL phosphate buffer (pH 7.4). This solution was scanned on the UV/Vis spectrophotometer

between 200 to 600 nm against a blank containing, 0.75 mL of the 500 times diluted blood solution, 11 mL phosphate buffer (pH 7.4) and 50 μL H_2O_2 (2.7%). Successive scans were obtained in order to show the change in absorbance with oxidation of ABTS.

The same solutions were prepared again but with the scan being run between 300–500 nm at various recorded time intervals. The absorbance values for the peak at 415 nm were recorded with increasing time and a graph of absorbance versus time since addition of H_2O_2 was produced (the H_2O_2 was added to the test and blank solutions last, with the time of the subsequent reaction being recorded from that point).

Effect of anti-coagulants

Collection of blood using an anti-coagulant helps matters considerably. However, normal fingerprints laid down in blood (in real-life situations) do not contain an anti-coagulant, so it was necessary to establish whether the presence of such a compound in our trials was likely to influence the ABTS/hemoglobin reaction in any way. For this purpose, three 10 mL samples of ovine blood were collected into three separate vaccutainer tubes, each containing one of three different anti-coagulants. These were EDTA(K_3), sodium heparin, and potassium oxalate/NaF. A fourth 10 mL sample of blood without anticoagulant was also collected. The tubes were inverted a few times to ensure thorough mixing, and 500 μL was immediately taken from each tube and diluted up to 250 mL in volumetric flasks (giving a dilution factor of 500).

Aliquots of the blood solutions (1:500) were then diluted again by 2 times to give final dilutions of 1000 times. UV/Vis absorbance spectra of these four blood samples were then obtained for comparison purposes.

A 500 mg/100 mL (5 g/L) ABTS stock solution was then prepared for use in testing for possible effects from the anti-coagulants on the ABTS–oxidation reaction. A UV/Vis spectrophotometer was used to investigate any effect on the oxidation of ABTS. For each run, a subsample of the following was added to the 10 mm quartz cuvette: 10.99 mL citric acid/phosphate buffer (pH 5.4), 0.75 mL blood solution

(1:500), 50 µL ABTS stock solution and 10 µL 2.7% H_2O_2. This solution was run against the following blank: 11.04 mL citric acid/phosphate buffer (pH 5.4), 0.75 mL blood solution (1:500) and 10 µL 2.7% H_2O_2. Absorbance values for each solution at 415 nm were recorded with increasing time, starting from the point where H_2O_2 was added to the solution.

2.3.3 Results and discussion

Determination of a suitable blood and ABTS concentration

The resultant spectrum (Table 2.2 and Fig. 2.6) obtained from UV/Vis analysis of a 1000 times diluted ovine blood solution was consistent with a porphyrin structure as would be expected for hemoglobin and was also consistent with the absorption spectrum of dry blood obtained by Jones (1997).

Table 2.2
Absorption data from a 1000 times diluted ovine blood sample.

Peak maximum (nm)	Absorbance
412.79	0.972
542.39	0.105
576.40	0.108
208.40	3.447*

*Quantative proportionality of the absorbance is probably not preserved in the case of the 208.40 nm peak; since an absorbance of 3.0 represents transmittance of less than 0.1% of the original light. However, the relative size of this peak compared with the others is a useful marker for the heme group in blood. The strong absorbance in this region is a characteristic of porphyrins, in the spectra of which it is given the general designation "B-band", or "Soret-band".

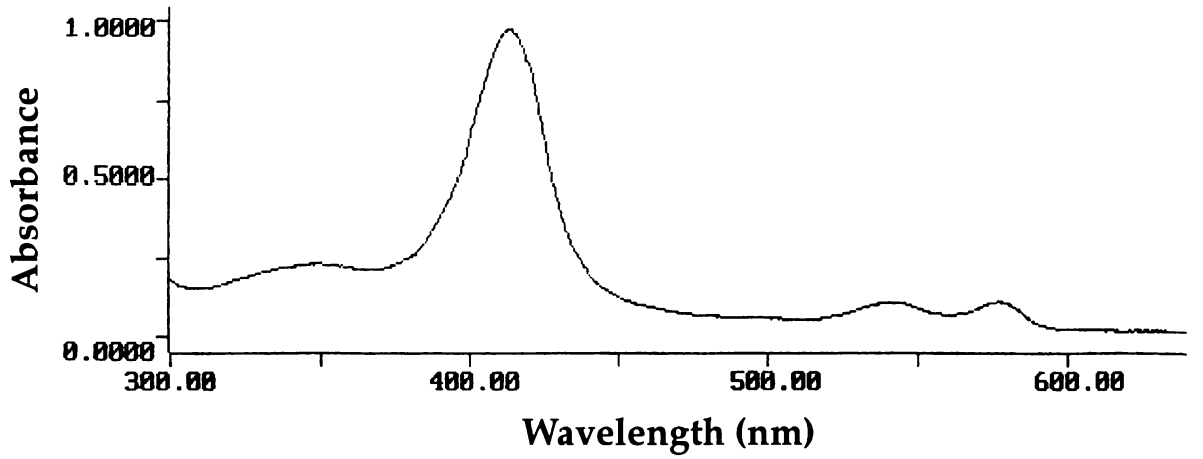

Fig. 2.6
Absorption spectrum (between 300–650 nm) of a 1000 times diluted ovine blood sample.

A flat baseline on the UV/Vis Spectrophotometer was achieved when the 1000 times diluted blood solution was run against a blank of itself; indicating complete subtraction had occurred.

A spectrum of an ABTS solution (0.025 g/L) in phosphate buffer (pH 7.4) was also obtained (Table 2.3 and Fig. 2.7).

Table 2.3
Absorption data for an ABTS solution (0.025 g/L at pH 7.4).

Peak maximum (nm)	Absorbance
342.80	1.731
252.40	2.083
227.20	2.421

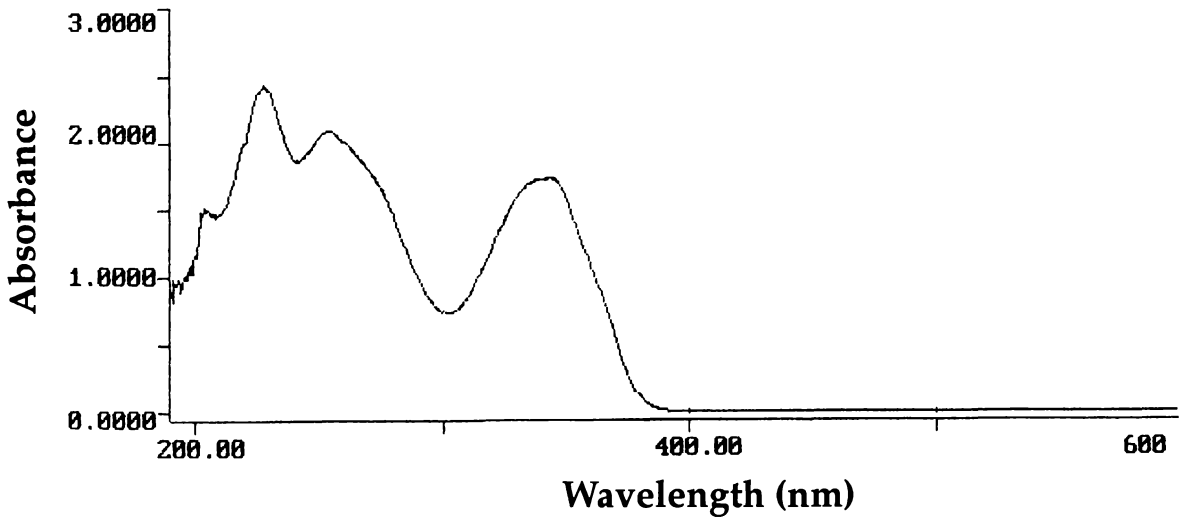

Fig. 2.7
Absorption spectrum of ABTS (0.025 g/L at pH 7.4) prior to oxidation.

The spectra of an ABTS solution (containing blood and H_2O_2), obtained 1 and 4 minutes after addition of the H_2O_2 contained large, poorly defined absorbances in the region between 300 to 400 nm. It was concluded that the H_2O_2 in the ABTS solution must have been effecting the absorbance of the blood because the absorbances due to the blood in the blank were not being properly subtracted. Therefore it was necessary to study the effect of H_2O_2 on the absorbance of blood.

The changes in the absorbance of a dilute ovine blood solution (7833 x dilution) at 412 and 208 nm were obtained before and after addition of 50 µL 2.7% H_2O_2. These absorbance changes are presented in Table 2.4.

Table 2.4
Absorbance change with time for a solution of ovine blood (7833 x dilution) and 50 µL 2.7% H_2O_2.

Time (m)	Absorbance	
	412 nm	208 nm
0	0.13	1.00
7.5	0.07	1.45
15.5	0.07	1.38
20	0.06	1.35

The changes in the absorbance of another blood solution (same dilution as above) were then obtained again before and after addition of 50 µL 2.7% H_2O_2 but with measurement of the absorbance peak at 412 nm only. These absorbance changes are presented in Table 2.5.

Table 2.5
Absorbance change at 412 nm with time for a solution of ovine blood (7833 x dilution) and 50 µL 2.7% H_2O_2.

Time (min)	Absorbance at 412 nm
0	0.12
2	0.09
25	0.04

The peak at 412 nm decreases with time after addition of H_2O_2. This effect is possibly due to oxidation of one of the chromatophores in the blood, and was found to be reproducible. In order to account for this, it was therefore necessary to add H_2O_2 to the blank as well for complete subtraction of the blank to occur.

A preliminary spectrum of the oxidation of an ABTS solution (0.021 g/L) containing diluted blood (7866.67 x dilution) with time after addition of 50 µL 2.7% H_2O_2, where changes in the hemoglobin absorption spectrum on exposure to H_2O_2 have been accounted for, is presented in Fig. 2.8.

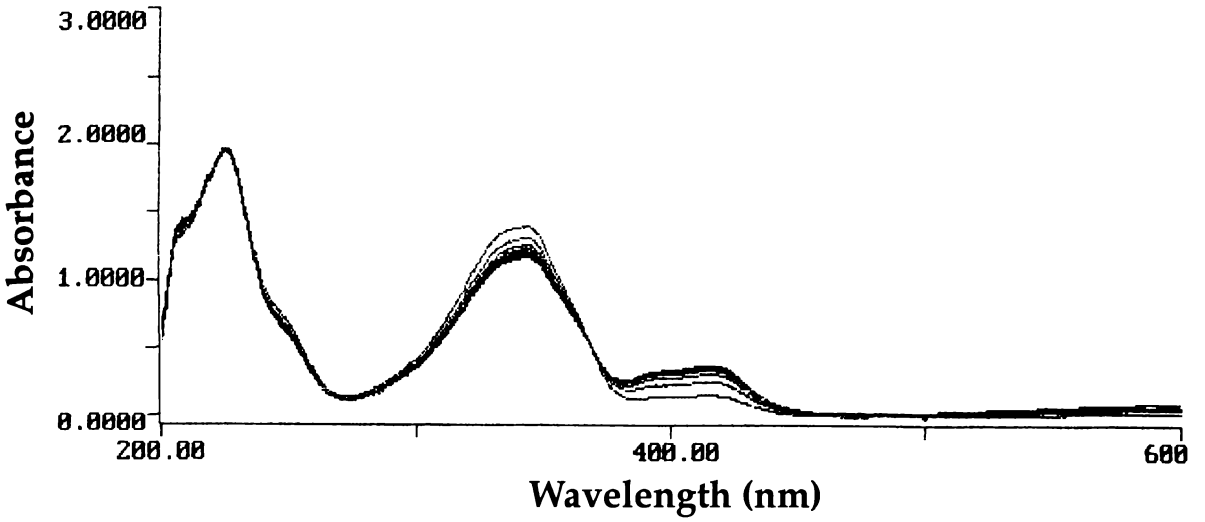

Fig. 2.8
Absorption spectrum of the oxidation of ABTS (0.021 g/L at pH 7.4) with time.

Changes in the absorbance spectrum during oxidation of ABTS occur between 300 and 500 nm; therefore it is necessary to centre on this region.

Changes in the absorbance spectrum during oxidation of ABTS were obtained again but with the time since addition of the H_2O_2 being accurately recorded and scans being made between 300 and 500 nm. An absorbance maximum of 415 nm was chosen for monitoring of the ABTS–oxidation reaction. The results are presented in Fig. 2.9, Fig. 2.10 and Table 2.6.

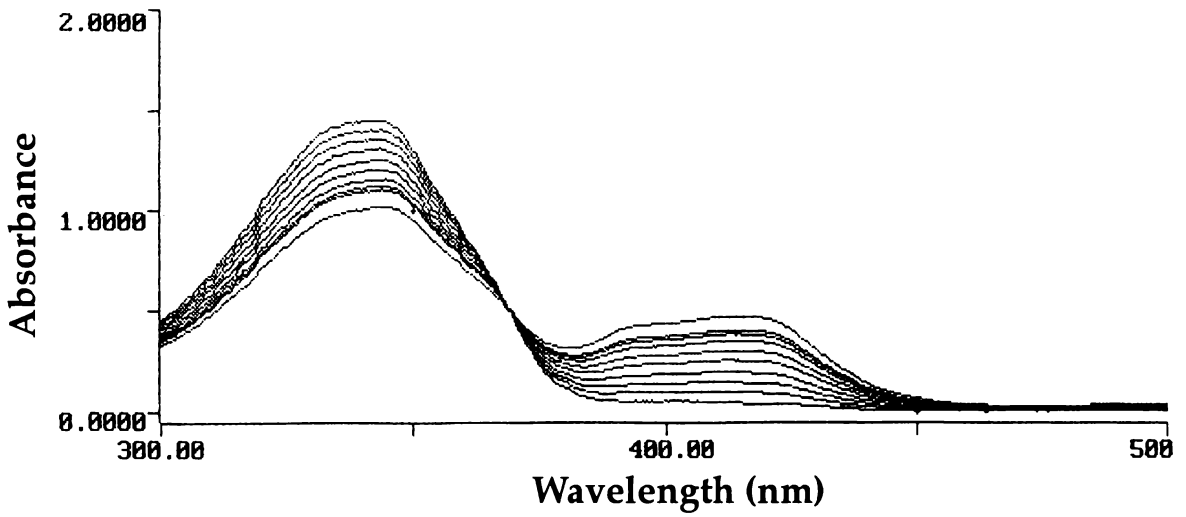

Fig. 2.9
Absorption spectrum (300–500 nm) of the oxidation of ABTS (0.021 g/L at pH 7.4) with time.

Table 2.6
Change of absorbance at 415 nm with time for the oxidation of ABTS (0.021 g/L at pH 7.4 and with 50 µL 2.7% H_2O_2).

Time (s)	110	180	258	332	415	485	562	633	918	2270
Absorbance	0.11	0.16	0.21	0.25	0.28	0.31	0.33	0.35	0.39	0.43

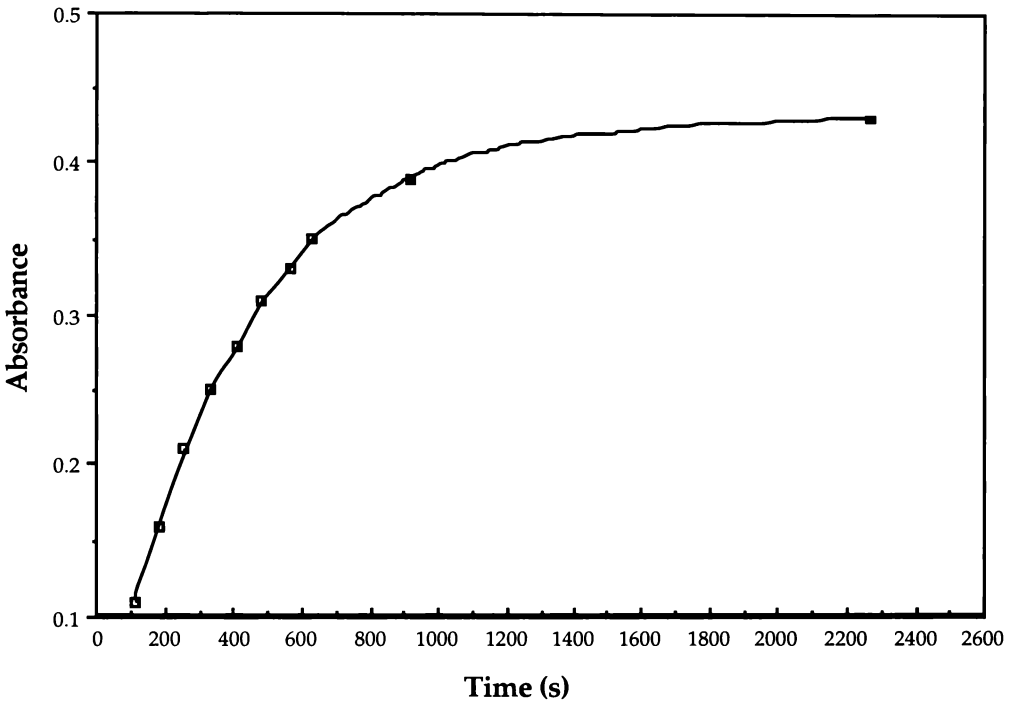

Fig. 2.10
Plot of change in absorption at 415 nm with time for the oxidation of ABTS (0.025 g/L at pH 7.4 and with 50 µL 2.7% H_2O_2).

From the UV/Vis spectrum of ABTS, it is evident that the peak at 415 nm steadily grows during oxidation, with the rate of growth initially rapid and then slowing. To the eye, this is observed as a colour change from pale green to dark green.

Optimisation of pH and H_2O_2 concentration

From the results obtained in the previous section it seems evident that 100 µL of ABTS stock solution (2.5 g/L) and 0.75 mL of the 1:500 blood solution made up to a final volume of 11.8 mL with a buffer and a 2.7% H_2O_2 solution are a suitable criteria for establishing the optimum pH and H_2O_2 concentration. Also the change in absorbance with time for the formation of the oxidised ABTS species should be monitored at 415 nm.

The results from the experiments to determine the optimal concentration of H_2O_2 at a pH value of 7.4 (using a phosphate buffer) are presented in Table 2.7. From these results it was established that 10 µL 2.7% H_2O_2 gives optimal colour development. Results from experiments to determine the optimal pH using a set volume of 10 µL 2.7% H_2O_2 were therefore obtained and are presented in Table 2.8 and Fig. 2.11.

Table 2.7
Effect of H_2O_2 volumes on colour development of ABTS (measured by absorbance at λ = 415 nm) at pH 7.4.

Volume of 2.7% H_2O_2 added																	
5 µL		10µL (a)		10 µL (b)		25 µL		37 µL		50 µL		60 µL		75 µL		100 µL	
T (s)	Ab.	T (s)	Ab.	T (s)	Ab.	T (s)	Ab.	T (s)	Ab.	T (s)	Ab.	T (s)	Ab.	T (s)	Ab.	T (s)	Ab.
129	0.04	124	0.06	110	0.04	115	0.06	107	0.08	110	0.11	99	0.08	108	0.08	80	0.08
197	0.08	196	0.10	182	0.08	188	0.12	180	0.13	180	0.16	173	0.15	180	0.13	140	0.12
275	0.11	265	0.14	256	0.11	262	0.17	256	0.18	258	0.21	248	0.20	256	0.17	240	0.16
352	0.15	351	0.19	332	0.15	336	0.22	350	0.23	332	0.25	321	0.24	369	0.21	320	0.18
451	0.19	459	0.25	411	0.19	476	0.29	423	0.26	415	0.28	437	0.28	486	0.25	398	0.20
526	0.22	571	0.29	488	0.22	570	0.32	523	0.29	485	0.31	511	0.29	606	0.27	472	0.21
641	0.27	719	0.34	646	0.28	644	0.35	598	0.30	562	0.33	628	0.30	726	0.28	543	0.23
820	0.32	848	0.37	721	0.30	765	0.38	730	0.33	633	0.35	778	0.31	799	0.29	616	0.22
953	0.36	926	0.40	794	0.32	907	0.40	880	0.34	918	0.39	851	0.31	967	0.30	727	0.22
1974	0.46	1977	0.47	867	0.34	971	0.41	1964	0.36	2270	0.43	1949	0.29	1987	0.31	866	0.23
				942	0.36	1920	0.46									2110	0.21
				1978	0.45												

Table 2.8
Effect of pH on colour development of ABTS (measured by absorbance at λ = 415 nm) with 10 μL 2.7% H_2O_2.

pH 4.4		pH 5.0		pH 5.4		pH 5.8		pH 6.8		pH 7.4*		pH 8.0	
T (s)	Ab.	T (s)	Ab.	T (s)	Ab.	T (s)	Ab.	T (s)	Ab.	T (s)	Ab.	T (s)	Ab.
107	0.29	108	0.91	126	0.83	107	0.55	106	0.13	117	0.05	103	0.01
180	0.53	180	1.25	198	1.18	184	1.04	197	0.27	189	0.09	180	0.03
254	0.75	254	1.25	273	1.25	259	1.24	287	0.41	260	0.13	286	0.05
327	0.92	363	1.23	349	1.25	331	1.23	377	0.54	341	0.17	402	0.06
455	1.10	484	1.23	426	1.23	409	1.22	466	0.65	474	0.23	483	0.07
576	1.17	602	1.22	546	1.22	529	1.20	556	0.74	609	0.29	587	0.07
696	1.19	722	1.21	664	1.21	607	1.20	636	0.80	720	0.32	679	0.08
816	1.19	842	1.20	845	1.20	727	1.19	791	0.87	857	0.36	827	0.08
936	1.18	962	1.20	1025	1.19	899	1.17	927	0.91	934	0.38	947	0.08
1981	1.15	2158	1.13	1986	1.14	2127	1.06	1986	0.92	1977	0.46	1984	0.10
				4455	1.03	3526	0.98						
						5955	0.86						
						67745	0.58						

*Average of two trials at pH 7.4.

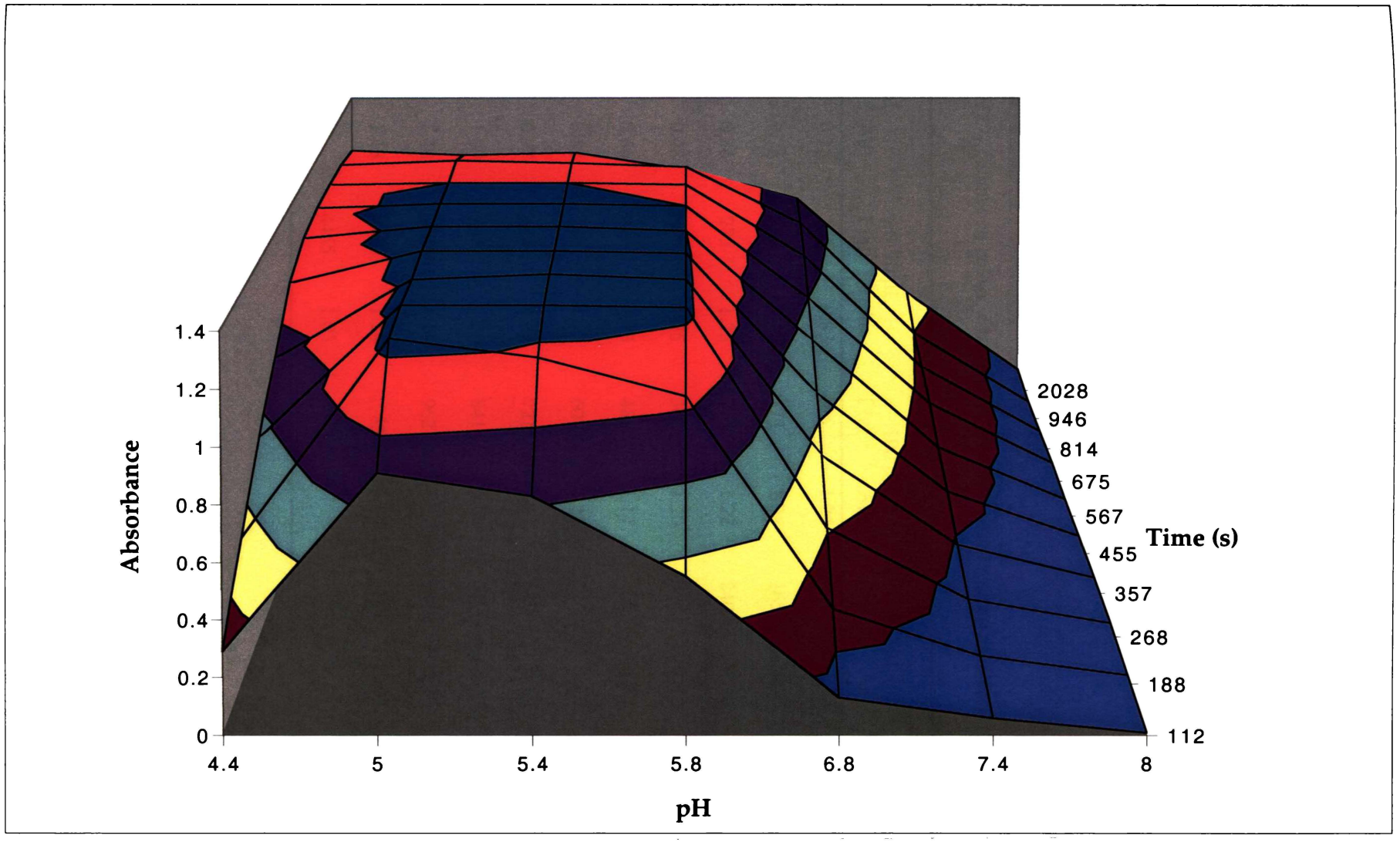

NB. Due to limitations with Microsoft Excel, the pH and time axes do not always increase in even increments.

Fig. 2.11
Plot of effect of pH on colour development of ABTS (measured by absorbance at λ = 415 nm) with 10 µL 2.7% hydrogen peroxide.

The results from Fig. 2.11 indicate that a pH value of 5.4 is optimal. Results from further experiments to determine the optimal concentration of H_2O_2 at this pH value of 5.4 (citric acid /phosphate buffer) are therefore presented in Table 2.9 and Fig. 2.12.

Table 2.9
Effect of H_2O_2 volume on colour development of ABTS (measured by absorbance at λ = 415 nm) at pH 5.4.

Volume of 2.7% H_2O_2 added									
1 µL		10 µL		100 µL		500 µL		1000 µL	
T (s)	Ab.	T (s)	Ab.	T (s)	Ab.	T (s)	Ab.	T (s)	Ab.
99	0.13	126	0.83	86	1.26	90	1.20	99	1.16
173	0.23	198	1.18	173	1.25	165	1.20	178	1.13
252	0.36	273	1.25	275	1.22	240	1.20	262	1.10
328	0.48	349	1.25	362	1.20	314	1.18	380	1.05
446	0.66	426	1.23	481	1.17	405	1.17	500	0.99
566	0.82	546	1.22	601	1.14	525	1.15	621	0.95
686	0.97	664	1.21	721	1.11	645	1.12	741	0.90
806	1.09	845	1.20	841	1.09	765	1.10	837	0.85
926	1.18	1025	1.19	962	1.07	945	1.06	960	0.81
2125	1.18	1986	1.14	1985	0.87	1986	0.86	1982	0.44
		4455	1.03						

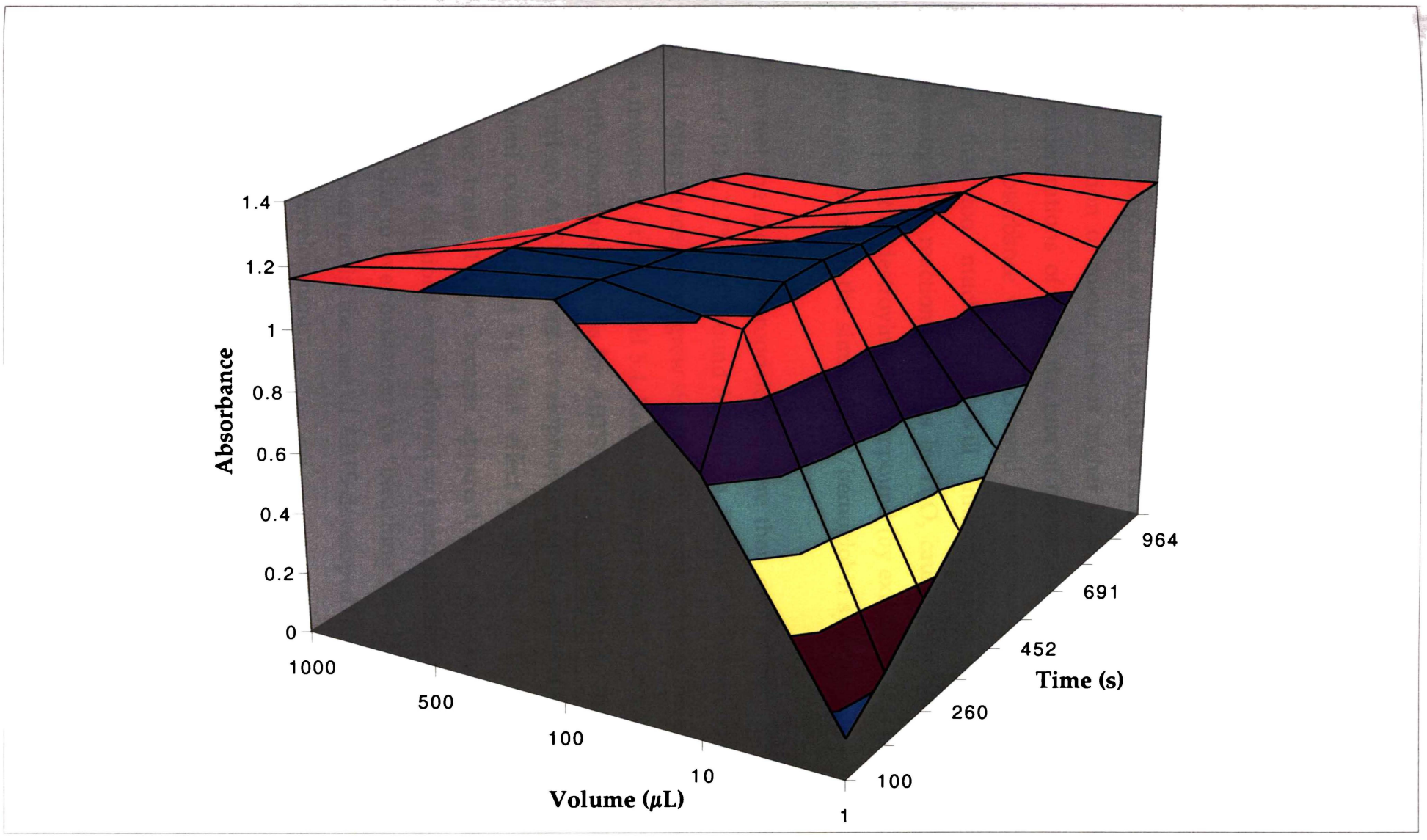

Fig. 2.12
Plot of effect of hydrogen peroxide volume on colour development of ABTS (measured by absorbance at λ = 415 nm) at pH 5.4.

NB. Due to limitations with Microsoft Excel, the volume and time axes do not always increase in even increments.

Discussion of optimisation results

The optimum amount of H_2O_2 required at pH 7.4 was determined firstly. Results of these trials are presented in Table 2.7. From these results, an optimal absorbance was obtained with use of 10 μL of H_2O_2 (2.7%). This corresponds to 1 g ABTS per 40 mL of 2.7% H_2O_2 for optimal colour development (full calculation of which is included in Appendix 2.3). At pH 7.4 colour development is not particularly sensitive to the amount of H_2O_2 added but use of the minimum volume which works (10 μL) compared with the higher volume of 25 μL was felt reasonable due to the observation of colour loss at higher concentrations (and long times). At higher concentrations of H_2O_2, the rate of colour development is similar at first, but the final absorbance values achieved are not so high. In other words it is apparent that too much H_2O_2 will inhibit colour development in the ABTS/hemoglobin reaction, perhaps by H_2O_2 causing further oxidation of the ABTS to the point of destroying the compound (by extension, it is possible that this effect may also occur in the similar DAB/hemoglobin system).

Trials to test the most appropriate pH were then carried out using the optimal volume of 10 μL 2.7% H_2O_2 found for pH 7.4. Results are presented in Table 2.8 and Fig. 2.11. Absorbance values grew significantly as the pH was lowered, appearing to reach a maximum at about pH 5.4. Raising the pH from 7.4 to 8.0 had the opposite effect, with absorbance values for ABTS falling substantially. Thus, in solution, the effect of pH on ABTS colour development is quite pronounced, and maximum development occurs at pH 5.4. This effect is illustrated graphically in Fig. 2.11. During these trials it also became apparent that absorbance values started to decrease again if solutions were allowed to stand for long periods (Fig. 2.13). This could also be due to over-oxidation (or "bleaching") by H_2O_2 in solution, and was not an effect observed in the case of ABTS-developed fingerprints, where H_2O_2 is rinsed off after development.

Once the optimum pH was determined, it was felt prudent to establish whether the optimum H_2O_2 volume of 10 μL still applied at the higher acidity. The results for different H_2O_2 volumes at pH 5.4 are presented in Table 2.9 and Fig. 2.12.

From these results it can be seen that 10 μL 2.7% H_2O_2 (H_2O_2:ABTS ratio of 40 mL:1 g) was still the best volume to use at the lower pH. It gives the smallest absorbance

decrease with time after the initial absorbance maximum is reached. Use of 1 µL leads to a lower rate of initial colour development, whereas use of 100, 500 and 1000 µL lead to increasingly greater rates of colour loss after development. This latter observation lends support to the idea that unreacted H_2O_2 is involved in the colour loss.

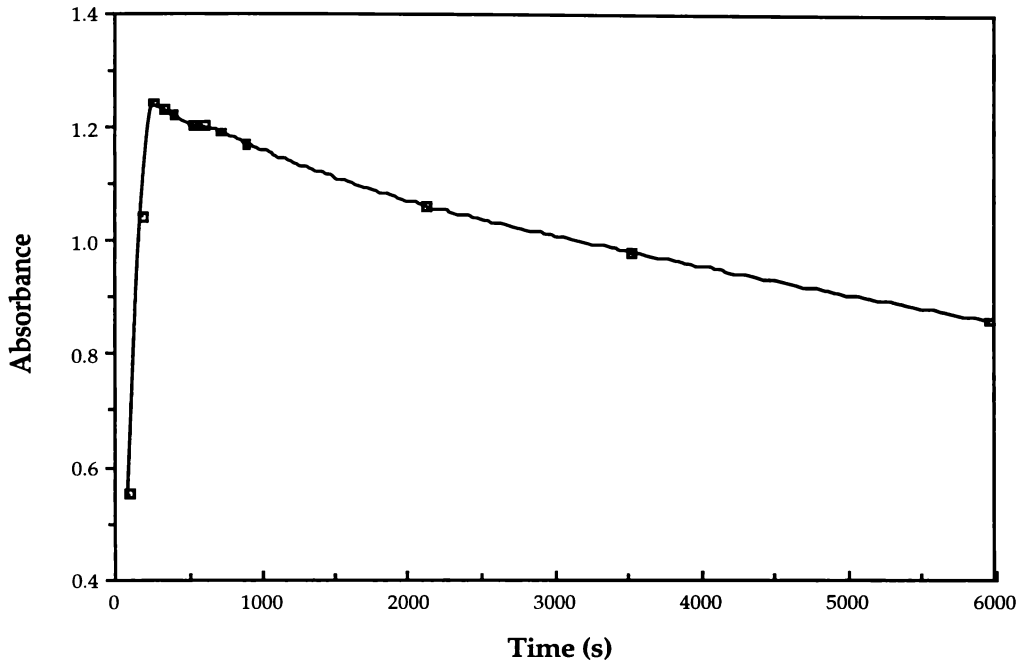

Fig. 2.13
Plot showing decrease in absorbance (λ = 415 nm) of oxidised ABTS over an extended time period (1 hr and 40 mins) at pH 5.8 and 10 µL 2.7% H_2O_2.

Overall, the cuvette-based solution trials yield the following as optimal for development of colour in the ABTS/hemoglobin system; pH 5.4, ratio of 1 g ABTS to 40 mL 2.7% H_2O_2, and a development time of 4 to 8 minutes. These were taken as starting conditions for testing the activity of ABTS on blood fingerprints. Unknowns in moving from solution work to development of blood on the surfaces were (a) whether the concentration of ABTS would have any effect on final colour development, and (b) the extent to which the oxidised ABTS would be able to deposit on the surface-bound blood and remain there (rather than move back into solution). This second parameter is quite important; in an earlier trial

involving phenolphthalein, it was found that although this reagent provides a strong, magenta colour immediately on reaction with a fixed print, within a few seconds this colour rises from the print surface and disperses back into solution. Obviously, part of the reason DAB (refer to section 2.1.1) is an effective reagent is that the oxidised form is less soluble in aqueous solution than the reduced form and will therefore precipitate and settle out on the fingerprint surface.

Effect of anti-coagulants

Absorbance values and their corresponding wavelengths for the blood solutions (1:1000) containing different or no anti-coagulants are presented in Table 2.10.

Table 2.10
Comparison of absorbance spectra of blood containing different or no anti-coagulants.

EDTA(K_3)		Sodium Heparin		Potassium Oxalate		No Anti-coagulant	
λ (nm)	Abs.	λ (nm)	Abs.	λ (nm)	Abs.	λ (nm)	Abs.
576.00	0.143	576.40	0.137	576.80	0.137	576.40	0.090
542.39	0.133	542.79	0.129	541.59	0.130	541.19	0.096
415.19	1.134	414.39	0.124	414.79	1.140	408.39	1.039
344.39	0.261	345.99	0.262	345.59	0.261	347.59	0.253
270.00	0.496	274.40	0.386	270.00	0.616	269.60	0.469
212.40	3.381	211.60	3.333	209.20	3.444	—	—
208.00	3.302	208.00	3.278	208.00	3.425	207.60	3.295

From these results it can be seen that the presence of anti-coagulants in the blood do not significantly alter the absorbance characteristics of hemoglobin itself, with absorbance values being largely indistinguishable from those obtained without anti-coagulants.

The change in absorbance values with time at 415 nm for ABTS solutions with blood containing different or no anti-coagulants are presented in Fig. 2.14 and Table 2.11.

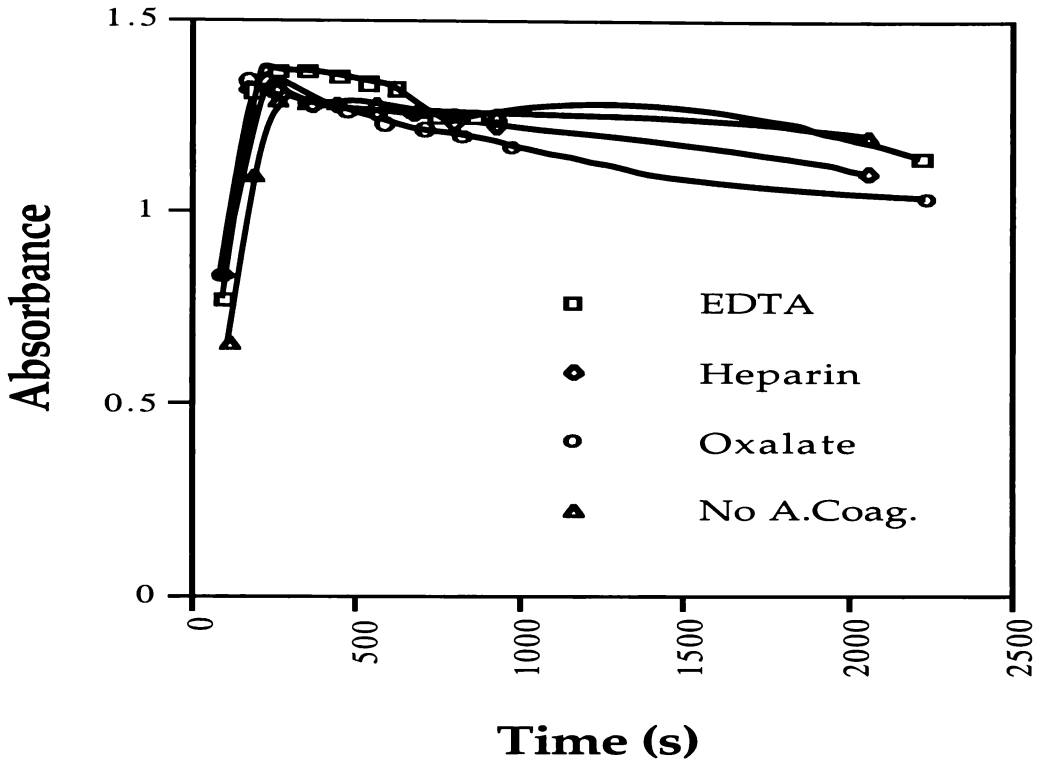

Fig. 2.14
Comparison of effect of anticoagulants on oxidation of ABTS with time for 10 μL H_2O_2 and pH 5.4 (absorbance measured at λ = 415 nm).

Table 2.11
Comparison of effect of anticoagulants on ABTS with time for 10 μL H_2O_2 and pH 5.4 (absorbance measured at λ = 415 nm).

EDTA(K_3)		Sodium Heparin		Potassium Oxalate/NaF		No anti-coagulant	
T (s)	Ab.	T (s)	Ab.	T (s)	Ab.	T (s)	Ab.
102	0.77	99	0.83	89	0.83	109	0.66
185	1.31	173	1.32	170	1.34	185	1.09
267	1.36	258	1.32	247	1.31	262	1.29
346	1.36	357	1.27	350	1.28	351	1.28
447	1.35	442	1.27	470	1.26	442	1.28
536	1.33	561	1.25	590	1.23	562	1.28
626	1.32	681	1.25	710	1.21	682	1.26
745	1.24	800	1.23	830	1.20	802	1.25
866	1.24	921	1.22	979	1.17	922	1.25
2227	1.14	2060	1.10	2235	1.03	2062	1.20

A proper comparison of the three different anti-coagulants, EDTA(K_3), sodium heparin, and potassium oxalate/NaF necessitates the determination of the absorbance at a specific time for each blood sample in order to establish whether there is any influence on the ABTS/hemoglobin reaction. The time chosen was 300 seconds, and absorbances at this time were calculated by interpolation of the data in Table 2.11 and which are presented in Table 2.12. The UV/Vis results previously obtained in the optimisation of pH and H_2O_2 concentrations subsection using an earlier blood sample with no anti-coagulant at pH 5.4 and with 10 μL 2.7% H_2O_2 were also used for purposes of comparison.

Table 2.12
Comparison of absorbances at 300 seconds for different and no anti-coagulants.

Anti-coagulant	Absorbance at 300 seconds
EDTA(K_3)	1.36
Sodium Heparin	1.30
Potassium Oxalate	1.30
No anti-coagulant	1.29
No anti-coagulant*	1.25

*Result obtained from an earlier blood sample used in optimisation subsection.

From these results it can be seen that the presence of anti-coagulants in the blood do not significantly suppress the reaction between ABTS, H_2O_2 and hemoglobin, with absorbance values being no smaller (and in fact largely indistinguishable) from those obtained without use of anti-coagulants.

2.4 *DAB solution optimisation trials*

2.4.1 Methodology

Optimisation of pH and H_2O_2 concentrations

It was decided that although methods for DAB treatment were already well established it would be prudent to investigate the optimisation of pH and H_2O_2 concentration in the same manner as was carried out for ABTS. The method currently recommended by the New Zealand Crown Research Institute, *ESR:Forensic* is the method used as the basis for comparison (Lavis, 1994). The method is included in Appendix 2.2.

A stock solution of DAB was prepared by dissolving 30 mg DAB with distilled water in a 250 mL volumetric flask (0.12 g/L). To help facilitate dissolution of the DAB a 30 minute treatment in an ultrasound bath was carried out. Aliquots of 1 mL were placed into 1.5 mL plastic snap lid "Eppendorf" vials and frozen. The freezing of the solutions was carried out to prevent stock solutions from slowly oxidising by themselves.

All solutions prepared contained 1 mL of DAB stock solution (previously thawed immediately prior to use), 750 μL of the 1:500 blood solution, a specified volume of 2.7% H_2O_2, and a sufficient volume of buffer solution to give a final volume of 12.5 mL. Changes in the absorbance of these solutions with time at 406.80 nm were then determined on the UV/Vis Spectrophotometer against a blank containing 750 μL of the 1:500 blood solution, the same volume of 2.7% H_2O_2 as in the sample, and a sufficient volume of buffer solution to give a final volume of 12.5 mL. The H_2O_2 was always added last, with the time of the subsequent reaction being recorded from that point.

Experiments to determine the optimal concentration of H_2O_2 were initially carried out at a pH value of 5.4 (using a citric acid/phosphate buffer). Volumes of H_2O_2 added were varied from 10 to 1000 μL. A single experiment was then carried out using 100 μL H_2O_2 at a pH value of 7.4 in order to compare the difference between DAB oxidation at pH 7.4 and pH 5.4. Experiments to determine the optimal pH were then performed using a set volume of 100 μL 2.7% H_2O_2 and varying the pH from 4.4 to 7.4. Further experiments to determine the optimal concentration of H_2O_2 at a pH value of 5.0 (citric acid/phosphate buffer) were carried out with H_2O_2 volumes ranging from 10 to 500 μL. All buffer solutions used were 0.1–0.2 *M* in strength. Buffers were prepared according to the proportions given previously in Table 2.1.

Determination of a suitable blood and DAB concentration

The preserved-500 times diluted ovine blood solution used in the previous trials for ABTS was three weeks old (stored in refrigerator) at the time of the DAB solution trials. A UV/Vis spectrum of a two fold dilution of this solution (1000 times total dilution) was obtained and used as evidence of possible degradation.

A DAB solution containing 500 µL DAB stock solution (0.12 g/L), 0.75 mL of the 500 times diluted blood solution, 100 µL H_2O_2 (2.7%) and 10.45 mL citric acid/phosphate buffer (pH 5.4) was then prepared. This solution was scanned on the UV/Vis spectrometer between 200 to 650 nm against a blank containing, 0.75 mL of the 500 times diluted blood solution, 10.95 mL citric acid/phosphate buffer (pH 5.4) and 100 µL H_2O_2 (2.7%).

2.4.2 Results and discussion

Determination of a suitable blood and DAB concentration

Results from the UV/Vis spectrum of a two fold dilution of preserved–500 times diluted three week old ovine blood solution is presented in Table 2.13. The results seem to reveal no degradation and a similar spectrum to that obtained three weeks earlier for the same solution. Therefore the same solution was used for further work.

Table 2.13
Absorption data from a 1000 times diluted ovine blood sample.

Fresh solution 3 weeks earlier		Aged solution after 3 weeks	
Peak maximum (nm)	Absorbance	Peak maximum (nm)	Absorbance
412.79	0.972	408.39	1.064
542.39	0.105	540.39	0.106
576.40	0.108	576.00	0.097
—	—	272.80	0.390
208.40	3.447	208.40	3.420

The UV/Vis spectrum obtained for oxidation of a DAB solution (0.0051 g/L) in citric acid/phosphate buffer (pH 5.4) with 100 µL 2.7% H_2O_2 added had a gradual increase in absorbance from 650 nm to 200 nm with little evidence of any absorbance maximum. After numerous scans it was determined that there was a small absorbance maximum in the visible region at 406.80 nm (Table 2.14 and Fig. 2.15).

Table 2.14
Change in absorbance and wavelength maximum with time for oxidation of DAB (0.0051 g/L) at pH 5.4 with 100 µL 2.7% H_2O_2 in the presence of hemoglobin.

Time (s)	Absorbance	Wavelength (nm)
98	0.178	406.80
236	0.315	407.60
353	0.370	409.60
497	0.388 &	413.20 &
	0.388	406.80
875	0.406	406.80

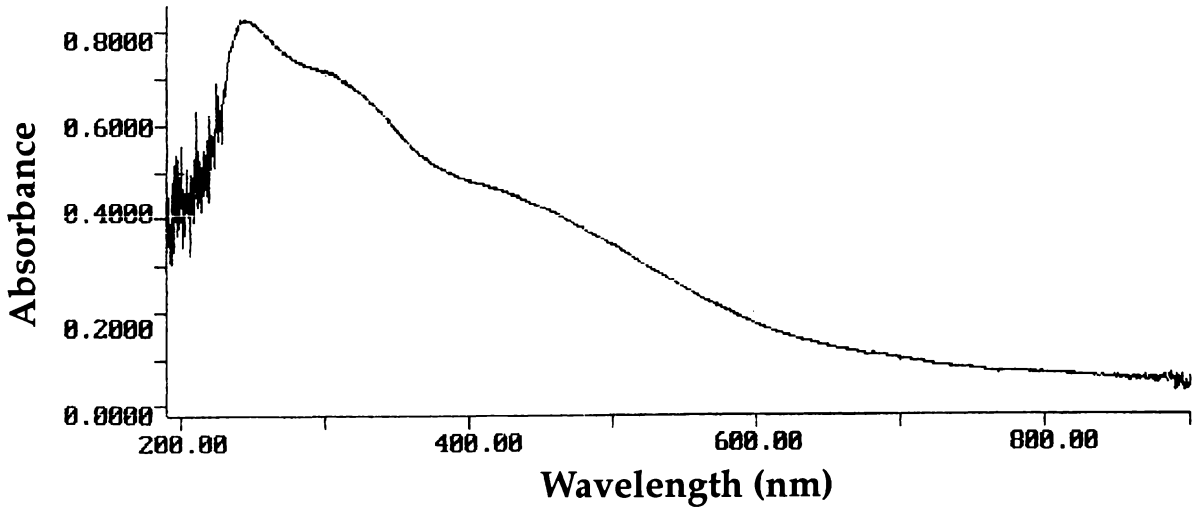

Fig. 2.15
Spectrum of oxidised DAB (0.0051 g/L at pH 5.4) obtained 20 minutes after addition of 100 µL 2.7% H_2O_2.

The UV/Vis spectrophotometer was therefore set up to record absorbance values at 406.80 nm for all subsequent analyses of DAB. The maximum absorbance value at this wavelength however, was still less than 0.25 even after 10 minutes. For this reason it was decided that the amount of DAB should be increased to 1 mL for subsequent analyses.

Optimisation of pH and H_2O_2 concentration

The optimum amount of H_2O_2 required at pH 5.4 was determined firstly. Results of these trials are presented in Table 2.15.

Table 2.15
Effect of H_2O_2 volume on colour development of DAB (measured by absorbance at λ = 406.80 nm) at pH 5.4.

Volume of 2.7% H_2O_2 added							
10 µL		100 µL		500 µL		1000 µL	
T (s)	Ab.	T (s)	Ab.	T (s)	Ab.	T (s)	Ab.
86	0.103	88	0.164	85	0.168	93	0.185
146	0.140	148	0.252	145	0.258	153	0.261
206	0.178	208	0.323	205	0.320	213	0.291
266	0.216	268	0.338	265	0.345	273	0.301
326	0.252	328	0.349	325	0.353	333	0.309
386	0.282	388	0.354	385	0.362	453	0.318
506	0.337	508	0.361	505	0.368	573	0.325
626	0.372	628	0.365	625	0.374	693	0.325
746	0.397	748	0.367	745	0.379	813	0.328
1886	0.388	1888	0.372	1885	0.378	1923	0.340

The results indicate that optimal colour development can be obtained with use of 100 µL of 2.7% H_2O_2. The choice of 100 µL rather than 500 µL was made even though both resulted in a similar rate of colour development because the risk of over-oxidation (or "bleaching") is minimised with the use of less H_2O_2. The use of 10 µL resulted in a slower rate of colour development while the use of 1000 µL resulted in a lower final absorbance.

Changes in absorbance with time for a DAB solution containing 100 µL 2.7% H_2O_2 at a pH value of 7.4 are presented in Table 2.16. The results when compared with those presented in Table 2.15 indicate that colour development in solution at a pH of 5.4 is significantly better.

Table 2.16
Change in absorbance of DAB with time at pH 7.4 and with 100 µL of H_2O_2.

Time (s)	76	136	196	256	316	436	556	676	796	1936
Absorbance	0.027	0.032	0.034	0.039	0.044	0.056	0.064	0.071	0.078	0.169

Following this results of the most appropriate pH were obtained using 100 µL of 2.7% H_2O_2 and buffers of various pH values. The results, presented in Table 2.17 and Fig. 2.16, indicate that a pH value of 5.0 provides the greatest rate of colour development. It should be noted that comparison is also made with the rate of colour development previously obtained at pH 5.4 using 100 µL of 2.7% H_2O_2 from Table 2.15.

Table 2.17
Effect of pH on colour development of DAB (measured by absorbance at λ = 406.80 nm) with100 µL 2.7% H_2O_2.

pH 7.4		pH 6.8		pH 6.0		pH 5.0		pH 4.4		pH 5.4*	
T (s)	Ab.	T (s)	Ab.	T (s)	Ab.	T (s)	Ab.	T (s)	Ab.	T (s)	Ab.
80	0.031	100	0.051	90	0.076	81	0.205	88	0.121	88	0.164
140	0.038	160	0.065	150	0.119	141	0.313	148	0.177	148	0.252
200	0.050	220	0.081	210	0.171	201	0.344	208	0.224	208	0.323
260	0.060	280	0.099	270	0.224	261	0.358	268	0.264	268	0.338
320	0.071	340	0.115	330	0.274	321	0.364	328	0.287	328	0.349
440	0.094	460	0.153	450	0.339	441	0.372	448	0.324	388	0.354
560	0.119	580	0.191	570	0.355	561	0.372	568	0.341	508	0.361
680	0.141	700	0.226	690	0.369	681	0.377	688	0.352	628	0.365
800	0.163	820	0.260	810	0.379	801	0.381	808	0.359	748	0.367
1880	0.278	1920	0.352	1920	0.377	1920	0.383	1920	0.391	1888	0.372

*These results taken from Table 2.15 for ease of comparison.

It should be noted here that the optimum pH of 5.0 for colour development of DAB in solution is different to the pH of 7.4 normally used by *ESR:Forensic* for visualisation of blood prints on surfaces.

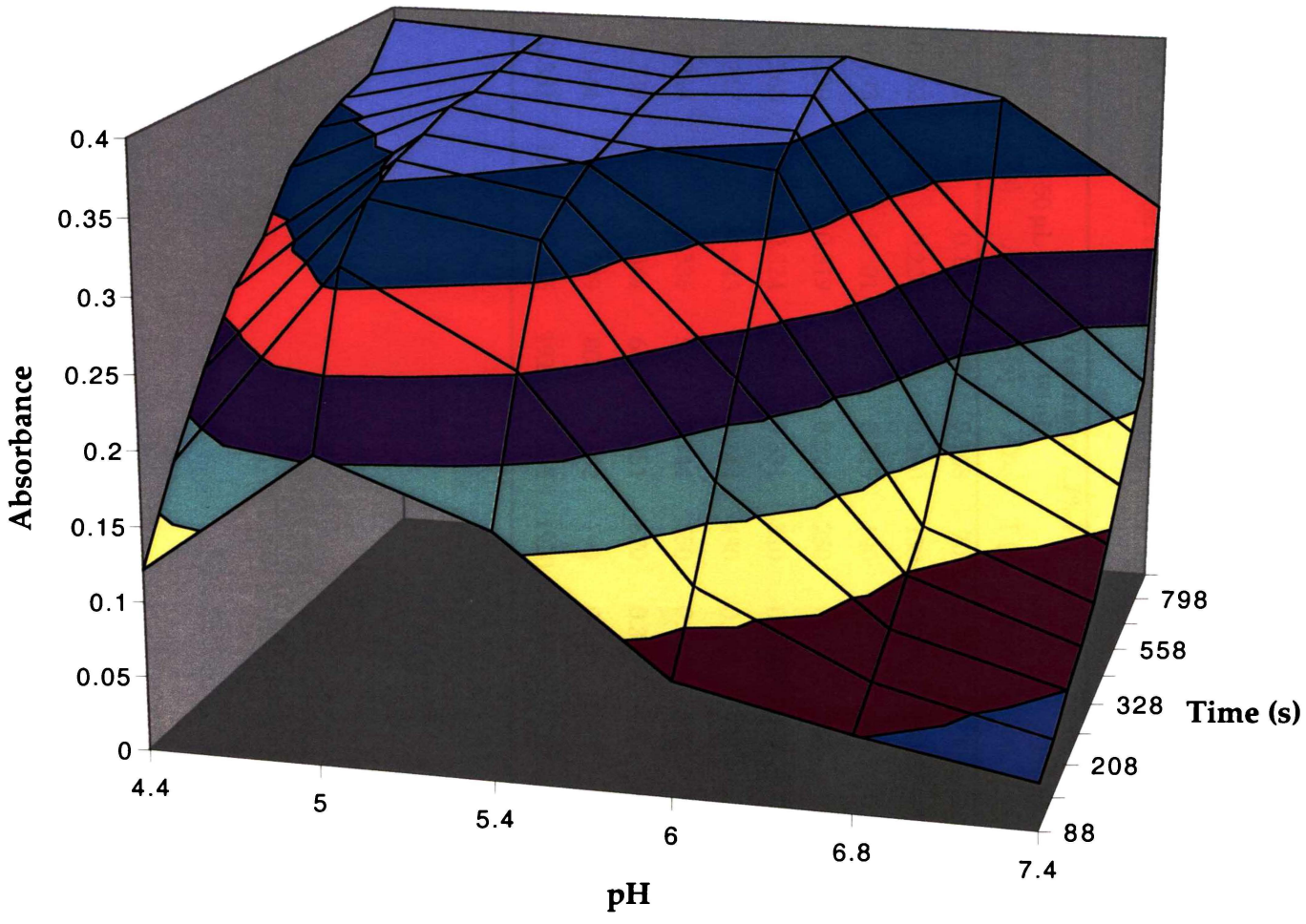

NB. Due to limitations with Microsoft Excel, the pH and time axes do not always increase in even increments.

Fig. 2.16
Plot of effect of pH on colour development of DAB (measured by absorbance at λ = 406.80 nm) with 100 µL 2.7% hydrogen peroxide.

In a continuation of the iterative procedure, results were then obtained for the optimum H_2O_2 concentration at a pH value of 5.0; these are presented in Table 2.18 and Fig. 2.17.

Table 2.18
Effect of H_2O_2 volume on colour development of DAB (measured by absorbance at λ = 406.80 nm) at pH 5.0.

Volume of 2.7% H_2O_2 added											
10 µL		50 µL		90 µL		120 µL		150 µL		500 µL	
T (s)	Ab.	T (s)	Ab.	T (s)	Ab.	T (s)	Ab.	T (s)	Ab.	T (s)	Ab.
108	0.111	75	0.132	80	0.148	70	0.153	73	0.152	80	0.186
168	0.152	135	0.226	140	0.250	130	0.258	133	0.24	140	0.239
228	0.193	195	0.301	200	0.315	190	0.312	193	0.304	200	0.262
288	0.230	255	0.319	260	0.326	250	0.327	253	0.331	260	0.271
348	0.263	315	0.324	320	0.331	310	0.334	313	0.342	320	0.276
468	0.317	435	0.343	440	0.344	430	0.341	433	0.351	440	0.283
588	0.348	555	0.336	560	0.344	550	0.344	553	0.359	560	0.285
708	0.339	675	0.344	680	0.351	670	0.349	673	0.364	680	0.288
828	0.344	795	0.349	800	0.352	790	0.350	793	0.366	800	0.287
1920	0.351	1920	0.355	1920	0.355	1920	0.353	1920	0.374	1920	0.292

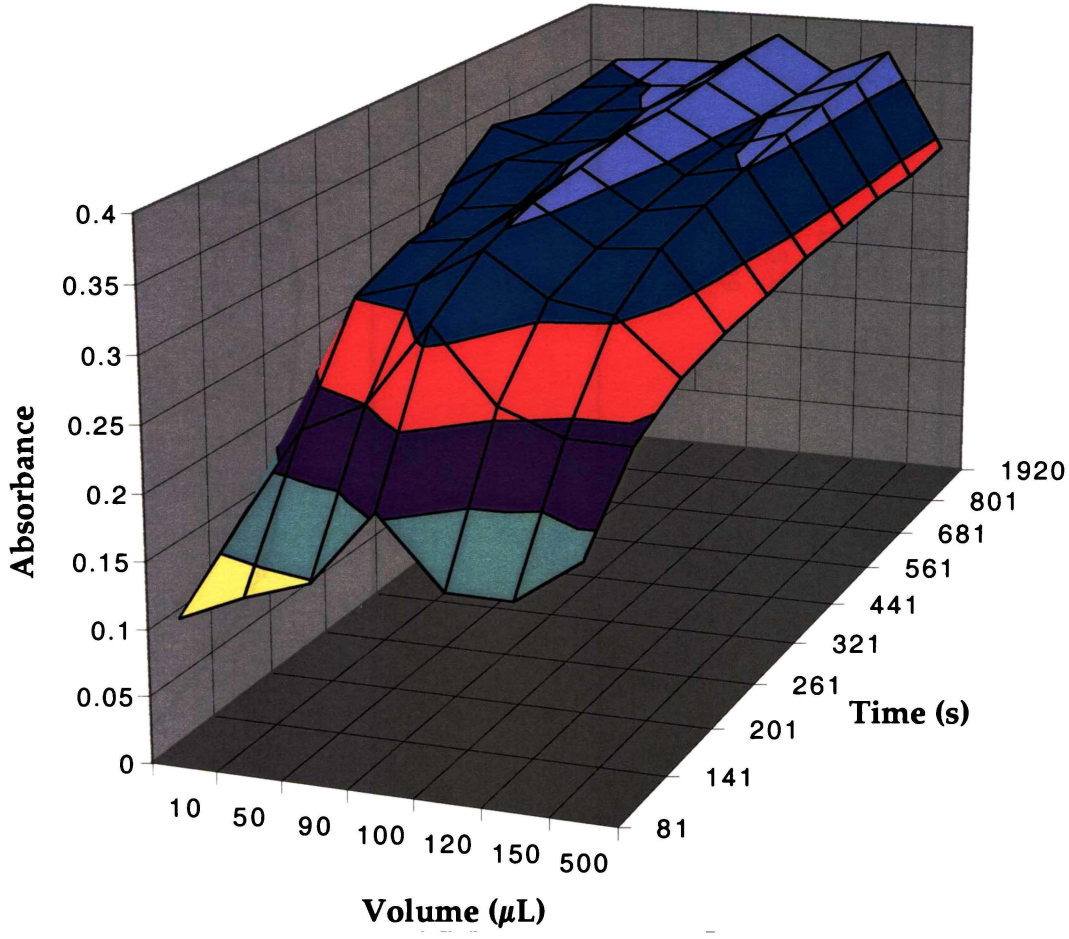

NB. Due to limitations with Microsoft Excel, the volume and time axes do not always increase in even increments.

Fig. 2.17
Plot of effect of hydrogen peroxide volume on colour development of DAB (measured by absorbance at λ = 406.80 nm) at pH 5.0.

At pH 5.0, the 100 μL 2.7% H_2O_2 volume seems to be still the optimum volume to use. This particular trial using 100 μL of 2.7% H_2O_2 and a pH of 5.0 was repeated but was extended over a longer time interval to determine whether the absorbance decreases with time after reaching a maximum, as was observed with ABTS. In the case of DAB the same effect was indeed found to occur with the absorbance decreasing with time after reaching an initial maximum. Results are presented in Fig. 2.18 and Table 2.19.

Table 2.19
Change in absorbance of DAB with time for 100 μL H_2O_2 and pH 5.0.

Time (s)	Absorbance	Time (s)	Absorbance
94	0.181	694	0.352
154	0.255	814	0.352
214	0.307	1920	0.359
274	0.320	3404	0.356
334	0.329	7209	0.338
454	0.340	11921	0.217
574	0.347		

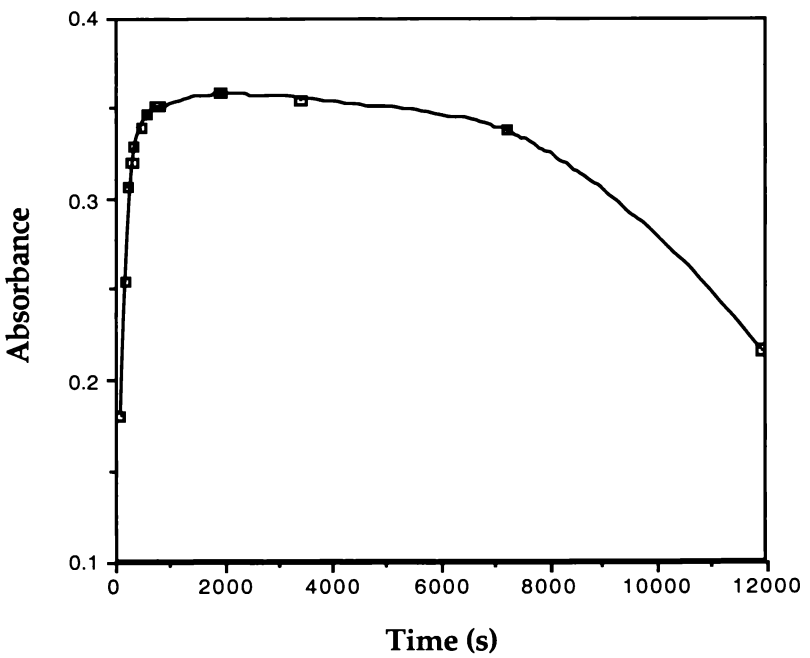

Fig. 2.18
Change in absorbance during oxidation of a solution of DAB with time for 100 μL H_2O_2 and pH 5.0.

Discussion of optimisation results

The optimum amount of H_2O_2 required at pH 5.4 was determined firstly. Results of these trials are presented in Table 2.15. From these results, an optimal absorbance was obtained with use of 100 µL of H_2O_2 (2.7%).

Trials to test the most appropriate pH were then carried out using the optimal volume of 100 µL 2.7% H_2O_2 found for pH 5.4. Results are presented in Table 2.17. Absorbance values grew significantly as the pH was lowered, appearing to reach a maximum at about pH 5.0 before decreasing again at lower pH. Thus, in solution, the effect of pH on DAB colour development is quite pronounced, and maximum development occurs at pH 5.0. Once the optimum pH was determined, it was felt prudent to establish whether the optimum H_2O_2 volume of 100 µL still applied at the higher acidity. The results for different H_2O_2 volumes at pH 5.0 are presented in Table 2.18.

From these results it can be seen that 100 µL 2.7% H_2O_2 was still the best volume to use at pH 5.0. These results also seem to indicate that the DAB/oxidation reaction is more stable up to around 1900 seconds compared with the ABTS/oxidation reaction which shows some sign of absorbance decrease at around 1900 seconds.

Overall, the cuvette-based solution trials yield the following as optimal for development of colour in the DAB/hemoglobin system; pH 5.0 and 0.96 g/L of DAB per 1 mL of H_2O_2 which was calculated from the optimal 100 µL H_2O_2 volume (full calculation of which is included in Appendix 2.4). These optimised results can be favourably compared (excluding the choice of pH) with the *ESR:Forensic* method of Lavis (1994) which uses 0.995 g/L of DAB per 1 mL of H_2O_2 and a pH of 7.4.

2.5 *Use of ABTS and DAB on blood fingerprints*

2.5.1 Methodology

General procedure

All blood fingerprints (previously laid down on paper, glass microscope slides or ceramic tiling) were firstly fixed with 5-sulfosalicylic acid (3 minute soak in 20 g/L

of aqueous 5-sulfosalicylic acid). This is the method of fixing a blood fingerprint currently recommended by the New Zealand Crown Research Institute, *ESR:Forensic* (Lavis, 1994). The prints were then rinsed in distilled water before being treated with either ABTS or DAB. Prints treated with ABTS were immersed for 5 minutes in 10 mL of ABTS solution (5 g/L in buffer at pH 5.4) to which had been added 200 μL of freshly prepared 2.7% H_2O_2. These were the conditions used unless otherwise stated and were the same proportions of reagents as determined from the optimisation of pH and H_2O_2 concentrations in solution. A number of variations on these conditions were trialed in order to test whether they were still optimal for development of blood prints on surfaces. This is because of a second factor which might be important on surfaces which is the ability of the oxidised chromophore to remain associated with the print (rather than be dissolved back in to the solution).

A preliminary investigation found that DAB treatment of blood fingerprints at the optimised pH of 5.0 was visually non-distinguishable in colour development from treatment at pH 7.4. A possible reason for this could be that, although oxidation occurs more readily at pH 5.0, the solubility of the oxidised product is higher, so the overall effect remains the same. It was therefore decided that the *ESR:Forensic* DAB method (Lavis, 1994) rather than the optimised DAB method from section 2.4.2 should be used for comparison with the optimised ABTS method.

Prints treated with DAB were immersed in 100 mL of DAB solution (1 g/L in buffer at pH 7.4) and 500 μL 27% H_2O_2 for 5 minutes. This is the method currently recommended by the *ESR:Forensic* (Lavis, 1994). Both ABTS and DAB treatments were then followed by a further rinse in distilled water. The following trials were carried out:

Treatment on porous surfaces

Blood fingerprints were deposited onto unused photocopy paper and each print was cut bilaterally down the centre of the print, so that a comparison could be made between treatment methods by treating the two corresponding halves differently.

1. *Treatment compared with no treatment.* One half of a print was treated with ABTS while the other half was left untreated.
2. *Varying H_2O_2 concentrations.* Four prints were used to compare treatment between 20 µL and 200 µL 2.7% H_2O_2. Another four prints were used to compare treatment between 200 µL (2.7%) and 200 µL (27%) H_2O_2.
3. *Varying ABTS concentrations.* Four prints were used to compare treatment between 2.5 g/L and 5 g/L ABTS solution. Another four prints were used to compare treatment between 5 g/L and 10 g/L ABTS solution.
4. *Varying soaking times in ABTS solution.* One print was used to compare a 2.5 minute treatment with a 5 minute treatment in ABTS solution. Another print was used to compare a 5 minute treatment with a 10 minute treatment in ABTS solution. A third print was used to compare a 5 minute treatment with a 30 minute treatment in ABTS solution.
5. *Varying fixative times.* Four prints were used to compare fixative treatment at 3 minute and 6 minute soaking times.
6. *Comparison of ABTS method at pH 5.4 and pH 7.4.* Sixteen prints were used to compare ABTS treatment at pH 5.4 and pH 7.4, using citric acid/phosphate and phosphate buffers, respectively.
7. *Comparison of ABTS with DAB.* Fifty prints were used to compare ABTS treatment with DAB treatment.
8. *Compatibility of ABTS with DAB.* Ten prints were used to compare the development obtained by using a mixture of ABTS and DAB with that obtained by using ABTS alone. 100 mL of ABTS solution (5 g/L) and 100 mL of DAB (1 g/L) solution both prepared in buffer pH 5.4 with 500 µL of added H_2O_2 (27%) was used for the mixture. A further seven prints were used to compare the development obtained by treatment with DAB followed by subsequent ABTS treatment, with DAB treatment alone. Four more prints were used to compare ABTS treatment followed by DAB treatment, with DAB treatment alone.
9. *Compatibility of ABTS with ninhydrin.* Two strips of paper each containing a latent fingerprint and a blood fingerprint were used to see if ABTS treatment could be followed by ninhydrin treatment and if ninhydrin treatment could be followed by ABTS treatment.
10. *Heat treatment.* In one literature reference (Takayanagi and Yashiro, 1984), incubation temperatures between room temperature and 50°C were tested on the ABTS oxidation reaction. The ABTS oxidation reaction produced greater absorbances at higher temperatures but was more unstable. It was therefore decided that ABTS treatment at 50°C should be compared to treatment at room temperature. The ABTS treatment at 50°C involved pre-warming the solution (apart from the 200 µL of 2.7% H_2O_2) by placing it in a laboratory oven at 50°C for 20 minutes. The halves of four blood fingerprints (previously fixed with 5-sulfosalicylic acid) were immersed in the heated solution (now containing 200 µL 2.7% H_2O_2 also) for 5 minutes in the oven. The other four corresponding blood fingerprint halves were treated with ABTS solution at room temperature in the usual way.

11. *Cold treatment.* Because the ABTS solution is stored in the fridge it was decided that the effectiveness of the ABTS solution at 12°C (approximate temperature of solution after it has been taken out of the fridge and been prepared for use) should be compared with the effectiveness of the solution after it has been allowed to warm up to 20°C (room temperature). The halves of four blood fingerprints (previously fixed with 5-sulfosalicylic acid) were immersed in the 12°C solution with 200 µL 2.7% H_2O_2 for 5 minutes. The other four corresponding blood fingerprint halves were treated with ABTS solution at 20°C for 5 minutes.

Treatment on non-porous surfaces

1. *Glass.* Four prints were placed onto glass microscope slides and subsequently fixed with 5-sulfosalicylic acid before being treated with ABTS. Another print was placed over two slides set side by side so that two halves of the same print could be obtained. The print was used to compare ABTS treatment with DAB treatment.
2. *Ceramic tile.* Twelve prints were placed on a white ceramic bathroom tile and subsequently fixed with 5-sulfosalicylic acid before being treated with ABTS.

2.5.2 Results

Treatment on porous surfaces

The following results were obtained in trials examining ABTS development of blood fingerprints on paper.

1. *Treatment compared with no treatment.* Treatment of a blood fingerprint with ABTS results in a much better bright green print with good ridge definition. An example of this is presented in Fig. 2.19 a and Fig. 2.19 b.
2. *Varying H_2O_2 concentrations.* The optimised ratio of H_2O_2 to ABTS from the cuvette trials translated to 200 µL of 27% H_2O_2 in these trials. However, on the print, treatment with ten times less H_2O_2 (200 µL 2.7%) resulted in equivalent development to 200 µL of 27% H_2O_2. Treatment with one hundred times less H_2O_2 (20 µL 2.7%) resulted in undeveloped patches compared with 200 µL (2.7%) treatment, which produced a distinctly stronger colour, better enhancement and with more ridge detail visible.
3. *Varying ABTS concentrations.* Treatment using ABTS at a concentration of 2.5 g/L resulted in prints which were lighter in colour than those obtained from ABTS at a 5 g/L concentration. However, further increasing the ABTS concentration to 10 g/L resulted in more background-staining with less distinct ridge-detail compared with the 5 g/L solution.

4. *Varying soaking times in ABTS.* There was no significant difference in the development obtained by treatment at 2.5, 5 and 10 minutes. The 30 minute treatment however, resulted in greater background-staining with less distinct-ridge detail.
5. *Varying fixative times.* There was no detectable difference in the final development for the fingerprint halves fixed with 5-sulfosalicylic acid for 3 or 6 minutes prior to ABTS treatment.
6. *Comparison of ABTS treatment at pH 5.4 and pH 7.4.* Treatment at pH 7.4 resulted in a grey development colour compared with treatment at pH 5.4 which resulted in the usual bright green development colour expected. The treatment at pH 5.4 resulted in slightly more background-staining but this actually proved to be an advantage in helping to better define the ridge-detail (there seemed to be more shades of colour). An example of this is presented in Fig. 2.19 c.
7. *Comparison of ABTS with DAB.* Nine ABTS-treated fingerprint halves were better developed than their corresponding DAB treated halves (Fig. 2.20 a.), nine ABTS-treated halves were of poorer development (Fig. 2.20 b.) and thirty two ABTS-treated halves were of equivalent development, or were indistinguishable (Fig. 2.20 c.). Overall, ABTS gives equivalent performance to DAB for prints on paper (but with the resulting colour being bright green) with the added advantage of being a non-toxic option. It should be noted that the preparation of the ABTS stock solution is easier than preparation of the DAB stock solution, because ABTS is very soluble in water compared with DAB. It was necessary to use an ultra-sonic bath in order to help dissolve the DAB.
8. *Compatibility of ABTS with DAB.* For the prints treated with a mixture of ABTS and DAB the development was the same as for those treated with DAB alone. The bright green colour of the ABTS solution totally disappeared after the DAB solution was added to it, indicating that the DAB was "masking" or deactivating the ABTS in some way. This effect may be because DAB is a stronger reducing agent than ABTS. It is conceivable that oxidation of DAB causes reduction of ABTS when the two are in close proximity. The prints treated with DAB followed by ABTS treatment were indistinguishable from the prints treated with DAB alone. In fact the bright green colour of the ABTS solution slowly disappeared after placing the DAB treated prints into the ABTS solution for 5 minutes. The prints treated with ABTS first, followed by DAB treatment resulted in the same development as the prints treated with DAB alone. The bright green colour of the ABTS treated prints slowly faded to a light grey colour before changing to the dark brown colour consistent with DAB treatment.
9. *Compatibility of ABTS with ninhydrin.* The fingerprint exhibit treated with ABTS first followed by ninhydrin resulted in only the blood fingerprint developing. The latent fingerprint did not develop at all. The other fingerprint exhibit initially resulted in purple development of the latent fingerprint after the ninhydrin treatment (the blood print became grey in colour with better visibility) followed by subsequent green development of the

blood fingerprint after ABTS treatment. The ninhydrin-developed latent print however, disappeared on immersion in the fixative solution.

10. *Heat Treatment.* There was no visible difference between ABTS treatment at 50°C and ABTS treatment at room temperature, and therefore no obvious advantage in heating.
11. *Cold treatment.* There was no visible difference between ABTS treatment at 12°C and ABTS treatment at 20°C. Therefore, it is not necessary to warm the ABTS solution to room temperature before use.

Treatment on non-porous surfaces

1. *Glass.* On this surface, reasonably good visual enhancement of blood fingerprints was obtained, with no background staining. It was necessary to hold the slide at the correct angle to the source of light for good visualisation, due to reflection from the surface. The DAB-treated half-fingerprint on glass was better developed and was easier to see on the glass than the ABTS-treated half. Reflection of light from the glass surface seems to cause more of a problem in visualising the ABTS-treated prints than those treated with DAB. Visualisation under UV light (254 nm and 366 nm) did not improve the print resolution.

On ceramic tile. On this surface, reasonable enhancement was obtained using ABTS, but this was not as good as on glass and certainly not as good as that achieved on paper.

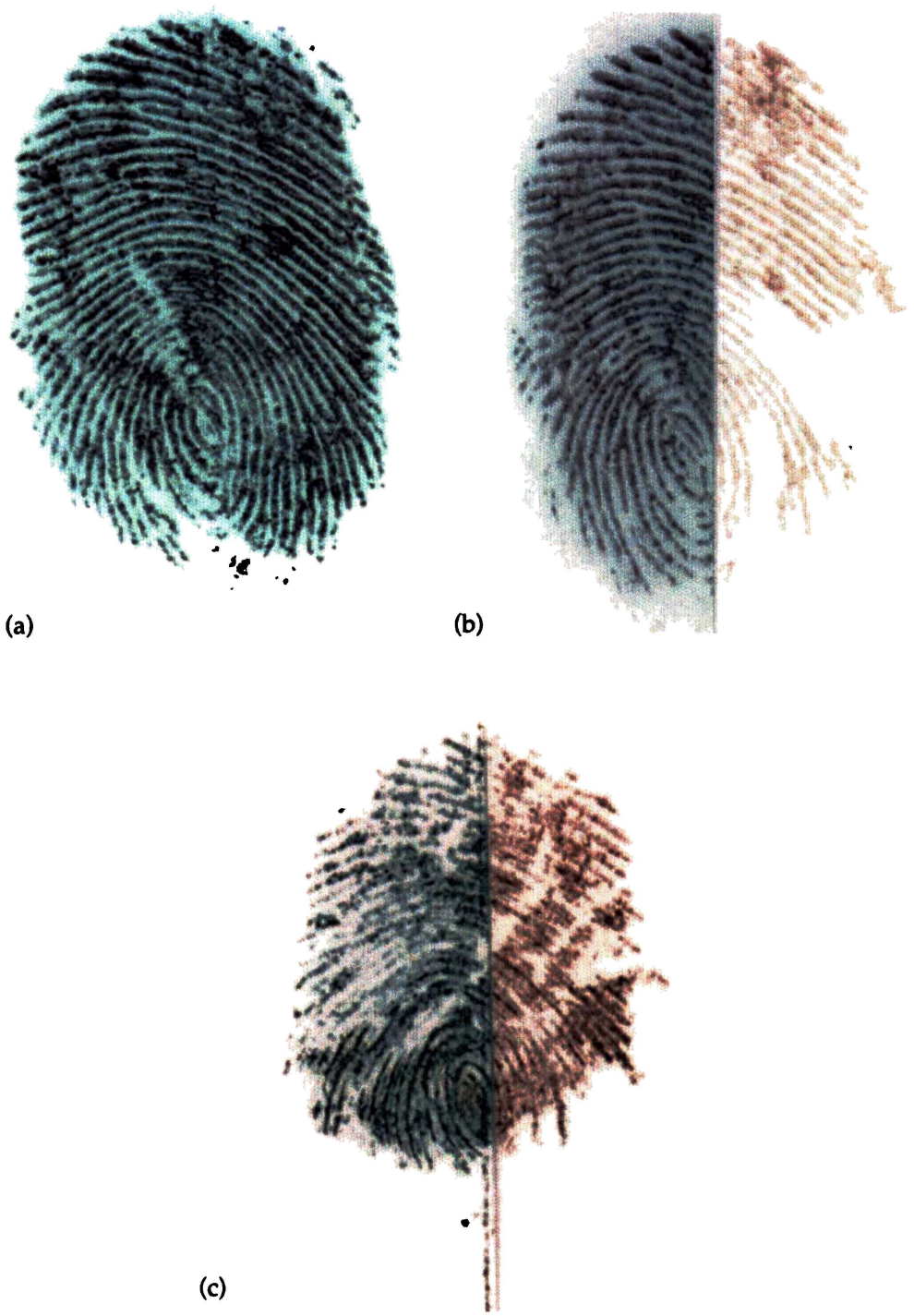

Fig. 2.19
(a) ABTS treatment, (b) ABTS treatment compared with no treatment, and (c) ABTS treatment at pH 5.4 (left) compared with treatment at pH 7.4 (right).

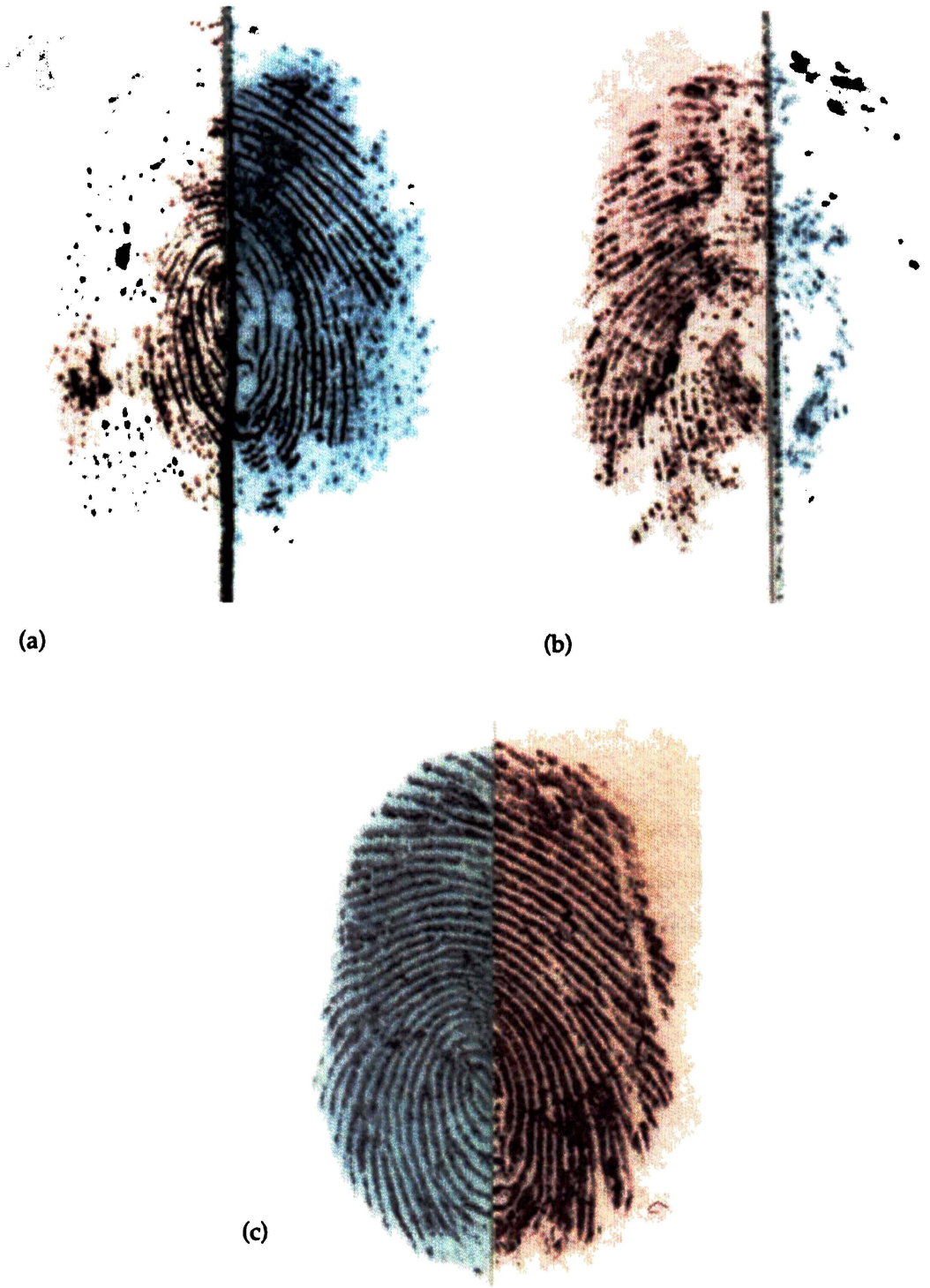

Fig. 2.20
ABTS treatment compared with DAB treatment. (a) ABTS treatment is better than DAB treatment, (b) DAB treatment is better than ABTS treatment, and (c) ABTS and DAB treatment are equivalent.

2.6 *Sensitivity of ABTS compared with DAB*

2.6.1 Methodology

Spot tests on filter paper

The procedure for the determination of ABTS sensitivity was based on the procedure used by Garner et al. (1976). A sample of the author's blood was diluted serially in isotonic saline. The following dilutions were prepared: $1x10^{-1}$, $1x10^{-2}$, $1x10^{-3}$, $1x10^{-4}$, $1x10^{-5}$, $1x10^{-6}$. A 10 µL aliquot of each dilution was placed onto a separate strip of filter paper and left to dry. This procedure was repeated twice so that there were three sets of filter paper strips each with the same series of dried, diluted blood spots. Three ABTS solutions were then prepared (in distilled water) with the following concentrations: 0.1 *M*, 0.05 *M* and 0.025 *M*. A drop of the 0.1 *M* solution was placed onto the blood spots on each strip of filter paper of the first set of filter paper strips followed by a drop of 2.7% of H_2O_2. The 0.05 and 0.025 *M* solutions were then placed onto the second two sets of filter paper strips respectively followed by 2.7% of H_2O_2. A control was also used with just ABTS and H_2O_2 on filter paper with no blood spots.

A positive result test (denoted by the symbol +) was assigned when the green spot produced on reaction with the blood migrated out across the paper but left a darker green spot in the centre. A negative result (denoted by the symbol –) was assigned when the colour of the green spot was no darker than that obtained from a control.

The whole procedure was then repeated but using 0.1 *M*, 0.05 *M* and 0.025 *M* DAB solutions in place of ABTS.

Microplate well tests

The procedure used for the spot tests above was repeated again for ABTS and DAB but instead of using filter paper, spot tests were carried out at the bottom of plastic microplate wells with a negative being assigned for wells producing the same result as a control (based visually on colour). The following dilutions were prepared: $1x10^{-1}$, $1x10^{-2}$, $1x10^{-3}$, $1x10^{-4}$, $1x10^{-5}$, $1x10^{-6}$. A 10 µL aliquot of each dilution was then placed into the individual wells of the first row of the microplate. This was then repeated for the second and third rows. The three ABTS or DAB

solutions were then prepared (in distilled water) with the following concentrations: 0.1 *M*, 0.05 *M* and 0.025 *M*. A drop of the 0.1 *M* solution was placed into each well of the first row of the microplate followed by a drop of 2.7% of H_2O_2. The 0.05 and 0.025 *M* solutions were then placed into the wells of rows 2 and 3 respectively of the microplate followed by 2.7% of H_2O_2.

A positive test (denoted by the symbol +) was determined by colour comparison with a control well containing only ABTS or DAB solution and H_2O_2. A negative test (denoted by the symbol –) was assigned when the colour in the test well was the same as that in the control well.

2.6.2 Results

Spot tests on filter paper

Results for ABTS and DAB spot tests on filter paper are presented in Tables 2.20 and 2.21 respectively.

Table 2.20
Determination of the sensitivity of ABTS using spot tests on filter paper.

ABTS concentrations	Blood dilution series $1x10^{-1}$	$1x10^{-2}$	$1x10^{-3}$	$1x10^{-4}$	$1x10^{-5}$	$1x10^{-6}$
0.1 *M*	+	+	+	–	–	–
0.05 *M*	+	+	+	–	–	–
0.025 *M*	+	+	+	–	–	–

Table 2.21
Determination of the sensitivity of DAB using spot tests on filter paper.

DAB concentrations	Blood dilution series $1x10^{-1}$	$1x10^{-2}$	$1x10^{-3}$	$1x10^{-4}$	$1x10^{-5}$	$1x10^{-6}$
0.1 *M*	+	+	+	+	–	–
0.05 *M*	+	+	+	–	–	–
0.025 *M*	+	+	–	–	–	–

Microplate well tests

Results for microplate well tests on ABTS and DAB are presented in Tables 2.22 and 2.23 respectively.

Table 2.22
Determination of the sensitivity of ABTS using microplate wells.

ABTS concentrations	Blood dilution series $1x10^{-1}$	$1x10^{-2}$	$1x10^{-3}$	$1x10^{-4}$	$1x10^{-5}$	$1x10^{-6}$
0.1 *M*	+	+	+	–	–	–
0.05 *M*	+	+	+	–	–	–
0.025 *M*	+	+	+	–	–	–

Table 2.23
Determination of the sensitivity of DAB using microplate wells.

DAB concentrations	Blood dilution series $1x10^{-1}$	$1x10^{-2}$	$1x10^{-3}$	$1x10^{-4}$	$1x10^{-5}$	$1x10^{-6}$
0.1 *M*	+	+	+	–	–	–
0.05 *M*	+	+	+	–	–	–
0.025 *M*	+	+	+/–	–	–	–

2.6.3 Discussion

These sensitivity results are not very accurate as a positive or negative test is assigned purely on the basis of colour matching with a control by eye (however, it is worth noting that indicative tests for blood using DAB are also reliant on visual inspection). Even the controls became as equally dark as the positives after several hours. All assignments were therefore made within 10 minutes of H_2O_2 addition and a positive test was only assigned if it was darker then the control. The results do indicate however, that ABTS is at least as sensitive as DAB which is confirmed by the work of Yatomi (1981). As well as this Boehringer Mannheim N.Z. Ltd sell a POD Substrate Enhancer which improves peroxidase (POD) detection using ABTS as the substrate by causing a 2– or 3–fold increase of sensitivity and a remarkable faster colour change (Boehringer Mannheim, 1996).

2.7 *Effect of ABTS and DAB treatment on DNA analysis*

Concurrent research by Boyd (1997) in collaboration with Larkin (1997) determined the effect of ABTS and DAB treatment of fixed blood fingerprints on subsequent DNA analysis. Blood fingerprints on porous and non-porous paper, glass slides and clear perspex using unpreserved human blood were used. Both ABTS and DAB treatment resulted in only partial DNA profiles. Boyd's interpretation of these results included the possibility that this could be due to the DNA being degraded as the blood was approximately 4 months old when the DNA was extracted. Boyd alternatively concluded that the result could be a consequence of the chemistry of the catalytic tests and their interaction with the DNA, although the nature of these interactions were said to be unknown. A third reason for the effect on DNA profiles however, could also be due to reaction of the fixative 5-sulfosalicylic acid with the DNA.

2.8 *Price comparison*

2,2′-azino-di-[3-ethylbenzthiazolinesulfonate(6)] diammonium salt (ABTS) can be purchased from Aldrich Chemical Company in 1 g quantities @ NZ$49.56 (1998-99 price listings). Alternatively ABTS diammonium salt can be purchased from Boehringer Mannheim (BM) Laboratories in 2 g quantities @ NZ$33.00 (1996 price listings). 3,3′-diaminobenzidine can be purchased from Aldrich Chemical Company in 25 g quantities @ NZ$231.27. All Aldrich Chemical Company prices are from the Australian 1998-99 price listings (prices converted by Australian/New Zealand exchange rate).

The price per 1 g of ABTS (used to prepare 200 mL of ABTS working solution) when purchased from Boehringer Mannheim (BM) Laboratories in New Zealand will therefore cost NZ$16.50. The price per 0.2 g of DAB (used to prepare 200 mL of DAB working solution) will cost NZ$1.85.

2.9 *Summary*

ABTS is an effective, non-carcinogenic alternative to DAB for development of blood fingerprints, especially on porous surfaces. Prints developed with ABTS are bright green in colour, which should show up more clearly than the dark brown of oxidised DAB on certain surfaces. ABTS is a "nothing-to-lose" reagent, because subsequent DAB treatment after ABTS treatment is as good as DAB treatment by itself. Although ABTS treatment can be used after ninhydrin treatment of any latent prints, ninhydrin treatment cannot be used after ABTS treatment. Research to date seems to indicate that the effect of ABTS or DAB treatment on subsequent DNA analysis is equally detrimental although further research is probably required for confirmation of this. On the negative side however, ABTS treatment is approximately ten times more expensive than DAB treatment but is still relatively cheap in the context of laboratory operations. The structure of ABTS as the diammonium salt has been determined by XRD and confirmed in this work as consisting of two independent halves of two centrosymmetric molecules with the inclusion of two water molecules of hydration. The recommended procedure for ABTS treatment of prints in blood is provided in Chapter 8 (section 8.1).

2.10 *References*

Boehringer Mannheim N.Z. Ltd biochemicals order brochure (1996). 15 Rakino Way, P.O. Box 62-089, Auckland, New Zealand.

Boyd L.A. (1997). *Chemical enhancement of fingerprints; Development and comparison of techniques.* Masters thesis, University of Auckland, Auckland, New Zealand, 105-111.

Bretherick L. (1986). *Hazards in the chemistry laboratory.* 4th edition. The Royal Society of Chemistry, Alden Press, Oxford, 189.

Choudhary G. (1996). Human health perspectives on environmental exposure to diaminobenzidine: a review. *Chemosphere,* **32**(2), 267-291.

Dawson R.M.C., Elliott D.C., Elliott W.H., Jones K.M. (1986). *Data for Biochemical Research.* 3rd edition. Oxford Science Publications, New York.

Garner D.D., Cano K.M., Peimer M.S., and Yeshion M.S. (1976). An evaluation of tetramethyldiaminobenzidine as a presumptive test for blood. *J. Forens. Sci.*, **21**, 816-821.

Holland V.R., Saunders A.L., Rose F.L., Walpole A.L. (1974). A safer substitute for diaminobenzidine in the detection of blood. *Tetrahedron,* **30,** 3299-3302.

Jean W., Leung S.S.F., Lam C.W.K., Ho S.C., Lam T., and Janus E.D. (1997). Plasma total antioxidant capacity in an adult Hong Kong Chinese population. *Clin. Biochem.*, **30**(7), 553-557.

Jones K. (1997). *A Review of blood enhancement techniques.* Report prepared for the New Zealand Police, Royal New Zealand Police College.

Kremer M.L. (1989). The reaction of hemin with H_2O_2. *Eur. J. Biochem.*, **185,** 651-658.

Larkin T. (1997). *Environmental and chemical insults and their effects on short tandem repeat (STR) analysis in a forensic context.* Masters thesis, University of Auckland, Auckland, New Zealand, 105-111.

Lavis A. (1994). *Workshop in advanced fingerprint techniques.* Training manual, prepared for ESR:Forensic, Auckland, New Zealand.

Lück H. (1965). *Methods of enzymatic analysis.* Edited by Hans-Ulrich Bergmeyer. Verlag Chemie, Academic Press, New York, 895-897.

Marklund S. (1978). Determination of plasma or serum hemoglobin by peroxidase activity employing 2,2'-azino-di-(3-ethyl-benzthiazolinsulphonate-6) as chromogen. *Scand. J. Clin. Lab. Invest.*, **38,** 543-547.

Miller E.C., Miller J.A., Hartman H.A. (1966). *N*-Hydroxy-2-acetylaminofluorene: A metabolite of 2-acetylaminofluorene with increased carcinogenic activity in the rat. *Cancer Res,* **21,** 815-824.

Olsen R.D. (1985). Sensitivity comparison of blood enhancement techniques. *Identification, News,* (August 1985) 10-14.

Rey H.G., Wielinger H., Rieckmann P. (1970). *Colorimetric determination of hydroperoxides.* Boehringer Mannheim G.m.b.H. German, 5 pp (patent), DE 1648840 700212, DE 671014.

Saferstein R.. (1988). *Forensic Science Handbook.* Prentice-Hall, Englewood Cliffs, N.J., 272-276.

Searle C.E. (1970). Chemical carcinogens and their significance for chemists. *Chem Br,* **6,** 5-10.

Stryer L. (1988). *Biochemistry.* 3rd edition.. W.H. Freeman and Company, New York. 143-148 and 422.

Takayanagi M., Yashiro T. (1984). Colorimetry of Hemoglobin in Plasma with 2,2'-Azino-di-(3-ethylbenzthiazoline-6-sulphonic acid) (ABTS). *Clin Chem,* **30**(3), 357-359.

Traylor T.G., and Xu F. (1990). Mechanisms of reactions of iron(III) porphyrins with hydrogen peroxide and hydroperoxides: Solvent and solvent isotope effects. *J. Am. Chem. Soc.*, **112,** 178-186.

Uno T., Takeda A., and Shimabayashi S. (1995). Effects of imadazoles and pH on the peroxidase activity of the hemin - hydrogen peroxide system. *Inorg. Chem.*, **34,** 1599-1607.

Yatomi, H. (1981). Test reagents for preliminary screening of blood stains. *Nichidai Igaku Zasshi,* **40**(8), 839-852.

Mousty C., Therias S., Aboab B., Molinie P., Queignec M., Leone P., Rossignol C., and Palvadeau P. (1997). Single crystal structure refinement and physical characterization of the 2,2'-azinobis(3-ethylbenzothiazoline-6-sulfonate)diammonium salt (ABTS). *New J. Chem.*, **21,** 1321-1330.

Chapter Three

Two new methods for the enhancement of blood fingerprints using *o*-, and *p*-phenylenediamine

3.1 *Introduction*

Ortho-phenylenediamine (OPD) and *para*-phenylenediamine (PPD) have been previously used as chromogens for the determination of plasma or serum hemoglobin. Both OPD and PPD undergo oxidation to a coloured form (orange and purple respectively) in the presence of H_2O_2 and hemoglobin. The coloured, oxidized derivative of PPD is thought to be a molecule formed from diamine and diimine (Lück, 1965).

Antigen-antibody associations occurring in a porous silica gel were optically detected via the reaction of peroxidase conjugate with OPD leading to the formation of a yellow colouration (Roux et al., 1997). A unique sandwich ELISA for the determination of ABH antigens in bloodstains was also developed using OPD (Kazuo et al., 1996). PPD has been used in the identification of ceruloplasmin in blood serum (Battistini, 1967). OPD was also used in the detection of seminal stains by sandwich ELISA which involved the use of a horseradish peroxidase-labelled antibody (Tyouichi, 1984).

OPD has also been used in the determination of hemoglobin in plasma and serum, where linear-sweep polarography rather than spectrophotometric methods have been used (Jun Feng et al., 1997).

OPD and PPD are both considered to be toxic by inhalation (may cause bronchial asthma), in contact with skin (may cause dermatitis; the skin becomes blackened), and if swallowed and may cause sensitisation by skin contact (Bretherick, 1986). The hazards however, seem to be somewhat less than those associated with 3,3'-

diaminobenzidine (DAB). For example OPD has been referred to as a less toxic aromatic by Donlon et al., 1997. Also, PPD was found to be only weakly mutagenic to Ames Salmonella strain TA98 with metabolic activation but was found to be non-mutagenic to the TA100 strain. However, PPD was found to induce a dose-related increase in chromosomal aberrations in Chinese hamster ovary cells (Chung et al., 1995).

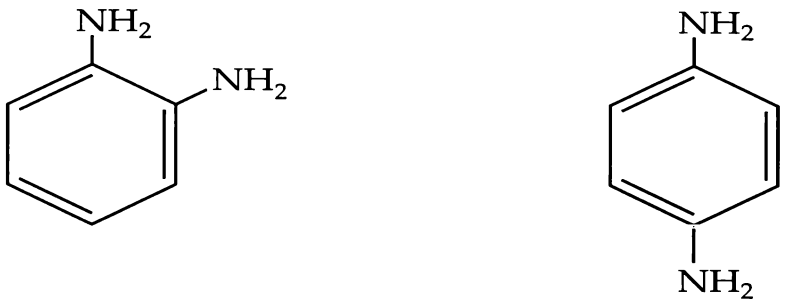

OPD **PPD**

Fig. 3.1
Ortho-phenylenediamine (OPD) and *para*-phenylenediamine (PPD).

3.2 *Materials and instrumentation*

Chemicals used in this research were purchased from the following sources:

- *o*- and *p*-phenylenediamine (flakes) and $Na_2HPO_4.12H_2O$ (AR) from BDH Laboratory Chemicals.
- 3,3′ diaminobenzidine from Aldrich Chemical Company.
- 5-sulfo-salicylic acid and $NaH_2PO_4.2H_2O$ from M&B Laboratory Chemicals.
- Citric acid monohydrate was supplied by Ajax Chemicals (Univar).

Other materials used in this research were obtained from the following sources:

- Blood was collected from the author's arm and diluted by a ratio of 1:500 using the same procedure as described previously in section 2.2.
- Paper (A4, 80gsm) was obtained from Copyright (Australian paper, Ltd.) and glass slides from Marienfeld.

The following instrumentation was used in this research:

- A Varian Cary 1 UV-Visible Spectrophotometer (SBW = 0.2 nm, signal averaging time = 0.100 sec) was used for solution trials.
- A Meterlab™ pH meter (model PHM240) was used for confirming the pH values of buffer solutions.

3.3 *Methodology*

3.3.1 Optimisation of pH and H_2O_2 concentrations

The optimal pH and H_2O_2 concentrations favouring best colour development of OPD or PPD in a solution containing small amounts of blood in a 10 mm quartz cuvette were firstly determined by UV/Vis spectroscopy on a Varian Cary 1 UV-Visible Spectrophotometer (SBW = 0.2 nm, Signal averaging time = 0.100 sec) by monitoring the change in absorbance with time at the peak maximum determined for OPD or PPD.

All solutions prepared contained 500 µL of OPD or PPD stock solution (50 mg OPD or PPD made up to 100 mL in distilled water), 750 µL of the 1:500 blood solution (discussed in the materials section above), a specified volume of 2.7% H_2O_2, and a sufficient volume of buffer solution to give a final volume of 12.2 mL. Changes in the absorbance of these solutions with time at 434 nm for OPD and 404 nm for PPD were then determined on the UV/Vis spectrophotometer against a blank containing 750 µL of the 1:500 diluted blood solution, the same volume of 2.7% H_2O_2 as in the sample, and a sufficient volume of buffer solution to give a final volume of 12.2 mL. The H_2O_2 was always added last, with the time of the subsequent reaction being recorded from that point. Establishment of the absorbance maximums for OPD and PPD were carried out using sample and blank solutions containing 50 µL of 2.7% H_2O_2 and buffer pH 5.4.

Experiments to determine the optimal concentration of H_2O_2 for OPD and PPD were carried out at a pH value of 5.4 (citric acid/phosphate buffer). A pH of 5.4 was chosen

initially as it had resulted in optimal colour development for ABTS in Chapter 2, and so seemed an appropriate pH to start with. Volumes of H_2O_2 added were varied from 10 to 500 µL for OPD and 10 to 1000 µL for PPD. Experiments to determine the optimal pH for OPD and PPD were then performed using a set volume of 50 µL 2.7% H_2O_2 and varying the pH from 4.4 to 7.4 (phosphate and citric acid/phosphate buffers). Buffers were prepared according to the directions presented in Table 2.1 in Chapter 2.

3.3.2 Fingerprint trials

General procedure

In order to assess the potential of OPD and PPD as alternatives to DAB for the enhancement of fingerprints in blood a comparison trial with DAB was carried out on blood fingerprints. Various other trials were also carried out to determine whether the optimised pH and H_2O_2 concentration conditions from the cuvette solution trials still applied on blood fingerprints.

All blood fingerprints (previously laid down on paper or glass microscope slides) were firstly fixed with 5-sulfosalicylic acid (3 minute soak in 20 g/L of 5-sulfosalicylic acid). The prints were then rinsed in distilled water before being treated with either OPD, PPD or DAB. Prints treated with OPD or PPD solutions were immersed for 5 minutes in 50 mL of either solution (0.5 g/L OPD or PPD in citric acid/phosphate buffer at pH 5.4) to which had been added 1 mL of 27% H_2O_2. These were the conditions used unless otherwise stated and were the conditions determined from the optimisation of pH and H_2O_2 concentrations in solution.* A number of variations on these conditions were trialed in order to test whether they were still optimal for development of blood prints on surfaces. Prints treated with DAB were immersed in 100 mL of DAB solution (1 g/L in buffer at pH 7.4) and 0.5 mL 27% H_2O_2 for 5 minutes. This is the method currently used by *ESR:Forensic* in New Zealand (Lavis, 1994). OPD, PPD and DAB treatments were then followed by a further rinse in distilled water.

---

* The optimised H_2O_2 volume determined for OPD however, was actually 0.5 mL at a pH of 5.4 but was changed to 1 mL after this larger volume was found to be better on blood fingerprints as opposed to in solution.

Treatment on porous surfaces

Blood fingerprints were deposited onto unused paper and each print was cut bilaterally down the centre of the print so that a comparison could be made between treatment methods by treating the two corresponding halves differently.

1. *Varying H_2O_2 concentrations:* Four prints were used to compare OPD treatment using either 50 µL or 100 µL 27% H_2O_2. Another four prints were used to compare OPD treatment using either 100 µL or 500 µL 27% H_2O_2. Four more prints were used to compare OPD treatment using either 500 µL or 1000 µL 27% H_2O_2. A further four prints were used to compare treatment using either 1000 µL or 1500 µL 27% H_2O_2. Four prints were then used to compare PPD treatment using either 0.2 mL or 1 mL 27% H_2O_2. Another four prints were used to compare PPD treatment using either 1 mL or 2 mL 27% H_2O_2.
2. *Treatment compared with no treatment:* One half of a print was treated with OPD while the other half was left untreated. The procedure was repeated using PPD.
3. *Varying OPD and PPD concentrations:* Four prints were used to compare treatment between 0.25 g/L and 0.5 g/L OPD solution. Another four prints were used to compare treatment between 0.5 g/L and 1 g/L OPD solution. The procedure was repeated using PPD.
4. *Varying soaking times in OPD or PPD:* One print was used to compare a 2.5 minute treatment with a 5 minute treatment in OPD solution. Another print was used to compare a 5 minute treatment with a 10 minute treatment in OPD solution. A third print was used to compare a 5 minute treatment with a 30 minute treatment in OPD solution. The procedure was repeated using PPD.
5. *Comparison of OPD and PPD methods at pH 5.4 and pH 7.4:* Sixteen prints were used to compare OPD treatment at pH 5.4 and pH 7.4, using citric acid/phosphate and phosphate buffers, respectively. The procedure was repeated using PPD.
6. *Comparison of OPD and PPD with DAB:* Fifty prints were used to compare OPD treatment with DAB treatment. The procedure was repeated using PPD.
7. *Compatibility of OPD and PPD with DAB:* One print was used to compare the development obtained by treatment with DAB followed by subsequent OPD treatment with DAB treatment alone. Another print was used to compare OPD treatment followed by DAB treatment with OPD treatment alone. The procedure was repeated using PPD.
8. *Compatibility of OPD and PPD with Ninhydrin:* Two strips of paper each containing a latent fingerprint and a blood fingerprint were used to see if OPD treatment could be followed by Ninhydrin treatment and if Ninhydrin treatment could be followed by OPD treatment. The procedure was repeated using PPD.

9. *Comparison of old PPD solution (prepared 48 hours earlier) with new PPD solution (prepared half hour earlier):* Four prints were used to compare the effectiveness of a 48 hour old PPD solution (dark purple) with a half hour old PPD solution (faint lilac colour).

Treatment on non-porous surfaces

Two glass microscope slides each with a fixed blood print were treated with OPD at pH 5.4 and pH 7.4. Two more glass microscope slides each with a fixed blood print were then treated with PPD at pH 5.4.

3.4 *Results*

3.4.1 Optimisation of pH and H_2O_2 concentration for OPD

Results for the establishment of the absorbance maximum for OPD (undergoing oxidation) in a citric acid/phosphate buffer (pH 5.4) with 50 µL 2.7% H_2O_2 added are presented in Table 3.1. An absorbance maximum of 434 nm was chosen as an appropriate wavelength for all subsequent analyses of OPD.

Table 3.1
Change in the absorbance and wavelength maximum with time for the oxidation of OPD in the presence of hemoglobin.

Wavelength (nm)	Absorbance	Time (mins)
408.19	0.153	3
434.39	0.760	10
434.39	1.053	16
435.19	1.210	21
432.59	1.615	115

Determination of optimal H_2O_2 concentration

Experiments to determine the optimal concentration of H_2O_2 were carried out at a pH value of 5.4 (citric acid/phosphate buffer). Volumes of 2.7% H_2O_2 added were varied from 10 to 500 µL. Results are presented in Table 3.2 and Fig. 3.2.

Table 3.2
Effect of hydrogen peroxide volume on colour development of OPD (measured by absorbance at λ = 434 nm) at pH 5.4.

Volume of 2.7% H_2O_2 added							
10 µL		50 µL		100 µL		500 µL	
Time (s)	Abs.	Time (s)	Abs.	Time (s)	Abs.	Time (s)	Abs.
120	0.02	120	0.08	120	0.11	120	0.28
180	0.06	180	0.18	180	0.18	180	0.42
300	0.16	300	0.40	300	0.31	300	0.61
420	0.26	420	0.62	420	0.43	420	0.69
540	0.35	540	0.80	540	0.53	540	0.73
660	0.43	660	0.95	660	0.62	660	0.75
780	0.50	780	1.08	780	0.70	780	0.75
900	0.56	900	1.17	900	0.78	900	0.74
1800	0.88	1800	1.55	1800	1.08	1800	0.85
2700	1.02	2700	1.65	2700	1.26	2700	0.86
				6360	1.43		

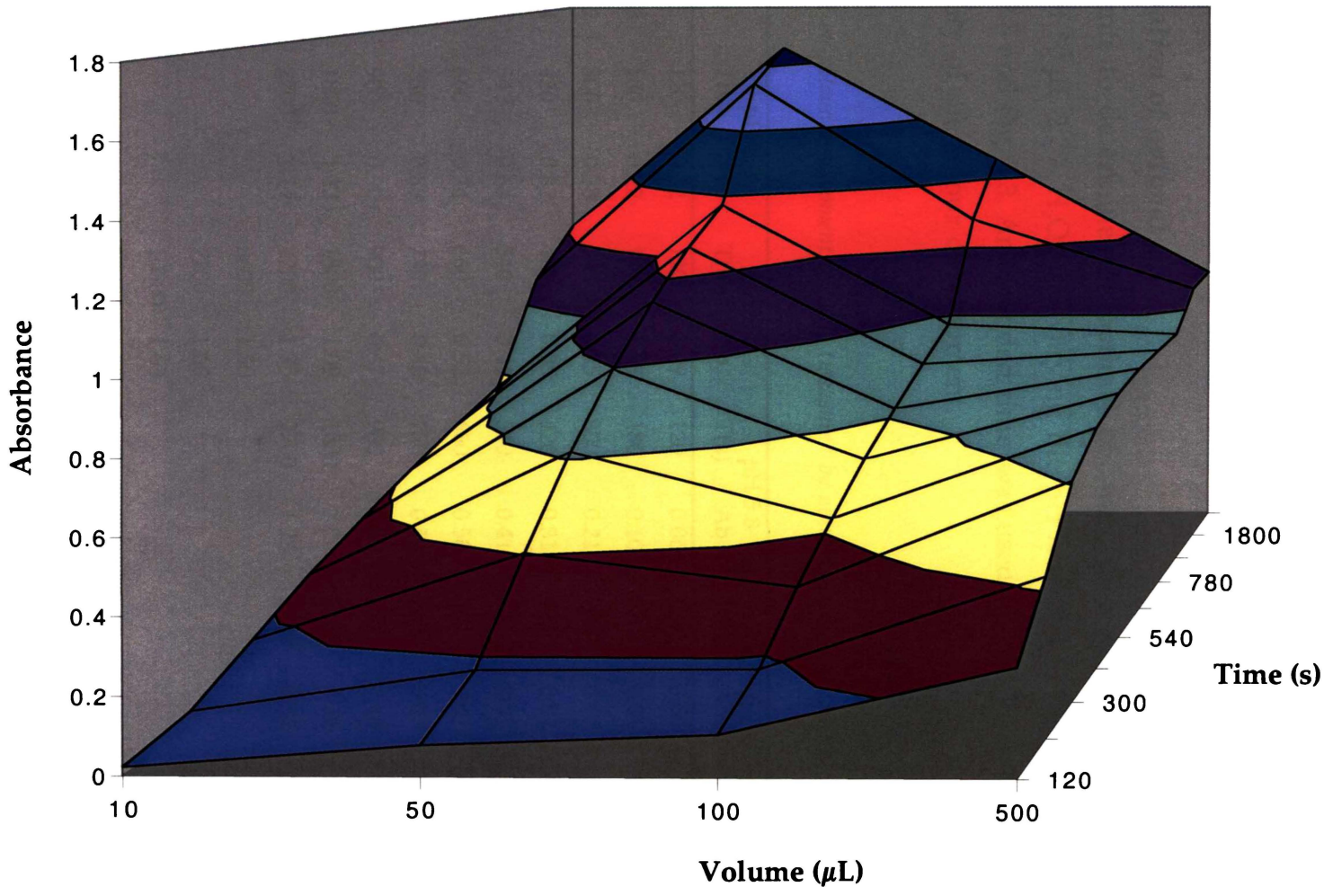

Fig. 3.2
Plot of effect of hydrogen peroxide volume on colour development of OPD (measured by absorbance at λ = 434 nm) at pH 5.4.

NB. Due to limitations with Microsoft Excel, the volume and time axes do not always increase in even increments.

From these results, an optimal absorbance was obtained with use of 50 µL of 2.7% H_2O_2. At higher concentrations of H_2O_2, the rate of colour development is similar at first, but the final absorbance values achieved are not so high. In other words it is apparent that too much H_2O_2 will inhibit colour development in the OPD/hemoglobin reaction, by H_2O_2 causing further oxidation of the OPD (as was observed and discussed for ABTS and DAB in Chapter 2).

Determination of optimal pH

Experiments to determine the optimal pH were then performed using the optimal volume of 50 µL 2.7% H_2O_2 and varying the pH from 4.4 to 7.4. Results are presented in Table 3.3 and Fig. 3.3. An extended time was used for pH 5.4 in order to determine the stability of the colour development.

Table 3.3
Effect of pH on colour development of OPD (measured by absorbance at λ = 434 nm) with 50 µL 2.7% H_2O_2.

pH 4.4		pH 5.0		pH 5.4		pH 5.8		pH 6.8		pH 7.4	
T(s)	Ab.	T(s)	Ab.	T(s)	Ab.	T(s)	Ab.	T(s)	Ab.	T(s)	Ab.
120	0.21	120	0.12	120	0.09	120	0.06	120	0.00	120	0.00
180	0.33	180	0.22	180	0.15	180	0.10	180	0.01	180	0.00
300	0.52	300	0.38	300	0.25	300	0.21	300	0.02	300	0.01
420	0.64	420	0.82	420	0.35	420	0.31	420	0.04	420	0.02
540	0.71	540	0.64	540	0.44	540	0.41	540	0.05	540	0.04
660	0.76	660	0.74	660	0.52	660	0.50	660	0.07	660	0.05
780	0.78	780	0.83	780	0.60	780	0.59	780	0.08	780	0.06
900	0.80	900	0.90	900	0.67	900	0.67	900	0.10	900	0.07
1800	0.82	1800	1.22	1800	1.09	1800	1.06	1800	0.21	1800	0.16
2700	0.83	2700	1.29	2700	1.35	2700	1.23	2700	0.32	2700	0.23
				3600	1.50						
				7200	1.66						
				10800	1.63						
				18000	1.62						
				26100	1.61						
				6 day	1.37						

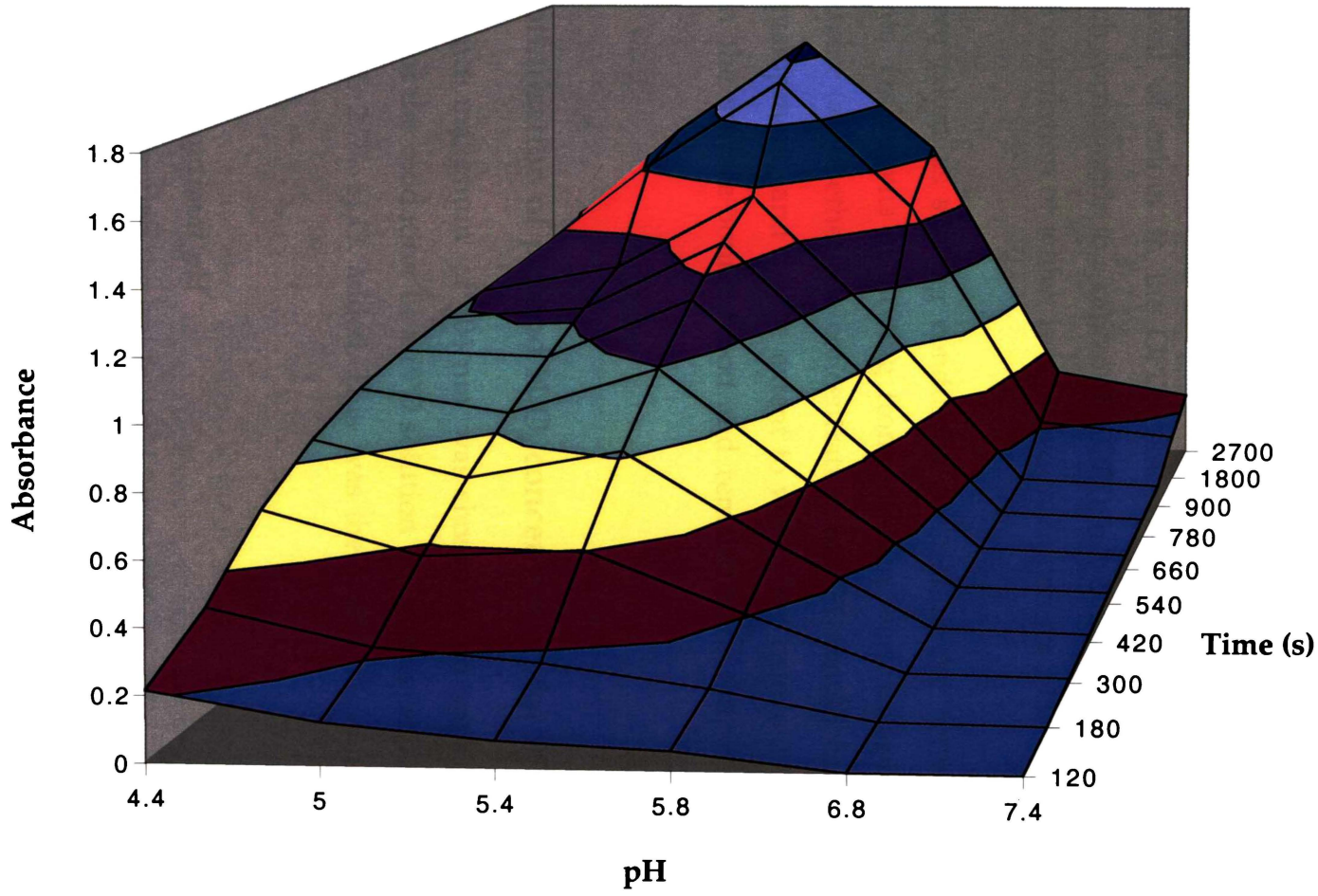

NB. Due to limitations with Microsoft Excel, the pH and time axes do not always increase in even increments.

Fig. 3.3
Plot of effect of pH on colour development of OPD (measured by absorbance at λ = 434 nm) with 50 µL 2.7% hydrogen peroxide.

Absorbance values grew significantly as the pH was lowered, appearing to reach a maximum at about pH 5.4. Raising the pH to 7.4 had the opposite effect, with absorbance values falling for OPD substantially. Thus, in solution, maximum colour development for OPD occurs at pH 5.4. The stability of OPD development in solution at pH 5.4 also seems to be fairly stable considering that only a small decrease in absorbance was observed over a period of six days.

Overall, the cuvette-based solution trials yield the following as optimal for development of colour in the OPD/hemoglobin system: pH 5.4, and 50 µL of 2.7% H_2O_2 which corresponds to a ratio of 1 g OPD to 200 mL of 2.7% H_2O_2 or 20 mL of 27% H_2O_2 (full calculation of which is included in Appendix 3.1).

These were taken as starting conditions for testing the activity of OPD on blood fingerprints. Unknowns in moving from solution work to development of blood on a surface were (a) whether the concentration of OPD would have any effect on final colour development, and (b) the extent to which the oxidised OPD would be able to deposit on the surface-bound blood and remain there (rather than move back into solution).

3.4.2 Optimisation of pH and H_2O_2 concentration for PPD

An absorbance maximum of 404 nm was chosen as an appropriate wavelength for monitoring of the oxidation of a PPD solution in a citric acid/phosphate buffer (pH 5.4) with 50 µL 2.7% H_2O_2 added. This was the wavelength used for all subsequent analyses of PPD.

Determination of optimal pH

Experiments to determine the optimal pH were performed using 50 µL 2.7% H_2O_2 and varying the pH from 4.4 to 7.4. The volume of 50 µL was chosen as a starting point for testing as it had been found to be the optimum H_2O_2 volume for OPD. Results are presented in Table 3.4 and Fig. 3.4.

Table 3.4
Effect of pH on colour development of PPD (λ = 404 nm) with 50 μL 2.7% H_2O_2.

Time (s)	pH of Buffer								
	4.4	5.0	5.4	5.8	6.0	6.6	7.0	7.4	8.0
60	0.161	0.198	0.092	0.178	0.110	0.102	0.119	0.124	0.123
120	0.202	0.246	0.130	0.217	0.134	0.121	0.135	0.131	0.123
180	0.219	0.288	0.166	0.253	0.160	0.139	0.149	0.140	0.127
240	0.228	0.325	0.203	0.292	0.184	0.155	0.162	0.150	0.134
300	0.232	0.354	0.241	0.328	0.206	0.171	0.174	0.159	0.141
360	0.234	0.374	0.275	0.362	0.227	0.184	0.186	0.168	0.148
420	0.234	0.391	0.307	0.390	0.248	0.198	0.198	0.177	0.154
480	0.234	0.406	0.334	0.416	0.266	0.210	0.208	0.185	0.160
540	0.234	0.418	0.357	0.437	0.284	0.222	0.219	0.193	0.167
600	0.233	0.428	0.378	0.454	0.300	0.232	0.229	0.201	0.173
660	0.233	0.436	0.397	0.470	0.315	0.243	0.238	0.207	0.178
720	0.236	0.442	0.414	0.481	0.329	0.252	0.250	0.214	0.184
780	0.237	0.448	0.428	0.491	0.341	0.262	0.254	0.221	0.189
840	0.235	0.453	0.441	0.498	0.353	0.270	0.259	0.227	0.194
900	0.242	0.458	0.453	0.504	0.363	0.279	0.264	0.234	0.199
960	0.241	0.461	0.463	0.508	0.373	0.286	0.269	0.239	0.203
1020	0.251	0.463	0.472	0.512	0.382	0.293	0.275	0.240	0.208
1080	0.250	0.465	0.477	0.515	0.390	0.301	0.281	0.245	0.212
1140	0.256	0.466	0.484	0.516	0.397	0.307	0.283	0.247	0.216
1200	0.263	0.466	0.490	0.518	0.403	0.309	0.285	0.248	0.220
1260	0.266	0.467	0.496	0.519	0.408	0.312	0.302	0.252	0.224
1320	0.275	0.470	0.506	0.519	0.413	0.317	0.307	0.256	0.228
1380	0.280	0.471	0.508	0.519	0.417	0.322	0.317	0.261	0.231
1440	0.281	0.470	0.515	0.519	0.421	0.326	0.320	0.259	0.234
1500	0.281	0.469	0.517	0.519	0.424	0.329	0.321	0.259	0.237
1560	0.282	0.470	0.518	0.519	0.427	0.332	0.324	0.263	0.239
1620	0.282	0.470	0.521	0.518	0.430	0.335	0.327	0.263	0.242
1680	0.283	0.471	0.523	0.518	0.432	0.338	0.323	0.268	0.244
1740	0.283	0.470	0.524	0.518	0.434	0.341	0.326	0.271	0.247
1800	0.283	0.469	0.525	0.517	0.435	0.343	0.325	0.274	0.250

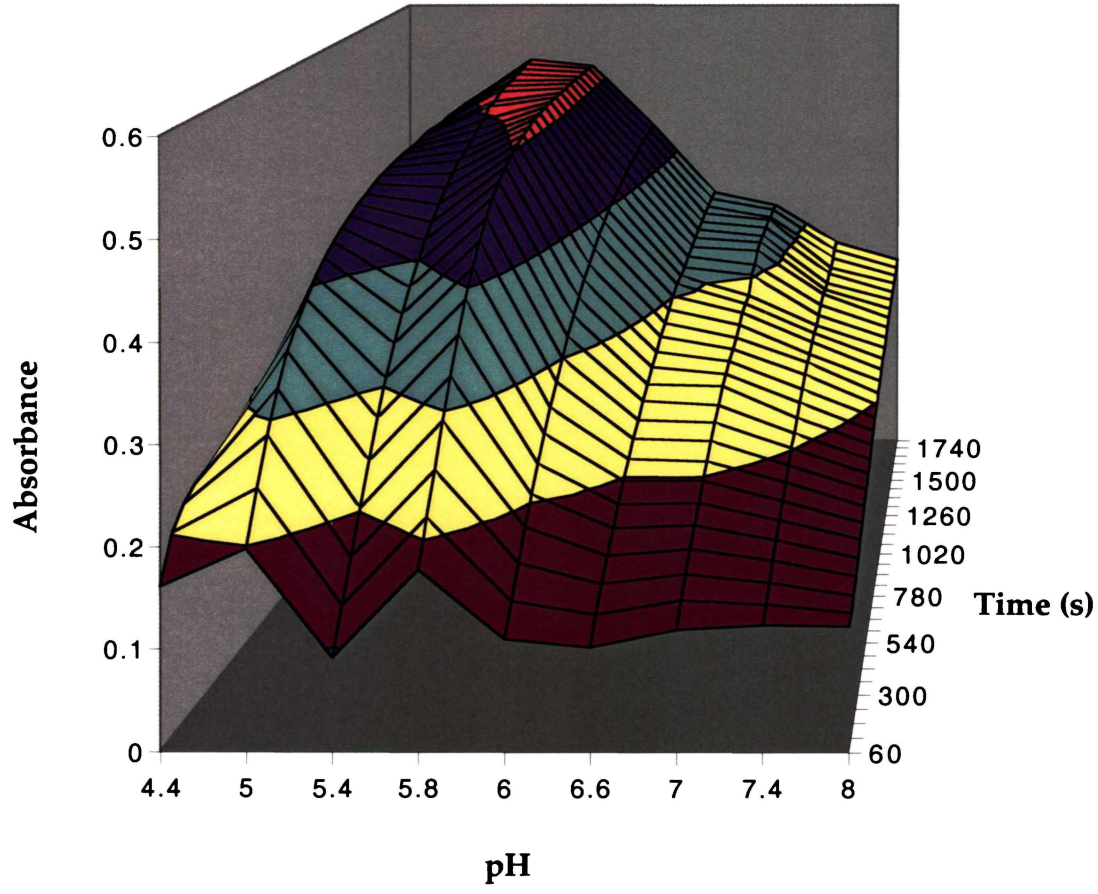

NB. Due to limitations with Microsoft Excel, the pH and time axes do not always increase in even increments.

Fig. 3.4
Plot of effect of pH on colour development of PPD (measured at λ = 404 nm) with 50 µL 2.7% hydrogen peroxide.

Absorbance values grew significantly as the pH was lowered, appearing to reach a maximum at about pH 5.4. Raising the pH to 7.4 had the opposite effect, with absorbance values falling for PPD substantially. Thus, in solution, maximum colour development for PPD occurs at pH 5.4.

Determination of optimal H_2O_2 concentration

Experiments to determine the optimal concentration of H_2O_2 were then carried out at a pH value of 5.4 (citric acid/phosphate buffer). Volumes of H_2O_2 added were varied from 10 to 1000 µL. Results are presented in Table 3.5 and Fig. 3.5.

Table 3.5
Effect of H_2O_2 volumes on colour development of PPD (λ = 404 nm) at pH 5.4.

Time (s)	Volume of 2.7% H_2O_2 added (µL)					
	10	25	50	100	500	1000
60	0.171	0.185	0.169	0.217	0.221	0.197
120	0.209	0.228	0.211	0.270	0.219	0.113
180	0.238	0.267	0.250	0.326	0.215	0.020
240	0.264	0.304	0.291	0.372	0.188	0.000
300	0.286	0.341	0.328	0.401	0.247	0.113
360	0.306	0.372	0.361	0.417	0.304	0.118
420	0.322	0.399	0.386	0.428	0.343	0.162
480	0.336	0.420	0.406	0.433	0.351	0.185
540	0.346	0.436	0.424	0.439	0.421	0.160
600	0.354	0.448	0.438	0.443	0.437	0.171
660	0.359	0.459	0.452	0.451	0.445	0.244
720	0.364	0.466	0.463	0.498	0.455	0.289
780	0.367	0.472	0.473	0.504	0.454	0.321
840	0.369	0.476	0.480	0.506	0.471	0.342
900	0.370	0.477	0.487	0.509	0.473	0.335
960	0.371	0.479	0.492	0.515	0.481	0.356
1020	0.371	0.480	0.493	0.519	0.499	0.337
1080	0.371	0.481	0.497	0.520	0.530	0.328
1140	0.371	0.482	0.500	0.522	0.537	0.332
1200	0.369	0.483	0.494	0.523	0.529	0.319
1260	0.368	0.481	0.498	0.525	0.536	0.367
1320	0.367	0.480	0.500	0.527	0.525	0.349
1380	0.366	0.478	0.505	0.527	0.530	0.402
1440	0.365	0.477	0.514	0.526	0.523	0.414
1500	0.364	0.477	0.514	0.525	0.526	0.406
1560	0.362	0.477	0.515	0.525	0.535	0.391
1620	0.362	0.478	0.516	0.526	0.538	0.417
1680	0.361	0.478	0.515	0.527	0.541	0.404
1740	0.360	0.478	0.516	0.524	0.526	0.405
1800	0.359	0.477	0.515	0.524	0.530	0.424

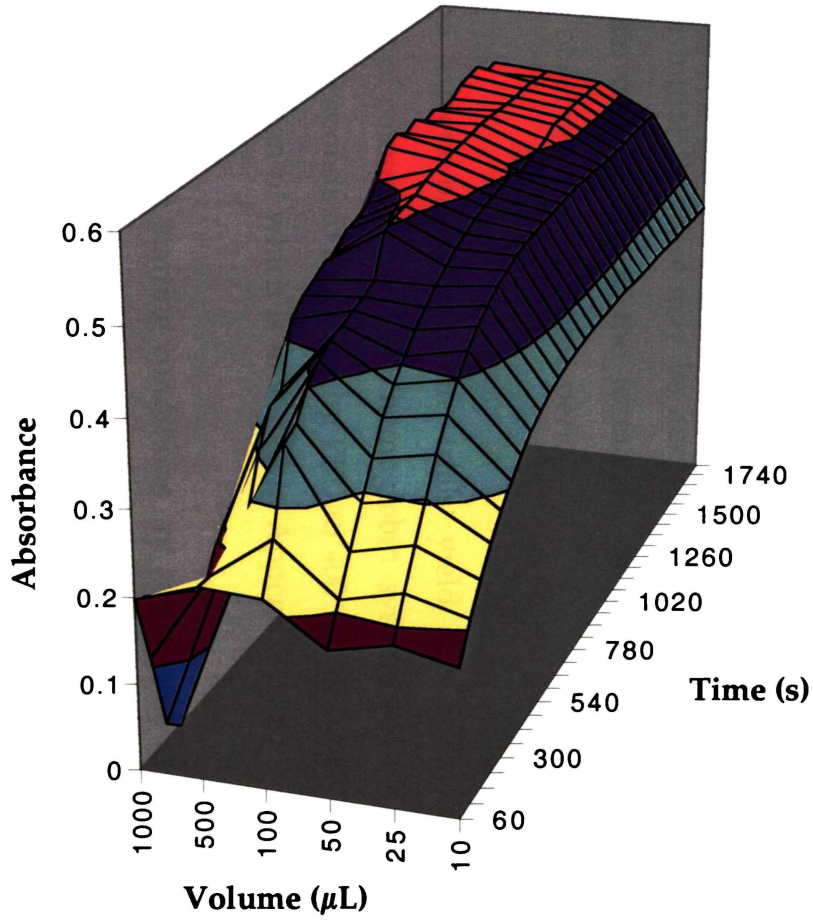

Fig. 3.5
Plot of effect of hydrogen peroxide volume on colour development of PPD (measured by absorbance at λ = 404 nm) at pH 5.4.

NB. Due to limitations with Microsoft Excel, the volume and time axes do not always increase in even increments.

The reason for the high initial absorbance readings in Table 3.5 can be explained by the staining of the sample cuvette by PPD from the previous trials on pH optimisation. The staining can be removed by a long soak in concentrated HCl. It was not practical to do this between trials and it was not thought necessary anyway as the final absorbance readings are not effected and also only a qualitative picture of the optimum conditions and not the absolute absorbance readings is required.

From these results, 100 µL of H_2O_2 seems to give the optimum absorbance value. At higher concentrations of H_2O_2, the rate of colour development is similar at first, but the final absorbance values achieved are not so high, as with OPD, ABTS and DAB. For the 500 and 1000 µL trials the absorbance readings decreased initially before subsequently increasing and reaching a rather jagged plateau (not too pronounced in Fig. 3.5). The initial decrease may be due to some side reaction occurring while the jagged plateau may be due to the formation of a large number of oxygen bubbles which were observed over the time period.

Overall, the cuvette-based solution trials yield the following as optimal for development of colour in the PPD/hemoglobin system; pH 5.4, and 100 µL of 2.7% H_2O_2 which corresponds to a ratio of 1 g PPD to 400 mL of 2.7% H_2O_2 or 40 mL of 27% H_2O_2 (full calculation of which is included in Appendix 3.2).

These were taken as the starting conditions for testing the activity of PPD on blood fingerprints. Unknowns in moving from solution work to development of blood on a surface are the same as those discussed for OPD in section 3.4.1.

3.4.3 OPD fingerprint trials

Treatment on porous surfaces

The following results were obtained in trials examining OPD development of bloody fingerprints on paper.

1. *Varying H_2O_2 concentrations:* The optimised ratio of H_2O_2 to OPD determined from the cuvette trials translated to 0.5 mL of 27% H_2O_2 in 50 mL OPD solution (0.5 g/L). The 50 µL (27%)

treatment resulted in slightly poorer development compared with the 100 µL (27%) treatment which produced a stronger colour, better enhancement and with more ridge detail visible. The 500 µL (27%) treatment resulted in better development than the 100 µL (27%) treatment. The 1000 µL (27%) treatment resulted in better development than the 500 µL (27%) treatment. There was no visible difference between the 1500 µL (27%) treatment and the 1000 µL (27%) treatment. It was decided therefore, that 1 mL of 27% H_2O_2 should be used for further fingerprint trials rather than the optimised volume of 0.5 mL determined in the previous cuvette trials.

2. *Treatment compared with no treatment:* The treated side had much better ridge definition and more detail was visible. The treated side was orange in colour. An example of this is presented in Fig. 3.6 a and Fig. 3.6 b.
3. *Varying OPD concentrations:* The treatment at the 0.25 g/L OPD concentration was lighter in colour than the 0.5 g/L concentration. Apart from more background staining the 1 g/L OPD concentration resulted in no difference compared with the 0.5 g/L concentration. It was therefore decided that the OPD concentration of 0.5 g/L should be retained for further trials.
4. *Varying soaking times in OPD:* There was no significant difference in the development obtained by treatment at 5, 10 and 30 minutes apart from greater background staining for the 30 minute treatment. The 2.5 minute treatment however, was lighter in colour and less visible. It was therefore decided that the treatment time of 5 minutes should be retained.
5. *Comparison of the OPD method at pH 5.4 and pH 7.4:* Treatment at pH 7.4 resulted in a browner development colour (like DAB) compared with treatment at pH 5.4 which resulted in the usual orange development colour expected. An example of this is presented in Fig. 3.6 d. It was therefore decided that a pH of 5.4 should be retained for further trials.
6. *Comparison of OPD with DAB:* Two OPD treated fingerprint halves were better than their corresponding DAB treated halves, forty one OPD treated halves were of equivalent development (or were indistinguishable) and seven OPD treated halves were of poorer development. So overall, OPD seems to give fairly equivalent performance to DAB for prints on paper (but with the resulting colour being orange). An example of this is presented in Fig. 3.6 c.
7. *Compatibility of OPD with DAB:* The print half treated with DAB first followed by OPD treatment resulted in the same development as the corresponding print half treated with DAB alone. The print treated with OPD first followed by DAB treatment resulted in the same development as the print treated with OPD alone.
8. *Compatibility of OPD with Ninhydrin:* The fingerprint exhibit treated with OPD first followed by ninhydrin resulted in only the blood fingerprint developing. The latent fingerprint did not develop at all. The other fingerprint exhibit initially resulted in purple development of the latent fingerprint after the ninhydrin treatment (the blood print became grey in colour with better visibility) followed by subsequent orange development of the blood fingerprint after

OPD treatment. The ninhydrin developed latent print however, disappeared on immersion in the fixative solution.

Treatment on non-porous surfaces

The development obtained on glass at pH 5.4 is poor compared to that obtained at pH 7.4 which gives good development with a reddish colour.

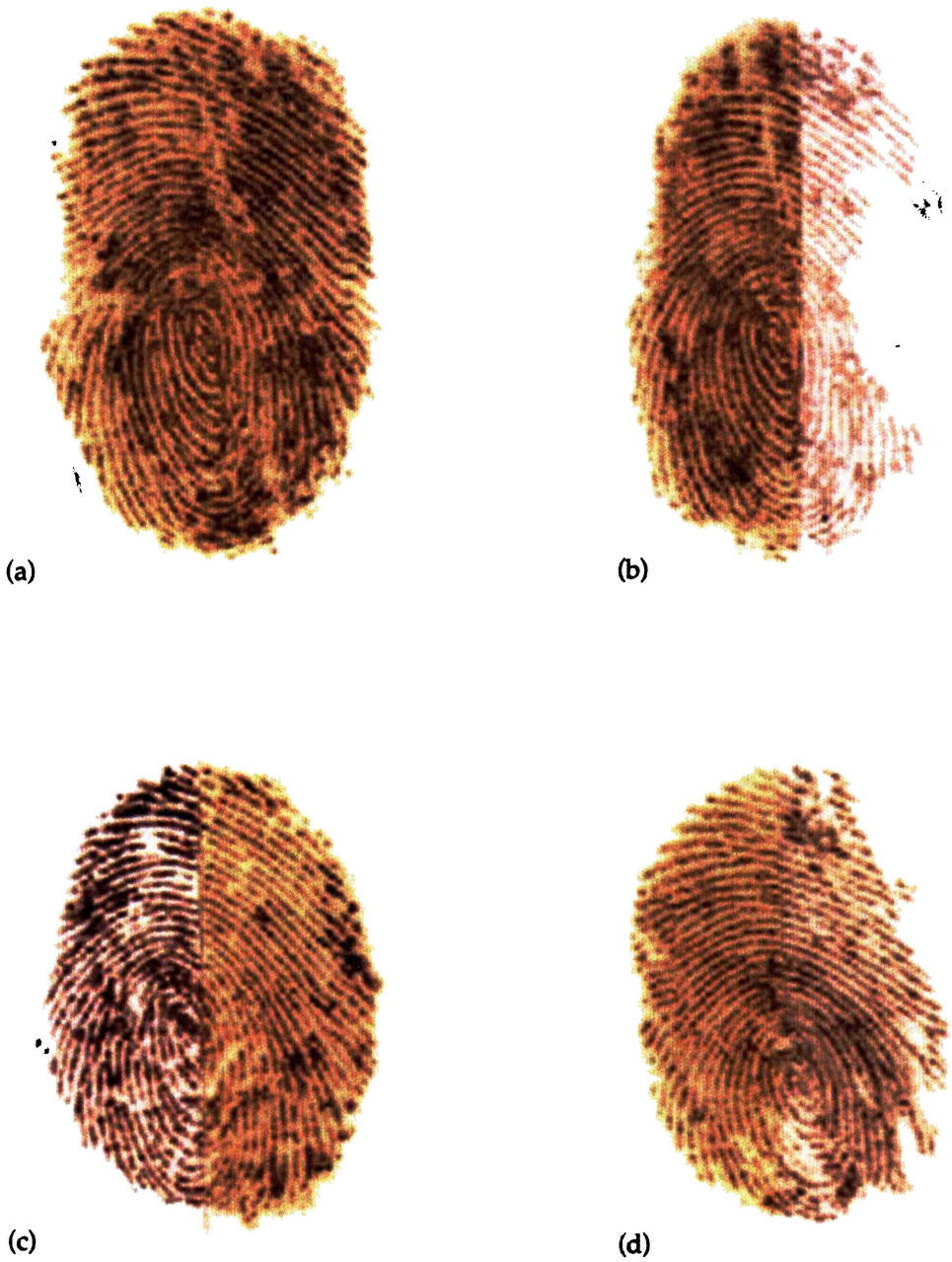

Fig. 3.6

Visualisation of blood fingerprints (a) OPD treatment, (b) OPD treatment vs. no treatement, (c) DAB treatment (left) vs. OPD treatment (right), and (d) OPD treatment at pH 5.4 (left) vs. OPD treatment at pH 7.4 (right).

3.4.4 PPD fingerprint trials

Treatment on porous surfaces

The following results were obtained in trials examining PPD development of bloody fingerprints on paper. It was observed that blood prints on paper turn green first in the initial stages of development before slowly turning black/purple after being immersed in the active solution.

1. *Varying H_2O_2 concentrations (The optimised ratio of H_2O_2 to PPD from the cuvette trials translated to 1 mL of 27% H_2O_2 in these trials):* Two out of four print halves treated with 1 mL 27% H_2O_2 resulted in better development compared with the 0.2 mL 27% H_2O_2 treatment. The other two print halves indicated no difference between the 1 and 0.2 mL 27% H_2O_2 treatment. There was no visible difference between the four print halves treated with 2 mL 27% H_2O_2 and the four corresponding print halves treated with 1 mL 27% H_2O_2. It was therefore decided to use 1 mL 27% H_2O_2 per 50 mL PPD (0.5 g/L) for all future work.
2. *Treatment compared with no treatment:* The treated side had much better ridge definition and more detail was visible. The treated side was black/purple in colour. An example of this is presented in Fig. 3.7 a and Fig. 3.7 b.
3. *Varying PPD concentrations:* The development obtained for all four print halves using the 0.25 g/L PPD concentration was lighter in colour than that obtained using the 0.5 g/L concentration. One of the prints was also not as well developed. The 1 g/L PPD concentration resulted in no difference compared with the 0.5 g/L concentration. It was therefore decided to keep using the 0.5 g/L PPD solution.
4. *Varying soaking times in PPD:* There was no significant difference in the development obtained by treatment at 2.5, 5, 10 and 30 minutes apart from greater background staining for the 10 and 30 minute treatments.
5. *Comparison of PPD method at pH 5.4 and pH 7.4:* Treatment at both pH 7.4 and pH 5.4 resulted in the same development colour (purple) but pH 7.4 resulted in slightly more background staining. An example of this is presented in Fig. 3.7 d.
6. *Comparison of PPD with DAB:* Seven PPD treated fingerprint halves were better than their corresponding DAB treated halves, thirty five PPD treated halves were of equivalent development (or were indistinguishable) and eight PPD treated halves were of poorer development. So overall, PPD seems to give fairly equivalent performance to DAB for prints on paper (but with the resulting colour being black/purple). An example of this is presented in Fig. 3.7 c.
7. *Compatibility of PPD with DAB:* The print half treated with DAB first followed by PPD treatment resulted in the same development as the corresponding print half treated with DAB

alone except that the DAB/PPD treated print was purple/brown in colour. The print treated with PPD first followed by DAB treatment resulted in the same development as the print treated with DAB alone except that the PPD/DAB treated print was purple/brown in colour. These results indicate that both PPD and DAB are similar in oxidising strength.

8. *Compatibility of PPD with ninhydrin:* The fingerprint exhibit treated with PPD first followed by ninhydrin resulted in only the blood fingerprint developing with its usual black/purple colour. The latent fingerprint did not develop at all. The other fingerprint exhibit initially resulted in purple development of the latent fingerprint after the ninhydrin treatment followed by subsequent black/purple development of the blood fingerprint after PPD treatment. The ninhydrin developed latent print however, disappeared on immersion in the fixative solution prior to PPD treatment.
9. *Comparison of old PPD solution (prepared 48 hours earlier) with new PPD solution (prepared half hour earlier):* One out of four print halves treated with the new solution was slightly better developed than the corresponding print half treated with the old solution. The other three print halves showed no difference. It is probably best however to follow a precautionary principle and prepare the PPD solution fresh each day.

Treatment on non-porous surfaces

The development obtained on glass with PPD was fairly equivalent to that obtained using DAB for both pairs of glass slides but with a more purple/brown colour for PPD.

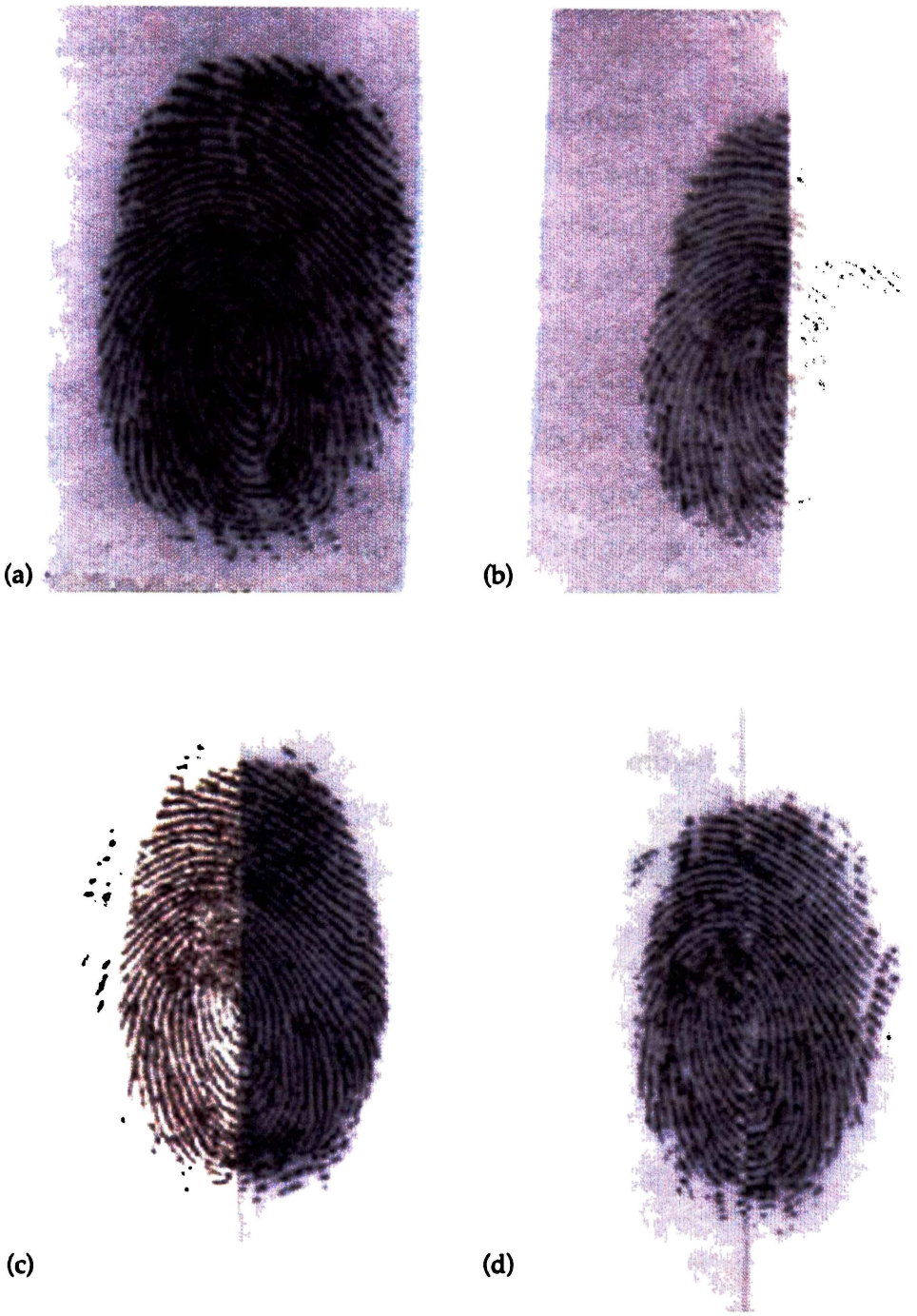

Fig. 3.7
Visualisation of blood fingerprints (a) PPD treatment, (b) PPD treatment vs. no treatment, (c) DAB treatment (left) vs. PPD treatment (right), and (d) PPD treatment at pH 5.4 (left) vs. PPD treatment at pH 7.4 (right).

3.5 *Sensitivity of OPD and PPD compared with DAB*

3.5.1 Methodology

As with the methodology used for ABTS in section 2.6.1 of Chapter 2, the procedure for the determination of OPD and PPD sensitivity was based on the procedure used by Garner et al., 1976. A sample of the author's blood was diluted serially in isotonic saline. The following dilutions were prepared: $1x10^{-1}$, $1x10^{-2}$, $1x10^{-3}$, $1x10^{-4}$, $1x10^{-5}$, $1x10^{-6}$. A 10 µL aliquot of each dilution was placed into the separate wells of a plastic microplate in three rows. Three OPD solutions were then prepared (in distilled water) with the following concentrations: 0.1 *M*, 0.05 *M* and 0.025 *M*. A drop of the 0.1 *M* solution was placed into each well of the first row of the microplate followed by a drop of 2.7% of H_2O_2. The 0.05 and 0.025 *M* solutions were then placed into the wells of rows 2 and 3 respectively of the microplate followed by 2.7% of H_2O_2. This procedure was then repeated again on separate microplate wells for PPD and DAB.

A positive test (denoted by the symbol +) was determined by colour comparison with control wells containing only OPD, PPD or DAB solution and H_2O_2. A negative test (denoted by the symbol –) was assigned when the colour in the well was the same as that in the control well.

3.5.2 Results and discussion

Results for microplate well tests on DAB, OPD and PPD are presented in Tables 3.6, 3.7, and 3.8 respectively.

Table 3.6
Determination of the sensitivity of DAB using microplate wells.

DAB concentrations	Blood dilution series $1x10^{-1}$	$1x10^{-2}$	$1x10^{-3}$	$1x10^{-4}$	$1x10^{-5}$	$1x10^{-6}$
0.1 *M*	+	+	+	–	–	–
0.05 *M*	+	+	+	–	–	–
0.025 *M*	+	+	+/–	–	–	–

Table 3.7
Determination of the sensitivity of OPD using microplate wells.

OPD concentrations	Blood dilution series $1x10^{-1}$	$1x10^{-2}$	$1x10^{-3}$	$1x10^{-4}$	$1x10^{-5}$	$1x10^{-6}$
0.1 *M*	+	+	+	–	–	–
0.05 *M*	+	+	+	–	–	–
0.025 *M*	+	+	+	–	–	–

Table 3.8
Determination of the sensitivity of PPD using microplate wells.

PPD concentrations	Blood dilution series $1x10^{-1}$	$1x10^{-2}$	$1x10^{-3}$	$1x10^{-4}$	$1x10^{-5}$	$1x10^{-6}$
0.1 *M*	+	+	+	–	–	–
0.05 *M*	+	+	+	–	–	–
0.025 *M*	+	+	+	–	–	–

As with ABTS, even the controls became as equally dark as the positives after several hours. All assignments were therefore made within 10 minutes of H_2O_2 addition and a positive test was only assigned if it was darker then the control. The results seem to indicate however, that OPD and PPD are at least as sensitive as DAB.

3.6 *Price comparison*

Ortho-phenylenediamine (OPD) and *para*-phenylenediamine (PPD) can be purchased as flakes from Aldrich Chemical Company in 100 g quantities @ NZ$31.86 and NZ$32.68 respectively. 3,3'-diaminobenzidine can also be purchased from Aldrich Chemical Company in 25 g quantities @ NZ$231.27. All prices are listed in the Australian 1998-99 Catalogue Handbook of Fine Chemicals (prices converted by Australian/New Zealand exchange rate).

The price per 100 mg of OPD or PPD (used to prepare 200 mL of OPD or PPD working solution) when purchased from Aldrich Chemical Company will therefore cost NZ$0.04. The price per 200 mg of DAB (used to prepare 200 mL of DAB working solution) will cost NZ$1.85.

3.7 *Chapter Summary*

OPD and PPD, although both still toxic, represent less of a hazard than the carcinogenic risks of DAB for development of blood fingerprints, while still being as effective. OPD works well on porous surfaces at pH 5.4 and on glass at pH 7.4. OPD development results in prints which are orange, which should show up more clearly than the dark brown of oxidised DAB on dark surfaces. PPD gives purple prints and works well on porous surfaces and on glass at pH 5.4. Like ABTS, OPD and PPD are "nothing-to-lose" reagents, because subsequent DAB treatment after OPD or PPD treatment is as good as DAB treatment by itself. In fact OPD and PPD treatment can be used before or after DAB treatment with the resulting colour being a mixture of the OPD or PPD colour with that of DAB. This is different from the situation with ABTS, where prior DAB use apparently renders the reagent inactive (refer to section 2.5.2). Although OPD or PPD treatment can be effectively used after ninhydrin treatment, ninhydrin treatment cannot be effectively used after OPD or PPD treatment. The recommended procedure for OPD and PPD treatment of prints in blood is presented in Chapter 8 (section 8.1).

3.8 *References*

Battistini A., and Casa, F. (1967). Quantitative starch gel electrophoresis. I. Interpretation of electrophoretic pattern. *Lattante*, **38**(1), 1-22.

Bretherick L. (1986). *Hazards in the chemistry laboratory*. 4th edition. The Royal Society of Chemistry, Alden Press, Oxford, 450-451.

Chung K., Murdock C.A., Edward Stevens S., Li Y., Wei C., Huang T., and Chou M.W. (1995). Mutagenicity and toxicity studies of PPD and its derivatives. *Toxicol. Lett.*, **81**(1), 23-32.

Donlon B., Razo-Flores E., Luijten M., Swarts H., Letlinga G., and Field J. (1997). Detoxification and partial mineralization of the azo dye Mordant Orange 1 in a continuous upflow anaerobic sludge-blanket reactor. *Appl. Microbiol. Biotechnol.*, **47**(1), 83-90.

Garner D.D., Cano K.M., Peimer M.S., and Yeshion M.S. (1976). An evaluation of tetramethylbenzidine as a presumptive test for blood. *J. Forens. Sci.*, **21**, 816-821.

Jun Feng S., Xiao Feng K., and Wei G. (1997). Determination of hemoglobin in plasma and serum by linear-sweep polarography. *J. Anal. Chem.*, **357**(1), 127-129.

Kazuo M., Ko-ich T., Isao Y., Hiroaki N., Yoko T., Tomoko I., Setsunori T., and Kojiro K. (1996). A unique and sensitive ELISA technique for typing ABH antigens in bloodstains using UEA-I lectin-the

removal of detergent with a Sephadex G-25 mini-column improves sensitivity. *J. Forensic Sci.*, **41**(1), 35-39.

Lavis A. (1994). *Workshop in advanced fingerprint techniques.* Training manual prepared for *ESR:Forensic*, Auckland, New Zealand.

Lück H. (1965). *Methods of enzymatic analysis.* Edited by Hans-Ulrich Bergmeyer. Verlag Chemie, Academic Press, New York, 895-897.

Roux C., Livage J., Farhati K., and Monjour L. (1997). Antibody-antigen reactions in porous sol-gel matrixes. *J. Sol-Gel Sci. Technol.*, **8**(1/2/3), 663-666.

Tyouichi T., Mitsuwo H., and Kimitaka S. (1984). Detection of seminal stains by sandwich ELISA using monoclonal.gamma.-seminoprotein antibody bound to acrylonitrile-butadiene-styrene beads. Forensic immunological studies of body fluids and secretion. XXIII. *Nippon Hoigaku Zasshi*, **38**(1), 83-87.

Chapter Four

An investigation into the utilisation of $Eu(fod)_3$ and related compounds for the fluorescent visualisation of latent fingerprints

4.1 *Introduction*

The utilisation of coordinatively–unsaturated (six–coordinate) europium and terbium complexes as reactive reagents for the direct visualisation of latent fingerprints on porous and non-porous surfaces has been investigated.

Previously, forensic research in the lanthanide area has tended to focus around rare earth-Ruhemann's Purple complexes and coordinatively–saturated europium complexes. Rare earth–Ruhemann's Purple complexes involve the reaction products of ninhydrin with amino acids, which react further with europium or terbium chloride hexahydrate ($EuCl_3.6H_2O$, $TbCl_3.6H_2O$) to form organo-rare earth complexes. These complexes exhibit Eu^{3+} luminescence at 615 nm with a lifetime of 0.4 ms (Menzel and Mitchell, 1990) and Tb^{3+} luminescence at 545 nm with a lifetime of 1.3 ms (Alaoui and Menzel, 1994).

Coordinatively–saturated eight–coordinate europium complexes are used as luminescent dyes to enhance fingerprints developed with cyanoacrylate. These complexes include thenoyl europium chelate (TEC) and its analogues (Wilkinson and Watkin, 1993; Wilkinson and Misner, 1994; and Lock et al., 1995) and exhibit Eu^{3+} luminescence at 614 nm.

Six-coordinate europium complexes differ from those currently in use as cyanoacrylate dyes in that they are likely to be reactive toward a number of functional groups present in fingerprints. In the past, such reagents have been widely employed as Lanthanide Shift Reagents for improving resolution in NMR spectroscopy (Shoffner, 1975). However, the increased magnetic field strength of today's NMR

instruments has resulted in a steady decline in their use for this purpose. Such reagents are all derived by tris-complexation of the lanthanide metal ion with enolic β-dicarbonyl compounds, and are commercially available. Chemical shift reagents operate by associating through the metal orbitals, with non-bonding electrons in the substrate, so that they are only effective with molecules belonging to such functional classes as amines, alcohols, ethers, aldehydes, ketones, esters, nitriles and epoxides (Kemp, 1986).

The main coordinatively–unsaturated europium complex investigated in this study is tris(6,6,7,7,8,8,8-heptafluoro-2,2-dimethyl-3,5-octanedionato) europium(III) [$Eu(fod)_3$] (Fig. 4.1). $Eu(fod)_3$ was first synthesised by Springer et al. (1967) and has since been used as an NMR shift reagent for the structural analysis of various organic compounds (Johnston et al., 1975; Shoffner, 1974 and 1975; Rondeau and Sievers, 1971; Morrill et al., 1973; Reuben, 1973; Bruder et al., 1974). $Eu(fod)_3$ is a covalent charge-neutral compound, soluble in non-polar solvents such as aliphatic hydrocarbons. It is still commercially available even though there is now less need for shift reagents with modern NMR spectrometers.

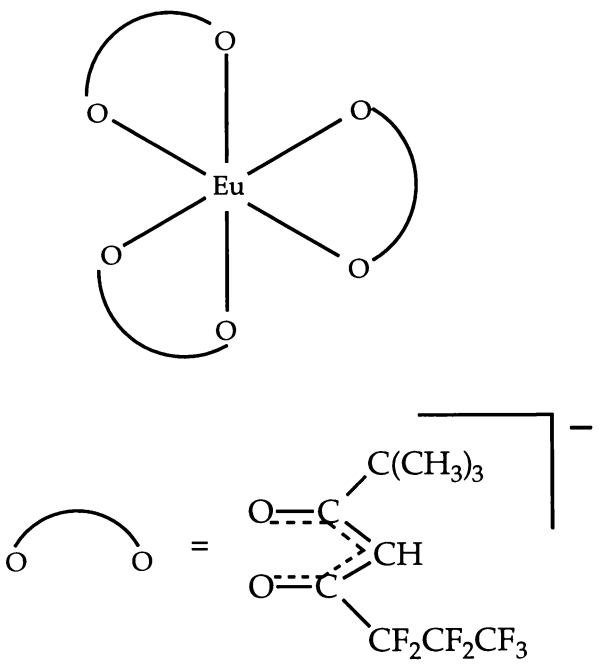

Fig. 4.1
Structure of $Eu(fod)_3$.

$Eu(fod)_3$ is likely to be reactive to a broad variety of functional groups. Direct experimental evidence (obtained using NMR) has been published which establishes that $Eu(fod)_3$ reacts with alcohols, ketones and carboxylic acids (Johnston et al., 1975; Shoffner, 1974); and similar compounds have been previously found to react with amine groups (Kemp, 1986). $Eu(fod)_3$ should therefore be quite reactive toward many of the constituents found in latent fingerprints, the most significant of which would be alcohols, carboxylic acids and amino acids. The reactivity of $Eu(fod)_3$ in this manner is due to the fact that it is a six-coordinate complex of a metal which 'prefers' to be eight-coordinate: two spare coordination sites are available around the metal for ligands to bind to.

Three related compounds were also briefly investigated in this work with respect to their potential to develop fingerprints. These were the europium compound tris(2,2,6,6-tetramethyl-3,5-heptane-dionato) europium(III) $[Eu(dpm)_3]$ and the terbium compounds tris(6,6,7,7,8,8,8-heptafluoro-2,2-dimethyl-3,5-octanedionato) terbium(III) $[Tb(fod)_3)]$ and the terbium chelate of diethylenetriamine pentaacetic acid-4-aminosalicylic acid (DTPA-pAS) (Fig. 4.2). This latter compound is not an NMR shift reagent, but has been used in a fluorescence immunoassay for human serum albumin (Bailey et al., 1984 and 1988). It involves the covalent linking of 4-aminosalicylic acid (p-AS) to diethylenetriamine pentaacetic acid anhydride (DTPAA). The resulting structure (DTPA-pAS) is then chelated to Tb^{3+}. The chelate is soluble in water and is fluorescent in aqueous solution.

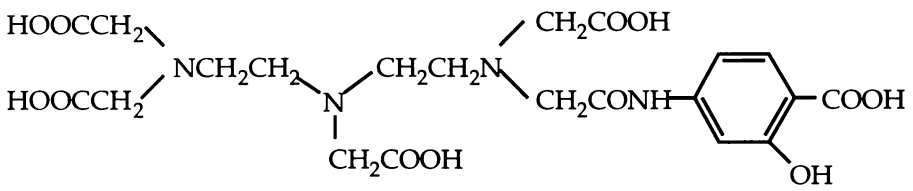

Fig. 4.2
Presumed structure of DTPA-pAS (Bailey et al., 1988).

In the case of human albumin, DTPA-pAS is used to label the albumin to which then is added a terbium chloride solution. The emission intensity at 545 nm from the resulting terbium chelate is then measured. Investigation into the fluorescence

properties of the terbium chelates of the reaction products had been achieved by the addition of terbium chloride solution and triethanolamine buffer to a solution of DTPA-pAS. It was proposed that if DTPA-pAS can be used in combination with Tb^{3+} to label human serum albumin, which is a component of human blood and can also be used in combination with triethanolamine and Tb^{3+}, then it could also be used to help visualise blood fingerprints (serum albumin) and latent fingerprints (amino acids).

In terms of their spectroscopy, the complexes of europium and terbium (and also of samarium and dysprosium) have certain properties which make them a good choice for visualisation of fingerprints. They have unusually long fluorescence lifetimes (1 μs to over 1 ms), very large Stokes shifts (over 200 nm) and exhibit emission spectra consisting of sharp lines (Bailey et al., 1988). It is these luminescent properties which make these lanthanide complexes ideal for optical filtering and time-resolved imaging (Murdock and Menzel, 1993), which can be useful when removal of background fluorescence from various surfaces is necessary. This combination of good reactivity with excellent optical properties mean that lanthanide shift reagents have high potential for direct single-step visualisation of latent fingerprints.

4.2 *Methodology*

4.2.1 Chemicals

Chemicals used in this research were purchased from the following sources:

- $Eu(fod)_3$ (Resolve-Al™ EuFOD, 99%), ninhydrin (ACS reagent), octanoic acid (AR), $TbCl_3.6H_2O$, sodium methoxide, pinacolone, ethyl heptafluorobutyrate, hydrated terbium(III) chloride, and *p*-aminosalicylic acid (p-AS) from Aldrich Chemical Company Ltd.
- $Eu(dpm)_3$ from Merck.
- $Tb(fod)_3$ was prepared using a method based on that of Springer et al. (1967) (section 4.2.2 and 4.2.3).
- DFO (1,8-diazafluoren-9-one) from Lumichem Ltd.
- Toluene, dichloromethane, chloroform, and hexane from R.P. Normanpur™ (AR).

- Petroleum spirits (b.p. 40-60°C) (AR), and petroleum spirits (b.p. 80-100°C) (AR), glycine (AR), methanol (AR), ethanol (AR) glacial acetic acid (AR), propionic acid (LR), molecular sieve 4A, sulfuric acid (AR), diethyl ether (AR), $NaNO_3$ (AR), and N,N-dimethylformamide (GPR) from BDH.
- Ethyl acetate (AR), urea (AR), sodium hydroxide (AR), and triethylamine (LR) from Ajax Chemicals.
- D-(+)-glucose from May and Baker Laboratory Chemicals.
- Freon (1,1,2 trichlorotrifluoroethane) from E.I. Dupont de Nemours and Company.
- 1,10-phenanthroline from Serva.
- Diethylenetriamine pentaacetic acid anhydride (DTPAA) (bicyclic anhydride of diethylenetriamine pentaacetic acid) (LR) from Hopkin and Williams Ltd.
- Dimethyl sulfoxide (DMSO) (AR) was obtained from Mallinckrodt®.
- X4 from the Marsden Point Refinery in New Zealand and is the equivalent of petroleum spirits (b.p. 40-60°C). It comes as a bulk solvent which is redistilled prior to use.

4.2.2 Synthesis of 1,1,1,2,2,3,3-Heptafluoro-7,7-dimethyl-4,6-octanedione, H(fod)

The β-diketone ligand H(fod) was synthesised by a Claisen condensation of ethyl heptabutyrate with pinacolone. The method used was based on that of Springer et al. (1967).

A 1000 mL three-necked round-bottomed flask was fitted with a condenser tube and a stoppered pressure-equalizing addition funnel and flushed with nitrogen via the condenser tube. Sodium methoxide (0.0926 mole, 5 g) (measured out under nitrogen) was suspended in 75 mL of absolute diethyl ether. Ethyl heptafluorobutyrate (0.0926 mole, 22.41 g) was added dropwise to the stirred mixture over a period of 45 mins from the stoppered pressure-equalizing addition funnel, whereupon a cream-coloured slurry resulted. A solution of pinacolone (0.09255 mole, 9.27 g) in 25 mL of absolute diethyl ether was added from the funnel over a period of 20 mins. When the addition was half complete, a clear yellow solution was present in the flask. This solution was basic (pH paper) after complete addition of pinacolone. It was stirred for 2 hr and then allowed to stand overnight. Sulfuric acid (40 mL, 2 *M*) was slowly added with stirring to the ether solution. The aqueous phase generated was basic (pH paper)

until all of the acid was added. The aqueous layer was separated and washed with fresh diethyl ether. The washings were combined with the original yellow organic layer; and, after partial evaporation using a rotary evaporator, the solution was vacuum distilled (water pump) using a micro distillation set–up with a vigreux column.

Three fractions were collected. The 1st fraction was collected at approximately 61°C (slight temperature fluctuation), the 2nd fraction at approximately 65°C (slight temperature fluctuation), and the 3rd fraction between 63-69°C (large temperature fluctuation). All fractions were colourless with a pungent odour but slowly turned yellow with time. ^{1}H and ^{19}F NMR obtained on a Bruker AC300 spectrometer was used for the analysis of the various fractions. NMR of the 2nd fraction showed contamination with pinacolone. NMR of the 3rd fraction showed only a small trace of pinacolone contamination. The 2nd fraction was redistilled. The 2nd fraction of this fraction was collected at 67°C and the 3rd fraction collected between 65-80°C. The NMR showed that the 2nd fraction was pure and that the 3rd fraction was contaminated. Therefore the 3rd fraction from the 1st distillation was combined with the 2nd fraction from the 2nd distillation to give a total yield of 2 g (7.7 %).

The ^{1}H NMR for fraction 3 from the first distillation revealed singlet peaks at 1.23 ppm due to $C(CH_3)_3$, a peak at 6.07 ppm due to CH and a broad peak centred around 14 ppm due to OH (indicating a slow exchange rate). Two small peaks at 2.19 and 7.26 ppm were probably due to pinacolone contamination. The ^{19}F NMR for this fraction confirmed the straight chain structure of the perfluoropropyl group; a triplet at 3.6 ppm due to CF_3CF_2, a quartet at -37.5 ppm due to CF_2CF_2CO and a singlet at -42.7 ppm due to $CF_3CF_2CF_2$.

The ^{1}H NMR for fraction 2 from the redistillation of fraction 2 revealed the same spectra as for fraction 3 from the first distillation but with no pinacolone contamination.

4.2.3 Synthesis of the Tris fod Complex of the Terbium(III) Ion

The terbium(III) chloride hexahydrate (0.0011 mole, 0.411 g) was dissolved in the minimum amount of absolute methanol. A solution of H(fod) (0.0033 mole, 0.977 g) in 1.5 mL of absolute methanol was neutralised with 801 μL of 4.12 *M* aqueous sodium hydroxide solution. Addition of an excess of sodium hydroxide or the use of a more concentrated basic solution was avoided in order to preclude hydrolysis of the ligand. Upon addition of the first portion of the aqueous NaOH solution, the formerly homogeneous solution separated into two phases, because the unneutralized H(fod) is insoluble in the resulting solvent mixture. When an equivalent amount of base has been added, the solution became homogeneous. The two solutions were then mixed with a magnetic stirrer, and a small amount of white $NaNO_3$ precipitated immediately. The resulting mixture was added dropwise over a period of approximately 20 minutes to *ca.* 40 mL of distilled water which was stirred vigorously. The solid complex precipitated, and the mixture was stirred until the precipitate was in the form of fine granules. A stirring rod was used during the precipitation to crush the granules and prevent coagulation into a tar. The final methanol concentration was kept very low to minimise the possibility of oiling. The suspended precipitate was isolated by suction filtration and air dried for approximately 1 hr.

Two batches of crude product were prepared and the yields for the first and second batch were 77.67 % and 85.74 % respectively.

The crude products were recrystallized twice by dissolving in the minimum amount of dichloromethane (distilled) at room temperature and cooling the solutions to approximately -8°C (salted icebath). The products were dried on a vacuum line (at room temperature) for *ca.* 12 hr between recrystallizations followed by freeze drying for *ca.* 12 hr for the second recrystallisation.

Melting points for the two batches were determined on a Reichert Thermovar melting point instrument (Reichert-Jung). The melting points for both batches started at about 175°C and were complete by 185°C. The majority had melted by 180°C. The literature melting point was between 190-196°C. The reason for this discrepancy

between experimental and literature values is probably due to the m.p. being taken several days after the product had been freeze dried. Some of the product may have incorporated a molecule of water into the complex producing the monohydrate over the intervening time between freeze drying and m.p determination. The monohydrate has a lower melting point which would lower the melting point relative to the pure anhydrous product.

4.2.4 Instrumentation and equipment

The following instrumentation and equipment were used in this research:

- A Perkin Elmer Luminescence Spectrometer LS 50B was used for collection of all fluorescence data; this utilises a xenon-lamp source.
- A Mineralight® hand-held UV lamp (model UV GL-58) was used with two wavelength settings of 254 and 366 nm for initial visualisation of treated fingerprints.
- When photos were required, use was made of an operational Polilight® (model PL10A) owned by the New Zealand Police; the 320 nm filter was used in conjunction with a TV camera and thermal printer.
- A Spectra Physics 164 argon-ion laser (1 watt) in combination with a 265 Exciter was used for visualisation of DFO treated fingerprints.
- A Fisons VG Platform II electrospray mass spectrometer was used to look for evidence of particular substrates binding to $Eu(fod)_3$ and $Tb(fod)_3$.
- White and green paper (A4, 80 gsm) was obtained from Copyright (Australian Paper, Ltd.).
- A Bruker AC300 NMR spectrometer was used for confirmation of the H(fod) synthesis.
- A Reichert Thermovar melting point instrument (Reichert-Jung), and a Büchi Rotavapor (R) rotary evaporator were all used in the synthesis and characterisation of $Tb(fod)_3$.

4.2.5 Solution trials

A preliminary investigation indicated that $Eu(fod)_3$ and $Tb(fod)_3$ readily dissolve in petroleum spirits (b.p. 40-60°C) and X4 (refer to chemical list in section 4.2.1) which were therefore, unless otherwise specified, used as the general reagents for fingerprint trials. Refer to Appendix 4.1 for emission and excitation spectra comparisons between the two solvents. Both $Eu(fod)_3$ and $Tb(fod)_3$ were also found to be soluble in methanol but solvents containing significant quantities of water are generally not

suitable, because direct coordination of water molecules to the europium centre has a tendency to quench the fluorescence (Bailey et al., 1988). $Eu(dpm)_3$ was found to have poor solubility in petroleum spirits and methanol but was found to be soluble in toluene.

Fluorescent maximum emission and excitation spectra of $Eu(fod)_3$ in either petroleum spirits (b.p. 40-60°C), petroleum spirits (b.p. 80-100°C) or X4 were obtained using a luminescence spectrometer. Five different solutions were prepared. Slit widths for both excitation and emission were set at 10 nm (for four of the five solutions), with solutions being held in a 10 mm quartz cuvette. One of these solutions was prepared using petroleum spirits (b.p. 80-100°C), while two of these solutions were prepared using lower boiling range petroleum spirits (b.p. 40-60°C) as the solvent, one of which was analysed on the spectrometer using excitation and emission slit widths set at 15 nm. The other petroleum spirits (b.p. 40-60°C) solution was prepared six months later using the same batch of $Eu(fod)_3$. The remaining two solutions were prepared using X4 as the solvent, one of which was prepared 6 months later than the other but using the same batch of $Eu(fod)_3$. A solution of $Eu(fod)_3$ in X4 was then analysed on the luminescence spectrometer using excitations of 254 and 366 nm. These are the wavelength settings of the hand-held UV lamp used for subsequent visualisation of $Eu(fod)_3$-treated fingerprints. All solutions were prepared by dissolving 10 mg $Eu(fod)_3$ (freshly dried in freeze drier) in 20 mL X4 or petroleum spirits (b.p. 40-60°C and b.p. 80-100°C).

Fluorescent maximum emission and excitation spectra of $Tb(fod)_3$ in X4 were obtained. Fluorescent maximum emission and excitation spectra were then obtained using a 50/50 mixture of $Eu(fod)_3$ and $Tb(fod)_3$ in X4. A three dimensional spectrum of emission and excitation versus intensity of $Eu(fod)_3$ and $Tb(fod)_3$ in X4 were then also obtained by exciting at 10 nm steps and obtaining emission spectra at each 10 nm step. Slit widths for both excitation and emission were set at 10 nm, with solutions being held in a 10 mm quartz cuvette. Solutions were prepared by dissolving 10 mg $Eu(fod)_3$ or 10 mg of $Tb(fod)_3$ (freshly dried in freeze drier) in 20 mL X4 or petroleum spirits (b.p. 40-60°C).

A fluorescent emission prescan of $Eu(dpm)_3$ was obtained using a luminescence spectrometer. Slit widths for both excitation and emission were set at 10 nm, with solutions being held in a 10 mm quartz cuvette. A solution was prepared by dissolving 50 mg $Eu(dpm)_3$ in 20 mL toluene.

4.2.6 Fingerprint trials

Preliminary comments

For the initial trials unless otherwise specified, latent fingerprints were placed on strips of white paper and then cut bilaterally down the centre in order that each half could be treated in a different way and thus accurate comparisons be made. In order to deposit the fingerprints on a given surface the finger or thumb was rubbed a few times across the forehead and then pressed firmly down on to the surface being investigated. Again, unless otherwise stated, treatment consisted of a short "dip" or immersion in a 6.67 g/L petroleum spirits (b.p. 40-60°C) solution of $Eu(fod)_3$ using a 20 second "dipping" time. Visualisation of the $Eu(fod)_3$-treated fingerprints was obtained using a Mineralight® hand-held UV lamp (Model UV GL-58). This has a mercury vapour source, with two wavelength settings of 254 and 366 nm, and it was found that the 254 nm setting gave the best visualisation. The use of orange goggles was necessary for successful viewing of the prints in order to filter out background fluorescence from the paper. For photographic purposes a Polilight® using the 320 nm wavelength filter was employed with an orange filter over the camera lens.

Optimisation of treatment time and reagent concentration

Preliminary trials were carried out on the optimum time and reagent concentrations required for development. A series of "dipping" times ranging from 10 seconds to 5 minutes at a solution concentration of 3.333 g $Eu(fod)_3$/L were compared. $Eu(fod)_3$ concentrations ranging from 0.133 g/L to 6.67 g/L using a 20 second "dipping" time were also compared.

Stability of prints after treatment

A trial was carried out on prints to establish the stability of the developed print (in air) after treatment. Print halves deposited on paper were used to compare stability of treatment 1 hour to 72 hours after treatment (this trial was carried out in triplicate).

To test the possibility that moisture in the air was reacting with the $Eu(fod)_3$-treated print a print deposited on paper was treated with $Eu(fod)_3$ and then cut bilaterally down the centre. One half was placed in a dry nitrogen atmosphere (drybox) for four days while the other half was left in a normal atmosphere for four days before both halves were compared.

Effect of print age

A trial was also carried out in order to establish whether the age of the latent print influenced the final development. Prints were deposited on paper and then cut in two. One half of each print was left for 10 minutes before being treated with $Eu(fod)_3$ while the other half of each print was left over a range of times from 1 minute to 72 hours before being treated with $Eu(fod)_3$. After each half print was treated it was placed in a nitrogen atmosphere to prevent further deterioration due to exposure to moisture while it awaited comparison with its corresponding print half (the trial was carried out in duplicate).

Age of solution

Two prints deposited on paper were cut in half down the centre. One half of each print was treated with a 1 week old $Eu(fod)_3$ solution. The other corresponding halves were treated with freshly prepared $Eu(fod)_3$ solution.

Effect of heat treatment

In order to test the effect of heat treatment on $Eu(fod)_3$ development one print was treated for 20 s and then cut in two, with one half being left to dry in air, and the other half left in an oven at 100°C for 2 mins (this was repeated in triplicate). A second print

was then cut in two, with one half being left in an oven at 100°C for 2 mins before both halves were treated with $Eu(fod)_3$ (this again was repeated in triplicate).

Compatibility with ninhydrin and DFO

The compatibility of $Eu(fod)_3$ treatment with two commonly-used reagents for the visualisation of latent fingerprints on porous surfaces was determined. The two reagents were ninhydrin, and DFO (1,8-diazafluoren-9-one), both of which react with the amino acid component of the print. Ninhydrin reacts to yield the coloured compound Ruhemann's Purple, whereas DFO forms a compound which emits in the yellow (550 nm) region when excited at 514.5 nm. An argon laser (1 watt) was used to produce the excitation light for DFO. Ninhydrin and DFO were both prepared in freon/acetic acid/ethanol solutions (Kent et al., 1986; and Lavis, 1994 respectively).

Comparison of three different solvents with petroleum spirits (b.p. 40-60 °C)

$Eu(fod)_3$ treatment using toluene, chloroform or freon as solvents compared with petroleum spirits (b.p. 40-60°C) was investigated. Fingerprints deposited on paper were cut in half down the centre. One set of halves was treated with $Eu(fod)_3$ in either toluene, chloroform or freon while the other corresponding halves were treated with $Eu(fod)_3$ in petroleum spirits (b.p. 40-60°C). The trial was carried out in duplicate.

Comparison of $Eu(fod)_3$/petroleum spirits (b.p. 40-60 °C) treatment on four different sufaces

$Eu(fod)_3$ treatment on four different surfaces was investigated using petroleum spirits (b.p. 40-60 °C) as the solvent. Fingerprints were deposited on a mylar (over-head transparency) sheet, aluminium foil, white ceramic tile and the outside painted surface of a coke can before being treated with $Eu(fod)_3$.

Selection of the best solvent for different surfaces

Various solvents were compared for use with $Eu(fod)_3$ treatment in order to establish the best one to use. Also, different solvents were tested in a systematic manner on different surfaces in order to establish which solvent works best for which surface. Up

to this point, petroleum spirits had been used as the solvent in all trials involving use of $Eu(fod)_3$. The selection of this was based mainly on the non-polar nature of $Eu(fod)_3$ and the need to exclude water. The possibility existed that other solvents might result in better development of prints, and for this reason, a range of formulations were trailed on a selection of surfaces. All solutions were prepared using a concentration of 6.67 g/L of $Eu(fod)_3$.

$Eu(fod)_3$ treatment using four different solvents was also compared on both the inside and outside painted surfaces of a coke can and on paper. Fingerprints were deposited onto strips cut from a coke can and onto strips of paper before being treated with either petroleum spirits (b.p. 40-60°C), ethyl acetate, hexane or dichloromethane.

$Eu(fod)_3$ treatment on different metals

Fingerprints were deposited on galvanized iron, stainless steel, brass, rusty iron and painted metal (type unknown). All five metal surfaces were then treated with $Eu(fod)_3$ in ethyl acetate.

$Eu(fod)_3$ treatment on a $5 banknote

$Eu(fod)_3$ treatment using either petroleum spirits (b.p. 40-60°C), ethyl acetate, or dichloromethane was investigated on fingerprints deposited on strips cut from a New Zealand $5 banknote.

Comparison of $Eu(fod)_3$ treatment with DFO treatment on porous surfaces

In order to get a reliable relative measure of the degree of fluorescence obtainable from $Eu(fod)_3$-treated prints fifty prints were deposited on paper and then cut down the centre into halves with half of each print being treated with $Eu(fod)_3$ and the other half with DFO, one of the most effective reagents in its class currently used (Kent et al., 1986). DFO–treated prints were excited at 514.5 nm, and $Eu(fod)_3$–treated prints were excited at 254 nm.

Comparison of Eu(fod)$_3$ treatment with superglue/panacryl treatment on non-porous sufaces

In order to gauge the efficiency of Eu(fod)$_3$ on non-porous surfaces, a comparison was made with the superglue fuming/staining method. Ten prints were deposited equally over ten pairs of galvanized iron strips and three prints were deposited equally over three pairs of aluminium coke can strips. One set of half prints were treated with Eu(fod)$_3$/ethyl acetate while the other corresponding set of half prints were treated with superglue followed by panacryl staining (Lavis, 1994).

Enhancement of luminescence following Eu(fod)$_3$ treatment

Two different methods for the possible enhancement of the luminescence after Eu(fod)$_3$ treatment were investigated. Liquid nitrogen was used to cool a Eu(fod)$_3$-treated latent fingerprint deposited on paper while being subjected to UV excitation. This method is often used for the enhancement of ninhydrin/$ZnCl_2$–treated fingerprints and is based on the idea that fluorescence becomes more likely as vibrational modes are frozen out (Skoog et al., 1996). A Eu(fod)$_3$–treated fingerprint deposited on paper was also treated with a solution of 75 mg 1,10–phenanthroline in 40 mL methanol and 10 mL acetone. This method has been used in the enhancement of lanthanide fluorescence (Lock et al., 1995) and is based on the known ability of a coordinate bidentate ligand to cause enhanced europium fluorescence (compared with coordination of two unidentate ligands) (Allred et al., 1997).

Eu(fod)$_3$ as a cyanoacrylate dye

The coordinatively-saturated eight-coordinate europium complexes such as thenoyl europium chelate (TEC) are used as luminescent dyes to enhance fingerprints developed with cyanoacrylate (Wilkinson and Watkin, 1993). It is possible that Eu(fod)$_3$, which is only six-coordinate, may also be able to act as a suitable luminescent dye for the enhancement of fingerprints developed with cyanoacrylate. Five fingerprints were placed onto five glass microscope slides and fumed in an oven with cyanoacrylate vapours according to the method of Lavis (1994). Eu(fod)$_3$ in methyl

ethyl ketone (MEK) (5g/L) was poured onto the surface of three of these slides and left to soak into the cyanoacrylate developed prints for 2, 5 and 10 minutes respectively. The solution was then run off onto a paper towel. $Eu(fod)_3$ solution was then poured onto the other two slides for 2 and 5 minutes respectively before both were rinsed in acetone (AR) for a few seconds. All five slides were then examined using the hand-held UV lamp (254 nm).

Effect of water

Twenty prints were deposited on strips of paper and then cut down the centre. One set of halves were immersed for one minute in distilled water and then left to air dry. Both sets of halves were then treated with $Eu(fod)_3$ in petroleum spirits.

Effect of lipids

Four prints were deposited on paper using Fernleaf semisoft butter as a "lipid mimic". The prints were then treated with $Eu(fod)_3$.

$Eu(dpm)_3$ fingerprint trial

Ten fingerprints were deposited on white paper and then treated with a solution of $Eu(dpm)_3$ in toluene (6.068 g/L) for 20 seconds before being placed under the UV hand-held lamp on both the 254 and 366 nm wavelength settings.

$Tb(fod)_3$ fingerprint trials

Ten fingerprints were deposited on white paper and treated with $Tb(fod)_3$ in petroleum spirits (b.p. 40-60°C) (6.67 g/L) for 20 seconds. Four fingerprints were then deposited on pink paper (less background fluorescence) and were treated for 1, 5, 20 seconds and 2 mins respectively. Two fingerprints deposited on glossy white paper were treated for 1 second. Fingerprints were also deposited on a glass microscope slide, aluminium foil, a clear plastic bag and a mylar (over-head transparency) sheet and treated with $Tb(fod)_3$ in petroleum spirits (b.p. 40-60°C) (6.67 g/L) for 20 seconds.

Tb-DTPA-pAS chelate trials

Two different DTPA-pAS solutions were prepared.

Solution One:

DTPAA (0.092 m*M*, 36 mg) was dissolved in 5 mL of dimethyl sulfoxide (DMSO), previously dried over molecular sieve 4A. *p*-aminosalicylic acid (0.092 m*M*, 14 mg) was dissolved in 0.46 mL DMSO. The two solutions were mixed together. $TbCl_3.6H_2O$ solution (0.092 m*M*, 1.83 mL), prepared by addition of 0.1867 g $TbCl_3.6H_2O$ to 10 mL water was added to the DTPA-pAS solution.

Solution Two:

DTPAA (0.183 m*M*, 72 mg) and triethylamine (0.2 m*M*, 28 µL) were dissolved in 1 mL of dimethyl sulfoxide (DMSO), previously dried over molecular sieve 4A. *p*-aminosalicylic acid (0.235 m*M*, 36 mg) was dissolved in 1 mL DMSO. The p-AS solution was added dropwise to the stirred DTPAA solution and the mixture was stirred for 30 minutes at room temperature. $TbCl_3.6H_2O$ solution (0.183 m*M*, 3.66 mL), prepared by addition of 0.1867 g $TbCl_3.6H_2O$ to 10 mL water containing 87 µL concentrated HCl, was added to the DTPA-pAS solution. The Tb-DTPA-pAS solution was then made up to 20 mL with phosphate buffer (pH 7.0).

A latent fingerprint deposited on paper was treated with the Tb-DTPA-pAS solution (Solution One) for 10 seconds and left to dry before being viewed under the hand-held UV lamp at 254 nm.

A latent fingerprint deposited on paper was treated with just the $TbCl_3.6H_2O$ solution for 10 seconds and left to dry before being viewed under the hand-held UV lamp at 254 nm.

A blood fingerprint deposited on paper (previously fixed – see section 2.5.1) was treated with the Tb-DTPA-pAS solution (Solution Two) for 10 seconds and left to dry before being viewed under the hand-held UV lamp at 254 nm.

A set of five latent and five blood fingerprints deposited on white paper were then treated with the Tb-DTPA-pAS solution (Solution Two) for 30 seconds after which they were left to dry before being viewed under the hand-held UV lamp at 254 nm.

4.2.7 Chemistry of the $Eu(fod)_3$ reaction with latent fingerprints

The following work was carried out in order to determine what types of fingerprint components $Eu(fod)_3$ is most likely to be reacting with.

Non-lipid fingerprint components

It is possible that $Eu(fod)_3$ could react with amino acids, amines, monosaccharides, urea and lactic acid, all of which are non-lipids and are found in latent fingerprints (Fig. 4.3).

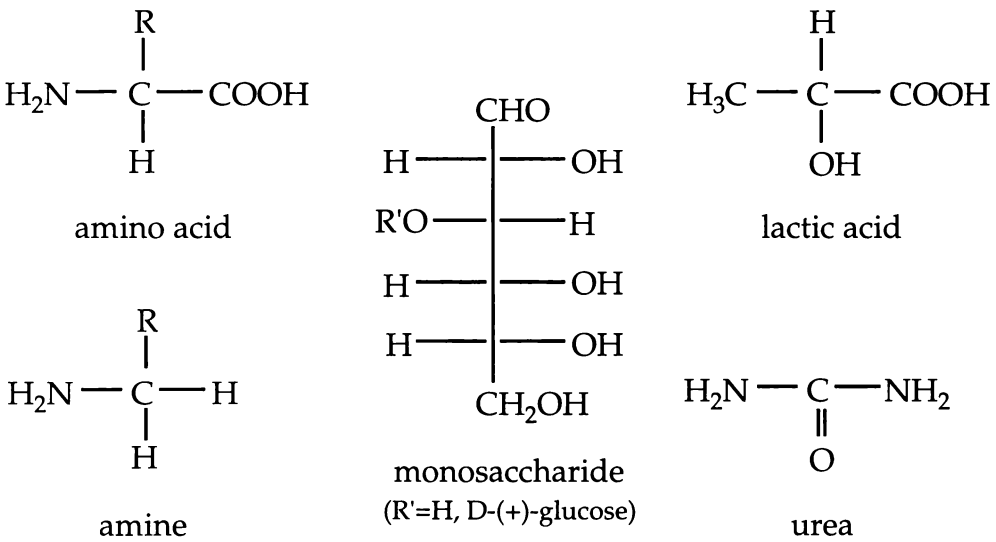

Fig. 4.3
Some non-lipid fingerprint components.

Evidence for the reactivity of $Eu(fod)_3$ with glycine (an amino acid), triethylamine (an amine), glucose (a monosaccharide), and urea was obtained by using a pasteur pipette to place a small spot of an aqueous solution of the substance under investigation on white paper. The paper was dried at 100°C for two minutes in an oven and then

treated with $Eu(fod)_3$ solution (6.67 g/L, Pet. Spirits) and examined under the hand-held UV lamp.

Evidence for the reactivity of $Eu(fod)_3$ (and $Tb(fod)_3$) with glycine, triethylamine, urea, and acetic acid and propionic acid (both contain the carboxylic acid group of amino acids), was obtained by adding each potential ligand into a solution containing the lanthanide chelate, and analysing ions formed using electrospray mass spectrometry (ESMS). ESMS spectra were recorded on a Fisons VG Platform II instrument. The sample was injected into the spectrometer via a Rheodyne injector fitted with a 10 µL sample loop. A Thermo Separation Products SpectraSystem P1000 LC pump delivered the solution to the mass spectrometer source at a flow rate of 0.01 mL min^{-1} and nitrogen was employed both as a drying and nebulising gas. The cone voltage was set at 20 V.

Previously, evidence for ligand exchange processes involving acetate ions and lanthanide (Ln) 2,2,6,6-tetramethyl-3,5-heptanedione (dpm) complexes $Eu(dpm)_3$, $Gd(dpm)_3$, $Yb(dpm)_3$ has been obtained using ESMS (Curtis et al, 1992a and 1992b). The following experimental methods are based on this work.

Acetic acid is the simplest of the water-soluble carboxylic acids likely to be found in the latent fingerprint. A 10 mg amount of $Eu(fod)_3$ (and $Tb(fod)_3$) was added to 20 mL of carrier solution. The carrier solution was prepared from 95 mL MeOH, 95 mL H_2O (1:1 ratio) and 10 mL acetic acid.

Propionic acid is the next simplest water-soluble carboxylic acid after acetic acid. A 10 mg amount of $Eu(fod)_3$ was added to 20 mL of carrier solution. The carrier solution was prepared from a 1:1 $MeOH/H_2O$ solution plus 13 mL propionic acid (200 mL total).

Glycine (NH_2CH_2COOH) is the simplest of the water-soluble amino acids likely to be found in the latent fingerprint. A 10 mg amount of $Eu(fod)_3$ and 2.17 mg (3 mole excess) of glycine was added to 20 mL of carrier solution. The carrier solution (200 mL

total) was prepared from a 1:1 MeOH/H_2O solution plus 10 mL acetic acid (acetic acid was required in this case to dissolve $Eu(fod)_3$).

Urea is also likely to be available in a latent fingerprint for reaction with $Eu(fod)_3$. A 10 mg amount of $Eu(fod)_3$ and 4.7 mg (large excess) of urea was added to 20 mL of carrier solution. The carrier solution (200 mL total) was prepared from a 1:1 MeOH/H_2O solution plus 1 % propionic acid (propionic acid was required to dissolve the $Eu(fod)_3$).

Triethylamine ($(CH_3CH_2)_3N$) is an example of a water-soluble amine. A 10 mg amount of $Eu(fod)_3$ and 50 µL (large excess) of triethylamine was added to 20 mL of carrier solution. The carrier solution (200 mL total) was prepared from a 1:1 MeOH/H_2O solution plus 10 mL acetic acid (acetic acid was required to dissolve the $Eu(fod)_3$).

Lipid fingerprint components

The lipid component of fingerprints is made up of mostly triglycerides (triacylglycerols) and free fatty acids (Morrison and Boyd, 1973) (Fig. 4.4).

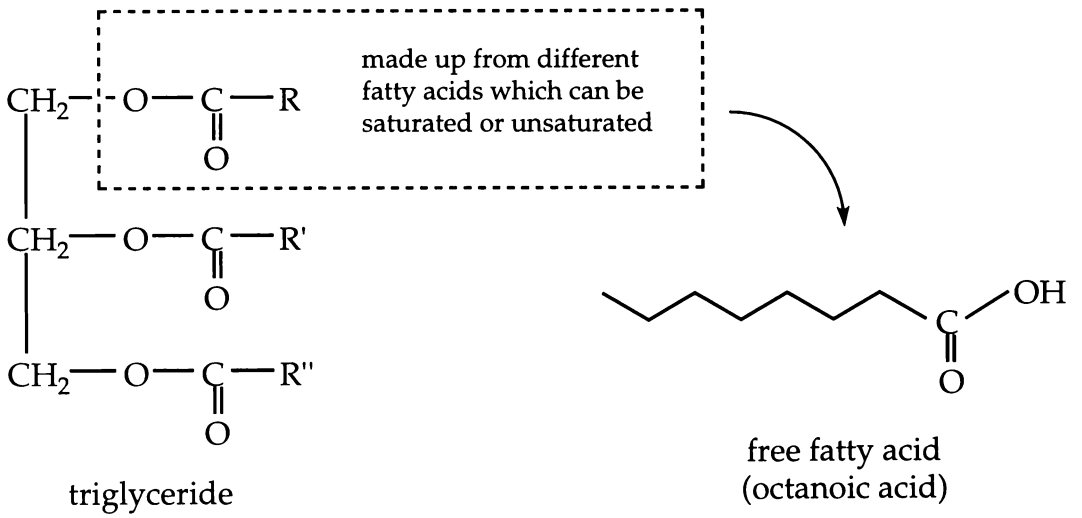

Fig. 4.4
Triglyceride and free fatty acid structures.

Evidence of hexanoic acid binding to $Eu(fod)_3$ has been published by Shoffner, 1974. Hexanoic acid seems to be on the boundary between what is considered a fatty acid and what is considered to be a water soluble carboxylic acid. For the purpose of this work however, it was decided that octanoic acid should be used as a representative free fatty acid.

Evidence of octanoic acid binding to $Eu(fod)_3$ (and $Tb(fod)_3$) was obtained by recording a fluorescence emission spectrum for a 0.5 g/L solution in petroleum spirits (b.p. 40-60°C). A large molar excess (10 µL) of octanoic acid was then added to 2 mL of the solution and a fluorescence emission spectrum was then recorded. Slit widths for both excitation and emission were set at 15 nm (10 nm for $Tb(fod)_3$ in X4), with solutions being held in a 10 mm quartz cuvette.

Supporting evidence for the binding or association of octanoic acid to $Eu(fod)_3$ was obtained by recording a UV/Vis spectrum of a 0.02 g/L solution of $Eu(fod)_3$ in petroleum spirits (b.p. 40-60°C). A large molar excess (10 µL) of octanoic acid was then added to the solution and a UV/Vis spectrum was then recorded. Solutions were held in a 10 mm quartz cuvette.

4.3 *Results and discussion of solution trials*

4.3.1 Excitation-emission spectra of $Eu(fod)_3$

A poorly defined spectrum with very broad and overlapping peaks was obtained for $Eu(fod)_3$ in petroleum spirits (80-100°C). This was probably due to fluorescent contributions from higher molecular weight aromatic hydrocarbons in the solvent. It was consequently decided that it would be too difficult to make a proper assessment of the $Eu(fod)_3$ spectrum in the presence of petroleum spirits (80-100°C) and this solvent was therefore dispensed with.

Very similar emission and excitation spectra were obtained for $Eu(fod)_3$ with both petroleum spirits (40-60°C) and X4 as the solvents, but with some differences in intensities occurring. It was decided therefore that either solvent could be used interchangeably for $Eu(fod)_3$. There was also little difference found in fluorescent excitation-emission spectra between $Eu(fod)_3$ solutions prepared six months apart, indicating that $Eu(fod)_3$ is reasonably stable. The sharp emission in the orange region at 614 nm, when excited at 340 nm, is the main emission most likely to be of use in fingerprint visualisation. Results are presented in Tables 4.1 to 4.4 and Figures 4.5 to 4.8.

Table 4.1
Emission wavelengths and intensities for $Eu(fod)_3$ in two solvents, when excited at between 340–342 nm.

$Eu(fod)_3$ in X4 with excitation at 340 nm		342 nm[a]		$Eu(fod)_3$ in Pet. Spirits with excitation at 342 nm[b]		341 nm[a]	
Emission λ	Intensity	Emission λ	Intensity	Emission λ	Intensity	Emission λ	Intensity
614.0	198	614.0	206	614.5	183	614.0	162
592.0	25	592.0	25	589.5	28	591.5	20
537.5	14	537.5	16	537.5	20	537.5	10
379.5	20	371.5	55	382.5	41	380.5	21

[a]results obtained 6 months later using new solutions, [b]15 nm slit width used.

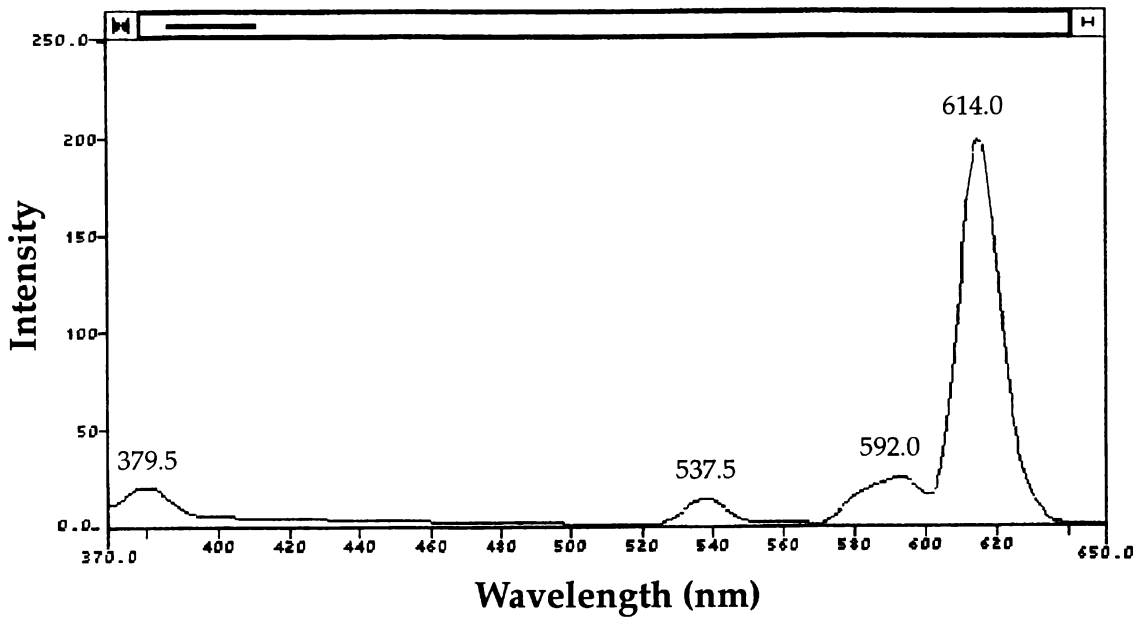

Fig. 4.5
Emission spectrum for $Eu(fod)_3$ in X4 with excitation at 340 nm.

Table 4.2
Emission wavelengths and intensities for $Eu(fod)_3$ in two solvents, when excited at between 222–226 nm.

$Eu(fod)_3$ in X4 with excitation at 225 nm		226 nm[a]		$Eu(fod)_3$ in Pet. Spirits with excitation at 225 nm[b]		222 nm[a]	
Emission λ	Intensity	Emission λ	Intensity	Emission λ	Intensity	Emission λ	Intensity
613.5	54	613.5	61	614.0	81	613.5	101
592.5	7	592.0	7	590.0	12	593.0	12
537.0	5	537.0	5	536.5	10	537.0	7
		459.0	23			451.5	76
350.5	212	351.5	206	352.0	785	350.0	152

[a]results obtained 6 months later using new solutions, [b]15 nm slit width used.

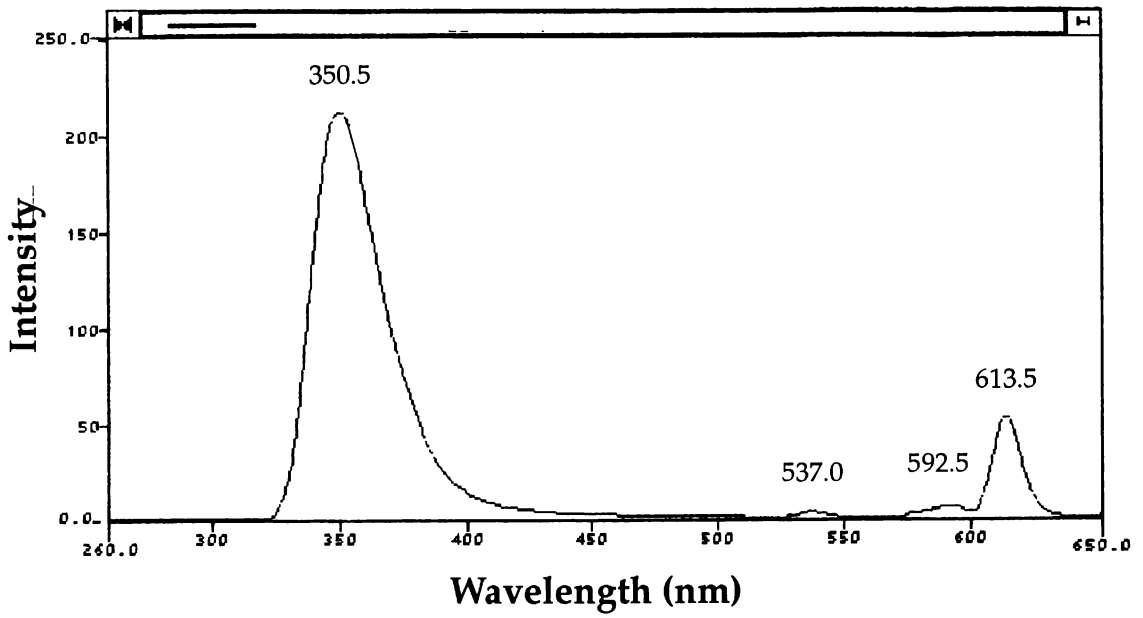

Fig. 4.6
Emission spectrum for $Eu(fod)_3$ in X4 with excitation at 225 nm.

Table 4.3
Maximum excitation wavelengths and intensities for the 614 nm emission from $Eu(fod)_3$ in two solvents.

$Eu(fod)_3$ in X4 for emission at 614 nm		$Eu(fod)_3$ in X4 for emission at 614 nm[a]		$Eu(fod)_3$ in Pet. Spirits for emission at 614 nm[b]		$Eu(fod)_3$ in Pet. Spirits for emission at 614 nm[a]	
Excitn. λ	Intensity	Excitn. λ	Intensity	Excitn. λ	Intensity	Excitn. λ	Intensity
340.0	199	342.0	206	342.0	185	341.0	162
238.0	68	240.5	72	242.0	83	241.5	91
228.5	67	229.0	64	225.5	85	225.0	107

[a]results obtained 6 months later using new solutions, [b]15 nm slit width used.

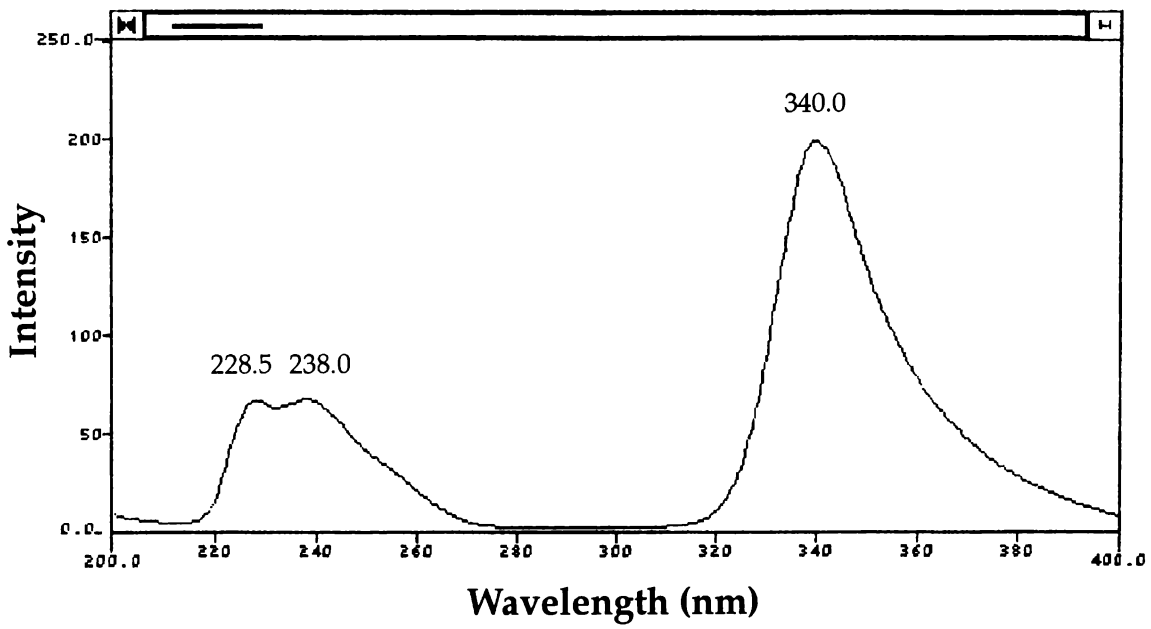

Fig. 4.7
Excitation spectrum for $Eu(fod)_3$ in X4 for the emission at 614 nm.

Table 4.4
Maximum excitation wavelengths and intensities for the 350–352 nm emission from Eu(fod)$_3$ in two solvents.

Eu(fod)$_3$ in X4 for emission at 351 nm		Eu(fod)$_3$ in X4 for emission at 351 nm[a]		Eu(fod)$_3$ in Pet. Spirits for emission at 352 nm[b]		Eu(fod)$_3$ in Pet. Spirits for emission at 350 nm[a]	
Excitn. λ	Intensity	Excitn. λ	Intensity	Excitn. λ	Intensity	Excitn. λ	Intensity
225.5	227	225.5	156	222.0	150	224.5	850

[a]results obtained 6 months later using new solutions, [b]15 nm slit width used.

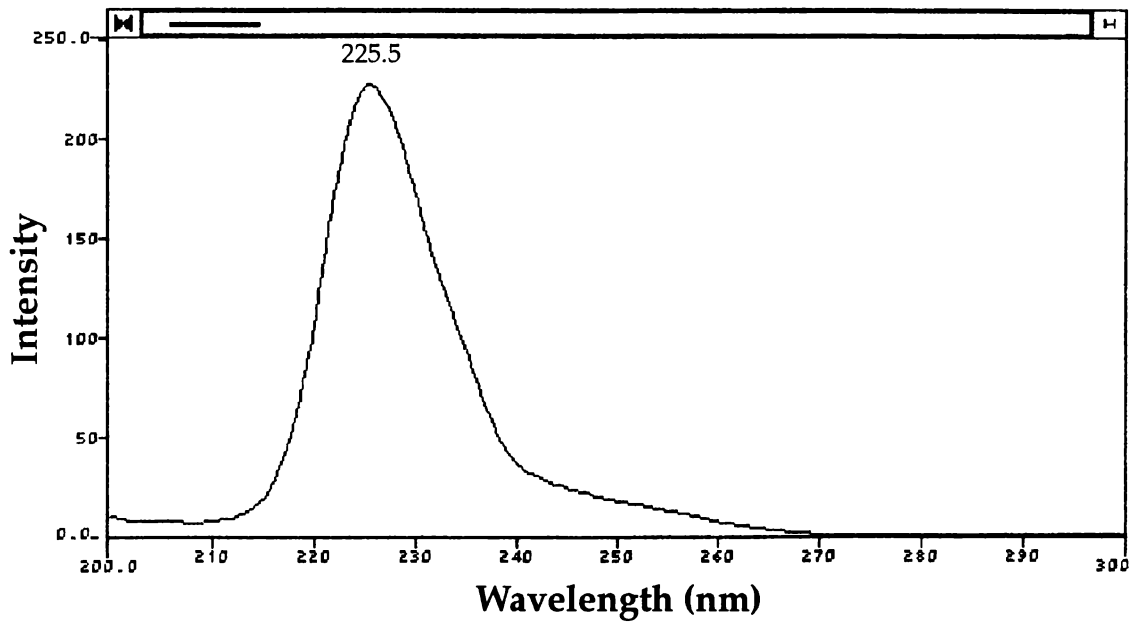

Fig. 4.8
Excitation spectrum for Eu(fod)$_3$ in X4 for the emission at 351 nm.

A three dimensional excitation–emission spectrum of Eu(fod)$_3$ in X4 was obtained (Fig. 4.9). It was felt that a three dimensional spectrum would be useful for determining the optimum emission wavelength using a particular excitation wavelength. This could be useful if a fingerprint examiner was trying to avoid getting interfering emissions from the background of a fingerprint exhibit. The raw data for Fig. 4.9 is included in Appendix 4.2. Retabulation of this data in a graphical spreadsheet database such as *Microsoft® Excel* will allow viewing of the excitation–emission spectrum from any convenient angle.

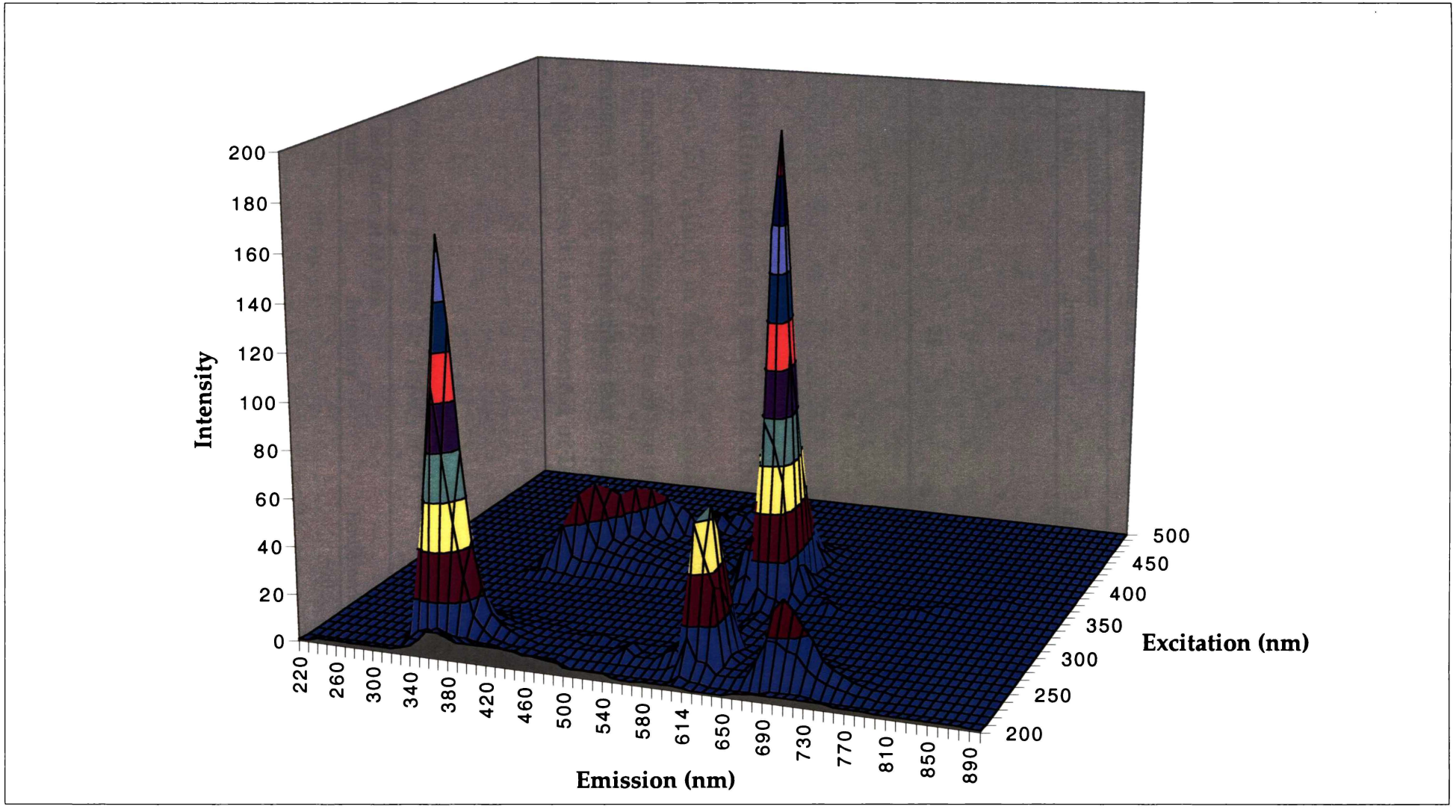

Fig. 4.9
Three dimensional excitation-emission spectrum of Eu(fod) 3 .

Emission intensities for the excitation of $Eu(fod)_3$ at 254 and 366 nm (the wavelength settings of the UV hand-held lamp) are presented in Table 4.5. Under these conditions, the 614 nm emission is twice as intense when excited at 366 nm compared with that obtained at 254 nm.

Table 4.5
Emission wavelengths and intensities for $Eu(fod)_3$ in X4.

Excitation at 366 nm		Excitation at 254 nm	
Emission λ (nm)	Intensity	Emission λ (nm)	Intensity
614.0	63	613.5	31
592.5	8	590.0	4
537.0	5	537.0	2
410.0	29		

4.3.2 Excitation-emission spectra of $Tb(fod)_3$

The emission for $Tb(fod)_3$ in the green region, at 547 nm, when excited at 337 nm, is the main emission most likely to be of use in fingerprint visualisation. The intensity of this emission is over three times that obtained for the main emission of $Eu(fod)_3$ in the visible region. Results are presented in Tables 4.6 and 4.7 and Figures 4.10 to 4.12.

Table 4.6
Emission wavelengths and intensities for $Tb(fod)_3$ in X4.

Excitation at 243 nm		Excitation at 337 nm	
Emission λ (nm)	Intensity	Emission λ (nm)	Intensity
620.0	3	620.5	8
585.0	11	585.5	28
546.5	294	547.0	719
491.0	138	491.0	340
		376.0	23

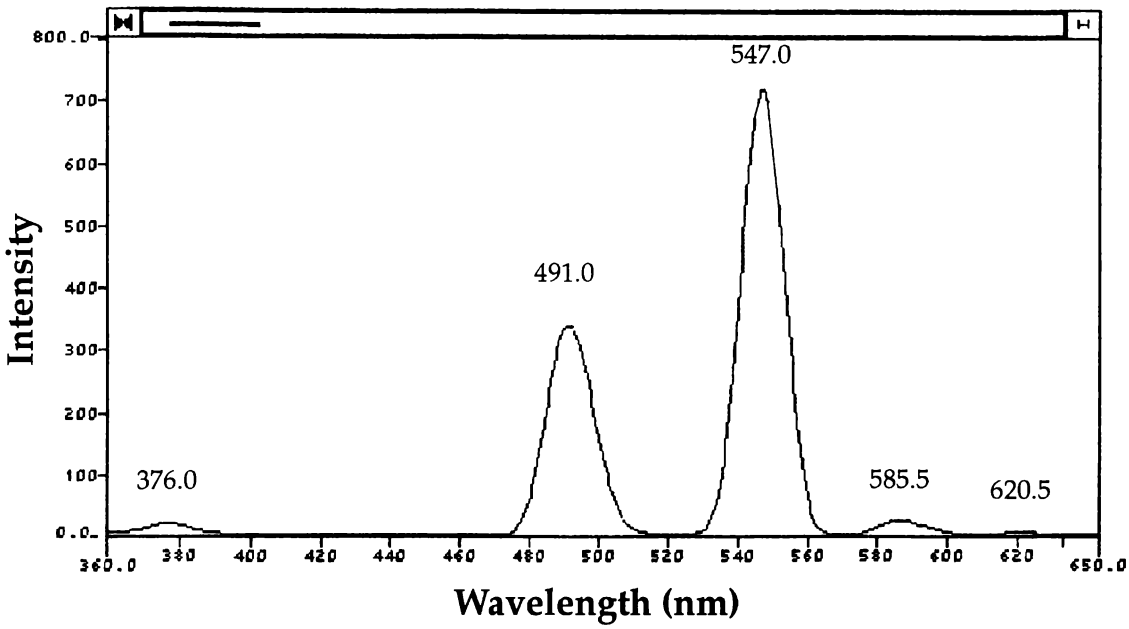

Fig. 4.10
Emission spectrum for $Tb(fod)_3$ in X4 with excitation at 337 nm.

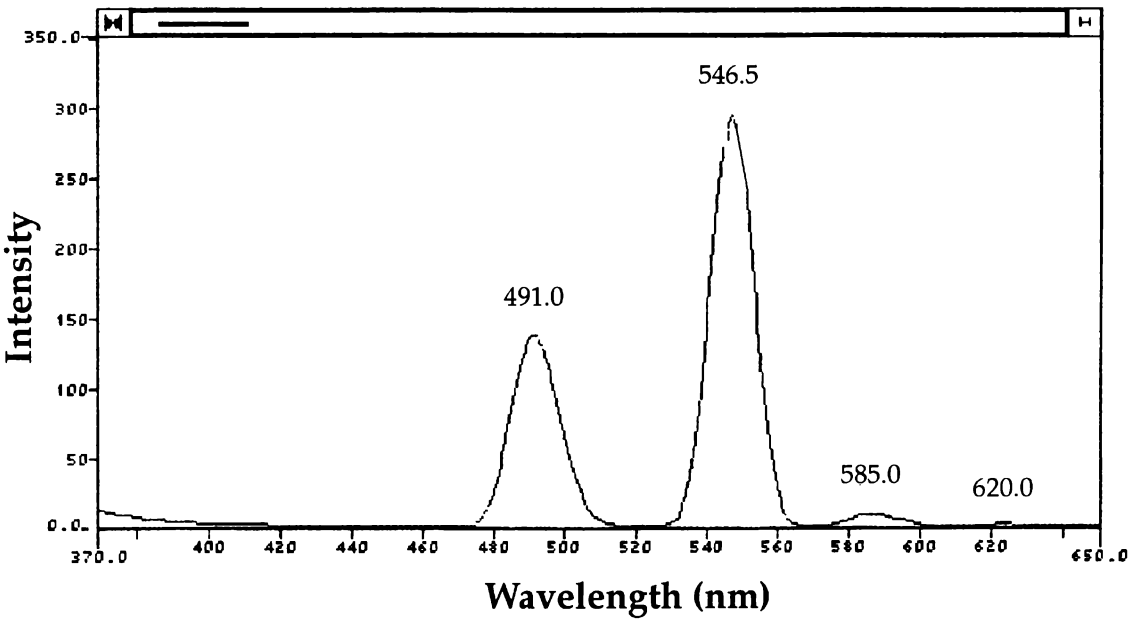

Fig. 4.11
Emission spectrum for $Tb(fod)_3$ in X4 with excitation at 243 nm.

Table 4.7
Excitation wavelengths and intensities for $Tb(fod)_3$ for the 547 nm emission.

Excitation wavelength (nm)	Intensity
472.0	2
337.0	716
243.0	299

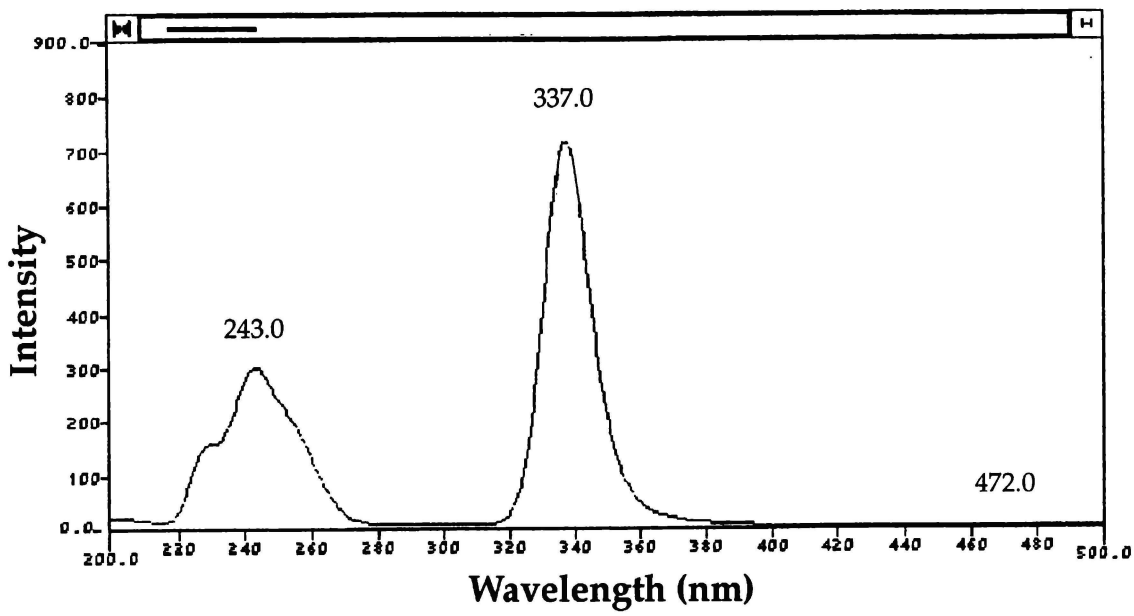

Fig. 4.12
Excitation spectrum for $Tb(fod)_3$ in X4 for emission at 547 nm.

A three dimensional excitation–emission spectrum of $Tb(fod)_3$ in X4 was obtained (Fig. 4.11). The raw data for this is provided in Appendix 4.2.

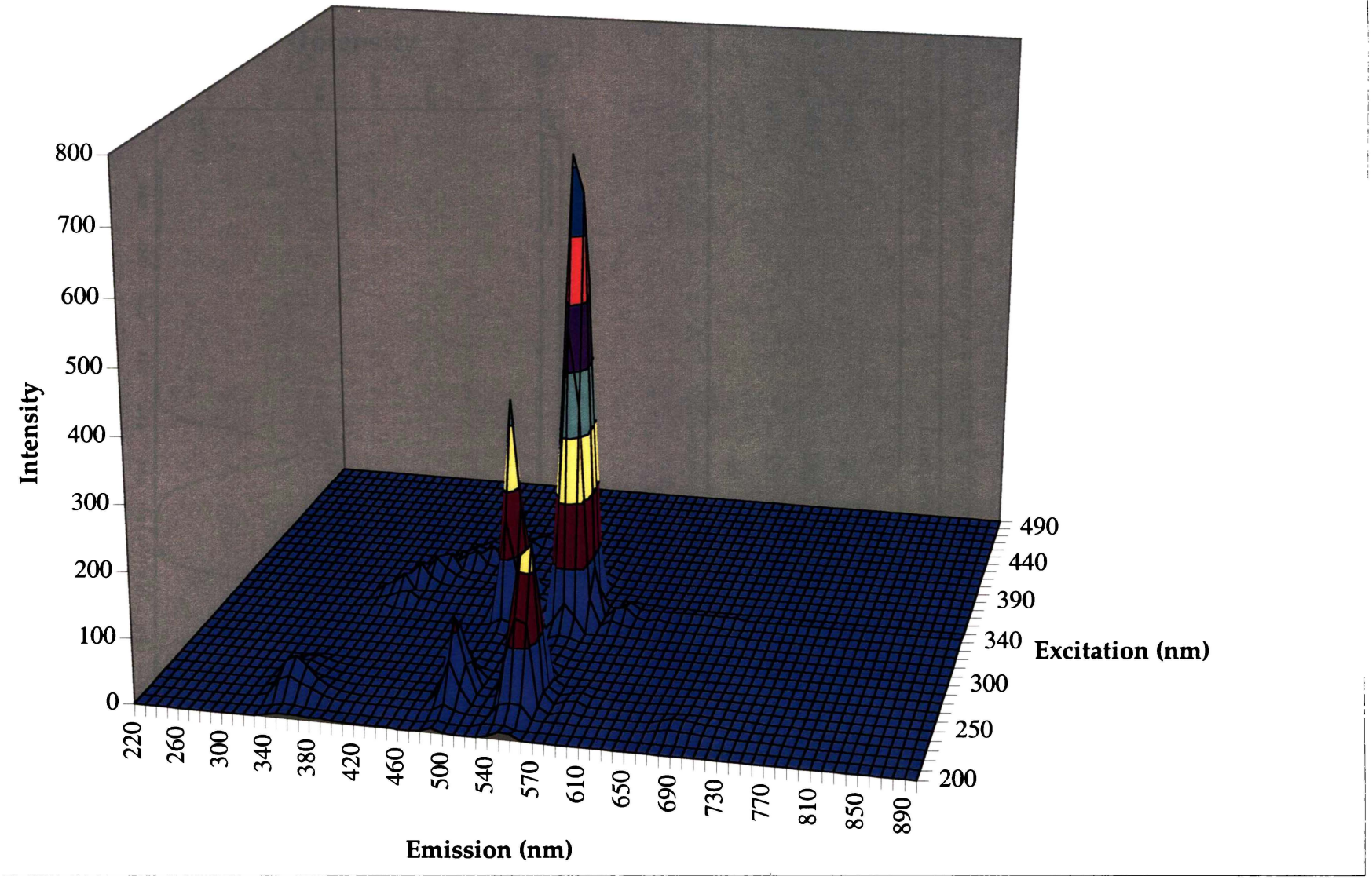

Fig. 4.13
Three dimensional excitation-emission spectrum of Tb(fod) $_3$.

4.3.3 Excitation-emission spectra of a mixture of $Eu(fod)_3$ and $Tb(fod)_3$

Excitation of a 50/50 mixture of $Eu(fod)_3$ and $Tb(fod)_3$ in X4 produced a mixture of the emissions whose wavelengths were not significantly different from those expected for each lanthanide complex individually. The 614 nm (europium) and 547 nm (terbium) emissions were both significantly reduced in intensity. Results are presented in Tables 4.8 and 4.9 and Figures 4.14 to 4.16 (individual emission graphs taken under similar conditions are provided in figures 4.5 and 4.10 respectively).

Table 4.8
Emission wavelengths and intensities for a mixture of $Eu(fod)_3$ and $Tb(fod)_3$ in X4 when excited at 338 nm.

Emission wavelength (nm)	Intensity	Corresponding source
614.0	156	Eu
588.5	29	Eu or Tb
546.5	282	Tb
491.0	131	Tb
377.0	19	Eu or Tb

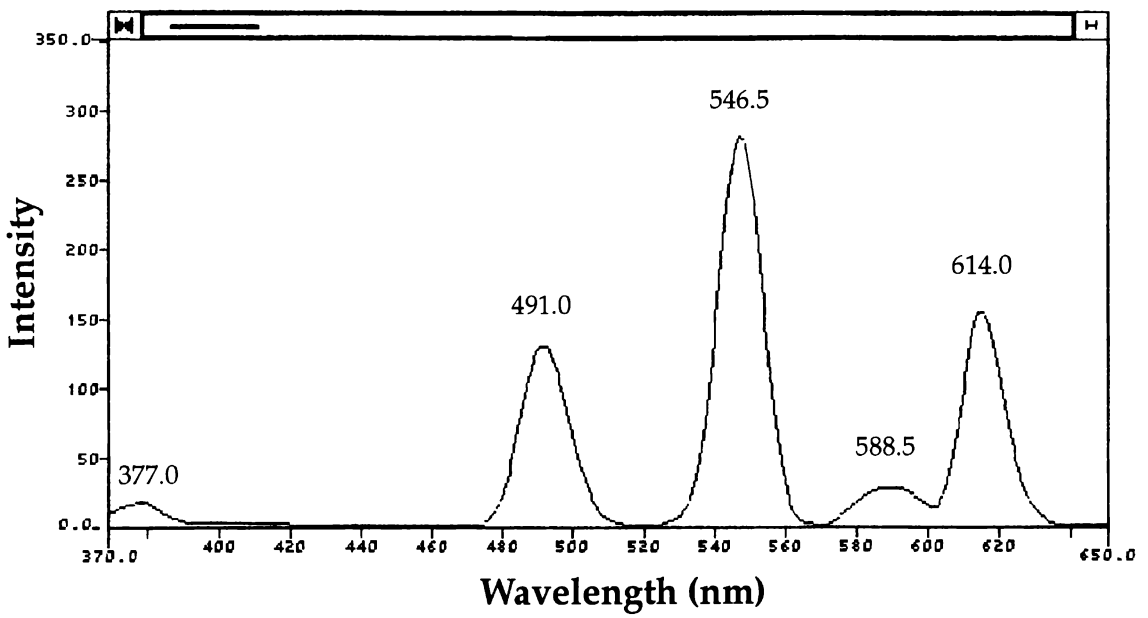

Fig. 4.14
Emission spectrum for a mixture of $Eu(fod)_3$ and $Tb(fod)_3$ in X4 with excitation at 338 nm.

Table 4.9
Excitation wavelengths and intensities for a mixture of $Eu(fod)_3$ and $Tb(fod)_3$ in X4.

547 nm Emission		614 nm Emission	
Excitation λ (nm)	Intensity	Excitation λ (nm)	Intensity
472.0	2	339.5	158
337.0	278	242.0	33
242.0	153		

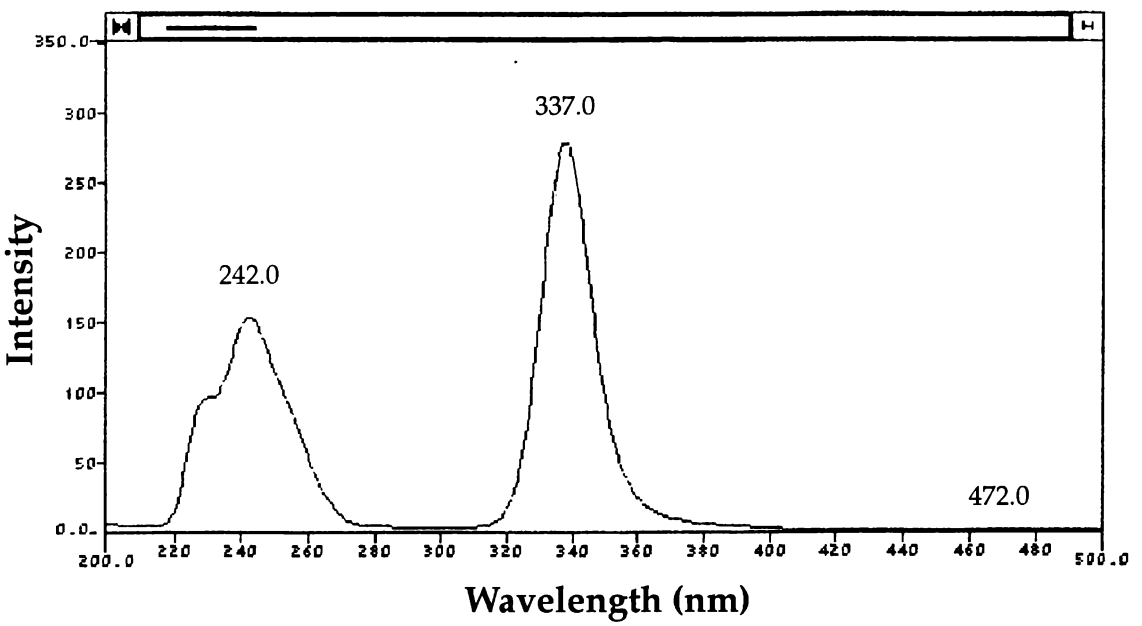

Fig. 4.15
Excitation spectrum for a mixture of $Eu(fod)_3$ and $Tb(fod)_3$ in X4 for emission at 547 nm.

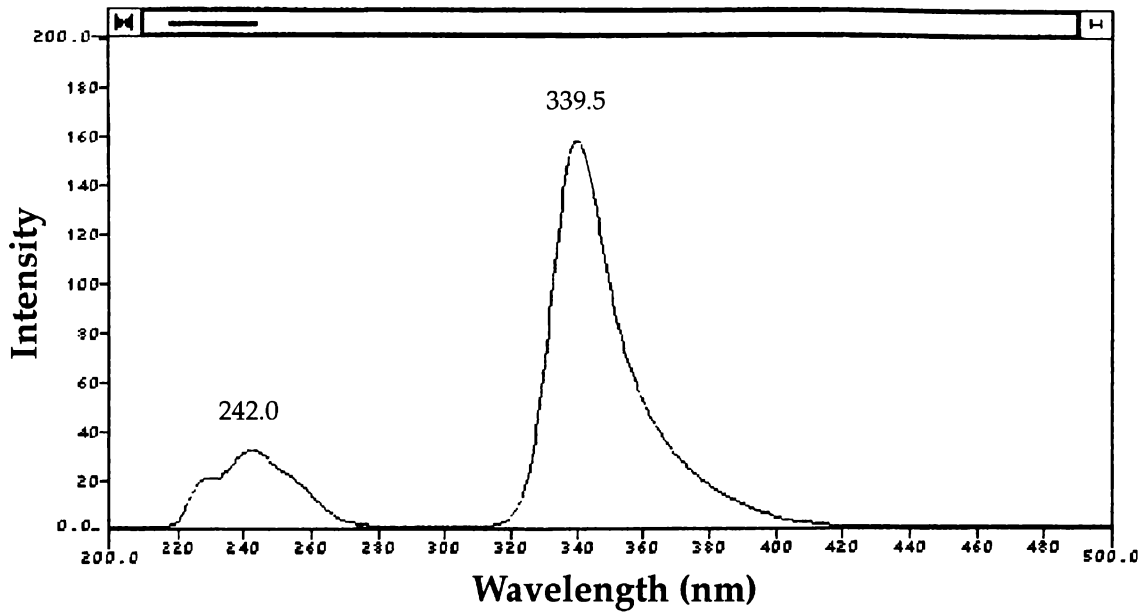

Fig. 4.16
Excitation spectrum for a mixture of $Eu(fod)_3$ and $Tb(fod)_3$ in X4 for emission at 614 nm.

4.3.4 Excitation–emission spectra of $Eu(dpm)_3$

A prescan of $Eu(dpm)_3$ in toluene produced the following results. Two emissions at 435 and 614 nm with intensities of 21 and 4 respectively were obtained by excitation at 385 nm. It was decided that the fluorescent intensities of this compound were too low to be of practical use.

4.4 *Results and discussion of fingerprint trials*

4.4.1 General remarks

In moving from solution studies to those of $Eu(fod)_3$, $Eu(dpm)_3$ and $Tb(fod)_3$-treated fingerprints on surfaces, the hand-held UV lamp was used. This has a mercury, vapour source, with two wavelength settings of 254 and 366 nm, and it was found that the 254 nm setting gave the best visualisation for $Eu(fod)_3$-treated prints. This is contrary to emission/excitation results obtained for $Eu(fod)_3$ in solution (see Table 4.5) which indicated that the 614 nm emission should be twice as intense when excited at 366 nm rather than at 254 nm. A possible reason for the difference between solution and surface results is that the 254 nm mercury line is simply more intense than that at 366 nm. This is borne out by the fact that the 254 nm line is the most sensitive mercury wavelength in atomic absorption spectroscopy. Alternatively, the difference may reflect genuine changes in the emission characteristics of the lanthanide shift reagent upon chemical complexation and/or immobilisation by absorption into the fingerprint.

4.4.2 $Eu(fod)_3$ fingerprint trials

Preliminary comments

Successful visualisation of prints was obtained on white photocopy paper (some background fluorescence from optical brightners*), galvanized iron, and aluminium drink cans, examples of which are presented in Figures 4.17, 4.18 and 4.19 respectively.

* About 80% of all optical brightening agents produced are derived from stilbene which absorbs at 342 nm. Absorbances of the optical brightners of the CC/DAS type (which are used specifically for paper) lie between 347 to 352 nm with fluorescence maximum emissions between 432 and 442nm (Zahradník, 1982).

Fig. 4.17
Visualisation of a $Eu(fod)_3$ treated print on white paper (excited at 320 nm).

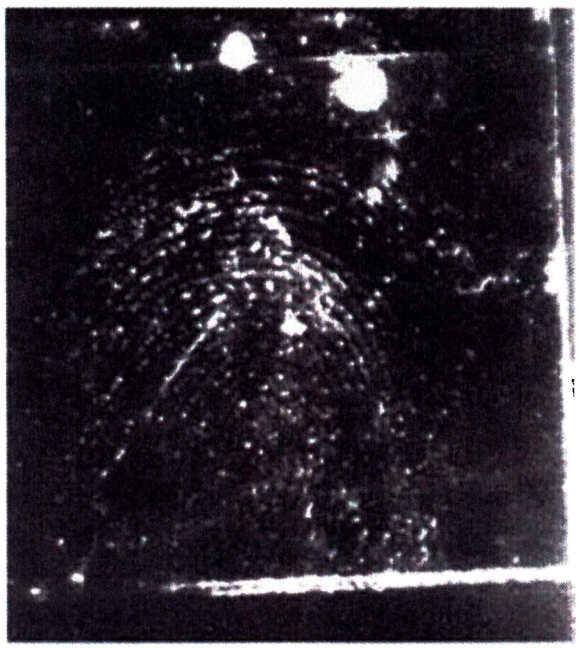

Fig. 4.18
Visualisation of a $Eu(fod)_3$ treated print on galvanized iron (excited at 320 nm).

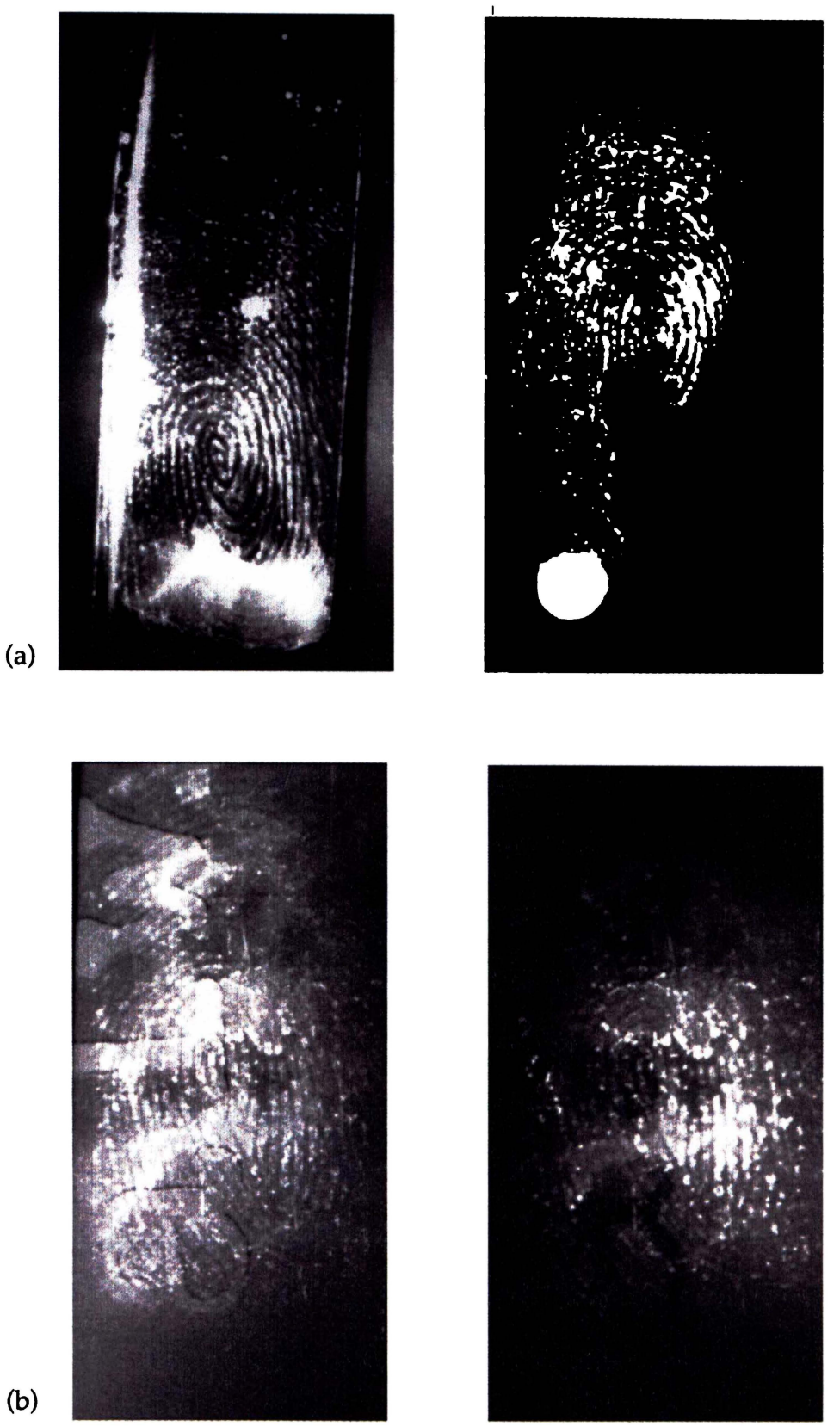

Fig. 4.19
Visualisation of $Eu(fod)_3$ treated prints on the inner (a) and outer (b) surfaces of an aluminium coke can (excited at 320 nm).

Optimisation of treatment time and reagent concentration

Twenty seconds was found to be the best "dipping" time from a series ranging from 10 seconds to 5 minutes at a solution concentration of 3.333 g $Eu(fod)_3$/L (Table 4.10). Using this dipping time, print development was found to get steadily better as the $Eu(fod)_3$ concentration was raised from 0.133 g/L (no prints visible) to 6.667 g/L (very good prints) (Table 4.11). It was decided that a twenty second dipping time in a solution of 6.667 g/L $Eu(fod)_3$ should be used for all further work. It is important to note when using this reagent that dipping times longer than 20 seconds result in poorer outcomes. This effect was examined using iodine vapour and found to be related to dissolution of the lipid fraction of the fingerprints in the petroleum spirits.

Table 4.10
Treatment time comparisons for a 3.333 g/L solution of $Eu(fod)_3$ on pairs of half prints.

Time (s)	Comparison of print halves
10 & 20	no difference between treatment times
20 & 120	slightly better development for 20 s treatment time
120 & 300	better development for 120 s treatment time

Table 4.11
Comparison of concentrations for $Eu(fod)_3$ treatment on pairs of half prints, using a 20 second dipping time.

Concentration (g/L)	Comparison of print halves
0.133 and 0.413	No prints visible
0.947 and	poor
2.747	moderately good
2.747 and	moderately good
6.667	good

Stability of prints after treatment

The results indicated that times up to 8 hours after development are still as good as when prints were freshly developed. However, after 24 hours, some fading is evident, and after 72 hours, only the outer parts of the print are visible (Table 4.12).

Table 4.12
Stability of $Eu(fod)_3$ treatment on print halves.

Time after development (hr)	Comparison of print halves
0 & 2	good
0 & 8	good
0 &	good
24	reasonable
0 &	good
72	only outer parts of print visible

It was speculated that the reason for this effect might be that moisture in the air was reacting with the $Eu(fod)_3$-treated print and reducing the fluorescence intensity. The results from the nitrogen atmosphere trial indicated that this could be possible. After four days, the half print left in the nitrogen atmosphere was still fully visible while the other half was only partially visible. The observed deterioration of $Eu(fod)_3$-treated prints in air is therefore likely to be caused by progressive entry of H_2O from the air into the inner coordination sphere around europium (and displacement of other ligands) a process which is known to quench lanthanide fluorescence (Bailey et al., 1988). It is assumed that on initial treatment, $Eu(fod)_3$ reacts with functional groups containing oxygen (eg. carboxylate) in the lipid or non-lipid component of the prints to form a more preferred 8-coordinate species.

Effect of print age

The trial was carried out in duplicate and the same results were obtained for both sets of prints. Results are presented in Table 4.13, and indicate that like many reagents, $Eu(fod)_3$ will work best on prints which are less than 24 hours old (relatively fresh). Further research in this area could lead to the possibility of $Eu(fod)_3$ being used as a test for the relative age of latent fingerprints, with good print development indicating that a print is likely to be less than 24 hours old.

Table 4.13
Effect of print age on the subsequent ability of $Eu(fod)_3$ to visualise it.

Print	Age of each print half in the pair being compared	Visualisation achieved
1	10 min &	good
	1 min	good
2	10 min &	good
	1 hr	good
3	10 min &	good
	4 hr	good
4	10 min &	good
	8 hr	good
5	10 min &	good
	24 hr	good
6	10 min &	good
	48 hr	poor
7	10 min &	good
	3 days	poor

Age of solution

Prints treated with a 1 week old and a freshly prepared $Eu(fod)_3$ solution (petroleum spirits (b.p. 40–60°C)) were equally well developed indicating that the $Eu(fod)_3$ solution is at least stable for a week.

Effect of heat treatment

There was no benefit found in heating a $Eu(fod)_3$-treated print. Pre-heating the print prior to treatment also had no additional effect.

Compatibility with ninhydrin and DFO

These trials revealed that it is possible to use $Eu(fod)_3$ as a preliminary treatment before either ninhydrin or DFO without appearing to compromise subsequent

development by the amino acid-targeting reagents. On the other hand, use of $Eu(fod)_3$ after ninhydrin or DFO yielded no further improvement in print development (Table 4.14), suggesting that ninhydrin and DFO inhibit the subsequent activity of $Eu(fod)_3$.

Table 4.14
Compatability of $Eu(fod)_3$ with ninhydrin and DFO on print halves.

Sequence of treatment	Development
Ninhydrin followed by $Eu(fod)_3$	no $Eu(fod)_3$ emission under UV light source but ninhydrin treatment still visible
$Eu(fod)_3$ followed by ninhydrin	ninhydrin treatment visible but no $Eu(fod)_3$ emission under UV light source
DFO followed by $Eu(fod)_3$	DFO visible but $Eu(fod)_3$ not visible
$Eu(fod)_3$ followed by DFO	DFO visible but $Eu(fod)_3$ not visible

Comparison of three different solvents with petroleum spirits (b.p. 40-60 °C)

Toluene, chloroform and freon were compared with petroleum spirits (b.p. 40-60°C) for use with $Eu(fod)_3$ treatment in order to establish the best solvent to use. Results are presented in Table 4.15.

Table 4.15
Comparison of different solvents with $Eu(fod)_3$ treatment.

Solvent	Development
toluene &	poor
petroleum spirits (b.p. 40-60°C)	good
chloroform &	poor
petroleum spirits (b.p. 40-60°C)	good
freon &	good
petroleum spirits (b.p. 40-60°C)	good

A good print was obtained on paper using petroleum spirits (b.p. 40-60°C) as the solvent (Fig. 4.15). Although freon gave similar results to petroleum spirits (b.p. 40-60°C) it was decided that further investigation of freon would not be useful as it is in

the process of being phased out due to its environmental implications (Hewlett et al., 1996).

Comparison of Eu(fod)$_3$/petroleum spirits (b.p. 40-60 °C) treatment on four different solvents

Results of Eu(fod)$_3$ treatment on a mylar (over-head transparency) sheet, aluminium foil, white ceramic tile and a coke can are presented in Table 4.16.

Table 4.16
Comparison of Eu(fod)$_3$ in petroleum spirits (b.p. 40-60°C) treatment on four different surfaces.

Surface	Development
Mylar (over-head transparency) sheet	even fluorescence all over (no print visible)
aluminium foil	swirly fluorescent coating (no print visible)
white ceramic tile	swirly fluorescent coating (no print visible)
coke can (outside surface)	reasonable print visible

The visualisation of a latent fingerprint on an aluminium coke can indicated that further investigation could be promising.

Selection of the best solvent for different surfaces

Results from Eu(fod)$_3$ treatment using ethyl acetate, hexane, dichloromethane or petroleum spirits (b.p. 40-60°C) on both the inside and outside painted surfaces of a coke can and on paper are presented in Table 4.17.

Table 4.17
Comparison of different solvents with Eu(fod)$_3$ treatment on two different surfaces.

Solvent	Coke can (both sides)	Paper
ethyl acetate	reasonable print	poor print
hexane	poor print	reasonable print
dichloromethane	no print visible	poor print
petroleum spirits	poor print	good print

Reasonable prints were visualised on both the outside painted surface of a coke can as well as the inside surface (Fig. 4.16) using ethyl acetate as the solvent. These prints however, were not as good as those obtained on paper using petroleum spirits. A fingerprint on an aluminium soft drink can has been previously visualised using treatment with europium nitrate–RP(5–methoxyninhydrin) and subsequent UV excitation, but time resolved imaging was necessary and the chemical treatment used requires more than one step (Mekkaoui and Menzel, 1993) unlike the one step process of $Eu(fod)_3$.

The results of a systematic comparison of different solvent treatments on latent fingerprints deposited on different surfaces are presented in Tables 4.18 to 4.20.

Table 4.18
Comparison of $Eu(fod)_3$ treatment using dimethylformamide (DMF) or petroleum spirits (b.p. 40-60°C) as the solvent on a range of different surfaces.

Surface	Solvent	
(2 print halves)	DMF	Petroleum Spirits
Paper	no print visible	print visible (good)
Vinyl wallpaper	no print visible	no print visible
Coke Can	no print visible	no print visible
Polyurethaned wood	no print visible	no print visible
Clear plastic	no print visible	no print visible

N.B. Treatment times of between 1 second and 2 minutes were tried but no development was visible.

Table 4.19
Comparison of $Eu(fod)_3$ treatment using dichloromethane (DCM) or petroleum spirits (b.p. 40-60°C) as the solvent on a range of different surfaces.

Surface	Solvent	
(2 print halves)	DCM	Petroleum Spirits
Paper	print visible (reasonable)	print visible (good)
Vinyl wallpaper	no print visible	no print visible
Coke Can	no print visible	no print visible
Polyurethaned wood	no print visible	no print visible
Clear plastic	no print visible	no print visible

Table 4.20
Comparison of $Eu(fod)_3$ treatment using ethyl acetate or hexane as the solvent on a range of different surfaces.

Surface (2 print halves)	Solvent	
	Ethyl Acetate	Hexane
Paper	print visible (poor)	visible print (reasonable)
Vinyl wallpaper	no print visible	no print visible
Coke Can	print visible (good)	print visible (reasonable)
Polyurethaned wood	no print visible	no print visible
Clear plastic	no print visible	no print visible

From this systematic comparison it can be concluded that of the surfaces investigated $Eu(fod)_3$ only works well on aluminium coke cans and paper. Also it can be concluded that the best solvent for $Eu(fod)_3$ treatment on paper is petroleum spirits (b.p. 40-60°C) and for $Eu(fod)_3$ treatment on a coke can ethyl acetate should be used.

$Eu(fod)_3$ treatment on different metals

Because of the promise shown by $Eu(fod)_3$ treatment on an aluminium coke can it was decided that an investigation of different metals should be carried out. The results of this trial are presented in Table 4.21.

Table 4.21
Comparison of $Eu(fod)_3$ in ethyl acetate on a range of different metals.

Metal	Development
galvanized iron	moderately good
rusty iron	fair
shiny metal (painted)	poor
stainless steel	barely visible
brass	barely visible

Only $Eu(fod)_3$ treatment on galvanized iron resulted in a photographable print (Fig. 4.17).

$Eu(fod)_3$ treatment on a $5 banknote

$Eu(fod)_3$ treatment using either petroleum spirits (b.p. 40-60°C), ethyl acetate, or dichloromethane on a New Zealand $5 banknote resulted in the development of no visible prints.

Comparison of $Eu(fod)_3$ treatment with DFO treatment on porous surfaces

In the comparison of $Eu(fod)_3$ with DFO on paper, all fifty prints were found to be visible with both treatment methods. In all cases the DFO–treated prints were significantly brighter than the $Eu(fod)_3$–treated prints, but in some cases the detail of the developed ridges was clearer and more continuous for $Eu(fod)_3$. DFO tended to produce blotchy, non-continuous ridge development. From these results it would appear that DFO would still be the reagent of choice for obtaining fluorescent prints on porous surfaces. However, use of $Eu(fod)_3$ prior to DFO might still be of value, given that the former appears capable of resolving more detail in some cases and doesn't inhibit use of the latter.

Comparison of $Eu(fod)_3$ treatment with superglue/panacryl treatment on non-porous surfaces

In this case the $Eu(fod)_3$ treated prints were found to be consistently better. Also, it must be kept in mind that treatment with superglue requires a fuming cabinet and can take many hours, whereas $Eu(fod)_3$ treatment takes less than half a minute. $Eu(fod)_3$ may offer a simple and inexpensive alternative to the superglue method on non-porous surfaces such as the metallic surfaces examined in this work. Further trials on more surfaces are certainly warranted.

Enhancement of luminescence following $Eu(fod)_3$ treatment

In practice, both the technique of using liquid nitrogen and the technique of using the bidentate ligand 1,10-phenanthroline resulted in severe background fluorescence with loss of print visibility altogether. After the liquid nitrogen treated print on paper had warmed back up to room temperature again, only a faint fluorescence was visible

with no ridge detail. One possibility for this result could be due to quenching of the europium fluorescence by coordination with water in the liquid nitrogen.

$Eu(fod)_3$ as a cyanoacrylate dye

Faint fluorescence was visible in the ridges of all three prints treated with cyanoacrylate vapour followed by $Eu(fod)_3$ treatment with no rinsing. No fluorescence was visible however, in the two prints treated with cyanoacrylate vapour followed by $Eu(fod)_3$ treatment with acetone rinsing. $Eu(fod)_3$ does not seem to make a good cyanoacrylate dye.

Effect of water and lipids

All twenty, water soaked halves resulted in only background fluorescence with no fingerprint visible. The other twenty halves which were treated in the normal way resulted in good development. One developed print half with a visible print was then subsequently soaked in water. The background was still fluorescent but the print was no longer visible.

All four "butter" prints resulted in good development. A spot of butter was then placed on paper without use of a finger. A fluorescent spot was observed after treatment with $Eu(fod)_3$.

The following is a possible explanation for the previous results obtained from both water-soaked and "butter" prints. The "butter" prints and spot test resulted in $Eu(fod)_3$ development which suggests that $Eu(fod)_3$ is reacting with the lipid components of fingerprints. However, latent fingerprints which had been previously soaked in water did not result in $Eu(fod)_3$ development suggesting that the $Eu(fod)_3$ is reacting with the water soluble components of the fingerprints. This result does not contradict the lipid results as it is possible that the $Eu(fod)_3$ reacts with both lipid and non-lipid components. Normally, the petroleum spirits would dissolve the lipid component of the fingerprint but not the non-lipid component hence development still occurs. Water, however, would dissolve the non-lipid component of the fingerprint but not

the lipid component. The lipid component which reacts with the $Eu(fod)_3$ however, may not be sufficient (compared with that of butter) to result in the fingerprint standing out from the background.

4.4.3 $Tb(fod)_3$ fingerprint trials

None of the ten fingerprints treated with $Tb(fod)_3$ were visible when viewed by the hand-held UV lamp at 366 nm and 254 nm. A strong green fluorescent background however, was visible.

Treatment of fingerprints deposited on a glass microscope slide, aluminium foil, a clear plastic bag and a mylar (over-head transparency) sheet resulted in a swirly green background fluorescence with no fingerprints visible.

From the 1 and 5 second treatments of fingerprints on pink paper the outline of a fingerprint could be discerned from the background but no ridge detail was visible.

Treatment of fingerprints deposited on glossy white paper resulted in ridge detail being visible from the background fluorescence. The fingerprints however, looked more like reverse prints where the $Tb(fod)_3$ had reacted with everything except the print.

Overall it seems that although $Tb(fod)_3$ exhibits strong fluorescence it maybe more reactive to cellulose in the paper than the fingerprint constituents themselves and thus any fluorescence from the prints are totally hidden by the background fluorescence.

$Tb(fod)_3$ treatment using either petroleum spirits (b.p. 40-60°C), ethyl acetate, or dichloromethane on a New Zealand $5 banknote resulted in the development of no visible prints.

4.4.4 $Eu(dpm)_3$ fingerprint trials

No prints were visible when latent fingerprints on paper were treated with $Eu(dpm)_3$ and viewed under the hand-held UV lamp at 366 nm and 254 nm.

4.4.5 Tb-DTPA-pAS chelate trials

Solution 1

Tb-DTPA-pAS treated latent and blood fingerprints viewed under the UV lamp at 254 nm resulted in no fluorescence of the ridges being visible on the blood fingerprint exhibits and no prints being visible at all for the latent fingerprint exhibits. Strong background fluorescence (green) was evident however, in both blood and latent fingerprint exhibits.

A $TbCl_3.6H_2O$ treated latent fingerprint viewed under the hand-held UV lamp at 254 nm resulted in no print being visible but strong background fluorescence (green) all over the paper however, was visible.

Solution 2

Tb-DTPA-pAS treated latent and blood fingerprints viewed under the UV lamp at 254 nm resulted in no fluorescence of the ridges being visible on the blood fingerprint exhibits and no prints being visible at all for the latent fingerprint exhibits. Strong background fluorescence (green) was evident however, in both blood and latent fingerprint exhibits.

4.5 *Results and discussion of the chemistry of the $Eu(fod)_3$ reaction with latent fingerprints*

4.5.1 Non-lipid fingerprint components

$Eu(fod)_3$ spot tests

$Eu(fod)_3$ treatment of a glycine, triethylamine and urea spot resulted in development of a fluorescent spot indicating that $Eu(fod)_3$ is reacting with all three substances. The fluorescence was fainter however, for the triethylamine spot presumably because triethylamine is volatile and would have evaporated to some extent.

$Eu(fod)_3$ treatment of a glucose spot resulted in formation of a fluorescent ring around the area of the spot. This indicates that $Eu(fod)_3$ is reacting with glucose but also seems to indicate that chromatography is occurring (migration of glucose from the centre of the spot). It is also probably the reaction of $Eu(fod)_3$ with cellulose (unbranched chains of glucose) which results in the background staining seen on paper when using $Eu(fod)_3$.

Electrospray mass spectrometry of $Eu(fod)_3$

The electrospray mass spectrometry (ESMS) results for the reactivity of $Eu(fod)_3$ with acetic acid, propionic acid, glycine, triethylamine and urea are presented in Tables 4.23 to 4.27 respectively. It should be noted that there were two main peaks found for each ion (twin peaks). The two peaks represent the isotope ratio of europium which has two major isotopes of similar intensity. An example of the theoretically calculated isotope pattern for the ion $Eu(fod)(MeO)_2 + H^+$ is presented in Table 4.22 where the two major calculated peaks are 511 and 509 with similar intensities.

Table 4.22
Theoretically calculated isotope pattern of $Eu(fod)(MeO)_2 + H^+$.

Mass to charge ratio (*m/z*)	Intensity
509	90.18
510	12.52
511	100
512	13.8
513	1.67
514	0.14
515	0.01

Table 4.23
Electrospray mass spectrometry data for $Eu(fod)_3$ *and acetic acid.*

Assigned formula	Mass to charge ratio (*m/z*)	Intensity
$Eu(fod)(MeO)_2+H^+$	509.2, 511.1	90, 100
$Eu(fod)(AcO)(MeO)_2+2H^+$ or $Eu(fod)(AcO)(MeOH)_2^+$	569.0, 571.0	8, 9
$Eu(fod)(AcO)_3+2H^+$	625.0, 627.0	2, 2
$Eu(fod)_2(AcO)_2+2H^+$	861.4, 863.2	3, 3

Table 4.24
Electrospray mass spectrometry data for $Eu(fod)_3$ *and propionic acid.*

Assigned formula	Mass to charge ratio (*m/z*)	Intensity
$Eu(fod)(PrO)^+$	519.1, 521.1	25, 28
$Eu(fod)(MeO)_3+2H^+$	541.0, 543.1	1.1, 1.3
$Eu(fod)(PrO)(MeO)+H^+$	550.9, 553.0	3.1, 3.5
$Eu(fod)(PrO)_2+H^+$	593.1, 595.1	90, 100
$Eu(fod)(PrO)_3+2H^+$	667.2, 669.4	3, 3
$Eu(fod)_2^+$	740.6, 742.7	3, 3
$Eu(fod)_3+H^+$	—, 1039.6	—, 0.3

Table 4.25
Electrospray mass spectrometry data for $Eu(fod)_3$ and glycine.

Assigned formula	Mass to charge ratio (*m/z*)	Intensity
$Eu^{II}(fod)(H_2O)^+$	464.0, 466.2	15, 19
$Eu(fod)(MeO)_2+H^+$	509.0, 511.0	89, 100
$Eu(fod)(AcO)(MeOH)_2^+$	568.8, 570.9	13, 14

Table 4.26
Electrospray mass spectrometry data for $Eu(fod)_3$ and urea.

Assigned formula	Mass to charge ratio (*m/z*)	Intensity
$Eu(fod)(PrO)^+$	519.1, 521.2	15, 16
$Eu(fod)(PrO)(MeO)+H^+$	551.2, 553.3	8, 8
$Eu(fod)(PrO)(Urea)^+$	579.1, 581.1	9, 11
$Eu(fod)(PrO)_2+H^+$	593.2, 595.1	12, 14
$Eu(fod)(PrO)(Urea)_2^+$	639.2, 641.0	11, 12
$Eu(fod)(PrO)(Urea)_3^+$	699.1, 701.2	5, 5

Table 4.27
Electrospray mass spectrometry data for $Eu(fod)_3$ and triethylamine.

Assigned formula	Mass to charge ratio (*m/z*)	Intensity
$Eu(fod)(MeO)_2+H^+$	508.9, 510.9	85, 100
$Eu(fod)_2(H_2O)_3(MeO)+H^+$	826.8, 829.4	12, 14

As an instrumental method, ESMS is unique in its ability to transform ions in solution directly to gas phase ions, allowing the direct detection of ionic facets of the solution chemistry. The results from the ESMS spectra suggest that there are ligand exchange processes occurring in solution which involve $Eu(fod)_3$ and acetic acid, propionic acid, and urea, as all of these adducts were observed (though suggestive, the results are not entirely definitive however, because when using ESMS, a possibility remains that the ion adducts observed at the detector are formed by recombination of ions in the gas phase).

No ions resulting from the ligand exchange of glycine or triethylamine (TEA) with $Eu(fod)_3$ were observed, but this may be because of the presence of acetic acid in the carrier solution (required for the dissolution of $Eu(fod)_3$) which was in a high concentration and may have preferentially undergone ligand exchange. It was hoped that adducts with glycine or TEA might appear in the same spectrum along with acetic acid adducts. It also should be kept in mind that the ESMS results are obtained only under the conditions provided by the electrospray mass spectrometer and may not occur in a latent fingerprint.

Electrospray mass spectrometry of $Tb(fod)_3$

The ESMS results for the reactivity of $Tb(fod)_3$ with acetic acid are presented in Table 4.28. In this case only single peaks were observed for the various ions as terbium has only one major isotope.

Table 4.28
Electrospray mass spectrometry data for $Tb(fod)_3$ and acetic acid.

Assigned formula	Mass to charge ratio (*m/z*)	Intensity
$Tb(fod)(MeO)_2+H^+$	517.2	100
$Tb(fod)(AcO)(MeO)_2+2H^+$	577.4	4
$Tb(fod)(AcO)_3+2H^+$	633.2	11
$Tb(fod)_2(AcO)_2+2H^+$	869.3	6

The results obtained above for $Tb(fod)_3$ are analogous to those obtained previously for $Eu(fod)_3$ (Table 4.23).

4.5.2 Lipid fingerprint components

$Eu(fod)_3$/ octanoic acid fluorescent emission results

The significant changes in $Eu(fod)_3$ emission intensities before and after addition of a small amount of octanoic acid (10 μL in 2 mL) provides possible evidence of octanoic acid binding to or associating with $Eu(fod)_3$ (however, the results are not clear cut). The results for this trial are presented in Table 4.29.

Table 4.29
Emission intensities for $Eu(fod)_3$ before and after octanoic acid addition.

Excitation λ (nm)	Emission wavelength (nm)									
	614.0		590.0		537.5		380.0		350.0	
	before	after	before	after	before	after	before	after	before	after
340.0	183	111	28	22	20	8	41	43	—	—
225.0	81	30	12	0	10	0	—	—	785	914

The results obtained after octanoic acid addition were monitored over a period of 1 minute to 1 hour after addition and were found to be stable at these intensity values.

$Eu(fod)_3$/ octanoic acid UV/Vis results

The significant change in the UV/Vis absorbance of a $Eu(fod)_3$ solution before and after addition of octanoic acid provides further possible evidence of octanoic acid associating with the europium complex in some way. This might involve either direct coordination with intact $Eu(fod)_3$, or coordination by displacement of a fod ligand. The absorbance of the solution was 0.604 at 294 nm before addition of octanoic acid and was 0.558 at 288 nm after addition of octanoic acid.

$Tb(fod)_3$/ octanoic acid fluorescent emission results

Similar changes were observed in $Tb(fod)_3$ emission intensities before and after addition of octanoic acid. These results are presented in Table 4.30.

Table 4.30
Emission intensities for $Tb(fod)_3$ before and after octanoic acid addition.

Excitation Wavelength (nm)	Intensity before (547 nm emission)	Intensity after (547 nm emission)
337.0	617	510
240.0	460	15

4.6 *Chapter summary*

Visualisation of latent fingerprints using $Eu(fod)_3$ was obtained on white photocopy paper, aluminium drink cans and galvanized iron. An investigation of the optimum treatment conditions indicated that a twenty second dipping time in a solution of 6.67 g/L $Eu(fod)_3$ was best. For prints on paper it was found that petroleum spirits (b.p. 40-60°C) produced the best results and for prints on aluminium and galvanised iron, ethyl acetate proved best.

The orange emission (614 nm) of $Eu(fod)_3$ is obtained by UV excitation at 340 nm and is the emission used for fingerprint visualisation. In practice however, visualisation was obtained using a hand held UV lamp with the 254 nm filter. Alternatively the 320 nm filter on the Polilight® produces good visualisation.

It was found that $Eu(fod)_3$ works best on latent prints less than 24 hours old which could lead to the possibility of $Eu(fod)_3$ being used as a test for the ageing of latent fingerprints. The stability of the $Eu(fod)_3$ treated prints is also less than 24 hours presumably due to the reaction of $Eu(fod)_3$ with moisture in the air.

$Eu(fod)_3$ treatment can be used first without affecting subsequent ninhydrin or DFO treatment meaning that $Eu(fod)_3$ could be used first to "age" the print before subsequent ninhydrin or DFO treatment. It was found however, that DFO treatment is better than $Eu(fod)_3$ treatment on paper (porous surfaces) but that $Eu(fod)_3$ is better on aluminium and galvanised iron surfaces (non-porous surfaces) than superglue/panacryl treatment.*

$Eu(fod)_3$, unlike most latent fingerprint reagents such as ninhydrin and DFO, can react not only with both lipid and non-lipid components of latent fingerprints but also with a variety of non-lipid components. Latent fingerprint components with which $Eu(fod)_3$ can react with include fatty acids, amines, amino acids, carboxylic acids and urea. However, in practice it would seem more likely that $Eu(fod)_3$ would react with the non-lipid components of latent fingerprints which are usually more abundant.

* Other fluorescent methods which have been used on aluminium surfaces such as coke cans are fuming with DMAC (Brennan et al, 1995) and staining with tris (2,2'-bipyridyl) ruthenium (II) chloride hexahydrate (Menzel, 1990) which would both require time-resolved imaging in order to avoid background interference due to the lower wavelength emissions obtained compared with $Eu(fod)_3$ treatment.

$Eu(dpm)_3$ was found to be unsuitable for visualisation of latent fingerprints due to the lack of any visible fluorescence. $Tb(fod)_3$, although highly fluorescent in the visible region (547 nm) was also found to be unsuitable for visualisation of fingerprints. The reason for this is probably due to greater reactivity of $Tb(fod)_3$ with the cellulose contained in paper than with the components of fingerprints themselves (this does not however, explain the non-visualisation of fingerprints on a coke can). Tb-DTPA-pAS also resulted in just background fluorescence with no enhancement or visualisation of treated latent and blood fingerprints observed.

4.7 *References*

Alaoui I.M., and Menzel R.E. (1994). Emission enhancement in terbium-Ruhemann's purple complexes. *Forens. Sci. Int.*, **66**, 203-211.

Allred C.E., Murdock R.H., and Menzel E.R. (1997). New lipid-specific, rare earth-based chemical fingerprint detection method. *J. Forens. Ident.*, **47**(5), 542-556.

Bailey M.P., Rocks B.F., and Riley C. (1984). Terbium chelate for use as a label in fluorescent immunoassays. *Analyst*, **109**, 1449-1450.

Bailey M.P., Rocks B.F., and Riley C. (1988). Chelated terbium as a label in fluorescence immunoassay. In: *Nonisotopic immunoassay*, 187-197.

Bruder A.H., Tanny S.R., Rockefeller H.A., and Springer C.S. (1974). *Inorg. Chem.*, **13**, 880.

Curtis J.M., Derrick P.J., Schnell A., Constantin E., Gallagher R.T., and Chapman J.R. (1992a). Electrospray mass spectrometry of lanthanide β-diketone complexes Part 1. Ligand exchange processes involving acetate ions and $Ln(thd)_3$ complexes (Ln=Eu, Gd, Yb; thd=2,2,6,6-tetramethyl-3,5-heptanedione). *Inorganica Chimica Acta*, **201**, 197-201.

Curtis J.M., Derrick P.J., Schnell A., Constantin E., Gallagher R.T., and Chapman J.R. (1992b). Electrospray mass spectrometry of lanthanide β-diketone complexes. II - Ligand exchange processes involving acetate ions and $Ln(tfc)_3$ complexes. *Organic Mass Spec.*, **27**, 1176-1180.

Hewlett D.F., Winfield P.G.R., and Clifford A.A. (1996). The Ninhydrin process in supercritical carbon dioxide. *J. Forens. Sci.*, **41**(3), 487-489.

Johnston M.D., Shapiro B.L., Shapiro M.J., Proulx T.W., Godwin A.D., and Pearce H.L. (1975). Lanthanide-induced shifts in proton nuclear magnetic resonance spectra. XI. Equilibrium constants and bound shifts for cyclohexanones and cyclohexanols. *J. Amer. Chem. Soc.*, **97**(3), 542-554.

Kemp W. (1986). *NMR in chemistry: A multinuclear introduction.* MacMillan Education Ltd, London, 77-79.

Kent T. (editor), Hardwick S.A., and Sears V.G. (1986). *Manual of fingerprint development techniques - A guide to the selection and use of processes for the development of latent fingerprints.* Printed in England for the Home Office by Heanor Gate, Derbyshire.

Lavis A. (1994). *Workshop in advanced fingerprint techniques.* Training manual prepared for ESR:Forensic, Auckland, New Zealand.

Lock E.R.A., Mazzella B.S., and Margot P. (1995). A new europium chelate as a fluorescent dye for cyanoacrylate pretreated fingerprints - EuTTAPhen: Europium ThenoylTrifluoroAcetone ortho-Phenanthroline. *J. Forens. Sci.*, **40**(4), 654-658.

Mekkaoui A.I., and Menzel E.R. (1993). Spectroscopy of rare earth-Ruhemann's Purple complexes. *J. Forens. Sci.*, **38**(3), 506-520.

Menzel E.R., and Mitchell K.E. (1990). Intramolecular energy transfer in the europium-Ruhemann's purple complex: application to latent fingerprint detection. *J. Forens. Sci.*, **35**(1), 35-45.

Morrill T.C., Opitz R.J., and Mozzer R. (1973). *Tetrahedron Letters*, **38**, 3715.

Morrison R.T., and Boyd R.N. (1973). *Organic Chemistry.* 3rd edition. Allyn and Bacon, Inc., Boston, 1055.

Murdock R.H., and Menzel R.E. (1993). A computer interfaced time-resolved luminescence imaging system. *J. Forens. Sci.*, **38**(3), 521-529.

Reuben J. (1973). *J. Amer. Chem. Soc.*, **95**, 3534.

Rondeau R.E., and Sievers R.E. (1971). New superior paramagnetic shift reagents for nuclear magnetic resonance spectral clarification. *J. Amer. Chem. Soc.*, **93**(6), 1522-1524.

Shoffner J.P. (1974). On the use of tris(6,6,7,7,8,8,8-heptafluoro-2,2-dimethyl-3,5-octanedionato) europium(III) as a shift reagent for carboxylic acids and phenols. *J. Amer. Chem. Soc.*, **96**(5), 1599-1601.

Shoffner J.P. (1975). Use of tris-(6,6,7,7,8,8,8-heptafluoro-2,2-dimethyl-3,5-octanedionato) europium(III) for the structure determination and quantitative analysis of phenols. *Anal. Chem.*, **47**(2), 341-343.

Skoog D.A., West D.M., and Holler F.J. (1996). *Fundamentals of Analytical Chemistry.*7th edition. Saunders College Publications, Florida, 604.

Springer C.S., Meek D.W., and Sievers R.E. (1967). Rare earth chelates of 1,1,1,2,2,3,3-heptafluoro-7,7,-dimethyl-4,6-octanedione. *Inorg. Chem.*, **6**(6), 1105-1110.

Wilkinson D.A., and Misner A.H. (1994). A comparison of Thenoyl Europium Chelate with Ardrox and Rhodamine 6G for the fluorescent detection of cyanoacrylate prints. *J. Forens. Ident.*, **44**(4), 387.

Wilkinson D.A., and Watkin J.E. (1993). Europium aryl-β-diketone complexes as fluorescent dyes for the detection of cyanoacrylate developed fingerprints on human skin. *Forens. Sci. Int.*, **60**, 67-79.

Zahradník M. (1982). *The production and application of fluorescent brightening agents.* New York, John Wiley and Sons, 31-39.

Brennan J., Bramble S., Crabtree S., and Wright G. (1995). *J. Forens. Ident.*, **45**(4), 373-380.

Menzel E.R. (1990). Laser Excited Fluorescence in Criminalistics. *Laser Techniques In Luminescence Spectroscopy,* ASTM STP 1066, Philadelphia, 36-49.

Chapter Five

Investigation of two *o*-phthalaldehyde analogues as potential latent fingerprint reagents

5.1 *Introduction*

The reaction of amino acids with *o*-phthalaldehyde (OPA) to give a fluorescent product was first reported by Roth (1971) using an alkaline solution of the compound in the presence of a reducing reagent such as 2-mercaptoethanol (Fig. 5.1).

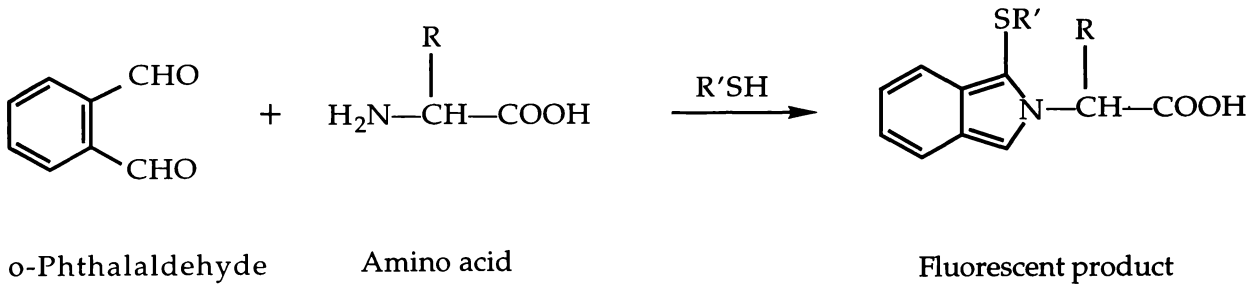

Fig. 5.1
Reaction of o-phthalaldehyde with amino acids.

Simons and Johnson (1978) later found that 2-mercaptoethanol could be substituted by ethanethiol. The use of the reagent to develop latent fingerprints has been reported by Mayer et al. (1978) employing a buffered solution of the reagent to which was added a detergent (Brij® 35) and 2-mercaptoethanol. Fluorescence of the fingerprints was then observed under irradiation from an ultra violet light.

The problem with the use of OPA is that emission from optical brighteners (Zahradník, 1982) and other components such as $CaCO_3$ and TiO_2 (Fisher, 1999) present in paper may interfere with the fluorescence produced by the treated fingerprint. The potential of derivatives of OPA to have different excitation and emission spectra from those of the background paper could make this a worthwhile fingerprint method.

One such derivative, 2,3-naphthalenedicarboxaldehyde (NDA) has been employed in the trace analysis of amino acids and primary amines by a number of workers (de Montigny et al., 1987; Carlson et al., 1986; Kwakman et al., 1990; Soper and Kuwana, 1989; Miura et al., 1984; and Matuszewski et al., 1987).

Montigny et al. (1987) found that the use of the cyanide ion as a reducing reagent with NDA rather than 2-mercaptoethanol resulted in increased fluorescence intensity and good chemical stability (Fig. 5.2 and Table 5.1). This increased chemical stability was also found for OPA but with a reduced fluoresence intensity (Table 5.1).

Table 5.1
Effect of reducing reagents for OPA and NDA on fluorescence.

Dialdehyde	Reducing Reagent	Excitation Max. (nm)	Emission Max. (nm)	Relative Fluorescent Intensity
OPA	2-ME*	340	450	1.00
	HSO_3^-	325	400	0.08
	CN^-	330	380	0.22
	N_3^-	—	—	—
	NCS^-	—	—	—
NDA	2-ME*	440	570	<0.01
	HSO_3^-	420	500	0.25
	CN^-	420	490	2.85
	N_3^-	—	—	—
	NCS^-	—	—	—

*2-mercaptoethanol

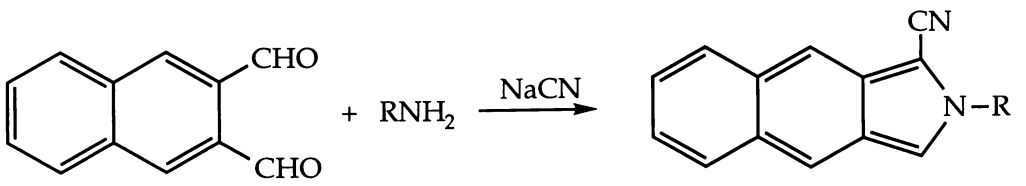

Fig. 5.2
Reaction of NDA with amino acids using the cyanide ion as a reducing reagent.

Another derivative of OPA is 2,3-anthracenedicarboxaldehyde (ADA) which has been employed in the trace analysis of amines by Kwakman et al. (1990). The cyanide ion was also used as the reducing reagent (Fig. 5.3).

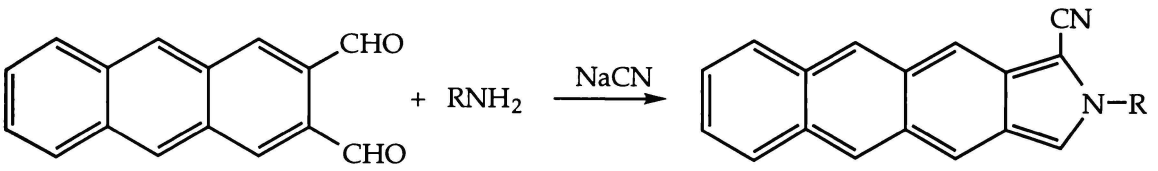

Fig. 5.3
Reaction of ADA with amines using the cyanide ion as a reducing reagent.

The best results for these types of reactions appear to be achieved under alkaline conditions. In an investigation of the effect of pH on the rate of NDA/CN^- derivatisation of alanine, Montigny et al. (1987) indicated that the maximal rate of derivatisation occurred at a pH of 9.5. This is consistent with the use of borate buffers with a pH of 9.5 for NDA and ADA by Kwakman et al. (1990). Similarly, Roth (1971) reported the determination of certain amino acids by reaction with OPA in basic or weakly acidic (pH 6.0) solutions, and Mayer (1978) reported use of a borate buffer with a pH of 10.4 for OPA fingerprinting.

The aim of this part of the work was to measure the emission characteristics of the products formed by reaction of amino acids with OPA, NDA and ADA, and assess how effective each of these compounds might be as fingerprint reagents.

5.2 *Methodology*

5.2.1 Materials and instrumentation

Chemicals used in this research were purchased from the following sources:

- *o*-phthalaldehyde, Brij® 35, and 2-mercaptoethanol from Aldrich Chemical Company.
- 2,3-naphthalenedicarboxaldehyde was initially synthesised by the method outlined in Appendix 5.1 but was later purchased from Aldrich Chemical Company.
- 2,3-anthracenedicarboxaldehyde was purchased from Molecular Probes (Eugene, OR, USA).
- NaCN, L-alanine*, boric acid, KOH, and methanol (AR) were all purchased from BDH.

* L-alanine was chosen for use as the amino acid as it results in more stable OPA derivatives than with glycine (Montigny et al, 1987).

The following instrumentation and materials were used in this research:

- A Perkin Elmer Luminescence Spectrometer LS 50B was used for collection of all fluorescence data; this utilises a xenon-lamp source.
- A Mineralight® hand-held UV lamp (model UV GL-58) was used with two wavelength settings of 254 and 366 nm for visualisation of treated fingerprints.
- A Spectra Physics 164 argon-ion laser (1 watt) in combination with a 265 Exciter was also used for visualisation of treated fingerprints.
- White and pink paper (A4, 80 gsm) was obtained from Copyright (Australian Paper, Ltd.)

5.2.2 Emission spectra of the reaction products formed by OPA, NDA and ADA with an amino acid

Emission spectra of the amino acid reaction products of OPA, NDA and ADA were investigated by preparing dilute solutions of these substances along with an appropriate nucleophile, and using analine as the representative amino acid. Solutions were prepared using variations on the methodology of Mayer et al. (1978) with a small amount of methanol being used to help dissolve the dialdehyde and with the addition of a certain amount of Brij® 35 detergent. A Perkin Elmer Luminescence Spectrometer LS 50B was used to obtain the spectra. Slit widths for both excitation and emission were set at 5 nm, with solutions being held in a 10 mm quartz cuvette.

The following stock solutions were prepared for use in the analysis of the reacted OPA, NDA and ADA emission spectra:

- A 30% solution of Brij® 35 detergent was prepared by dissolving 30 mg of the solid in 100 mL of distilled water. A 10 mL portion of this solution was then diluted by 2x to give a 15% solution.
- An *L*-alanine solution (6.6×10^{-7} *M*) was prepared by dissolving 5.9 mg of *L*-alanine in 100 mL of distilled water.
- Borate buffer was prepared by dissolving 25 g boric acid in 950 mL distilled water and adjusting the pH of the solution to 10.4 with 6 mol/L KOH.
- A 2-mercaptoethanol stock solution was prepared by dissolving 1 mL of 2-mercaptoethanol into a final volume of 10 mL distilled water (3.3×10^{-5} *M*).

- A NaCN stock solution was prepared by dissolving 16 mg of NaCN into a final volume of 10 mL distilled water (0.0326 *M*).

Borate buffer was used to prepare the following OPA solution which was 3.3×10^{-5} *M* after dilution:

- A 4.4 mg amount of OPA, 23 µL of 2-mercaptoethanol stock solution and 1 mL of 6.6×10^{-7} *M* *L*-alanine solution (added just before analysis) were made up to 100 mL using borate buffer. A 1 mL aliquot of this solution was then diluted by 10x with more borate buffer to give a final concentration of 3.3×10^{-5} *M*. Emission intensities of this solution were then obtained at various time intervals after the time of *L*-alanine addition by excitation at 337 nm.

More 3.3×10^{-5} *M* OPA solutions were then prepared using borate buffer but with the following variations:

- A 3.3×10^{-5} *M* OPA solution was prepared as before but with the 4.4 mg amount of OPA being firstly dissolved in 37 µL methanol and with the addition of 11µL Brij® 35 (15% solution). The mole ratios of the various substances used in this solution were the same as those used by Mayer et al. (1978). Emission intensities of this solution were then obtained at various time intervals after the time of *L*-alanine addition by excitation at 337 nm. A 2 mL volume of methanol was then added to the remaining 99 mL of the concentrated solution (3.3×10^{-4} *M*) in order to assess the effect of methanol on the emission intensities. A 1 mL sample of this solution was then diluted by 10x as before with borate buffer. Emission intensities of this diluted solution (3.3×10^{-5} *M*) were then obtained at various time intervals after the initial time of the *L*-alanine addition to the original 100 mL solution with an excitation wavelength of 337 nm.
- A 37 µL volume of methanol was used to dissolve the OPA and with the addition of 11µL Brij® 35 (15% solution).
- A 100 µL volume of methanol was used to dissolve the OPA and with the addition of 300 µL Brij® 35 (30% solution).
- A 2 mL volume of methanol was used to dissolve the OPA and with the addition of 300 µL Brij® 35 (30% solution).
- A 2 mL volume of methanol was used to dissolve the OPA and with the addition of 11 µL Brij® 35 (15% solution).

The following NDA solutions (3.3×10^{-5} *M*) were prepared:

- An NDA solution was prepared by dissolving 6.1 mg NDA in 2 mL methanol and adding 1 mL NaCN stock solution, 1 mL of L-alanine solution (added just before analysis) and making up to 100 mL with borate buffer. A 1 mL aliquot of this solution was then diluted by 10x with borate buffer to give a final concentration of 3.3×10^{-5} *M*. Emission intensities of this solution were then obtained at various time intervals after the time of *L*-alanine addition by excitation at 418 nm.
- An NDA solution was prepared as before but with the addition of 11 µL 15% Brij® 35.

An ADA solution was prepared by adding 3.9 mg ADA, 1 mL NaCN stock solution, 1 mL of L-alanine solution (6.6×10^{-7} *M*) (added just before analysis) and making up to 50 mL with methanol. It was found that ADA required a large amount of methanol for complete dissolution. A 1 mL aliquot of this solution was then diluted by 10x with borate buffer to give a final concentration of 3.3×10^{-5} *M*. Emission intensities of this diluted solution were then obtained at various time intervals after the time of L-alanine addition by excitation at 405 nm.

5.2.3 Fingerprint trials

Latent fingerprints deposited on paper were treated with a solution of OPA which had been prepared according to the method used by Mayer et al. (1978). Treatment however, involved immersion in the solution compared with Mayer's method of spraying on the solution with a Babington nebulizer. Treated prints on paper were left to dry for 5-10 minutes before being viewed using a UV hand-held lamp at 366 nm with orange goggles.

Prints deposited on white or pink paper were treated with a solution of OPA using a 20 second immersion time and then compared.

An investigation into the best immersion time for treatment with OPA was carried out. Prints on pink paper were immersed in a solution of OPA for 10 seconds, 20 seconds, 1, 2 and 5 minutes.

An investigation was also carried out on OPA treatment of latent fingerprints deposited on a range of different surfaces. Previously OPA treatment of latent fingerprints had only been investigated on paper (Mayer et al., 1978). Surfaces investigated included pink paper, a New Zealand $5 banknote, a coke can (both inside and outside surfaces), and a sheet of mylar (used for overhead transparencies).

Latent fingerprints deposited on white or pink paper were also treated with solutions of NDA and ADA. Treatment involved immersion in the solution for one half minute. NDA and ADA treated prints were then viewed using a UV hand-held lamp at 366 nm and an argon laser at 457.9 nm.

The OPA solution (0.018 *M*) was prepared by dissolving 0.12 g OPA in 1 mL methanol and adding 0.1 mL 2-mercaptoethanol, 0.15 mL 30% Brij® 35 and making up to 50 mL with borate buffer. The NDA solution (0.018 *M*) was prepared by dissolving 49.5 mg NDA and 13.2 mg NaCN in 15 mL methanol (NDA is very insoluble in aqueous solution). The ADA solution (0.007 *M*) was prepared by dissolving 17 mg NDA and 3.6 mg NaCN in 10 mL methanol.

5.3 *Results*

5.3.1 Emission spectra of OPA, NDA and ADA reaction products

Changes in emission intensities with time for various analine–OPA solutions prepared with and without Brij® 35 detergent and with and without methanol are presented in Fig. 5.4. Excitation was carried out at 337 nm with emission intensities being recorded using a 10 mm quartz cuvette, for the peak which falls between 446.0 to 453.5 nm (small variations were observed to occur in the exact location of the peak maximum). Raw data points from which this figure were derived are provided in Appendix 5.2.

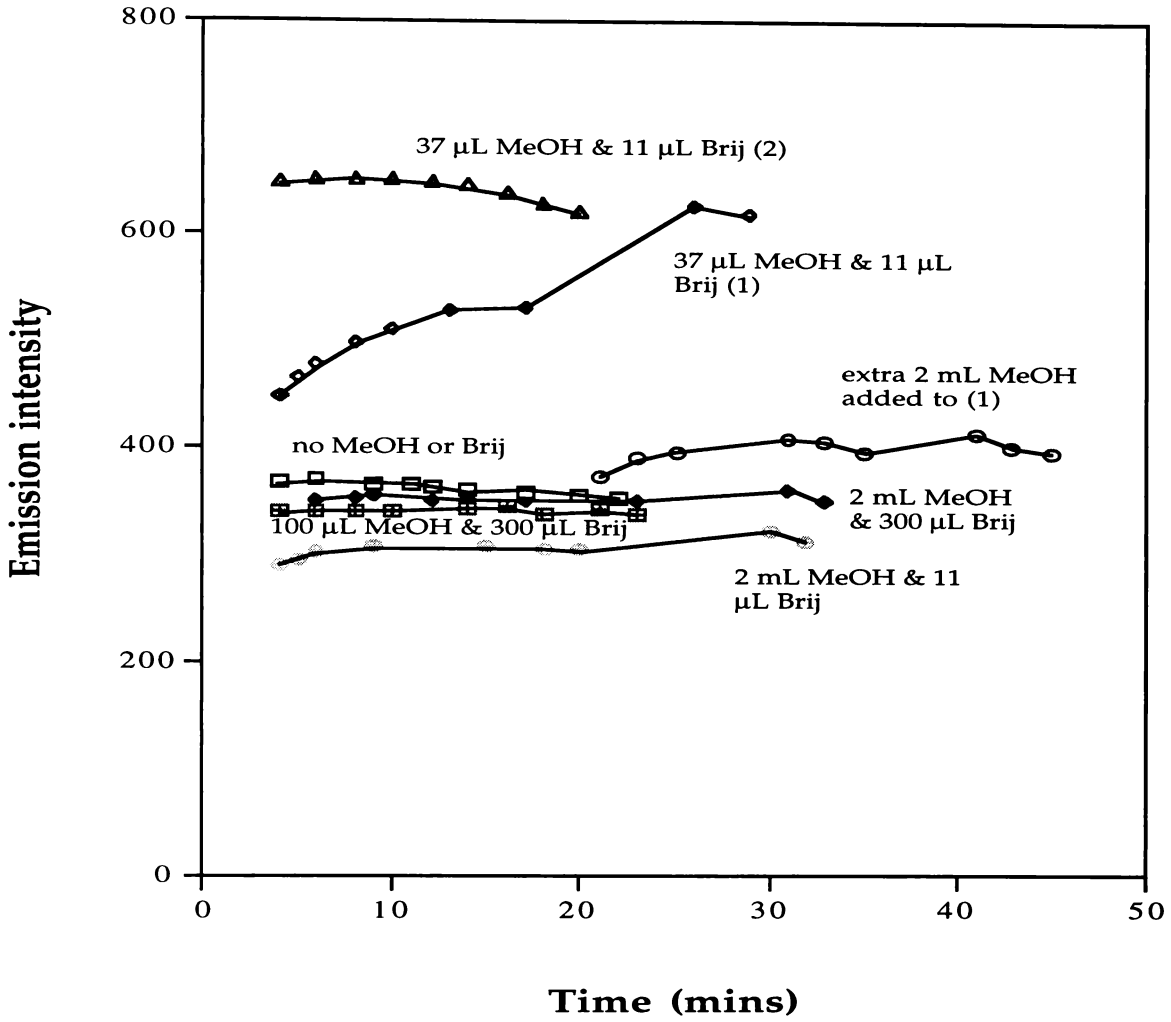

Fig. 5.4
Changes with time in the emission intensities of the peak between 446-454 nm for the reaction products of various analine–OPA solutions.

The results indicate that the use of excess methanol results in a reduction in the emission intensity of the fluorescent product of OPA. Use of either no Brij® 35 detergent, or an amount larger than that specified by Mayer et al. (1978) also results in a decrease in luminescence. This investigation therefore confirms that the OPA solution of Mayer et al. (1978) provides the best fluorescence intensity, with only the minimum amount of methanol being used to dissolve the OPA and with the addition of a small amount of Brij® 35 detergent.

Changes in emission intensities with time for an NDA solution prepared with and without Brij® 35 detergent are presented in Fig. 5.5, which is derived from the data

given in Appendix 5.2. Excitation was carried out at 418 nm with emission intensities being recorded between 473.5 to 479.5 nm, and the amount of Brij® 35 added in this case was based on the best proportion found for OPA.

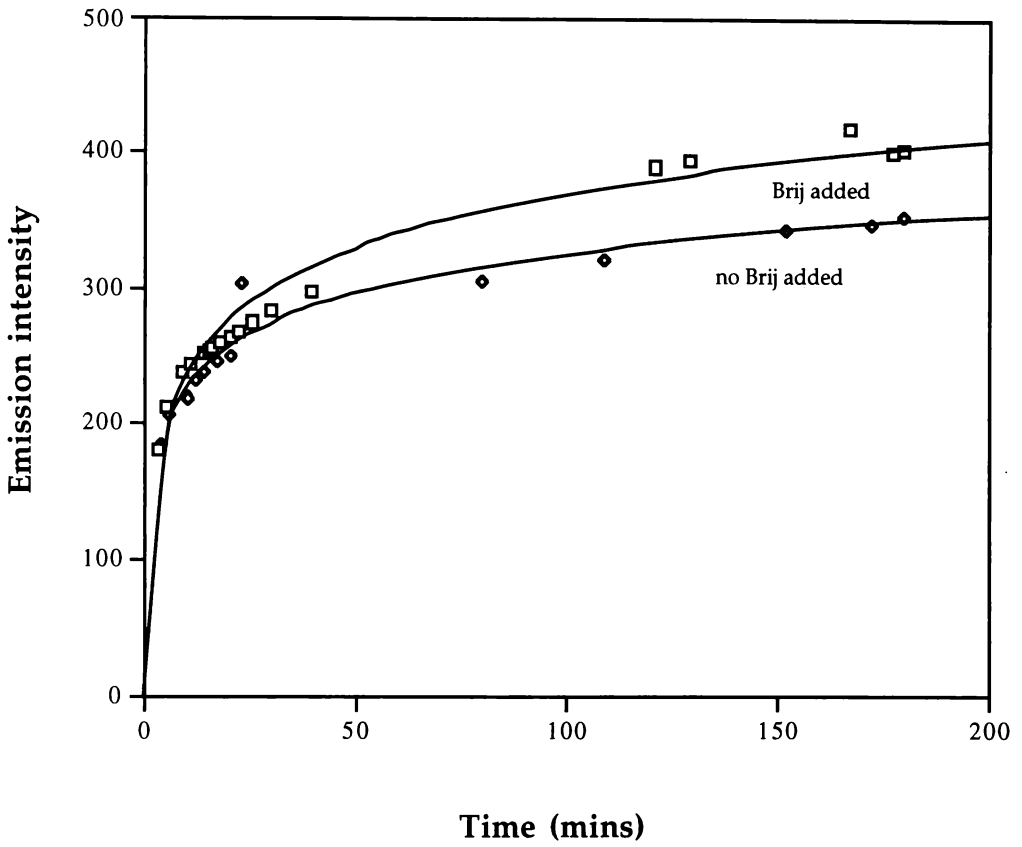

Fig. 5.5
Changes in emission intensities (473.5–479.5 nm peak) with time for the reaction products of an analine–NDA solution with and without Brij® 35 detergent.

The results indicate that, particularly over longer periods, not using Brij® 35 detergent results in a measurable reduction in emission intensity of the fluorescent product of NDA compared with using Brij® 35 detergent.

Changes in emission intensities with time for the reaction products of an analine–ADA solution are presented in Fig. 5.6 (raw data is given in Appendix 5.2). Excitation was carried out at 405 nm with emission intensities being recorded between 532.5 to 540.5 nm (the exact composition of this solution is outlined in section 5.2.2).

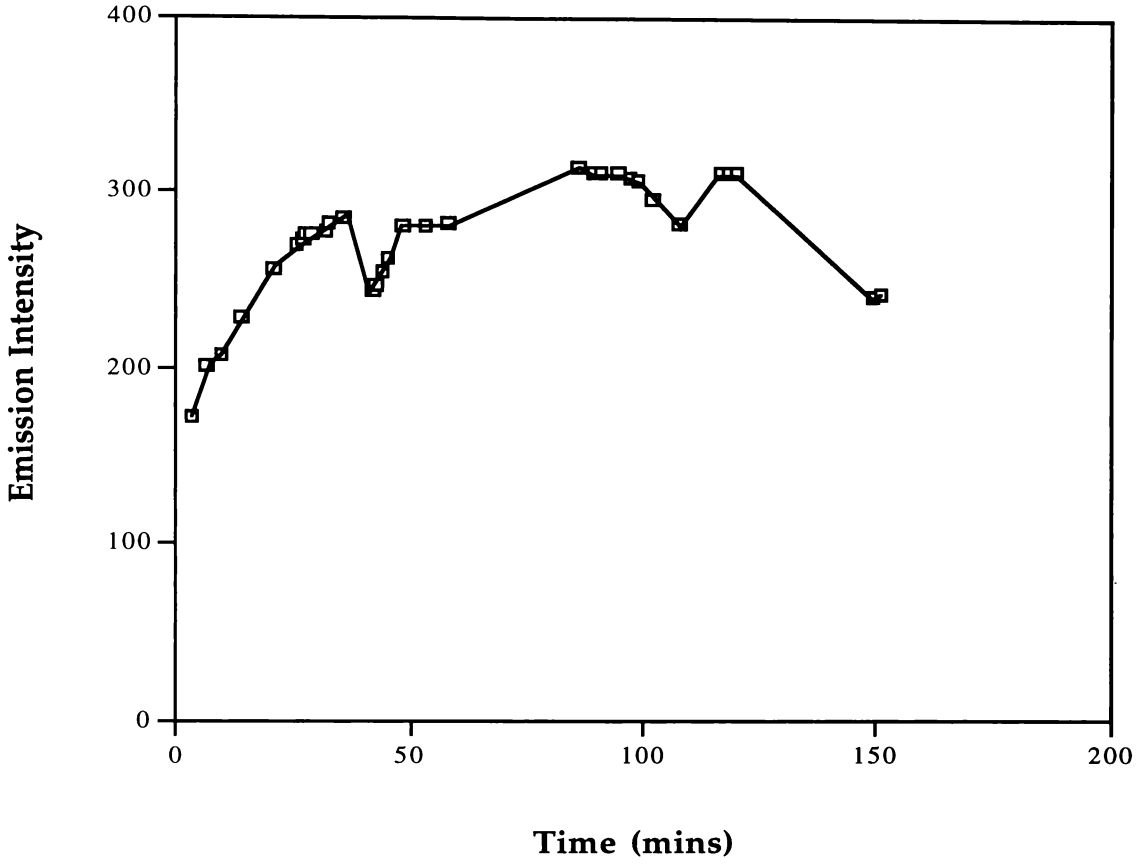

Fig. 5.6
Changes in emission intensities (532.5–540.5 nm peak) with time for the reaction products of an analine–ADA solution.

In this case no Brij® 35 detergent was employed as the solubility of ADA required it to be initially dissolved in 50 mL methanol before subsequent 10x dilution in aqueous buffer. It therefore became obvious at this stage that the OPA, NDA and ADA solutions could no longer be prepared in a comparable way with or without Brij® 35 detergent. Results displayed in Fig. 5.6 however, confirm that the three–ring compound ADA is also capable of developing significant fluorescence in the presence of an amino acid and a nucleophile. The dips observable in the apparent plateau in Fig. 5.6 could possibly be due to side reactions caused by reduced stability of the alanine -ADA reaction product.

Emission spectra were obtained for the alanine reaction products of OPA (2 mL methanol and 11 µL 15% Brij® 35), NDA (2 mL methanol and 11 µL 15% Brij® 35) and ADA (50 mL methanol and no Brij® 35). The solution conditions used for the OPA solution are not the optimal conditions determined previously from Fig. 5.4 but were used in order to obtain a proper comparison with NDA. The overlayed spectra are presented in Fig. 5.7. It should be noted that the spectrum for NDA was not obtained at the exact maximum intensity of 419 actually reached and that only OPA and NDA solutions were prepared in the same way.

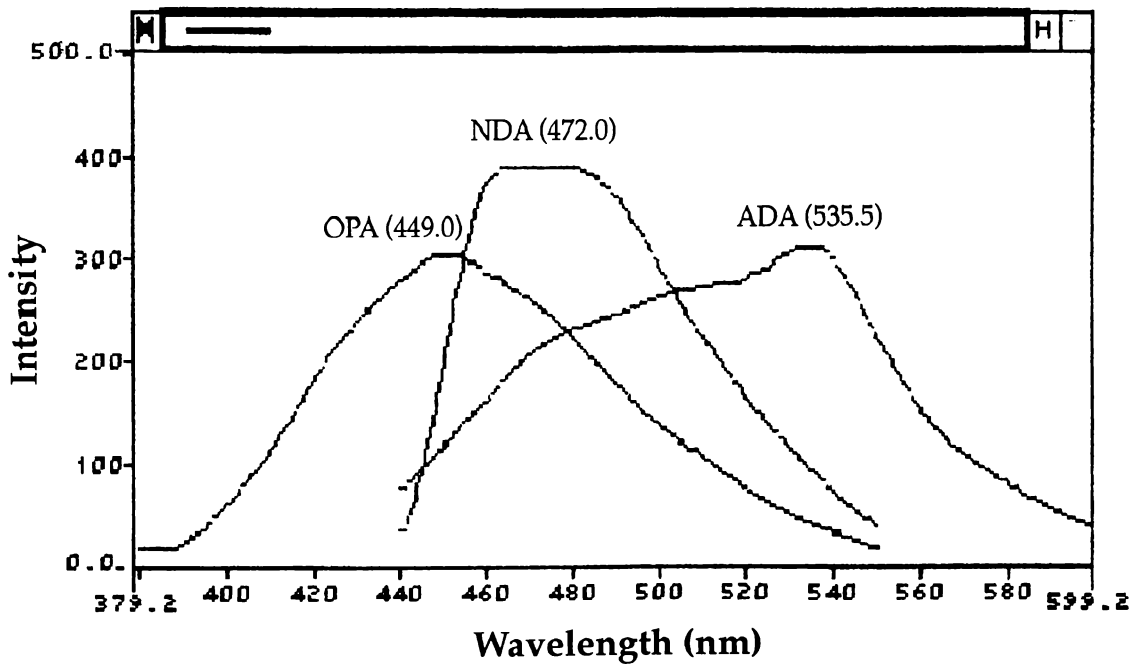

Fig. 5.7
Overlayed emission spectra for the reaction products of OPA, NDA and ADA with analine (excitation wavelengths are 337 nm, 418 nm and 405 nm respectively).

A summary of the excitations and their corresponding emissions for reaction products formed by OPA, NDA and ADA are presented in Table 5.2.

Table 5.2
Summary of excitations and emissions for the reaction products of OPA, NDA and ADA with analine.

Dialdehyde	Excitation λ (nm)	Emission λ (nm)
OPA	337	450
NDA	418	475
ADA	405	537

All three reagents yield emission peaks which are quite broad. The addition of one and two extra rings to OPA moves the resulting emissions of the reaction products to consecutively longer wavelengths. This result is in agreement with findings of Montigny et al. (1987) who compared OPA and NDA. Absorbances of the optical brightners normally used in paper lie around 350 nm with fluorescence maximum emissions between 432 and 442 nm (Zahradník, 1982). This makes OPA rather unsuitable as a reagent for direct fluorescent visualisation of fingerprints on most papers (although the possibility of time–resolved imaging may remain open, depending on the product's luminescent lifetime). The product from the reaction of NDA with NaCN however, produces a significant "red shift" in emission wavelength compared with that obtained in the case of OPA (and with respect to the emissions of optical brightners). The excitation wavelength for the fluorescence product of NDA is also a lot further into the red end of the spectrum compared with that of OPA. For this reason NDA may be more suitable for the detection of fingerprints on paper with respect to background fluorescence than OPA. ADA produces a very significant "red shift" in emission and excitation wavelength and could therefore be more suitable than both NDA and OPA for use in detection of fingerprints on paper and other surfaces with background emissions in the blue region.

5.3.2 Fingerprint trials

OPA treated fingerprints deposited on white paper resulted in no visible prints, a result which was probably due to background fluorescence emissions (blue) of the paper interfering with the blue emission of OPA (450 nm). By contrast, OPA treated fingerprints deposited on pink paper did result in visible prints (as previously

determined by Mayer et al., 1978); however, these were very blotchy in appearance, with only partial development.

On pink paper, only the 20 second and 1 minute OPA treated prints resulted in reasonable development. Shorter or longer treatment times resulted in poorer development. The immersion method of OPA treatment seems to be inferior to spraying with a Babington nebulizer, as used by Mayer et al., 1978 (comparative trials of spraying versus immersion were not attempted in this case due to time constraints). The results indicate however, that by immersion, a half minute dip in OPA solution will give the best development.

Results obtained from the OPA treatment of fingerprints on five different surfaces are presented in Table 5.3.

Table 5.3
Comparison of OPA treatment on a range of different surfaces.

Surfaces	Development
paper (pink)	reasonable
NZ$5 banknote	none
coke can (inside surface)	faintly visible
coke can (outside surface)	none
mylar (overhead transparency) sheet	none

NDA treated prints on both pink and white paper resulted in speckled green fluorescence on top of green background fluorescence when viewed under the UV hand-held lamp at 366 nm and the argon laser at 457.9 nm. In these cases it appeared as if the fingerprint had smeared or migrated out across the paper resulting in the speckled fluorescence observed.

ADA treated prints on pink and white paper resulted in speckled orange fluorescence when viewed under the UV hand-held lamp at 366 nm and the argon laser at 457.9 nm. Again the same reasoning for the speckled fluorescence could be applied.

If the speckling observed was partially related to migration of water–soluble print components, it is possible that better results might be obtained with a fine mist, or better still identifying an appropriate non–aqueous solvent system which is still compatible with the reaction chemistry. For example, the two commonly used latent fingerprint reagents, ninhydrin and DFO which work by reaction with amino acids are prepared in freon (Kent et al., 1986).

5.4 *Chapter summary*

Overall, OPA, NDA and ADA performed comparatively poorly when it came to visualising fingerprints on paper, despite their being reactive with amino acids and despite the fluorescence products of NDA and ADA having more favourable excitation and emission characteristics in solution. However, it is suspected that part of this poor performance problem could be due to the aqueous nature of the reagent systems, with a resultant tendency of water soluble amino–acid residues in the print to show some migration. It is possible that NDA and ADA may be good reagents for latent fingerprint development if they can be introduced successfully from a less polar solvent system. Recommendations for future research in this area are provided in Chapter 8.

5.5 *References*

Carlson R.G., Srinivasachar K., Givens R.S., and Matuszewski B.K. (1986). New derivatizing agents for amino acids and peptides. 1. Facile synthesis of N-Substituted 1-cyanobenz[f]isoindoles and their spectroscopic properties. *J. Org. Chem.*, **51**, 3978-3983.

Fisher, T.H.W. (1999). *Aspects of forensic chemistry of trace evidence: Explosive residue analysis, and detection of fingerprints on banknotes.* Masters thesis, University of Waikato, Hamilton, New Zealand.

Kent T. (editor), Hardwick S.A., and Sears V.G. (1986). *Manual of fingerprint development techniques - A guide to the selection and use of processes for the development of latent fingerprints.* Printed in England for the Home Office by Heanor Gate, Derbyshire.

Kwakman P.J.M., Koelewijn H., Kool I., Brinkman U.A. Th., and de Jong G.J. (1990). Naphthalene- and anthrancene- 2,3- dialdehyde as precolumn labelling reagents for primary amines using reversed- and normal-phase liquid chromatography with peroxyoxalate chemiluminescence detection. *Journal of Chromatography.*, **511**, 155-166.

Matuszewski B.K., Givens R.S., Srinivasachar K., Carlson R.G., and Higuchi T. (1987). N-Substituted 1-cyanobenz[f]isoindole: Evaluation of fluorescence efficiencies of a new fluorogenic label for primary amines and amino acids. *Anal. Chem.*, **59**, 1102-1105.

Mayer S.W., Meilleur C.P., and Jones P.F. (1978). The use of ortho-phthalaldehyde for superior fluorescent visualization of latent fingerprints. *J. Forens. Sci Soc.*, **18**, 233-235.

Miura T., Kashiwamura M., and Kimura M. (1984). A fluorometric method for the specific determination of serum arginine with 2,3-naphthalenedicarbaldehyde. *Anal. Biochem.*, **139**, 432-437.

de Montigny P., Stobaugh J.F., Givens R.S., Carlson R.G., Srinivasachar K., Sternson L.A., and Higuchi T. (1987). Naphthalene-2,3-dicarbaldehyde/cyanide ion: A rationally designed fluorogenic reagent for primary amines. *Anal. Chem.*, **59**, 1096-1101.

Roth M. (1971). Fluorescence reaction for amino acids.*Anal. Chem.*, **43**, 880-882.

Simons S.S., and Johnson D.F. (1978). Reaction of o-phthalaldehyde and thiols with primary amines: Formation of 1-alkyl(and aryl)thio-2-alkylisoindoles. *J. Org. Chem.*, **43**(14), 2886-2891.

Soper S.A., and Kuwana T. (1989). Matrix-isolated luminescence of primary amines derivatized with naphthalenedialdehyde. *Applied Spec.*, **43**(5), 883-886.

Weeks R.W., Yasuda S.K., and Dean B.J. (1976). Fluorescent detection of Hydrazines via Fluorescamine and isomeric phthaldehydes. *Anal. Chem.*, **48**, 159-161.

Zahradník M. (1982). *The production and application of fluorescent brightening agents.* New York, John Wiley and Sons, 31-39.

Chapter Six

Fluorescein diacetate: a preliminary appraisal of its potential use for the estimation of age of blood

6.1 *Introduction*

In the reconstruction of crimes involving homicide it is advantageous to be able to estimate the time of death (or the post-mortem interval—PMI) of a decomposing corpse.

One of the two current methods for estimating the PMI, the forensic entomological approach, is based on the time required for growth of insects and other arthropod species found browsing on the cadaver, or for longer time periods on the basis of arthropod populations and their position of appearance in established faunal succession schemes. It is assumed however that insects, usually flies, will discover the corpse soon after death or time of corpse exposure. This is not always a reliable assumption especially with indoor and closed-container death scenes, or where weather conditions are extreme (Catts and Goff, 1992). The other currently used method for estimating the PMI involves the solving of an equation for the post-mortem cooling of bodies. This method is only useful for bodies which have been deceased for less than 24 hours. The method also includes approximations, as various parameters such as the rectal temperature at time of death and ambient temperature used for solving the equation have to be assumed (Lynnerup, 1993).

Because of the problems associated with the current methods of PMI estimation it would be useful to have another more accurate method. In many cases it would also be advantageous to be able to estimate the age of a blood stain or blood fingerprint. In doing so it would not only be possible to place a suspect at the scene of a crime but to also determine whether that person was at the scene of the crime on or around the time the crime was committed.

The hydrolysis of the non–fluorescent compound fluorescein diacetate (FDA) by esterases present in the cytoplasm of red blood cells to the highly fluorescent product fluorescein has been used by Oh et al. (1995) in an assay for monitoring live haematopoietic cell numbers. The hydrolysis of FDA has also been used by Battin (1997) as a means of measuring the total esterase activity in natural stream sediment biofilms.

As a starting point of this work, it was postulated that in an ambient environment, esterase activity in blood from a deceased body might decrease at a certain, determinable rate, as the blood becomes older and various enzyme systems become denatured. If this is the case, it should be possible to estimate the PMI from this by comparing the rate of hydrolysis of FDA at the time of discovery with that which is usually obtainable at the time of death.

The aim of this part of the work was to assess the validity of the preliminary hypothesis that the total esterase (and pseudo–esterase) activity of a sample of stored human blood should decrease with time, with this decrease being reflected in a decrease in the rate of hydrolysis of FDA as the blood ages.

6.2 *Methodology*

6.2.1 Materials and instrumentation

The following materials and instrumentation were used in the preliminary appraisal of FDA for the aging of blood:

- $Na_2HPO_4.12H_2O$ (AR), aluminium oxide (Brockman Grade II), and acetone (AR) were purchased from BDH.
- NaOH (AR) and citric acid (Univar) were purchased from Ajax Chemicals.
- Acetic anhydride (AR) was purchased from M&B.
- Dichloromethane (AR) was purchased from R.P. Normanpur™.
- Fluorescein was purchased from Merck.
- HCl (AR) and pyridine were purchased from Aldrich Chemical Company.
- $CaCl_2$ was purchased from Riedel-de Haën.
- Blood was collected freshly from the arm of the author at the University of Waikato Medical Centre, Hamilton, New Zealand. The blood was collected directly into a 5 mL vaccutainer containing EDTA as an anti-coagulant.

- A Perkin Elmer Luminescence Spectrometer LS 50B was used for collection of all fluorescence data; this utilises a xenon-lamp source.
- A Bruker AC300 NMR spectrometer was used for confirmation of FDA synthesis.

6.2.2 Synthesis of fluorescein diacetate

Fluorescein diacetate (FDA) was synthesised following the method of a colleague (Hill, 1997). It is also commercially available from Sigma.

An 8.217 g amount of fluorescein (0.025 mole) was weighed into a round–bottomed flask fitted with a $CaCl_2$ drying tube. The resulting solid clump that formed on addition of 10 mL pyridine (0.124 mole) was heated on a hotplate for 20–30 minutes with stirring. An 11.67 mL volume of acetic anhydride (0.124 mole) was then added dropwise over 5 minutes to the resulting orange coloured solution. Heating of the reaction mixture was continued overnight with stirring and the drying tube connected.

The reaction mixture was then washed with distilled water and poured through a Buchner filter funnel. The resulting crystals which were dark yellow in colour were washed with two washings of 2 *M* NaOH and one washing of 1 *M* HCl followed by a wash with water.

At this stage, the crystals still retained some yellow colour due to the presence of small amounts of unreacted fluorescein. A column was therefore prepared using a 250 mL separating funnel filled to two thirds with aluminium oxide (Brockman Grade II), using dichloromethane as the eluent. The yellow crystals were dissolved and passed through the column using 500 mL of dichloromethane. The dichloromethane runoff was rotary evaporated leaving a white solid which was dried on a vacuum line.

A 7.1554 g (0.0172 mole) amount of white solid was obtained which was confirmed as fluorescein diacetate by ^{13}C NMR spectroscopy. The yield was 69.5%.

A ^{13}C NMR spectrum was obtained on a Bruker AC300 instrument using CCl_3D as the solvent. The results from this spectrum are presented in Table 6.1. Refer to Fig. 6.1 for numbered structure of FDA.

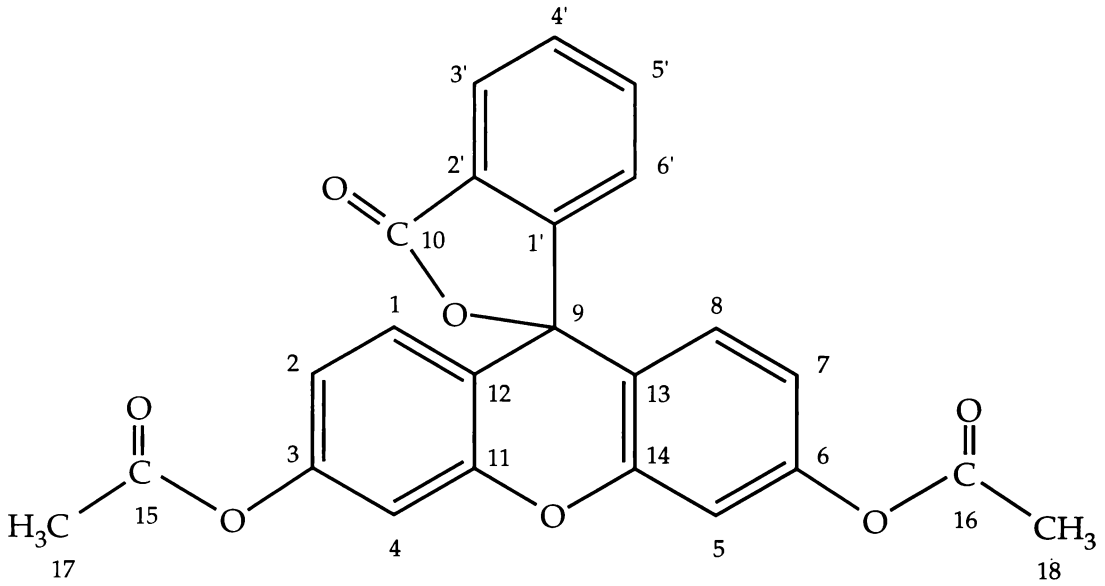

Fig. 6.1
Numbered structure of fluorescein diacetate (NMR shifts of the atoms numbered are listed in Table 6.1).

Table 6.1
^{13}C NMR results for synthesis of FDA.

Carbon number	Carbon environment	δ (ppm)
1′	C	152.10
2′	>C-COO-	126.10
3′	CH	124.13
4′	CH	130.08
5′	CH	135.30
6′	CH	125.26
1(8)	CH	128.99
2(7)	CH	117.78
3(6)	>C-O	no peak
4(5)	CH	110.42
9	C-O	82.15
10	>C-COO-	no peak*
11(14)	C-O	151.62
12(13)	C	116.52
15(16)	CH_3COO-	168.85
17(18)	CH_3COO-	21.15

*Probably hidden by stronger combined peak of C15 and C16.

6.2.3 Blood solution trials

A 0.48 *mM* solution of FDA was prepared by dissolving 20 mg in 100 mL acetone.

A fluorescein solution (0.9 *μM* was prepared in phosphate buffer (pH 7.4) in order to establish useful fluorescent emissions for monitoring of the hydrolysis of FDA. A luminescence spectrometer was used with slit widths for both excitation and emission being set at 2.5 nm and the fluorescein solution being held in a 10 mm quartz cuvette.

A 200 μL aliquot of the blood which had been collected directly into a 5 mL vaccutainer containing EDTA as an anti-coagulant was then diluted with citric acid/phosphate buffer (pH 7.4—refer to table 2.1 in Chapter Two) to a final volume of 100 mL in a volumetric flask (500 times dilution). Under these conditions, all the still–intact blood cells are expected to rupture (lyse) immediately, releasing their contents to the solution (Molan, 1998).

In order to establish any background fluorescent emissions other than those from fluorescein, scans of the FDA solution and the 500 times diluted blood solution were obtained between 450 and 550 nm using a luminescence spectrometer. Excitation was carried out at 240 nm with slit widths for both excitation and emission being set at 5 nm and with solutions being held in a 10 mm quartz cuvette.

A 100 μL sample of the FDA solution was then diluted to 20 mL with the 500 times diluted blood solution, to give a final FDA concentration of 2.4 *μM*. The time at which the FDA solution was added to the blood solution was recorded and the intensity of the 512 nm emission of the FDA/blood solution was obtained at various time intervals using a luminescence spectrometer. Excitation was carried out at 240 nm with slit widths for both excitation and emission being set at 5 nm and with solutions being held in a 10 mm quartz cuvette.

The original blood sample which had been obtained at a recorded time was stored in the vaccutainer it had been collected in, out of direct sunlight (in a shaded but not totally dark area) at an average temperature of approximately 18°C. Aliquots of this blood (200 μL) were taken at various times over a 35 day period and used to prepare more FDA/blood solutions for analysis on a luminescence spectrometer.

6.3 *Results*

The maximum emission for fluorescein (the hydrolysis product of FDA) when excited at 240 nm was found to occur at 512 nm. A solution of FDA in acetone however, had no emissions between 450 and 550 nm when excited at 240 nm. The solution of blood was found to have an emission at 484 nm when excited at the same wavelength. This emission however, did not interfere with that of fluorescein at 512 nm. Changes in intensity of the emission of fluorescein at 512 nm for a blood sample treated with FDA are presented in Table 6.2. The rate of change in intensity was measured at particular times over a period of 0 to 35 days from the time when the blood sample was originally obtained. In all cases the initial FDA concentration was 0.48 mM, the blood solution used was 500 times diluted and the pH of the buffer was 7.4. Development was allowed to occur in the cuvette. Although temperature was not regulated (due to lack of a temperature device in the luminescence spectrometer), the ambient temperatures over the times of the trials were relatively constant at approximately (20 ± 2) °C

Table 6.2
Changes in emission intensity with time at 512 nm for a blood sample treated with FDA (0 to 35 days from time when blood sample was obtained). Other conditions were as outlined in the text.

Number of days since blood sample was obtained															
0		1/4		1		2		3		4		21		35	
T (m)	Int.	T (m)	Int.	T (m)	Int.	T (m)	Int.	T (m)	Int.	T (m)	Int.	T (m)	Int.	T (m)	Int.
0	0	0	0	0	0	0	0	0	0	0	0	0	0	0	0
6	19.3	6	14.8	6	27.8	6	17.1	6	15.8	6	15.6	10	21.5	6	11.8
10	41.7	10	25.9	10	52.7	10	30.7	10	29.9	10	21.7	14	28.4	10	20.3
14	74.1	14	48.5	14	87.6	14	56	14	51.9	14	31.3	18	35	14	30.2
18	112.3	18	85.2	18	126.2	18	94.9	18	86.6	18	44.7	22	44.6	18	41.6
22	156.2	22	139.8	22	170	22	140.9	22	130.2	22	63	26	54.5	22	53.4
26	204.2	26	200.7	26	223.2	26	199.3	26	182.6	26	89.2	30	68.1	26	66.6
30	255.3	30	275.4	30	276.3	30	270.3	30	244.3	30	119.9	34	82	30	80.9
34	308.9	34	348.6	34	331.5	34	343.2	34	311.9	34	159.6	60	259.1	34	96.9
60	624.3	65	850.6	57	646.6	60	737.8	60	705.7	60	539.4	64	296	60	228.3
76	819.8			64	724.3	64	775.3	64	748.9	64	568.6			64	253.8
						77	896.8								

Linear regression lines of variations in the rate of FDA hydrolysis over a 35 day period are presented in Fig. 6.2 (r^2 values lie between 0.913 and 0.988).

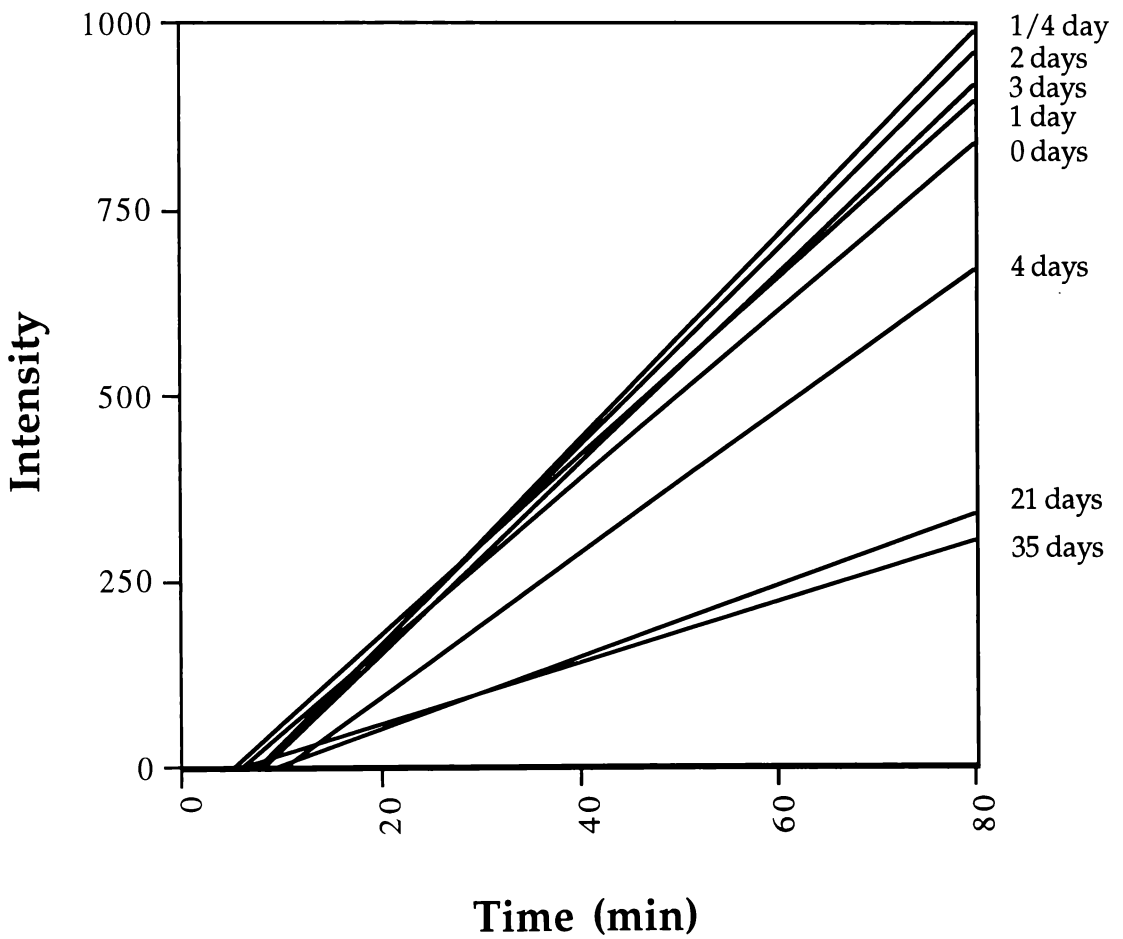

Fig. 6.2
Linear regression lines for variation in rate of FDA hydrolysis when brought into contact with human blood over a 35 day period.

The change in intensity of the fluorescein emission at 512 nm at 60 minutes is presented for a 35 day period in Fig. 6.3.

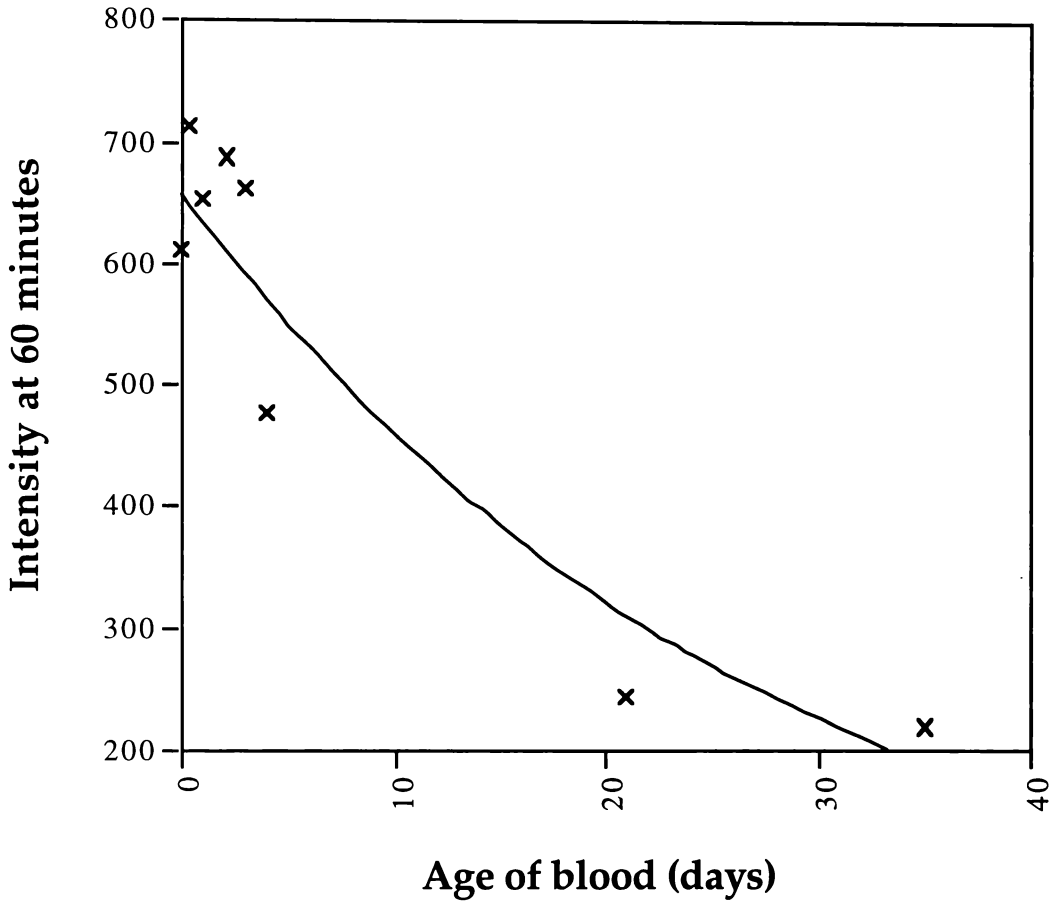

Fig. 6.3
Change in 512 nm fluorescein emission intensity at 60 minutes (based on linear regression lines) for blood varying in age from 0 to 35 days.

Over the first three days there is very little difference in the rate of FDA hydrolysis. The rate change is also rather ambiguous and seems to indicate no specific relationship. By the time the blood is four days old however, there is an obvious decrease in the rate of FDA hydrolysis. This decrease in rate continues for the 21 and 35 day analyses in a manner consistent with an inverse relationship. It should be noted that the rate of hydrolysis should be temperature dependent to some extent, as it is a chemical reaction. As noted above, the luminescence spectrometer used was not equipped with a temperature regulation device so therefore variation in temperature during the time over which the reaction was monitored could be the source of some of the variability observed over the first few days.

6.4 *Chapter summary*

The results from this preliminary appraisal indicate that FDA may be useful in estimating the PMI or age of blood stains and blood prints. Blood which was left for a period of 35 days in a vaccutainer with EDTA as an anti-coagulant showed an obvious decrease in the rate of FDA hydrolysis as the blood got older. The hypothesis that esterase activity in stored blood decreases with age, and that this decrease is reflected in the ability of the blood to hydrolyse FDA, is validated.

This however, is only a preliminary appraisal of the potential for FDA to be used as a marker of blood age, and does not emulate the actual conditions under which blood in a body or a blood stain would age, for which precise empirical calibration would be required following a standard protocol, as well as research access to cadavers of the recently deceased (or perhaps porcine models). A thorough investigation would be necessary in order to establish the actual effect of aging blood on FDA hydrolysis under the conditions provided by a body or dried stain, as well as identify biochemical issues such as the best organ to extract blood from. Recommendations for further research in this area are given in Chapter 8.

6.5 *References*

Battin T.J. (1997). Assessment of fluorescein diacetate hydrolysis as a measure of total esterase activity in natural stream sediment biofilms. *The Science of the Total Environment*, **198**, 51-60.

Catts E.P., and Goff M.L. (1992). Forensic entomology in criminal investigations. *Annual Review of Entomology*, **37**, 253-272.

Hill S. (1997). Personal communication. Department of Chemistry, University of Waikato, Hamilton, New Zealand.

Lynnerup N. (1993). A computer program for the estimation of time of death. *J Forens. Sci.*, **38**, 816-820.

Molan P. (1998). Personal Communication. Department of Biology, University of Waikato, Hamilton, New Zealand.

Oh K.W., Ng T., and See L.H. (1995). A fast assay for developing serum free media for cord blood haematopoietic cells. *Biotechnology Techniques*, **9(8)**, 577-582.

Chapter Seven

Various attempts at new methods for visualisation of latent and blood fingerprints

7.1 *Overview*

Various other attempts at developing new methods for visualisation of latent and blood fingerprints were investigated. Although most of the methods outlined in this chapter proved unsuccessful it was felt prudent that a description of the various methods should still be included in order to provide guidance with future research in the area.

7.2 *Materials and instrumentation*

The following chemicals and materials were all used in the various attempts at developing new methods for visualisation of latent and blood fingerprints outlined in this chapter:

- $AuCl_4H$, sulfuric acid (AR), petroleum spirits (b.p. 40-60°C) (AR), diethyl ether (AR), methanol (AR), octanol (GPR), $Na_2HPO_4.12H_2O$ (AR) sodium perborate (GPR), sodium bromide (GPR), and acetic acid (AR) were all purchased from BDH.
- Citric acid (univar), triethylamine (LR), and NaOH (AR) were purchased from Ajax Chemicals.
- Toluene (AR), and dichloromethane (AR) were purchased from R.P. Normanpur™.
- 9-(chloromethyl)anthracene, thiourea, Tween 20, 2-aminoethanethiol.HCl, dansyl chloride, bis(2-ethylhexyl)amine, 1-dodecanethiol thiocarbanilide, hydrochloric acid, sodium carbonate, anhydrous magnesium sulfate, and 5-amino-2,3-dihydrophthalazine (luminol) were all purchased from Aldrich Chemical Company.
- Acetone (AR) sodium citrate (AR), 5-sulfosalicylic acid, and $NaH_2PO_4.2H_2O$ were all purchased from M&B Laboratory Chemicals.
- Fluorescein was purchased from Merck.
- Hydrogen peroxide (27%) was purchased from Andrew Chemicals Division.

- Peroxidase-conjugated rabbit anti-human albumin was purchased from Dako, and SYPRO™ Orange was purchased from Bio-Rad Laboratories, and ABTS®-$(NH_4)_2$, was purchased from Boehringer Mannheim (BM) Laboratories.
- Fast Red A (β-naphthylamine sulfonic acid) was obtained from a colleague (Henderson, 1997) who had prepared it in house; tetraphenyl porphyrin, and disodium phthalocyanine were obtained from another colleague (Murphy, 1997) who had also prepared them in house.
- Paper (A4, 80 gsm) was obtained from Copyright (Australian Paper, Ltd.) and glass slides from Marienfeld.
- Blood was collected freshly from the arm of the author at the University of Waikato Medical Centre, Hamilton, New Zealand. Blood was collected directly into a 5 mL vaccutainer containing EDTA as an anti-coagulant.

The following instrumentation was used in this part of the work:

- A Mineralight® hand-held UV lamp (model UV GL-58) was used with two wavelength settings of 254 and 366 nm for visualisation of fingerprints treated with fluorescent chemicals.
- A Spectra Physics 164 argon-ion laser (1 watt) in combination with a 265 Exciter was also used for viewing of prints.
- A Hewlett Packard (5970) mass detector, quadrapole design, interfaced to a HP 5890 GC was used to obtain mass spectra. Selected ion mode (SIM) was used for anthracene thiol characterisation. A HP-1 Crosslinked Methyl Siloxane column was used with dimensions, 25 m x 0.2 mm x 0.33 μm film thickness.
- A Perkin Elmer Luminescence Spectrometer LS 50B was used as previously outlined for collection of fluorescence data.
- A Hitachi S4000 Scanning Electron Microscope was used to establish the presence of Au-S bonds. The instrument uses a cold emission tip electron source.
- A Varian Cary 1 UV-Visible Spectrophotometer (SBW = 0.2 nm, signal averaging time = 0.100 sec) was used for solution trials.
- A Meterlab™ pH meter (model PHM240) was used for confirming the pH values of buffer solutions.

7.3 *Modification of colloidal gold method*

7.3.1 Introduction

Colloidal gold, or multi-metal deposition, is a relatively new technique that is effective on a range of both porous and non-porous surfaces. The sensitivity obtained on plastic and polythene surfaces has been shown to be at least equal to, and at times superior to, *Super Glue™* fuming and vacuum metal deposition (Lavis, 1994).

The colloidal gold technique is a two stage process. In the first stage colloidal gold in aqueous solution binds to amino acids, peptides and proteins present in latent prints to give a gold deposit. The second stage involves treatment with a silver–based aqueous reagent (modified physical developer). The bound colloidal gold from the first stage provides a nucleation site around which silver precipitates in the second incubation step making the method very sensitive (Lavis, 1994).

For the purpose of this research it was proposed that a new method to replace the physical developer step be investigated. The reason for this is because the physical developer step is difficult to carry out and does not always work properly.

Colloidal gold is particularly effective on non-porous surfaces, especially plastics and polythenes. Surfaces on which it has been shown to be effective include:

- cling film
- photographs
- perspex
- waxed paper
- shotgun cartridges
- expanded polystyrene
- masking tape (adhesive and non-adhesive sides)
- beer bottle labels
- condoms

It is also effective on articles which have been wetted and the technique has revealed fingerprints on several surfaces for which there is no suitable method available.

There may be a loss in sensitivity with the technique if surfaces have been subjected to other chemical treatments (*eg. Super Glue™* fuming).

7.3.2 Methodology

Colloidal gold treatment

Latent fingerprints deposited on various surfaces were initially treated with a solution of colloidal gold. The method for colloidal gold treatment of latent fingerprints is provided as follows. This is the method currently being used by the Crown Research Institute *ESR:Forensic* in New Zealand (Lavis, 1994). After this initial treatment with colloidal gold, fingerprints were then subjected to a variety of treatments in order to establish a new method for replacing the physical development step usually employed after colloidal gold treatment.

All glassware was scrupulously cleaned. Internal surfaces of dishes were wiped with paper tissue under cold running tap water and then rinsed 3 times with distilled water before use. After use, dishes were washed thoroughly under a tap to prevent staining and were then dried with a paper tissue.

Solutions were prepared using the following procedures:

Gold chloride solution:

A solution of gold chloride was prepared by dissolving 1 g of $AuCl_4H$ in 10 mL of distilled water in a clean, well stoppered glass flask.

Sodium citrate solution:

A solution of sodium citrate was prepared by dissolving 1 g of sodium citrate in 100 mL of distilled water in a clean, well stoppered flask.

Citric acid solution:

A solution of citric acid was prepared by dissolving 96 g of citric acid in 1 L of distilled water in a clean, well stoppered flask.

All three of these solutions are stable and may be stored indefinitely at room temperature.

Working Solution:

1. A 1 mL aliquot of gold chloride solution was added to 1 L of distilled water in a 2 litre clean glass beaker.
2. The solution was brought rapidly to the boil and 15 mL of sodium citrate solution was added.
3. The solution was kept boiling gently for 10 minutes (solution was port wine in colour after addition of sodium citrate).
4. While still hot 5 mL of Tween 20 (detergent) was stirred in. The solution was left to cool.
5. The pH of the solution was checked with pH paper and citric acid solution was added 1 mL at a time until a pH of approximately 3 was obtained.
6. Distilled water was added to restore the volume to 1 litre.

The working solution of colloidal gold will remain stable for several months if kept in the refrigerator.

Procedure for treating fingerprints:

1. The article to be treated was washed in distilled water. Approximately 10 minutes was allowed for non-porous items and 30 minutes for porous items.
2. The article was immersed in the colloidal gold working solution. Gentle agitation of the solution was used to aid development which took between 10 and 60 minutes. Prints developed at this stage had a faint purple colouration.
3. The article was then rinsed in distilled water, briefly for non-porous surfaces, about 15 minutes for porous items with, in these cases, several changes of water.

Various treatments were then employed in an effort to visualise the latent prints further. These treatments were based on the knowledge that long chain n-alkanethiols ($HS(CH_2)_xX$), where X is not a methyl group, absorb spontaneously from solution onto gold surfaces (Laibinis et al., 1995). Laibinis et al. (1995) achieved this with n-alkanethiols were X was an OR group. It was proposed that a bridging molecule with a thiol group could be attached to the gold in the fingerprint and then a fluorescent marker be attached to the thiol containing bridging molecule.

2-aminoethanethiol treatment

It was envisaged that the thiol end of 2-aminoethanethiol could be reactive with colloidal gold treated fingerprints with subsequent reaction of dansyl chloride (which forms a fluorescent compound on reaction with amines) with the amine end of 2-aminoethanethiol. A UV lamp could then be used to enhance the visualisation of the prints.

2-aminoethanethiol.HCl was dissolved in water and a few drops of triethylamine was added to convert it to 2-aminoethanethiol. A colloidal gold treated fingerprint exhibit on paper and a glass microscope slide were immersed for approximately 45 minutes before being removed and left to dry.

Dansyl chloride (a fluorescent marker) was then dissolved in toluene (0.016 mol/L). The dry fingerprint exhibits were immersed in this solution for 2 minutes before being removed and left to dry.

The whole procedure was repeated but with the exhibits immersed in the thiolamine solution for shorter times.

In a variation on the delivery method, a colloidal gold treated fingerprint on filter paper was also treated with aminethiol solution for 20 s and then treated with dansyl chloride solution for 30 min. The same procedure was then repeated but with the filter paper being soaked in distilled water for 10 min after the aminethiol treatment.
A colloidal gold treated fingerprint on normal paper was placed between two pieces of filter paper, previously soaked in aminethiol solution. A towel was placed over the top and a steam iron applied over the towel for 1 min. The fingerprint exhibit was dried and then immersed in dansyl chloride solution for 2 minutes. The same procedure was carried out again on colloidal gold treated fingerprints on normal paper, filter paper and a glass slide.

The absorption maximum for "dansylated" fingerprints has been reported by Burt and Menzel (1985) to be at 360 nm with an emission at 475 nm. Therefore all exhibits were viewed under a UV hand-held lamp with the 366 nm filter setting.

Long chain thiol/dye treatment

This method involved the reaction of a long chained thiol ($C_{12}H_{25}SH$) in petroleum spirits (b.p. 40-60 °C) with the colloidal gold treated fingerprint. It was envisaged that the long chain would reduce the reactivity of the thiol group enough to prevent the colloidal gold being pulled back into solution (an effect found to be a problem for short–chain thiols — section 7.3.3). The fingerprint was then treated with a variety of compounds. It was hoped that these compounds would become entrapped in the lipophilic ends of the long chained thiol and thus act as dyes.

A dansyl amine adduct was prepared by dissolving 0.0017 mole of bis(2-ethylhexyl)amine, $[CH_3(CH_2)_3CH(C_2H_5)\text{-}CH_2]NH$, and 0.0008 mole of dansyl chloride in 50 mL toluene. Before applying this solution to colloidal gold/thiol treated fingerprints it was applied directly to four untreated fingerprints on paper in the hope that the dansyl chloride/amine adduct would react with the lipid component of the fingerprints.

Four prints on paper treated initially with colloidal gold were immersed in the thiol solution for 30 seconds before two of the prints were immersed in the dansyl amine adduct solution for 30 seconds and the other two prints were immersed for 5 minutes.

Four prints on paper treated initially with colloidal gold were immersed in the thiol solution for 30 seconds before two of the prints were immersed for 30 seconds and two of the prints were immersed for 5 minutes in a tetraphenyl porphyrin/toluene solution (2g/L).

Four prints on paper treated initially with colloidal gold were then immersed in the thiol solution for 30 seconds before being immersed in a disodium

phthalocyanine/acetone solution (2 g/L) for a few seconds. The prints were then rinsed in acetone.

Four prints on paper treated initially with colloidal gold were immersed in the thiol solution for 30 seconds before two of the prints were immersed in a fluorescein/water solution (0.91 m*M*) for 30 seconds and two of the prints were immersed for 5 minutes.

Fast Red A (β-naphthylamine sulfonic acid) is water soluble when it is basified and organic soluble when acidified. This provides a mechanism by which the dye could be forced into the organic soluble lipophilic end of the thiol. Fast Red A was dissolved in water as the basic sodium salt. A pre-colloidal gold and thiol treated fingerprint on paper was then immersed in the Fast Red A solution and dilute H_2SO_4 was added dropwise (5 mL).

Anthracene thiol

Anthracene is naturally fluorescent, and thiols are reactive to gold. Anthracene thiol was prepared in the following manner*. A 50 mL methanol solution containing 99.7 mg (0.44 μmole) of $AnCH_2Cl$ (chloromethyl anthracene) and 31.2 mg (0.44 μmole) of $(NH_2)_2CS$ was refluxed for 3 hours. The reaction mixture was rotary evaporated down to 3-4 mL. Diethyl ether was added to precipitate out the salt. The salt was filtered off and dissolved in water and a large excess of OH^-. The solid would not dissolve in water after OH^- was added. Methanol was therefore added to increase the solubility. It still did not dissolve even after refluxing for a further 3 hours. Acid was then added to a pH 4. The solution was rotary evaporated down. A diethyl ether/ water extraction was carried out in order to separate out the anthracene thiol into the ether layer. The ether layer was rotary evaporated down to leave a yellow solid.

Gas chromatography–mass spectrometry (GC–MS) was used to help characterise the yellow solid. Fluorescent spectra of the yellow solid (in dichloromethane) and chloromethyl anthracene (in dichloromethane) were also obtained on a luminescence spectrometer with excitation at 458 nm and a 5 nm slit width.

* Henderson (1997).

A solution of anthracene thiol was prepared in dichloromethane and used to treat two colloidal gold prints on paper, two colloidal gold prints on glass slides and one colloidal gold print on perspex.

Scanning Electron Microscopy (SEM) was carried out on a colloidal gold treated fingerprint on paper and glass slide with subsequent anthracene thiol treatment (anthracene thiol in dichloromethane) to establish if Au–S bonds were present. Carbon coating was performed to prevent charging of surfaces.

7.3.3 Results

Results for colloidal gold treated latent fingerprints with subsequent 2-aminoethanethiol and dansyl chloride treatments are presented in Table 7.1.

Table 7.1
Attempted fluorescent visualisation of colloidal gold treated fingerprints with subsequent 2-aminoethanethiol and dansyl chloride treatment using excitation at 366 nm.

Exhibit Type	Immersion Time in Thiolamine	Fluorescent Enhancement
paper	30 m	none
glass	30 m	none
paper	5 s	none
glass	5 s	none
paper	20 s	none
glass	20 s	none
paper	60 s	none
glass	60 s	none

After 2-aminoethanethiol treatment the faint purple colour, usually visible with colloidal gold treated prints, was found to be no longer visible. Also no fluorescent enhancement of the prints was observed after subsequent dansyl chloride treatment. Disappearance of the gold colour from the prints is unusual. It is suspected that reaction did occur between the thiol and deposited gold in the fingerprint (after

Laibinis et al., 1995). However, the next step after reaction with the short–chain thiol appears to have been removal of the reacted gold from the surface into solution.

A colloidal gold treated fingerprint on filter paper treated with aminethiol and dansyl chloride resulted in the whole area of the paper appearing fluorescent where it had previously been immersed in the aminethiol solution. The aminethiol had obviously soaked into the filter paper. No fluorescence was observed however, when the same procedure was repeated but with the filter paper being soaked in distilled water for 10 min after the initial aminethiol treatment.

The following results were obtained for colloidal gold treated fingerprints on normal paper, filter paper and a glass slide which had been placed between two pieces of aminethiol soaked filter paper and with subsequent steam iron application. After dansyl chloride treatment no fluorescence was observed on the paper, fluorescence was observed all over the filter paper and for the glass slide the colloidal gold print disappeared on application of the steam iron with no subsequent fluorescence being observed.

As mentioned above, it was speculated that the thiolamine was successfully complexing to the colloidal gold in the fingerprint, but then pulling it back into solution. A "softer" method of linking the fluorescent tag to the gold was therefore required.

Thiol/dye treatment

Before abandoning the possibility that the gold–thiol adduct might have still been present on the surface, the following trials were attempted in order to show it up if it were still present. The dansyl amine adduct was applied to four colloidal gold/thiol treated fingerprints and directly to four untreated fingerprints on paper. No fluorescence or enhancement however, was observed on viewing with a UV lamp at 366 nm. Similarly, treatment of four colloidal gold/thiol treated fingerprints on paper with a tetraphenyl porphyrin/toluene solution also resulted in no staining of the prints.

Four colloidal gold/thiol treated fingerprints on paper which were treated with a disodium phthalocyanine/acetone solution with a subsequent rinse in acetone resulted in almost immediate staining of the paper but with no visible enhancement of the print.

Four colloidal gold/thiol treated fingerprints on paper which were treated with a fluorescein/water solution resulted in no fluorescence or enhancement being observed on viewing with a UV lamp at 366 nm. Treatment of four colloidal gold/thiol treated fingerprints with a Fast Red A solution also had no result in terms of staining.

Anthracene thiol

Two prints on paper, two prints on glass slides and one print on perspex previously treated with colloidal gold before subsequent treatment with anthracene thiol solution resulted in no prints being visible when viewed under the argon laser at 488 nm.

SEM analysis on a colloidal gold treated fingerprint on paper and a glass slide with subsequent anthracene thiol treatment did not detect the presence of any Au–S bonds. The colour of the colloidal gold in the print, however, remained. It appears that in this case, the thiol did not react with the colloidal gold.

7.3.4 Section discussion and summary

Treatment of colloidal gold prints with short and long chain alkanethiols in order to coat the surface with a fluorescent tag was unsuccessful. Long chain n-alkanethiols ($HS(CH_2)_xX$) where X is not a methyl group could be investigated further, as Laibinis et al. (1995) has achieved adsorption of alkanethiols of the type ($HS(CH_2)_nOR$) onto the surfaces of evaporated gold films. However, it is possible that the surface integrity of a gold film is far greater than the gold deposited in a latent fingerprint from colloidal gold solution, and that gold film has a much greater stability to dissolution. The suspected main problem in these trials was dissolution of previously deposited gold

after complexation with the thiol. This behaviour has a well known precedent in chemical engineering, where sulfur–containing flotation agents are used to solubilise small gold particles during mining operations. An example of this is the commercial extractant Aerophine (sodium di-isobutyl-dithiophosphinate) which has been used as a flotation reagent ("collector") for separation of galena, chalcopyrite, and precious metals from complex sulfide ores (Raksasataya, 1998).

7.4 *Octanol as a model for the lipid component of a latent fingerprint*

7.4.1 Introduction

Fluorescein is a strongly fluorescent chemical which is most soluble in an alkaline solution (Haugland, 1992). Fluorescein has been discussed as a field-worthy latent bloodstain detection system by Cheeseman and DiMeo (1995). The method involves the preparation of a fluorescin solution (fluorescein in the reduced state) using zinc powder. This solution unlike a solution of fluorescein is colourless and is only stable for less than 48 hours. As well as this the preparation of the solution is reasonably involved. The solution is applied to barely visible blood prints only and requires a subsequent application of hydrogen peroxide. Oxidation of fluorescin then occurs in the presence of peroxidase or pseudo peroxidase (blood) and the print can be viewed under a near UV light source.

It was proposed that by acidifying an alkaline solution of fluorescein it may be possible to force some of the fluorescein into the lipid component of a latent fingerprint. n-Octanol was used to mimic the lipid component in a separating funnel with an aqueous solution of fluorescein. Octanol is used as a model for chemical transport across the skin, as it has the same dielectric constant and polarity as a cell membrane (Florence et al., 1992). The optimum conditions for increasing the fluorescein concentration in the octanol layer were investigated using UV/Vis spectroscopy. It was proposed that distribution constants (K_d) could be calculated for various octanol/aqueous mixtures.

7.4.2 Methodology

Fluorescent emission solution trials

The change in fluorescent emission intensity of flourescein with pH was initially investigated to see if this could be used as a method for establishing the amount of fluorescein which could be forced over into the octanol layer.

A 0.91 m*M* stock solution of fluorescein was prepared by dissolving 15 mg of fluorescein up to 50 mL using phosphate buffer pH 8. Dilute fluorescein solutions of varying pH values were then prepared using buffers (refer to Table 2.1 in Chapter 2 on phosphate and citric acid/phosphate buffers) to dilute 50 µL aliquots of the fluorescein stock solution up to 50 mL (0.91 µ*M*). The exact pH of these solutions was determined with a pH meter. Emission intensities at 512 nm were determined by excitation at 240 nm on a luminescence spectrometer. Slit widths for both excitation and emission were set at 2.5 nm, with solutions being held in a 10 mm quartz cuvette.

A 0.91 m*M* solution of fluorescein in octanol was prepared. A 50 µL aliquot of this solution was then diluted up to 50 mL (0.91 µ*M*) with octanol. Emission intensities were determined on a luminescence spectrometer. Slit widths for both excitation and emission were set at 2.5 nm, with the solution being held in a 10 mm quartz cuvette.

A fluorescent scan of octanol by itself was obtained in order to assess the effect it may be having on the emission spectra of fluorescein. Slit widths for both excitation and emission were set at 2.5 nm, with the solution being held in a 10 mm quartz cuvette.

UV/Vis solution trials

A 0.018 m*M* fluorescein solution was prepared by diluting 1 mL of stock solution (0.91 m*M*, pH 8) up to 50 mL with a citric acid/phosphate buffer (pH 5.55). A UV/Vis scan of this solution was obtained on a Varian Cary 1 UV-Visible Spectrophotometer (SBW = 0.2 nm, signal averaging time = 0.100 sec). A 20 mL portion of the solution was then poured into a 100 mL separating funnel with 20 mL of octanol (octanol floats on top). The funnel was stoppered and shaken vigorously a few times. UV/Vis scans

of the aqueous and octanol layers were then obtained for comparison with the previously obtained scan of the aqueous solution. A UV/Vis scan of neat octanol was also obtained in order to establish whether there was any absorbance contribution from it. Citric acid/ phosphate buffer was used as a blank for UV/Vis scans of the aqueous layers while octanol was used as a blank for UV/Vis scans of the octanol layers. All solutions were held in 10 mm quartz cuvettes.

A 0.036 m*M* fluorescein solution was prepared by diluting 2 mL stock solution (pH 8) up to 50 mL with a phosphate buffer (pH 9.01). A UV/Vis scan of this solution was obtained. A 20 mL portion of this solution was then poured into a 100 mL separating funnel with 20 mL of octanol. The funnel was stoppered and shaken vigorously a few times. UV/Vis scans of the aqueous and octanol layers was obtained. Concentrated HNO_3 (1 mL) was added to the funnel and the funnel then shaken as before. After this had been left to stand a while a UV/Vis scan of the aqueous layer was obtained. Phosphate buffer was used as a blank for all UV/Vis scans with solutions being held in 10 mm quartz cuvettes.

A 0.036 m*M* fluorescein solution was prepared by diluting 2 mL stock solution up to 50 mL with citric acid (pH 2). A 20 mL portion of this solution was then poured into a 100 mL separating funnel with 20 mL of octanol. The funnel was stoppered and shaken vigorously a few times. A visual examination of the colours in the two layers was then conducted.

Another 0.036 m*M* fluorescein solution was prepared by diluting 2 mL stock solution (pH 8) up to 50 mL with a phosphate buffer (pH 9.01). A five times diluted sample of this aqueous solution was scanned on the UV/Vis spectrometer. A 20 mL portion of the solution was then poured into a 100 mL separating funnel with 20 mL of octanol and 0.5 mL concentrated HNO_3 was added before stoppering and shaking. A sample of the octanol layer was then scanned on the UV/Vis spectrometer after the layers had separated on standing. This procedure was repeated three more times but with 1,2, and 4 mL of HNO_3 added.

A 0.182 m*M* fluorescein solution was prepared by diluting 10 mL of stock solution (pH 8) up to 50 mL with phosphate solution (pH 9.01). A twenty times diluted sample of this aqueous solution was scanned on the UV/Vis spectrometer. A 20 mL portion of this solution was then poured into a 100 mL separating funnel with 20 mL of octanol and 0.5 mL concentrated HNO_3 was added before stoppering and shaking. A sample of the octanol layer was then scanned on the UV/Vis spectrometer after the layers had separated on standing. This procedure was repeated three more times but with 1,2, and 4 mL of HNO_3 added.

It was at this point remembered that the original stock solution of fluorescein (0.91 m*M*) had been prepared with a buffer pH 8. Because 1/5th of the 0.182 m*M* fluorescein solution was prepared using this stock solution it was decided that the results may be affected by the buffering capacity of the solution. A new 0.91 m*M* stock solution of fluorescein using 0.2 *M* $Na_2HPO_4.12H_2O$ solution (pH 9.01) was therefore prepared.

UV/Vis scans of 0.036 and 0.182 m*M* aqueous fluorescein solutions before and of the corresponding octanol fluorescein solutions after addition of HNO_3 were again obtained but using the new stock solution (pH 9.01).

A 0.991 and a 1.521 m*M* solution were then prepared by dissolving 16.3 and 25 mg of fluorescein respectively up to 50 mL using 0.2 *M* $Na_2HPO_4.12H_2O$ solution (pH 9.01). UV/Vis scans of these more concentrated fluorescein solutions were obtained as previously but with the addition of just 4 mL of concentrated HNO_3.

Fingerprint trials

A fluorescein solution (1.521 m*M*) was prepared by dissolving 25 mg of fluorescein up to 50 mL using 0.2 *M* $Na_2HPO_4.12H_2O$ solution (pH 9.01). The solution was then acidified by addition of 4 mL concentrated HNO_3. This solution was then used to treat various fingerprint exhibits in the following ways:

- One fingerprint which had been deposited on a glass slide using Fernleaf semisoft butter as a "lipid mimic" was placed in the solution for three hours. An untreated "butter-print" was used for comparison purposes.
- One fingerprint which had been deposited on paper using Fernleaf semisoft butter as a "lipid mimic" was placed in the solution for ten minutes.
- One half of a latent fingerprint deposited on a glass slide was placed in the solution for 48 hours. The other half of the print was left untreated for comparison purposes.
- One half of a blood print deposited on a glass slide was left in the solution for a few hours. The other half of the blood print was left untreated for comparison purposes.

The fingerprint exhibits were then viewed with a Polilight® using the 320 nm wavelength setting. Exhibits were held up at an angle to the light source and clear goggles were worn.

The compound fluorescein isothiocyanate is reactive towards proteins. A fluorescein isothiocyanate solution (0.064 m*M*) was then prepared by dissolving 25 mg of fluorescein isothiocyanate up to 50 mL using 0.2 *M* $Na_2HPO_4.12H_2O$ solution (pH 9.01). This solution was then used to treat various fingerprint exhibits in the following ways:

- One half of a blood print deposited on a glass slide was left in the solution for an hour. The other half of the blood print was left untreated for comparison purposes.
- One half of a blood print deposited on paper was left in the solution for an hour. The other half of the blood print was left untreated for comparison purposes.

The fluorescein isothiocyanate solution was then acidified by addition of 4 mL concentrated HNO_3.

- One half of a blood print deposited on paper was left in the solution for 24 hours. The other half of the blood print was left untreated for comparison purposes.

The fingerprint exhibits were then viewed with a Polilight® using the 320 nm wavelength setting. Exhibits were held up at an angle to the light source and clear goggles were worn.

7.4.3 Results

Fluorescent emission solution trials

Results for the change in emission intensity at 512 nm for 0.91 μM solutions of fluorescein with pH values ranging from 2 to 9 are presented in Table 7.2.

Table 7.2
Changes in emission intensity of fluorescein at 512 nm with varying pH.

pH	Emission Intensity at 512 nm
2.07	72
4.51	58
5.43	137
6.40	507
7.37	855
8.06	895
9.18	934

Fluorescent emission results for a 0.91 μM solution of fluorescein in octanol are presented in Table 7.3.

Table 7.3
Fluorescent emissions of a solution of fluorescein in octanol.

Excitation λ (nm)	Emission λ (nm)	Emission Intensity
240	523.0	47
222	589.5	210
	& 528.5	& 34

The emission intensity of fluorescein seems to be greatly reduced in octanol. In addition to this octanol seems to be altering the fluorescent spectra of fluorescein.

Results of a fluorescent scan of octanol are presented in Table 7.4.

Table 7.4
Fluorescent emission of octanol when excited at 222 nm.

Excitation λ (nm)	Emission λ (nm)	Emission Intensity
222.0	589.5	222

Due to some impurity the octanol seems to have its own fluorescence. Also the emission intensity of fluorescein changes quite significantly with pH and seems to be greatly reduced in octanol. It was therefore decided to use UV/Vis spectroscopy for determining the distribution of fluorescein between the aqueous and octanol layers.

UV/Vis solution trials

Two wavelength maxima were obtained for the fluorescein solution (0.018 m*M*) prepared with a pH of 5.55 with one peak at 232 nm and the other at 476 nm (both having similar absorbances). It was decided that the peak in the visible region (476 nm) should be used for monitoring of the fluorescein transferal.

A UV/Vis scan of neat octanol between 300 to 700 nm produced no absorbance in this region (a flat baseline was obtained).

On standing after the aqueous solution had been shaken with octanol in a separating funnel the two layers slowly separated out leaving a visibly green colour still in the aqueous layer and a clear, untainted colour still in the octanol layer. UV/Vis spectroscopy however, indicated that there was now a small absorbance at 476 nm in the octanol layer were no absorbance had previously been. A slightly puzzling result however, was obtained for the aqueous absorbance value at 476 nm after shaking. The absorbance was only 0.075 even though a visibly green colour was still present in the aqueous layer. A possible explanation for this is that the absorbance maximum was actually shifted to a slightly different wavelength as a result of shaking with the octanol layer. Results are presented in Table 7.5 and suggest that a small degree of fluorescein transferal had occurred.

Table 7.5
Absorbances for aqueous and octanol layers containing fluorescein (0.018 mM) at pH 5.55.

Layer	Wavelength (nm)	Absorbance
aqueous (before)	476	0.580
aqueous (after)	476	0.075
octanol (after)	476	0.037

The wavelength maxima in the visible region for a fluorescein solution (0.036 m*M*) prepared with a pH of 9.01 was then observed at 490 nm before and after shaking with octanol. There seemed to be little difference observed in the absorbance values as well as was visibly observed in fluorescein colour before and after shaking with octanol. After concentrated HNO_3 was added to the funnel however, it was visibly observed that most of the fluorescein colour had now transferred over to the octanol layer, leaving a clear colour and reduced absorbance maximum (at a lower wavelength) in the aqueous layer. Results are presented in Table 7.6 and suggest that a high degree of fluorescein transferal had occurred upon acidification of the aqueous layer.

Table 7.6
Absorbances for aqueous layer containing fluorescein (0.036 mM) before and after shaking with octanol and after addition of HNO_3.

Layer	Wavelength (nm)	Absorbance
aqueous (before shaking)	490	2.555
aqueous (after shaking)	490	2.585
aqueous (after HNO_3 added)	438	0.169

On standing after an aqueous solution of fluorescein (0.036 m*M* at pH 2) had been shaken with octanol in a separating funnel the two layers slowly separated out. A visual examination indicated that most of the colour had disappeared from the aqueous layer with only a slight hint of colour having appeared in the octanol layer.

From these results it was decided that the best way of forcing the fluorescein from the aqueous layer to the octanol layer is by starting with an alkaline fluorescein solution

and acidifying it later when it is in the separating funnel and in contact with the octanol layer.

UV/Vis results for 0.036 m*M* and 0.182 m*M* fluorescein solutions of pH 9.01*, (prepared with both the pH 8 or pH 9 stock solutions) obtained before and after 0.5, 1, 2, and 4 mL of HNO_3 were added and subsequent mixing with octanol in a separating funnel was carried out, are presented in the following two tables. The average absorbance values (since several solutions of the same concentration were prepared) for the aqueous layers before addition of HNO_3 are presented in Table 7.7 while the actual absorbance values for the corresponding octanol layers after addition of HNO_3 are presented in Table 7.8. It was necessary to dilute samples of some of the aqueous and octanol layers before obtaining UV/Vis results due to high absorbance values. The wavelength maximum was found to be 496 nm in the aqueous layer (Fig. 7.1) and 454 nm in the octanol layer (Fig. 7.2).

Table 7.7
Average absorbances for aqueous layers before addition of HNO_3 (measured at 496 nm).

	Average absorbances in aqueous layer			
	0.036 m*M*	0.182 m*M*	0.036 m*M**	0.182 m*M**
Diluted absorbance value	0.615	0.757	0.611	0.765
Diluted absorbance value x dilution factor	3.076	15.14	3.053	15.29

*Solutions prepared with new stock solution of pH 9.01.

The values obtained using old and new stock solutions (pH 8 and 9 respectively) are very comparable suggesting that the first two solutions prepared with the pH 8 stock solution were at a pH of 9.01.

* The pH may vary from this value slightly for the first 0.182 mM solution as 1/5th of it was prepared with a stock solution of pH 8 compared with the second 0.182 mM solution which was prepared with stock solution of pH 9.

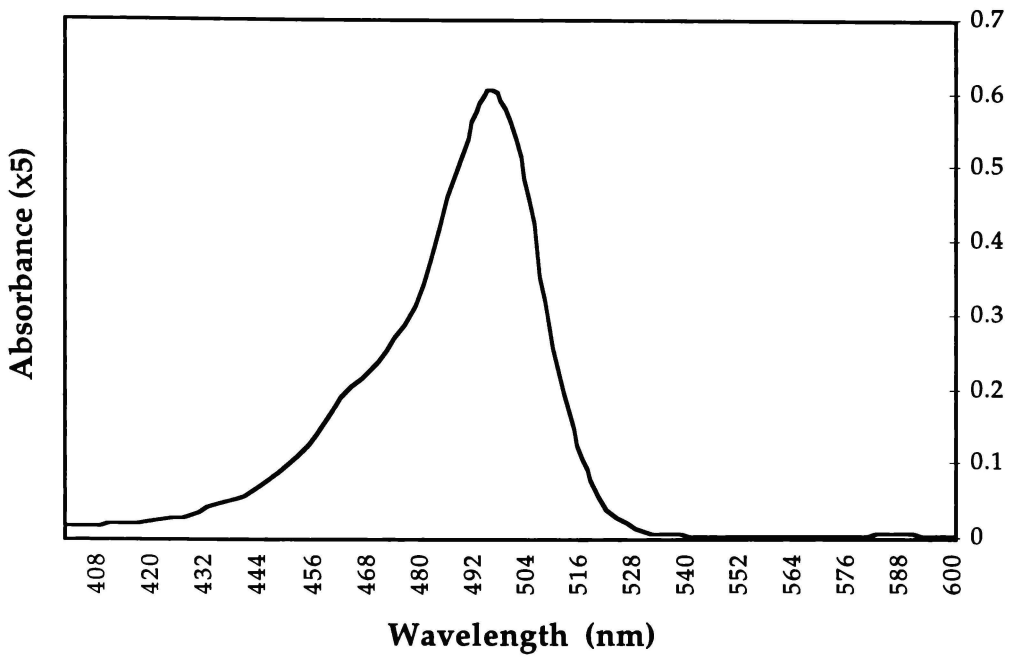

Fig. 7.1

Visible absorption spectrum of aqueous fluorescein (wavelength maximum at 496 nm).

Table 7.8

Absorbances for octanol layers after addition of HNO_3 (measured at 454 nm).

Volume HNO_3 (mL)	Relative absorbances in octanol layer[a]			
	0.036 m*M*	0.182 m*M*	0.036 m*M*[b]	0.182 m*M*[b]
0.5	0.389	1.626	0.325	0.915
1	0.910	3.621 (1.207)	1.212	2.89 (0.578)
2	1.609	5.616 (1.872)	1.663	5.163 (1.721)
3	—	—	—	6.07 (1.214)
4	1.671	5.71 (1.903)	1.858	7.685 (1.537)
5	—	—	—	7.905 (1.581)

[a]Values given represent the product of absorbance x dilution factor, while values in brackets are the actual absorbance values obtained from the diluted samples.
[b]Solutions prepared with new stock solution of pH 9.

The results indicate that there is definite transferal of fluorescein over to the octanol layer on addition of HNO_3. The amount transferred also increases with the amount of HNO_3 added. The average relative absorbance value for the 0.036 m*M* aqueous layer (i.e. absorbance for the diluted sample multiplied by the dilution factor) was 3 and the average relative absorbance value for the 0.182 m*M* aqueous layer was 15. With the addition of 4 to 5 mL HNO_3 to the 0.182 m*M* aqueous layer prepared with the new stock solution (pH 9) approximately half (7.5–8) of the absorbance value of fluorescein is "transferred" to the octanol layer.

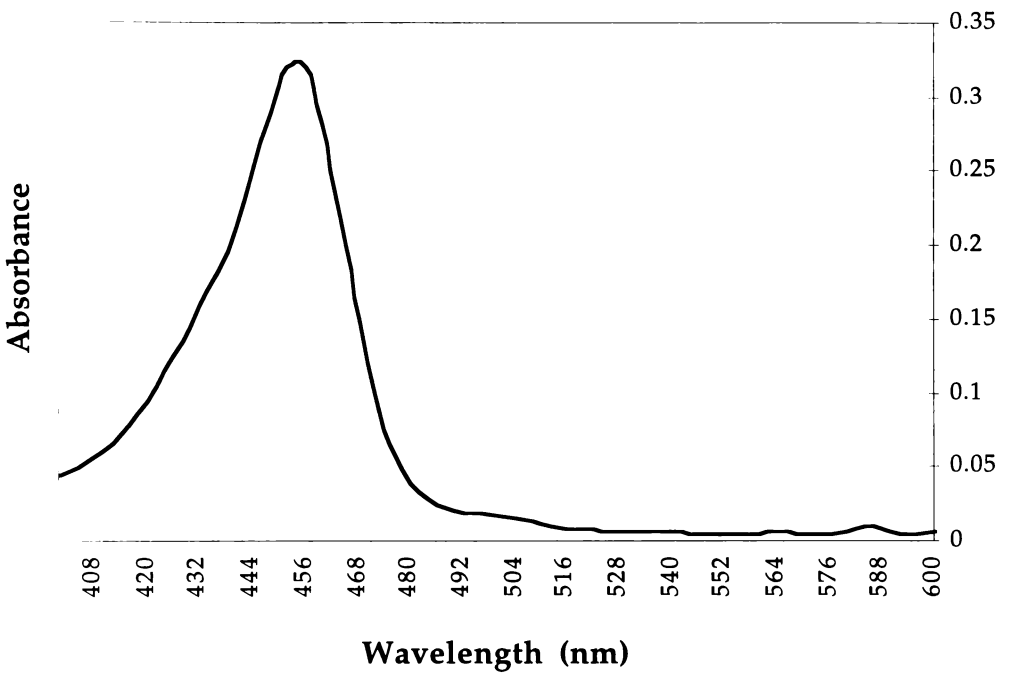

Fig. 7.2
Visible absorption spectrum of fluorescein in octanol (wavelength maximum at 454 nm).

A plot of the change in relative absorbance of fluorescein in the octanol layer with increasing volume of HNO_3 added to the 0.036 m*M* and 0.182 m*M* aqueous fluorescein solutions (prepared with both the pH 8 or pH 9 stock solutions) is presented in Fig. 7.3. The results indicate that the 0.182 m*M* solution prepared from the two different stock solutions does produce different absorbance readings in the corresponding octanol layer. The higher values obtained from using the more

alkaline stock solution suggest that fluorescein transferal is increased by beginning with a more alkaline aqueous solution and making it more acidic.

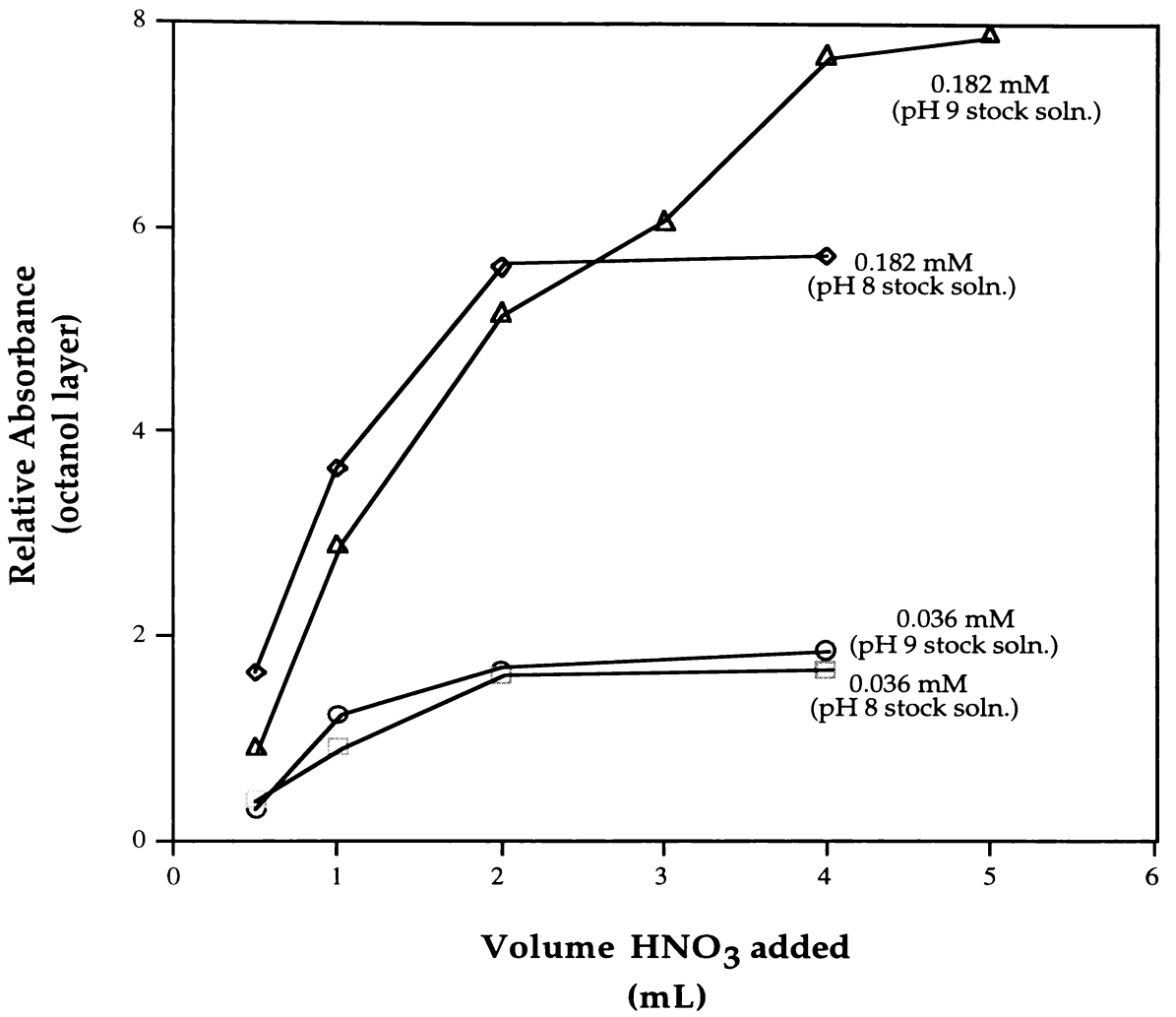

Fig. 7.3
Change in relative absorbance of fluorescein with volume of HNO_3 added.

UV/Vis results for a 0.991 m*M* and a 1.521 m*M* fluorescein solution (pH 9.01—using new stock solution) before and after 4 mL of HNO_3 was added and with subsequent mixing with octanol in a separating funnel was carried out are presented in Table 7.9. The absorbance for the aqueous layer was re-calculated from a 50 and a 100 times dilution respectively (for both concentrations) while the absorbance for the octanol layer was re-calculated from a 20 times dilution for both concentrations.

Table 7.9
Absorbances for aqueous layers before and corresponding octanol layers after addition of 4 mL HNO_3 (measurement at 496 and 454 nm respectively).

Conc. of aqueous solution (m*M*)	Relative absorbance in aqueous layer	Relative absorbance in octanol layer
0.991	82.8 (1.656)	23.7 (1.185)
1.521	124.2 (1.242)	34.58 (1.729)

NB Values in brackets are the actual absorbance values obtained from the diluted samples.

Changes in relative absorbance with increasing fluorescein concentration for the aqueous layer before and the corresponding octanol layer after addition of 4 mL of HNO_3 is presented in Fig. 7.4. Absorbance values used are those obtained from the 0.036, 0.182, 0.991 and 1.521 m*M* fluorescein solutions using the new stock solution.

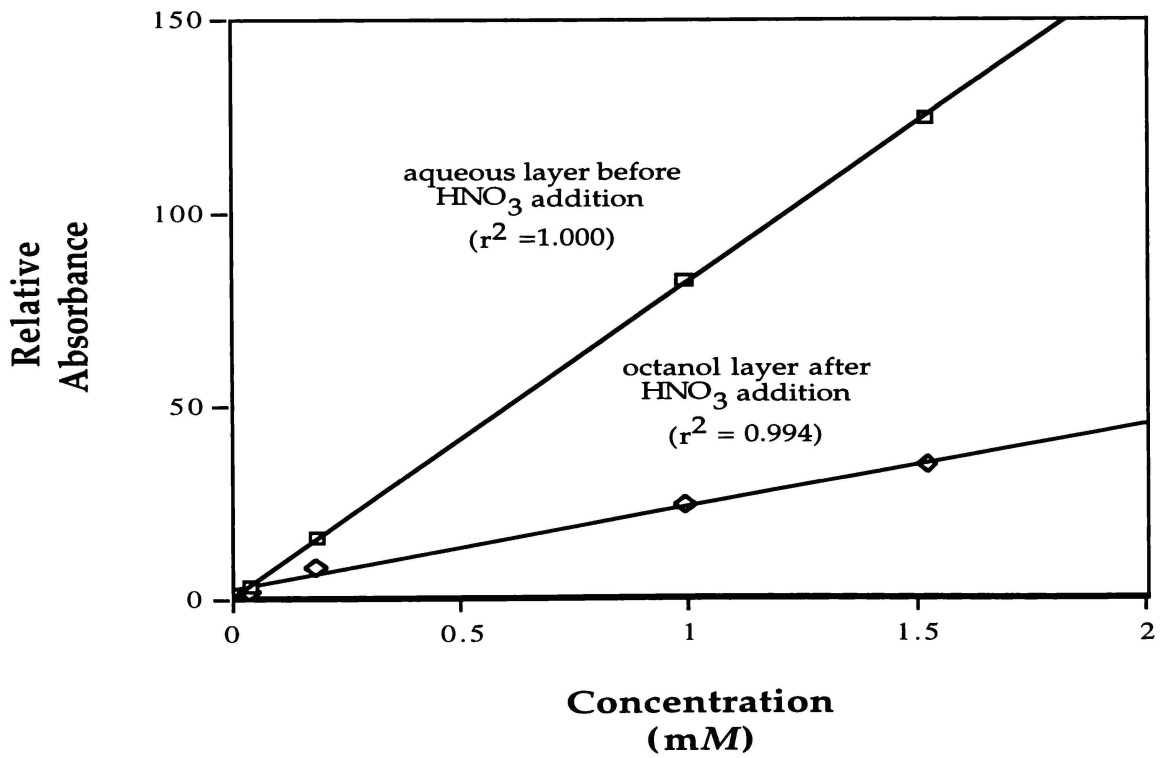

Fig. 7.4
Changes in relative absorbance with increasing fluorescein concentration before and after addition of 4 mL of HNO_3.

This plot indicates that the percentage transferal of fluorescein decreases with increasing fluorescein concentration. This pattern is also reflected in the partition coefficients for the aqueous to octanol layers presented in Table 7.10.

Table 7.10
Partition coefficients for ratio of fluorescein between aqueous and octanol layers obtained after addition of 4 mL HNO_3.

Concentration of aqueous layer (m*M*)	Absorbance in aqueous layer (x diln. factor)	Absorbance in octanol layer (x diln. factor)	Partition coefficient (aqueous/octanol)
0.036	3.053	1.858	1.643
0.182	15.29	7.685	1.990
0.991	82.8	23.7	3.494
1.521	124.2	34.58	3.592

Fingerprint trials

Optimum conditions determined in the above model trials which favoured transfer of fluorescein from the aqueous to the octanol layer were then applied to the treatment of blood and latent fingerprints. Initially, alkaline solutions containing fluorescein were brought into contact with the exhibit and acidified, in order to force some fluorescein to transfer to the lipids. Results for latent, butter and blood fingerprints treated with fluorescein are presented as follows:

- The fluorescein treated blood print on a glass slide when viewed under the Polilight® at 320 nm produced good orange fluorescence. The print was also a lot more visible to the eye under ambient lighting conditions compared with the untreated half.
- The fluorescein treated latent and butter prints on glass slides produced poor fluorescence with only parts of the prints being visible when viewed under the Polilight® at 320 nm.
- The fluorescein treated butter print on paper was not visible at all due to excessive background staining when viewed under the Polilight® at 320 nm.

Results for latent and blood fingerprints treated with fluorescein isothiocyanate are presented as follows:

- The fluorescein isothiocyanate treated blood print on a glass slide when viewed under the polilight at 320 nm produced good orange fluorescence. The print was also a lot more visible to the eye under ambient lighting conditions compared with the untreated half and more so than the fluorescein treated blood print.

- The fluorescein isothiocyanate treated blood print on paper did not produce fluorescence but was more visible to the eye when viewed under ambient lighting conditions and the Polilight® at 320 nm compared with the untreated half.

- The fluorescein treated latent print on glass produced poor fluorescence with only parts of the prints being visible when viewed under the Polilight® at 320 nm.

7.4.4 Section summary

Octanol/water was used as a solubility model of the interface between an aqueous solution and the lipid part of a latent fingerprint. The best way to encourage fluorescein to transfer from an aqueous to a lipid phase was found to involve introducing the fluorescein in an alkaline solution and then acidifying it. Although the method of forcing fluorescein into the lipid component by acidification of an alkaline fluorescein solution did not work sufficiently well to produce good fluorescence on real latent fingerprints, the method did seem to work to some extent on blood fingerprints. Further work in the area should focus on barely visible blood fingerprints as the dark colour of blood tends to hide any fluorescence on an easily visible blood fingerprint.

7.5 *Modification of the luminol technique*

7.5.1 Introduction

The oxidation reaction of 5-amino-2,3-dihydrophthalazine (luminol) is based on the peroxidase activity of hemoglobin in the presence of hydrogen peroxide (Fig. 7.5). This is the same reaction as that of DAB, ABTS, OPD, and PPD but differs however, in that it produces chemiluminescence rather than a colour change (Lytle and Hedgecock, 1978).

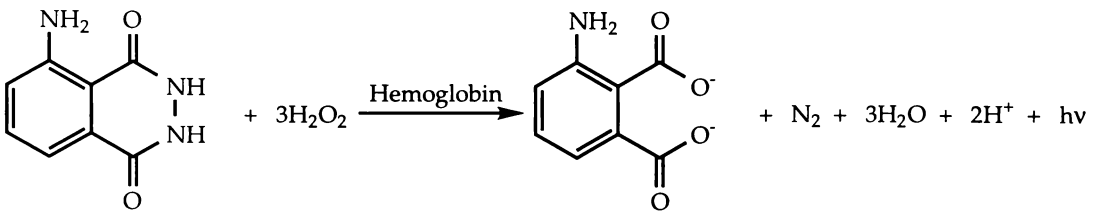

Fig. 7.5
Oxidation reaction of luminol (Mayer and Neuenhofer, 1994).

Sodium perborate is often used in place of hydrogen peroxide because even though the resulting luminescence intensity is lower, the duration of the chemiluminescence is significantly longer (*i.e.* 30 seconds compared with 5 seconds) (Zweidinger et al., 1973).

Several compounds, some of which are porphyrins, which enhance the activity of luminol with hydrogen peroxide and peroxidase have been found (Tumosa, 1996).

Chang and Patterson (1980), investigated the enhancement of iron(II) catalysis of luminol chemiluminescence using hydrogen peroxide with halide ions. In the presence of 0.3 mol/L bromide ion (Br^-), an increase of 3.5-fold of chemiluminescence signal was observed. This has potential significance to the luminol–blood reaction, because iron is the metal acting in the porphyrin catalytic centres of the hemoglobin protein. The mechanism by which luminol is oxidised in the presence of hydrogen peroxide and hemoglobin is believed to parallel the oxidation of DAB (section 2.1.1).

A proposed mechanism for the halide effect of the metal ion catalysed chemiluminescence reaction is presented in Fig. 7.6 (Chang and Patterson, 1980).

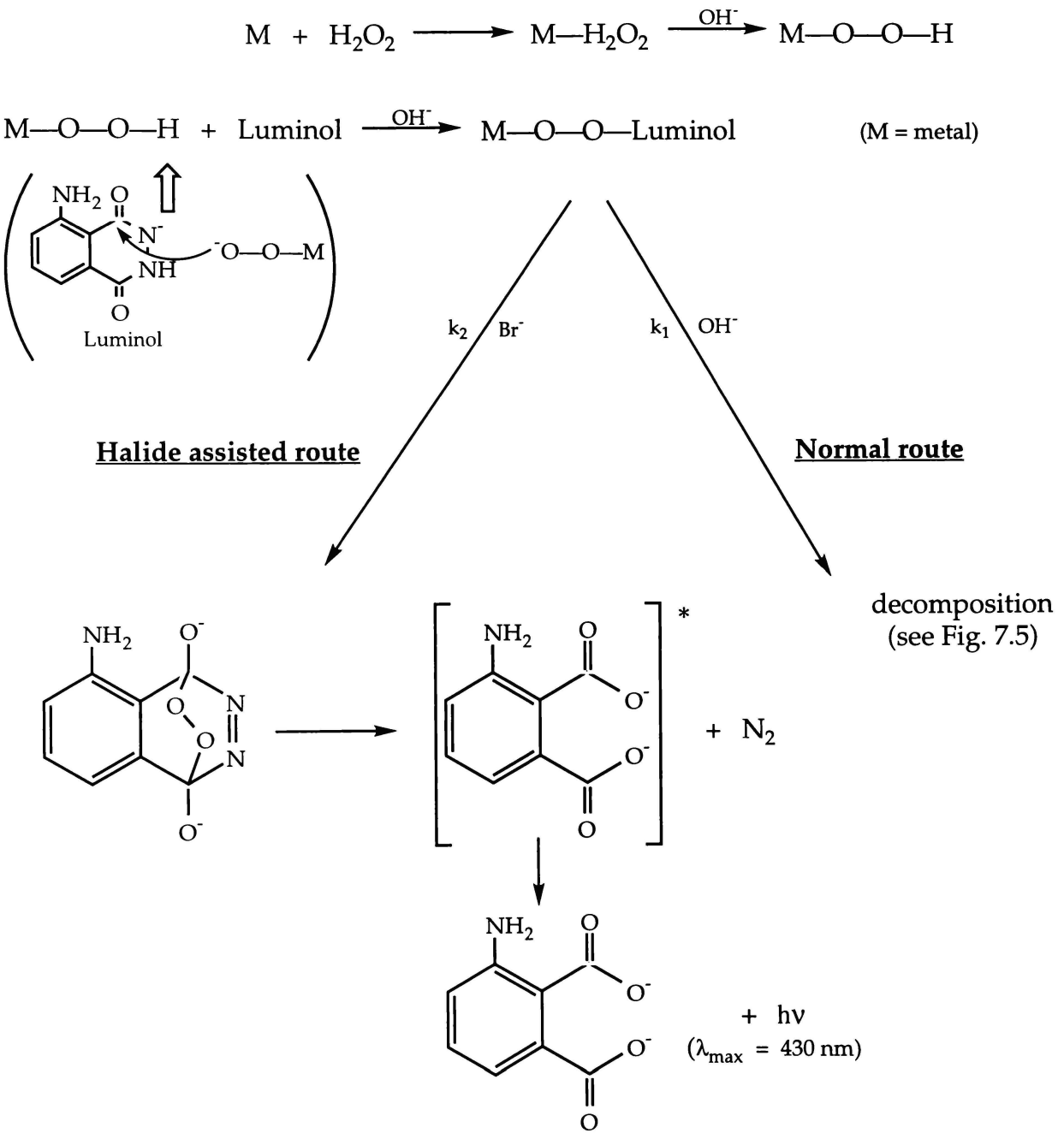

Fig. 7.6
A proposed mechanism for the halide effect of the metal ion catalysed chemiluminescence reaction (Chang and Patterson, 1980).

It was decided that this method of enhancement should be tested out on blood fingerprints (or blood stains) to see if this increased chemiluminescence signal in the presence of halide ions could be observed with hemoglobin catalysis.

7.5.2 Methodology

Two luminol solutions were prepared using the standard luminol reagent (Lytle and Hedgecock, 1978) which contains 0.1 g luminol, 5.0 g sodium carbonate, 100 mL of distilled water, and 0.7 g sodium perborate which is added just prior to use. To one of these solutions was added 3.087 g (0.3 *M*) NaBr. Both solutions were then sprayed onto fixed and non-fixed blood fingerprints on paper and their chemiluminescence compared visually by eye in a dark room (refer to section 2.5.1 for the methodology used for fixing of a blood fingerprint).

Two more luminol solutions were then prepared but with hydrogen peroxide (13.85 mL) substituting the sodium perborate. To one of these solutions was added 3.087 g (0.3 *M*) NaBr. Both solutions were then sprayed onto fixed and non-fixed blood fingerprints on paper and their chemiluminescence compared visually by eye in a dark room.

7.5.3 Results and summary

Equivalent luminescence intensity was visually observed with both bromide and non-bromide/luminol treatment with standard and non-standard luminol reagents.

There seems to be no visual benefit in the addition of NaBr to the luminol solution for the treatment of blood fingerprints. One reason for this lack of observed enhancement could be that both faces of the Fe(II) atom are involved when the catalysis involves free atoms in solution (such as in the work of Chang and Patterson, 1980); whereas the iron in the porphyrin group of hemoglobin is fixed and can only be approached from one direction (Fig. 7.7).

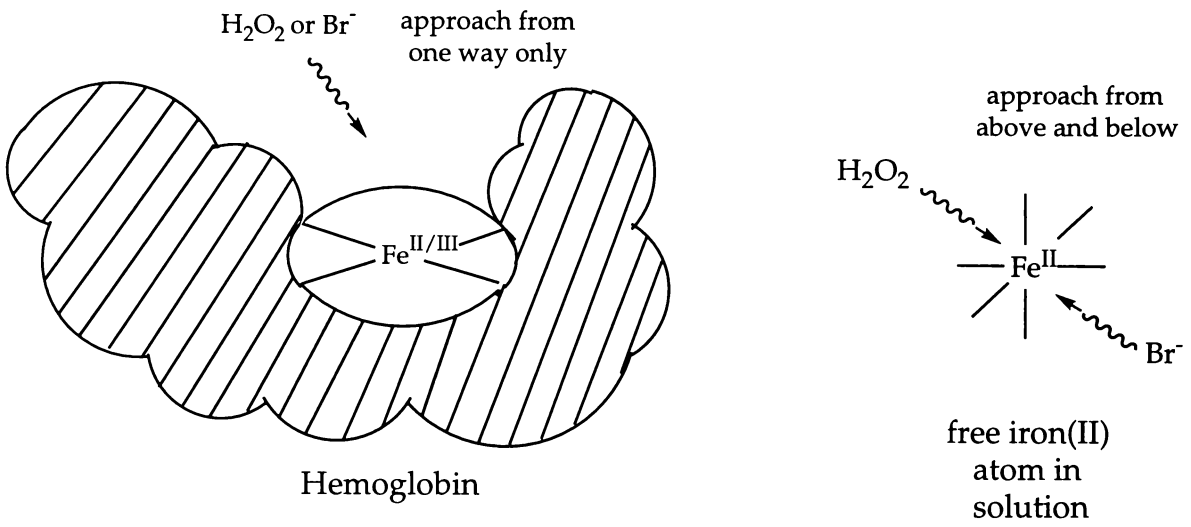

Fig. 7.7
Proposed means by which hydrogen peroxide and bromide approach an iron(II) centre in two different environments.

7.6 *Antibody-conjugate treatment*

7.6.1 Introduction

The use of peroxidase-conjugated rabbit anti-human albumin (an antibody-conjugate) for the enhancement of blood fingerprints was briefly investigated. It was proposed that the antibody-conjugate would react with albumin present in the blood of a blood fingerprint. The peroxidase end of the antibody-conjugate would then promote the oxidation of a chromophore such as ABTS in the presence of hydrogen peroxide. The rationale behind this is due to the fact that hemoglobin is only a pseudo–peroxidase and is about 100 times less efficient than a real peroxidase (Kremer, 1989). By having a real peroxidase available for promotion of ABTS oxidation the colour development should hopefully be enhanced due to the extent and speed of the reaction by (a) reducing the possibility of side reactions and (b) providing more peroxidases for

oxidation of ABTS (peroxidase activity will exist wherever there is albumin as well as hemoglobin).

7.6.2 Methodology

The peroxidase-conjugated rabbit anti-human albumin was diluted by 100 fold in phosphate buffer pH 7.4 (refer to Table 2.1 in Chapter 2). Fresh human blood which had been collected in a vaccutainer with no anticoagulant (refer to section 2.2) was deposited as blood fingerprints on paper. After being left to dry, the prints were fixed with sulfosalicylic acid according to the procedure used in section 2.5.1. They were then cut bilaterally down the centre into halves. One set of halves were immersed in the peroxidase-conjugated rabbit anti-human albumin solution for five minutes. The print halves were then rinsed in distilled water before being immersed in ABTS working solution (section 8.1) for another five minutes. The other corresponding set of print halves were then developed with ABTS working solution only and used as a comparison with the peroxidase-conjugated rabbit anti-human albumin/ABTS treated print halves.

7.6.3 Results and summary

Unfortunately, the development of the peroxidase-conjugated rabbit anti-human albumin/ABTS treated print halves was no better than that observed with standard ABTS treatment. Furthermore, in the presence of the extra peroxidase enzyme, prints were rendered less visible due to excessive background staining of the paper. This may possibly have been due to some of the peroxidase-conjugated rabbit anti-human albumin becoming mechanically trapped in the pores of the paper prior to the ABTS treatment. Also while the catalytic effect of hemoglobin is kinetically about 100 times less efficient than peroxidase the end result or colour development may well still be the same.

ABTS development involves two steps:

a) ABTS ———> oxidised ABTS

b) Accumulation of oxidised ABTS on the surface due to precipitation

The antibody would effect the rate of step (a) and the number of places it can happen simultaneously, but the results of this work show that these factors have little effect on step (b) and thus the overall colour development.

7.7 *SYPRO™ Orange protein stain*

7.7.1 Introduction

SYPRO™ Orange protein stain is a fluorescent reagent for the rapid staining of proteins with high sensitivity and low background following 1-D, 2-D or native polyacrylamide gel electrophoresis. The stained proteins are visualised by ultraviolet illumination (optimally 302 nm). The SYPRO™ Orange protein stain does not stain nucleic acids. In solution it is purported to be sensitive down to nanogram levels of proteins.

Blood plasma consists of over nine-tenths water and contains sugars, nutrients, acids, salts, minerals and proteins (Jones, 1997). It was proposed that SYPRO™ Orange protein stain could be used for staining proteins in blood plasma and there by providing a new technique for fluorescent visualisation of blood fingerprints.

7.7.2 Methodology

SYPRO™ Orange protein stain is provided as a 5000x concentrate in dimethyl sulfoxide (DMSO). A working solution of SYPRO™ Orange was prepared by adding 10 µL of stain to 50 mL of acetic acid (7.5%).

Two blood fingerprints were deposited on paper and two on glass microscope slides. The blood prints were then fixed with sulfosalicylic acid according to the procedure used in section 2.5.1.

One blood print deposited on paper and a glass slide were immersed in the SYPRO™ Orange working solution for 30 minutes while the other print on paper and a glass slide were immersed for 90 minutes. After being left to dry the prints were then viewed under a UV hand-held lamp with the 254 and 366 nm settings.

7.7.3 Results and summary

Treatment of blood fingerprints on paper and glass with SYPRO™ Orange protein stain did not result in any visual enhancement. SYPRO™ Orange however, did stain the paper resulting in strong fluorescence all over when viewed under UV light at 254 nm. One possibility for this result is that SYPRO™ Orange is reactive towards lignin or cellulose (CH_2O groups) in the paper.

7.8 *References*

Burt J.A. and Menzel E.R. (1985). Laser detection of latent fingerprints: Difficult surfaces. J. Forens. Sci., **13**(2), 364-370.

Chang C.A. and Patterson H.H. (1980). Halide ion enhancement of chromium(III), iron(II), and cobalt(II) catalysis of luminol chemiluminescence. *Anal. Chem.*, **52**, 653-656.

Cheeseman R., and DiMeo L.A. (1995). Fluorescein as a field-worthy latent bloodstain detection system. *J. Forensic Ident.*, **45**(6), 631-646.

Florence T.M., Morrison G.M., and Stauber J.L. (1992). Determination of trace element speciation and the role of speciation in aquatic toxicity. *Sci. Total Environ.*, **125**, 1-13.

Haugland R.P. (1992). *Handbook of fluorescent probes and research chemicals.* 5th edition. Molecular Probes, Inc. Eugene, OR, USA.

Jones K. (1997). *A Review of blood enhancement techniques.* Report prepared for the New Zealand Police, Royal New Zealand Police College.

Kremer M.L. (1989). The reaction of hemin with H_2O_2. *Eur. J. Biochem.*, **185**, 651-658.

Laibinis P.E., Bain C.D., Nuzzo R.G., and Whitesides G.M. (1995). Structure and wetting properties of ω-Alkoxy-n-alkanethiolate monolayers on gold and silver. *J. Phys. Chem.*, **99**, 7663-7676.

Lavis A. (1994). *Workshop in advanced fingerprint techniques.* Training manual prepared for *ESR:Forensic*, Auckland, New Zealand.

Henderson W. (1997). *Personal communication.* Department of Chemistry, University of Waikato, Hamilton, New Zealand.

Lytle L.T., Hedgecock D.G. (1978). Chemiluminescence in the visualisation of forensic bloodstains. *J. Forensic Science*, **23**, 550-562.

Mayer A., and Neuenhofer S. (1994). Luminescent labels—More than just an alternative to radioisotopes? *Angew. Chem. Int. Ed. Engl.*, **33**, 1044-1072.

Molan P. (1988). Personal Communication, Biology Department, University of Waikato, Hamilton, New Zealand.

Raksasataya M. (1998). *Aspects of the chemistry of lead in multiphase soil model systems and the environment.* Doctoral thesis, University of Waikato, Hamilton, New Zealand.

Tumosa S.C. (1996). The detection and species identification of blood – A bibliography of relevant papers from 1980 to 1995. *Forensic Sci. Rev.*, **8**(2), 74–90.

Zweidinger R.A., Lytle L.T. and Pitt C.G. (1973). Photography of bloodstains visualized by luminol. *J. Forensic Science*, **18**, 296-302.

Chapter Eight

Summary and recommendations

8.1 *Blood reagents*

8.1.1 ABTS, OPD and PPD

ABTS, OPD and PPD have all proven to be effective, alternatives to DAB for development of blood fingerprints with the relative costs being of the order; ABTS >DAB > OPD & PPD. OPD and PPD, although both still toxic, represent less of a hazard than the carcinogenic risks of DAB for development of blood fingerprints, while ABTS as far as is known is non-toxic. The recommended procedures for best visualisation of fingerprints deposited in blood using ABTS, OPD and PPD are provided as follows. The procedures are based on the combined results obtained from the solution and fingerprint optimisation trials in Chapters 2 and 3.

Fixative solution

Dissolve 20 g of 5-sulfosalicylic acid in 1 L distilled water in a 2 L glass beaker. Transfer to a labeled, laboratory bottle with a screw top (use either a dark glass bottle or cover with silver foil). Store in dark at room temperature.

Citric acid/phosphate buffer (pH 5.4)

Dissolve 71.64 g of $Na_2HPO_4.12H_2O$ or 35.61 g $Na_2HPO_4.2H_2O$ in distilled water and make up to the mark in a 1 L volumetric flask (0.2 *M*) shaking vigorously to ensure that all solids are dissolved. Transfer the solution to a labeled laboratory bottle with a screw top. Dissolve 21.01 g of citric acid monohydrate in distilled water and make up to the mark in a 1 L volumetric flask (0.1 *M*) shaking vigorously to ensure that all solids are dissolved. Transfer the solution to a labeled laboratory bottle with a screw top. Measure out 223 mL $Na_2HPO_4.12H_2O$ or $Na_2HPO_4.2H_2O$ solution (0.2 *M*) and 177 mL of citric acid monohydrate (0.1 *M*) into a labeled laboratory bottle with a screw top, and mix well.

ABTS working solution

Completely dissolve 1.25 g of ABTS in citric acid/phosphate buffer solution (pH 5.4) in a 250 mL volumetric flask. Invert a few times to ensure that all ABTS is dissolved. Transfer to a labeled, laboratory bottle with a screw top. Store in fridge (away from light) for up to a week.

OPD and PPD stock solutions

Dissolve 50 mg of OPD or PPD in 100 mL of citric acid/phosphate buffer solution (pH 5.4) in a labeled, laboratory bottle with a screw top. Unaided, OPD and PPD take a while to dissolve. This process can be facilitated by shaking vigorously or placing in an ultra-sound bath for 10 minutes. Store in fridge (away from light) for up to a week for OPD and use on the day for PPD.

(A) Immersion Method

- Place blood fingerprint exhibit in a clean, shallow, glass dish.
- Pour out sufficient fixative solution into the dish to cover exhibit. Leave for about 3 minutes before removing exhibit and rinsing in distilled water.
- Place exhibit in a clean, shallow, glass dish. Pour out 50 mL of the ABTS, OPD or PPD working solution into a laboratory bottle with a screw top followed by 0.5 mL of 27% H_2O_2 and shake to ensure thorough mixing (if 50 mL is not enough to cover exhibit then add more and adjust the H_2O_2 volume accordingly).
- Pour the activated working solution over the exhibit and leave to develop for 5 minutes. Remove the exhibit and rinse in distilled water.
- Leave exhibit to air dry in a dark place.

(B) Reservoir Method

- Lay a piece of clean, dry filter paper over the area of the blood fingerprint exhibit to be treated.
- Saturate the filter paper with fixative solution, using a pasteur pipette, and keep the paper saturated with the solution for three minutes. Remove the paper and wash the area under treatment with distilled water.
- Lay a piece of clean, dry filter paper over the area of the exhibit to be treated.
- Saturate the filter paper with activated working solution (previously mixed). Keep the paper saturated with the solution for 5 minutes. Remove the paper and wash the area under treatment with distilled water.
- Leave the exhibit to air dry in a dark place.

ABTS treated fingerprints should be photographed as soon as possible, and preferably within two weeks of development, as noticeable fading in colour was observed over a one month period (developed fingerprints could also be stored in the dark so as to slow down the fading process).

8.1.2 FDA

The results from a preliminary appraisal indicate that FDA may be useful in estimating the PMI or age of blood stains and blood prints. Factors which would need considering before this method could be applied to forensic casework would basically involve calibration of the method to the problem under consideration.

- In using FDA to determine PMI, it would first be necessary to establish the empirical relationship which exists between FDA hydrolysis of blood withdrawn from a given organ or body cavity and the time since death, and how this might be influenced by the ambient temperature, bacterial colonisation, cell lysis and any other factors.
- In the case of a blood stain, it might be expected that the rate of degradation of the blood would be greater, and the calibration scale might be considerably shorter. An additional factor to consider here would be the best means of re-suspending the blood (enzymatic components) back into solution for reaction with FDA.

Overall, it is felt that the amount of research involved in arriving at a reliable recommended protocol might amount to the equivalent of 2-3 PhD projects, and in scope would need to cover the areas forensic chemistry/biochemistry, physics, and pathology. However, the importance of being able to estimate PMI or the age of a bloodstain with greater accuracy suggests that such work would be worthwhile.

8.2 *Latent reagents*

8.2.1 $Eu(fod)_3$

$Eu(Fod)_3$ has proven to be effective in the fluorescent visualisation of latent fingerprints using a one step process. Although it was less effective than DFO on

porous paper it was found to work to a limited extent on aluminium drink cans and galvanized iron.

$Eu(dpm)_3$ and $Tb(fod)_3$ did not prove as effective as $Eu(fod)_3$. However, it may be possible that other ligands would result in better luminescence and/or reactivity of europium or terbium complexes. This aspect could be investigated further.

8.2.2 OPA, NDA and ADA

OPA, NDA and ADA all performed poorly in the fluorescent enhancement of latent fingerprints, a result which could be partially due to the aqueous nature of the reagent systems, with a resultant tendency of water soluble amino–acid residues in the print to show some migration. The three–ring analogue ADA combines two favourable features however, which might make it the best prospect for future development in this area. These are (a) its amino acid reaction product shows the greatest "red–shift" in emission wavelengths, and (b) it is the least water–soluble of the three compounds to begin with. For these reasons, it is recommended that future work in this area be focused in locating a solvent system for the reagent ADA which facilitates the amino acid reaction while minimizing migration of water–soluble components of the print.

8.3 *Other reagents*

Attempts to improve the colloidal gold method of latent fingerprint treatment by trying to coat the colloidal gold surface with a coloured or fluorescent tag via attachment to a thiol was unsuccessful. The suspected reason for this being the dissolution of previously deposited gold after complexation with the thiol.

By acidifying an aqueous solution of fluorescein in alkaline buffer it was found that fluorescein could be "forced" into octanol (lipid model). When this was attempted on latent fingerprints on paper and glass it was found that fluorescence in the prints was poor or non–existent. Fluorescence was obtained however, from blood fingerprints on glass when alkaline solutions of fluorescein and fluorescein isothiocyanate were

acidified. Fluorescence from blood fingerprints on paper however was not obtained using fluorescein isothiocyanate. Treatment of blood fingerprints on paper with SYPRO™ Orange protein stain was also unsuccessful.

An attempt to increase the chemiluminescence from luminol–treated blood fingerprints in the presence of bromide ions was unsuccessful. The reason for this is probably due to the structure of hemoglobin preventing the approach of bromide ions into the iron centre while H_2O_2 is already undergoing reaction with iron.

The use of an albumin antibody conjugated to peroxidase did not result in better enhancement of ABTS colour development. The reason for this could be that the use of a peroxidase compared with a pseudo–peroxidase (hemoglobin) would only increase the rate of colour development and not the overall colour development.

Appendices

Chapter Two

Appendix 2.1 (XRD data for ABTS)

Appendix 2.1 (a)
Bond lengths for molecules 1 and 2.

Molecule 1		Molecule 2	
Bonds	Bond lengths (Å)	Bonds	Bond lengths (Å)
S(11) - O(13)	1.457 (18)	S(21) - O(23)	1.466 (19)
S(11) - O(11)	1.465 (19)	S(21) - O(21)	1.459 (19)
S(11) - O(12)	1.469 (17)	S(21) - O(22)	1.457 (2)
S(11) - C(14)	1.773 (2)	S(21) - C(24)	1.767 (2)
S(12) - C(12)	1.764 (2)	S(22) - C(22)	1.761 (2)
S(12) - C(11)	1.775 (2)	S(22) - C(21)	1.774 (3)
N(11) - C(11)	1.289 (3)	N(21) - C(21)	1.280 (3)
N(11) - N(11)	1.410 (4)	N(21) - N(21)	1.420 (4)
N(12) - C(11)	1.380 (3)	N(22) - C(21)	1.384 (3)
N(12) - C(17)	1.390 (3)	N(22) - C(27)	1.385 (3)
N(12) - C(18)	1.463 (3)	N(22) - C(28)	1.465 (3)
C(12) - C(13)	1.386 (3)	C(22) - C(23)	1.383 (3)
C(12) - C(17)	1.402 (3)	C(22) - C(27)	1.403 (3)
C(13) - C(14)	1.401 (3)	C(23) - C(24)	1.392 (3)
C(14) - C(15)	1.396 (3)	C(24) - C(25)	1.391 (3)
C(15) - C(16)	1.387 (3)	C(25) - C(26)	1.382 (4)
C(16) - C(17)	1.389 (3)	C(26) - C(27)	1.388 (3)
C(18) - C(19)	1.516 (4)	C(28) - C(29)	1.507 (4)

Appendix 2.1 (b)
Bond angles for molecules 1 and 2.

Molecule 1		Molecule 2	
Bond angle	Degrees	Bond angle	Degrees
O(13) - S(11) - O(11)	111.97 (12)	O(21) - S(21) - O(23)	111.07 (11)
O(13) - S(11) - O(12)	111.84 (11)	O(22) - S(21) - O(23)	111.60 (13)
O(11) - S(11) - O(12)	112.26 (11)	O(22) - S(21) - O(21)	112.86 (13)
O(13) - S(11) - C(14)	107.72 (11)	O(23) - S(21) - C(24)	106.90 (12)
O(11) - S(11) - C(14)	106.46 (11)	O(21) - S(21) - C(24)	107.35 (11)
O(12) - S(11) - C(14)	106.15 (11)	O(22) - S(21) - C(24)	106.69 (11)
C(12) - S(12) - C(11)	90.32 (11)	C(22) - S(22) - C(21)	90.35 (12)
C(11) - N(11) - N(11)	111.2 (2)	C(21) - N(21) - N(21)	110.4 (3)
C(11) - N(12) - C(17)	114.7 (2)	C(21) - N(22) - C(27)	114.3 (2)
C(11) - N(12) - C(18)	121.8 (2)	C(21) - N(22) - C(28)	121.3 (2)
C(17) - N(12) - C(18)	123.1 (2)	C(27) - N(22) - C(28)	124.2 (2)
N(11) - C(11) - N(12)	122.9 (2)	N(21) - C(21) - N(22)	123.4 (2)
N(11) - C(11) - S(12)	126.4 (2)	N(21) - C(21) - S(22)	125.7 (2)
N(12) - C(11) - S(12)	110.73 (17)	N(22) - C(21) - S(22)	110.86 (18)
C(13) - C(12) - C(17)	120.8 (2)	C(23) - C(22) - C(27)	121.5 (2)
C(13) - C(12) - S(12)	127.88 (18)	C(23) - C(22) - S(22)	127.37 (19)
C(17) - C(12) - S(12)	111.34 (17)	C(27) - C(22) - S(22)	111.16 (18)
C(12) - C(13) - C(14)	118.5 (2)	C(22) - C(23) - C(24)	117.7 (2)
C(15) - C(14) - C(13)	120.5 (2)	C(25) - C(24) - C(23)	121.2 (2)
C(15) - C(14) - S(11)	118.95 (18)	C(25) - C(24) - S(21)	118.76 (19)
C(13) - C(14) - S(11)	120.55 (18)	C(23) - C(24) - S(21)	120.02 (19)
C(16) - C(15) - C(14)	120.8 (2)	C(26) - C(25) - C(24)	120.7 (2)
C(15) - C(16) - C(17)	118.8 (2)	C(25) - C(26) - C(27)	118.9 (2)
C(16) - C(17) - N(12)	126.7 (2)	C(26) - C(27) - N(22)	126.9 (2)
C(16) - C(17) - C(12)	120.5 (2)	C(26) - C(27) - C(22)	120.0 (2)
N(12) - C(17) - C(12)	112.7 (2)	N(22) - C(27) - C(22)	113.2 (2)
N(12) - C(18) - C(19)	112.0 (2)	N(22) - C(28) - C(29)	112.7 (2)

Appendix 2.1 (c)

Atomic coordinates and equivalent isotropic displacement parameters for ABTS as one third of the trace of the orthogonalized Uij tensor.

Atom	x	y	z	U(eq)
S(11)	0.9650(1)	0.1588(1)	0.0308(1)	0.021(1)
S(12)	0.6409(1)	0.0370(1)	-0.2375(1)	0.025(1)
O(11)	0.9442(2)	0.1966(1)	-0.0244(2)	0.034(1)
O(12)	0.8780(2)	0.1505(1)	0.1686(2)	0.027(1)
O(13)	1.1279(2)	0.1492(1)	0.0674(2)	0.031(1)
N(11)	0.5315(3)	0.0135(1)	-0.5474(3)	0.028(1)
N(12)	0.6858(2)	0.0659(1)	-0.5175(2)	0.024(1)
C(11)	0.6110(3)	0.0369(1)	-0.4554(3)	0.024(1)
C(12)	0.7431(3)	0.0784(1)	-0.2392(3)	0.020(1)
C(13)	0.8040(3)	0.0992(1)	-0.1058(3)	0.021(1)
C(14)	0.8839(3)	0.1312(1)	-0.1349(3)	0.020(1)
C(15)	0.9038(3)	0.1414(1)	-0.2948(3)	0.023(1)
C(16)	0.8396(3)	0.1209(1)	-0.4281(3)	0.023(1)
C(17)	0.7579(3)	0.0895(1)	-0.3998(3)	0.020(1)
C(18)	0.6736(3)	0.0732(1)	-0.6938(3)	0.026(1)
C(19)	0.5399(3)	0.0985(1)	-0.7504(4)	0.043(1)
S(21)	0.4026(1)	0.1965(1)	0.5448(1)	0.024(1)
S(22)	0.1035(1)	0.0642(1)	0.4047(1)	0.026(1)
O(21)	0.3002(2)	0.2079(1)	0.3997(2)	0.032(1)
O(22)	0.3889(3)	0.2193(1)	0.6875(2)	0.045(1)
O(23)	0.5634(2)	0.1941(1)	0.5098(2)	0.036(1)
N(21)	0.0425(3)	0.0037(1)	0.5777(3)	0.031(1)
N(22)	0.2049(3)	0.0486(1)	0.7091(2)	0.025(1)
C(21)	0.1119(3)	0.0343(1)	0.5753(3)	0.025(1)
C(22)	0.2153(3)	0.0965(1)	0.5255(3)	0.021(1)
C(23)	0.2559(3)	0.1311(1)	0.4796(3)	0.021(1)
C(24)	0.3462(3)	0.1521(1)	0.5957(3)	0.022(1)
C(25)	0.3953(3)	0.1388(1)	0.7519(3)	0.027(1)
C(26)	0.3513(3)	0.1045(1)	0.7982(3)	0.028(1)
C(27)	0.2602(3)	0.0832(1)	0.6845(3)	0.022(1)
C(28)	0.2288(3)	0.0292(1)	0.8661(3)	0.027(1)
C(29)	0.1192(4)	0.0414(1)	0.9836(4)	0.042(1)
O(1)	0.9799(3)	0.2902(1)	-0.0863(3)	0.036(1)
N(1)	0.8119(3)	0.2335(1)	-0.3230(3)	0.033(1)
O(2)	0.6321(3)	0.1984(1)	0.1903(3)	0.038(1)
N(2)	0.3288(3)	0.2909(1)	0.5289(3)	0.029(1)

Appendix 2.2 (DAB method as used by *ESR:Forensic*)

General procedure

Fingerprints contaminated with blood are enhanced with DAB by first stabilising or fixing the blood by immersion in sulfosalicylic acid. Articles are then washed in distilled water followed by immersion in freshly activated DAB working solution to stain the blood to a dark brown colour. This is followed by a wash in distilled water after which articles are allowed to dry at room temperature.

1. Pour sufficient sulfosalicylic acid solution to treat article in a clean, dry, glass dish and immerse article for two to three minutes.
2. Wash article in a dish of distilled water.
3. Pour sufficient freshly activated DAB working solution into a clean, dry, glass dish to treat article. Immerse article in working solution until fingerprints become a dark brown colour. This will take approximately four minutes.
4. Thoroughly wash article in a dish of distilled water, then allow to air dry.
5. Photograph useful fingerprints.

Preparation of Sulfosalicylic Acid (fixative solution)

1. Weigh out 20 grams of 5-sulfosalicylic acid. Place in a clean 2 litre glass beaker.
2. Add 1 litre of distilled water and stir with a magnetic stirrer until all the powder has dissolved.
3. Transfer to a clean, labeled, 1 litre glass bottle with a well fitting screw top. Use either a dark glass bottle or cover with silver foil. Store in the dark at room temperature.

Preparation of Phosphate Buffer

Add 100 mL of 1 Molar phosphate buffer, pH 7.4, to 800 mL of distilled water in a clean, labeled, 1 litre glass bottle with a well fitting screw top.
The solution can be stored at room temperature and will keep indefinitely.
To make up 1 litre of 1 Molar phosphate buffer dissolve 178 g of di-sodium hydrogen orthophosphate dihydrate ($Na_2HPO_4.2H_2O$) in 1 litre of distilled water. Adjust the pH to 7.4 with 85% phosphoric acid. It is important that the phosphate buffer used does not contain sodium azide as preservative.

Preparation of Preliminary DAB Solution

1. Weigh out 5 grams of DAB (3,3'-diaminobenzidine) into a clean 1 litre beaker.
2. Add 500 mL of distilled water and stir with a magnetic stirrer until all the powder has dissolved.
3. Transfer to clean, labeled, 20 mL glass vials. Store in the freezer at -20°C until required. (The vials used must be good quality glass to withstand freezing and re–thawing.)

Preparation of DAB Activated Working Solution

This solution must be made up fresh just prior to use.

1. Thaw out a 20 mL aliquot of DAB solution.
2. Mix together 180 mL of phosphate buffer and 20 mL of thawed DAB solution.
3. Add 1 mL of 30% hydrogen peroxide.

Appendix 2.3 (calculation of the correct ratio of ABTS to H_2O_2)

In the cuvette trials 10 µL of 2.7% H_2O_2 at pH 5.4 was found to be optimal for ABTS colour development. The concentration of the ABTS stock solution used to prepare solutions for the cuvette trial was 2.5 g/L (125 mg /50 mL). A 100 µL aliquot of this ABTS stock solution was added to 11.7 mL to give a final volume of 11.8 mL. Therefore the dilution factor is 8.475×10^{-3} (0.1 mL /11.8 mL). The concentration of ABTS in the diluted solution is 0.02119 g/L ($8.475 \times 10^{-3} \times 2.5$ g/L).

The mass of ABTS contained in this 0.02119 g/L ABTS solution is 2.5×10^{-4} g [0.02119 g/L x (11.8 mL /1000 mL]. If 1 g ABTS /2.5×10^{-4} g ABTS equals 4000 then 10 µL 2.7% H_2O_2 multiplied by this factor of 4000 equals 40 mL.

So 1 g ABTS requires 40 mL of 2.7% H_2O_2 (or 4 mL of 2.7% H_2O_2)for optimal colour development.

Appendix 2.4 (calculation of the correct ratio of DAB to H_2O_2)

In the cuvette trials 100 µL of 2.7% H_2O_2 at pH 5.0 was found to be optimal for DAB colour development. The concentration of the DAB stock solution used to prepare solutions for the cuvette trial was 0.12 g/L (30 mg /250 mL). A 1 mL aliquot of this DAB stock solution was added to 11.5 mL to give a final volume of 12.5 mL. Therefore the dilution factor is 0.08 (1 mL /12.5 mL). The concentration of DAB in the diluted solution is 9.6×10^{-3} g/L (0.08 x 0.12 g/L).

This result can be compared with that calculated for the *ESR:Forensic* method. The concentration of the DAB stock solution used is 10 g/L (5 g /500 mL). A 20 mL aliquot of this DAB stock solution is made up to 200 mL with phosphate buffer (pH 7.4) and 1 mL 27% H_2O_2 is added. Therefore the dilution factor is 0.0995 (20 mL /201 mL). The concentration of DAB in the diluted solution is 0.995 g/L (0.0995 x 10 g/L).

1 mL of this diluted solution is 27% H_2O_2 which is equivalent to 10 mL of 2.7% H_2O_2.

10 mL 2.7% H_2O_2 (*ESR:Forensic* method) /0.1 mL 2.7% H_2O_2 (optimised method) = 100

Therefore 100 x 0.0096 g/L (DAB concentration for optimised method) = 0.96 g/L

Optimised ratio = 0.96 g/L of DAB per 1 mL of H_2O_2 *ESR:Forensic* ratio = 0.995 g/L of DAB per 1 mL of H_2O_2

Appendices

Chapter Three

Appendix 3.1 (calculation of the correct ratio of OPD to H_2O_2)

In the cuvette trials 50 µL of 2.7% H_2O_2 at pH 5.4 was found to be optimal for OPD colour development. The concentration of the OPD stock solution used to prepare solutions for the cuvette trial was 0.5 g/L (50 mg /100 mL). A 500 µL aliquot of this OPD stock solution was added to 11.7 mL to give a final volume of 12.2 mL. Therefore the dilution factor is 40.98 x 10^{-3} (0.5 mL /12.2 mL). The concentration of OPD in the diluted solution is 0.02049 g/L (40.98 x 10^{-3} x 0.5 g/L).

The mass of OPD contained in this 0.02049 g/L OPD solution is 2.5 x 10^{-4} g [0.02049 g/L x (12.2 mL /1000 mL]. If 1 g OPD /2.5 x 10^{-4} g OPD equals 4000 then 50 µL 2.7% H_2O_2 multiplied by this factor of 4000 equals 200 mL.

So 1 g OPD requires 200 mL of 2.7% H_2O_2 (or 20 mL of 27% H_2O_2) for optimal colour development.

Appendix 3.2 (calculation of the correct ratio of PPD to H_2O_2)

In the cuvette trials 100 µL of 2.7% H_2O_2 at pH 5.4 was found to be optimal for PPD colour development. The concentration of the PPD stock solution used to prepare solutions for the cuvette trial was 0.5 g/L (50 mg /100 mL). A 500 µL aliquot of this PPD stock solution was added to 11.7 mL to give a final volume of 12.2 mL. Therefore the dilution factor is 40.98 x 10^{-3} (0.5 mL /12.2 mL). The concentration of PPD in the diluted solution is 0.02049 g/L (40.98 x 10^{-3} x 0.5 g/L).

The mass of PPD contained in this 0.02049 g/L PPD solution is 2.5 x 10^{-4} g [0.02049 g/L x (12.2 mL /1000 mL]. If 1 g PPD /2.5 x 10^{-4} g PPD equals 4000 then 100 µL 2.7% H_2O_2 multiplied by this factor of 4000 equals 400 mL.

So 1 g PPD requires 400 mL of 2.7% H_2O_2 (or 40 mL of 27% H_2O_2) for optimal colour development.

Appendices

Chapter Four

Appendix 4.1 (comparison of the excitation-emission spectra of X4 and petroleum spirits (b.p. 40-60°C))

Fluorescence spectra of X4 and petroleum spirits (b.p. 40-60°C) were obtained to provide a comparison between the two solvents. A 5 nm slit width was used for excitation and emission. Results are presented in Tables 4.1(A) to 4.3(A).

Appendix 4.1(a)
Emissions for X4 and Petroleum Spirits (b.p. 40-60°C).

X4 (excitation at 266 nm)		Pet. Spirits (b.p. 40-60°C) (excitation at 201 nm)	
Emission λ	Intensity	Emission λ	Intensity
292.5	561	293.6	508
322.5	260		
335.5	241		
		405.2	41
534.5	125		
569.0	491		
579.5	491	581.4	411
640.0	100		

Appendix 4.1 (b)
Excitations for X4 and Petroleum Spirits (b.p. 40-60°C).

X4 (for 292 nm emission)		Pet. Spirits (40-60°C) (for 293 nm emission)	
Excitation λ	Intensity	Excitation λ	Intensity
		201.0	489
225.5	322	215.0	474
266.5	566	269.0	60

Appendix 4.1 (b)
Excitations for X4 and Petroleum Spirits (40-60°C).

X4 (for 580 nm emission)		Pet. Spirits (40-60°C) (for 581 nm emission)	
Excitation λ	Intensity	Excitation λ	Intensity
		200.0	418
225.5	266	216.0	405
266.5	490	268.0	57

Appendix 4.2 (a)

Raw intensity data for three dimensional emission–excitation spectrum of Eu(fod) 3

Emission	Excitation wavelength (nm)																														
Wavelength (nm)	200	210	220	230	240	250	260	270	280	290	300	310	320	330	340	350	360	370	380	390	400	410	420	430	440	450	460	470	480	490	500
220	1	0	0	0	0	0	0	0	0	0	0	0	0	0	0	0	0	0	0	0	0	0	0	0	0	0	0	0	0	0	0
230	1	0	0	0	0	0	0	0	0	0	0	0	0	0	0	0	0	0	0	0	0	0	0	0	0	0	0	0	0	0	0
240	2.1	0	0	0	0	0	0	0	0	0	0	0	0	0	0	0	0	0	0	0	0	0	0	0	0	0	0	0	0	0	0
250	2.1	0	0	0	0	0	0	0	0	0	0	0	0	0	0	0	0	0	0	0	0	0	0	0	0	0	0	0	0	0	0
260	2.1	0	0	0	0	0	0	0	0	0	0	0	0	0	0	0	0	0	0	0	0	0	0	0	0	0	0	0	0	0	0
270	2.1	0	0	0	0	0	0	0	0	0	0	0	0	0	0	0	0	0	0	0	0	0	0	0	0	0	0	0	0	0	0
280	2.1	0	0	0	0	0	0	0	0	0	0	0	0	0	0	0	0	0	0	0	0	0	0	0	0	0	0	0	0	0	0
290	2.1	0	0	0	0	0	0	0	0	0	0	0	0	0	0	0	0	0	0	0	0	0	0	0	0	0	0	0	0	0	0
300	2.1	0	0	0	0	0	0	0	0	0	0	0	0	0	0	0	0	0	0	0	0	0	0	0	0	0	0	0	0	0	0
310	2.1	0	0	0	0	0	0	0	0	0	0	0	0	0	0	0	0	0	0	0	0	0	0	0	0	0	0	0	0	0	0
320	2.1	0	2.1	2.1	0	1.6	0	0	0	0	0	0	0	0	0	0	0	0	0	0	0	0	0	0	0	0	0	0	0	0	0
330	3.1	1	17	22	4.7	2.1	1.4	0	0	0	0	0	0	0	0	0	0	0	0	0	0	0	0	0	0	0	0	0	0	0	0
340	7.3	4.2	65	112	23	14	6	0	0	0	0	0	0	0	0	0	0	0	0	0	0	0	0	0	0	0	0	0	0	0	0
350	11	8.9	107	167	35	19	8.5	1.6	0	0	0	0	0	1.6	0	0	0	0	0	0	0	0	0	0	0	0	0	0	0	0	0
360	11	7.9	79	131	28	17	6.8	1.6	0	0	0	0	0	1.6	7.3	0	0	0	0	0	0	0	0	0	0	0	0	0	0	0	0
370	13	6.3	51	79	20	12	4.9	1	0	0	0	0	0	3.7	11	12	0	0	0	0	0	0	0	0	0	0	0	0	0	0	0
380	12	4.7	29	42	13	7.9	3.3	1	0	0	0	0	0	2.1	21	18	13	0	0	0	0	0	0	0	0	0	0	0	0	0	0
390	11	4.7	14	23	9.4	5.8	2.7	1	0	0	0	0	0	2.1	7.3	33	15	12	0	0	0	0	0	0	0	0	0	0	0	0	0
400	11	4.7	8.4	13	6.3	4.7	2	1	0	0	0	0	0	1	5.2	18	35	12	11	0	0	0	0	0	0	0	0	0	0	0	0
410	9.4	4.7	5.2	8.4	5.2	3.1	1.7	1	0	0	0	0	0	1	5.2	9.4	25	31	9.9	11	0	0	0	0	0	0	0	0	0	0	0
420	9.4	4.7	4.2	6.3	4.2	3.1	1.7	0	0	0	0	0	0	1	5.2	8.4	11	29	23	8.9	11	0	0	0	0	0	0	0	0	0	0
430	9.4	4.7	3.1	4.2	3.1	2.1	1.4	0	0	0	0	0	0	1	4.2	7.3	9.4	11	30	16	7.3	7.3	0	0	0	0	0	0	0	0	0
440	7.9	4.2	3.1	3.1	2.1	2.1	1.1	0	0	0	0	0	0	1	4.2	6.3	8.4	8.9	11	27	9.4	5.2	6.3	0	0	0	0	0	0	0	0
450	7.9	3.1	3.1	2.1	2.1	1.6	1	0	0	0	0	0	0	0	3.1	6.3	7.3	7.9	7.3	12	22	6.3	4.2	4.2	0	0	0	0	0	0	0
460	6.8	3.1	2.1	2.1	2.1	1.6	0	0	0	0	0	0	0	0	2.1	5.2	6.3	6.8	6.3	5.8	13	15	2.6	3.1	3.1	0	0	0	0	0	0
470	6.8	2.6	2.1	2.1	2.1	1.6	0	0	0	0	0	0	0	0	2.1	5.2	5.2	5.8	5.2	4.7	4.7	12	8.4	2.1	2.6	2.6	0	0	0	0	0
480	6.8	2.1	2.1	2.1	2.1	1.6	0	0	0	0	0	0	0	0	2.1	4.2	4.7	4.7	4.2	4.2	4.2	3.7	12	4.7	1.6	2.1	2.1	0	0	0	0
490	6.8	1.6	1	2.1	1	2.1	0	0	0	0	0	0	0	0	2.1	3.1	3.7	3.7	3.7	3.1	2.6	2.1	4.2	8.4	3.1	1	2.1	1.6	0	0	0
500	3.7	0	1	2.1	1	3.1	0	0	0	0	0	0	0	0	2.1	2.1	3.1	3.1	3.1	2.6	2.1	2.1	1.6	4.2	6.3	2.1	1	1.6	0	0	0
510	3.7	0	1	2.1	1	1.6	0	0	0	0	0	0	0	0	2.1	2.1	2.6	2.6	2.6	2.1	2.1	1.6	1	1	5.2	5.2	1	1	1	0	0
520	3.7	0	1	2.1	1	1	0	0	0	0	0	0	0	0	2.1	2.1	2.1	2.1	2.1	1.6	1.6	1	1	1	1.6	4.2	2.1	0	1	0	0
530	3.7	0	1	2.1	2.6	1	0	0	0	0	0	0	0	3.1	9.4	6.3	4.2	3.1	2.6	2.1	1.6	1	1	1	1	1.6	3.7	1	0	0	0
540	3.7	0	1	5.2	4.7	1	0	0	0	0	0	0	0	6.3	14	11	6.8	4.2	3.1	2.1	1.6	1	0	0	0	1	1.6	2.6	0	0	0
550	2.1	0	1	2.1	1	1	0	0	0	0	0	0	0	1	2.1	2.1	1.6	1.6	1	1	1	0	0	0	0	0	0	1.6	1	0	0
560	1.6	0	1	2.1	1	1	0	0	0	0	0	0	0	1	2.1	2.1	1.6	1	1	0	0	0	0	0	0	0	0	0	1	0	0
570	1.6	0	1	2.1	1	1.6	0	0	0	0	0	0	0	1.6	2.1	13	1	1	1	1	0	0	0	0	0	0	0	0	0	0	0
580	2.1	0	1	5.2	4.7	4.2	1.9	0	0	0	0	0	0	7.3	18	17	6.8	4.2	3.1	1	1	0	0	0	0	0	0	0	0	0	0
590	2.1	0	2.1	7.3	7.3	5.2	2.8	0	0	0	0	0	1	11	25	11	9.4	5.8	3.7	2.1	1	0	0	0	0	0	0	0	0	0	0

Appendix 4.2 (a) (continued...)

Raw intensity data for three dimensional emission–excitation spectrum of Eu(fod) 3

Emission	Emission wavelength (nm)																														
Wavelength (nm)	200	210	220	230	240	250	260	270	280	290	300	310	320	330	340	350	360	370	380	390	400	410	420	430	440	450	460	470	480	490	500
600	2.1	0	4.2	5.2	5.2	3.7	1.9	0	0	0	0	0	1	7.3	17	93	6.3	3.7	2.6	2.1	1	0	0	0	0	0	0	0	0	0	0
610	2.1	3.1	16	60	59	37	19	4.7	0	0	0	0	8.9	78	157	122	63	37	20	12	6.3	2.6	1.6	0	0	0	0	0	0	0	0
614	1.7	1.3	7	46	66	53	34	8.3	1.9	1.7	1.9	2.1	5.6	69	199	161	101	64	40	23	11	4.7	2.1	0	0	0	0	0	0	0	0
620	1	1	6.3	35	31	23	12	0	0	0	0	0	4.7	53	107	83	53	33	16	8.9	4.7	2.6	1	0	0	0	0	0	0	0	0
630	1	0	2.1	2.1	4.2	3.1	1.1	0	0	0	0	0	1	5.8	15	13	6.3	2.6	2.6	1	1	1	1	0	0	0	0	0	0	0	0
640	1	0	2.1	2.1	1.6	1	0	0	0	0	0	0	0	1	2.1	2.1	1	1	1	0	0	0	0	0	0	0	0	0	0	0	0
650	1	0	2.1	2.1	1.6	1	0	0	0	0	0	0	0	1	2.1	1	0	0	0	0	0	0	0	0	0	0	0	0	0	0	0
660	2.1	0	3.1	2.1	1.6	1	0	0	0	0	0	0	0	1.6	2.1	0	0	0	0	0	0	0	0	0	0	0	0	0	0	0	0
670	2.6	0	11	13	2.6	2.1	0	0	0	0	0	0	0	3.7	0	0	0	0	0	0	0	0	0	0	0	0	0	0	0	0	0	0
680	3.1	0	19	28	5.8	3.1	1.7	0	0	0	0	0	0	1	0	0	0	0	0	0	0	0	0	0	0	0	0	0	0	0	0	0
690	3.1	1.6	19	34	6.3	3.7	1.7	0	0	0	0	0	0	0	0	0	0	0	0	0	0	0	0	0	0	0	0	0	0	0	0	0
700	3.1	1.6	16	29	6.3	3.7	1.7	0	0	0	0	0	0	0	0	0	0	0	0	0	0	0	0	0	0	0	0	0	0	0	0	0
710	3.1	1.6	15	23	6.3	3.1	1.4	0	0	0	0	0	0	0	1	0	0	0	0	0	0	0	0	0	0	0	0	0	0	0	0	0
720	3.1	1.6	9.4	18	4.7	2.6	1.1	0	0	0	0	0	0	0	0	0	0	0	0	0	0	0	0	0	0	0	0	0	0	0	0	0
730	3.1	1	6.3	11	3.7	2.1	0	0	0	0	0	0	0	0	0	0	0	0	0	0	0	0	0	0	0	0	0	0	0	0	0	0
740	3.1	0	4.2	7.3	2.6	1.6	0	0	0	0	0	0	0	0	1	0	0	0	0	0	0	0	0	0	0	0	0	0	0	0	0	0
750	3.1	0	3.1	5.2	1.6	1	0	0	0	0	0	0	0	0	1.6	0	0	0	0	0	0	0	0	0	0	0	0	0	0	0	0	0
760	2.1	0	2.1	3.1	1	1	0	0	0	0	0	0	0	0	2.1	0	0	0	0	0	0	0	0	0	0	0	0	0	0	0	0	0
770	2.1	0	1	2.1	1	1	0	0	0	0	0	0	0	0	1	1	0	0	0	0	0	0	0	0	0	0	0	0	0	0	0	0
780	2.1	0	1	1	0	0	0	0	0	0	0	0	0	0	0	1.6	0	0	0	0	0	0	0	0	0	0	0	0	0	0	0	0
790	2.1	0	0	1	0	0	0	0	0	0	0	0	0	0	0	1	0	0	0	0	0	0	0	0	0	0	0	0	0	0	0	0
800	1.6	0	0	0	0	0	0	0	0	0	0	0	0	0	0	0	0	0	0	0	0	0	0	0	0	0	0	0	0	0	0	0
810	1.6	0	0	0	0	0	0	0	0	0	0	0	0	0	0	0	0	0	0	0	0	0	0	0	0	0	0	0	0	0	0	0
820	1.6	0	0	0	0	0	0	0	0	0	0	0	0	0	0	0	0	1	0	0	0	0	0	0	0	0	0	0	0	0	0	0
830	1.6	0	0	0	0	0	0	0	0	0	0	0	0	0	0	0	0	1	0	0	0	0	0	0	0	0	0	0	0	0	0	0
840	1.6	0	0	0	0	0	0	0	0	0	0	0	0	0	0	0	0	1	0	0	0	0	0	0	0	0	0	0	0	0	0	0
850	1.6	0	0	0	0	0	0	0	0	0	0	0	0	0	0	0	0	0	0	0	0	0	0	0	0	0	0	0	0	0	0	0
860	1.6	0	0	0	0	0	0	0	0	0	0	0	0	0	0	0	0	0	0	0	0	0	0	0	0	0	0	0	0	0	0	0
870	1.6	0	0	0	0	0	0	0	0	0	0	0	0	0	0	0	0	0	0	0	0	0	0	0	0	0	0	0	0	0	0	0
880	1.6	0	0	0	0	0	0	0	0	0	0	0	0	0	0	0	0	0	0	0	0	0	0	0	0	0	0	0	0	0	0	0
890	1	0	0	0	0	0	0	0	0	0	0	0	0	0	0	0	0	0	0	0	0	0	0	0	0	0	0	0	0	0	0	0
900	1	0	0	0	0	0	0	0	0	0	0	0	0	0	0	0	0	0	0	0	0	0	0	0	0	0	0	0	0	0	0	0

Appendix 4.2 (b)

Raw intensity data for three dimensional emission–excitation spectrum of Tb(fod) 3

Emission	Excitation wavelength (nm)																																
Wavelength (nm)	200	210	220	230	240	250	260	270	280	290	300	310	320	330	337	340	350	360	370	380	390	400	410	420	430	440	450	460	470	480	490	500
220	0	0	0	0	0	0	0	0	0	0	0	0	0	0	0	0	0	0	0	0	0	0	0	0	0	0	0	0	0	0	0	0
230	0	0	0	0	0	0	0	0	0	0	0	0	0	0	0	0	0	0	0	0	0	0	0	0	0	0	0	0	0	0	0	0
240	0	0	0	0	0	0	0	0	0	0	0	0	0	0	0	0	0	0	0	0	0	0	0	0	0	0	0	0	0	0	0	0
250	0	0	0	0	0	0	0	0	0	0	0	0	0	0	0	0	0	0	0	0	0	0	0	0	0	0	0	0	0	0	0	0
260	0	0	0	0	0	0	0	0	0	0	0	0	0	0	0	0	0	0	0	0	0	0	0	0	0	0	0	0	0	0	0	0
270	0	0	0	0	0	0	0	0	0	0	0	0	0	0	0	0	0	0	0	0	0	0	0	0	0	0	0	0	0	0	0	0
280	0	0	0	0	0	0	0	0	0	0	0	0	0	0	0	0	0	0	0	0	0	0	0	0	0	0	0	0	0	0	0	0
290	0	0	0	0	0	0	0	0	0	0	0	0	0	0	0	0	0	0	0	0	0	0	0	0	0	0	0	0	0	0	0	0
300	0	0	0	0	0	0	0	0	0	0	0	0	0	0	0	0	0	0	0	0	0	0	0	0	0	0	0	0	0	0	0	0
310	0	0	0	0	0	1	0	0	0	0	0	0	0	0	0	0	0	0	0	0	0	0	0	0	0	0	0	0	0	0	0	0
320	0	0	1.6	1.6	3.1	1	0	0	0	0	0	0	0	0	0	0	0	0	0	0	0	0	0	0	0	0	0	0	0	0	0	0
330	0	0	6.8	10	4.7	5.8	2.6	0	0	0	0	0	0	0	0	0	0	0	0	0	0	0	0	0	0	0	0	0	0	0	0	0
340	3.1	3.1	29	44	20	18	12	1.6	0	0	0	0	0	0	0	0	0	0	0	0	0	0	0	0	0	0	0	0	0	0	0	0
350	6.8	7.3	36	53	20	20	14	2.4	0	0	0	0	0	2.6	0	0	0	0	0	0	0	0	0	0	0	0	0	0	0	0	0	0
360	6.8	6.8	26	39	16	13	9.4	1.6	0	0	0	0	0	3.7	4.2	11	0	0	0	0	0	0	0	0	0	0	0	0	0	0	0	0
370	6.8	4.2	20	21	11	8.4	5.2	1.4	0	0	0	0	0	6.3	7.6	18	13	0	0	0	0	0	0	0	0	0	0	0	0	0	0	0
380	4.7	3.1	12	11	7.9	4.7	3.7	0	0	0	0	0	0	2.6	15	33	21	16	14	0	0	0	0	0	0	0	0	0	0	0	0	0
390	5.2	2.6	6.3	6.3	4.7	4.2	2.1	0	0	0	0	0	0	1.6	19	7.3	39	16	9.9	0	0	0	0	0	0	0	0	0	0	0	0	0
400	3.1	2.1	5.2	3.9	3.1	2.6	1.6	0	0	0	0	0	0	1.6	7.6	7.3	18	37	28	12	0	0	0	0	0	0	0	0	0	0	0	0
410	2.6	1.6	5.2	2.4	3.1	2.6	1.6	0	0	0	0	0	0	1	7.6	7.3	7.9	21	33	7.9	11	0	0	0	0	0	0	0	0	0	0	0
420	2.1	1.6	4.7	2.4	3.1	1.6	1.6	0	0	0	0	0	0	1	3.8	7.3	5.2	11	6.8	20	6.8	10	0	0	0	0	0	0	0	0	0	0
430	2.1	0	4.2	2.4	3.1	1.6	1.6	0	0	0	0	0	0	1	3.8	7.3	5.2	5.2	4.2	28	12	6.3	7.4	0	0	0	0	0	0	0	0	0
440	2.1	0	4.2	2.4	3.1	1	1	0	0	0	0	0	0	1	3.8	7.3	5.2	5.2	3.7	7.3	25	6.8	4.4	5.5	0	0	0	0	0	0	0	0
450	2.1	0	3.1	2.4	3.1	1	1	0	0	0	0	0	0	1	3.8	7.3	5.2	2.6	3.1	3.7	9.4	20	3.8	3.8	4.2	0	0	0	0	0	0	0
460	0	0	3.1	2.4	3.1	1	1	0	0	0	0	0	0	1	3.8	7.3	5.2	2.6	2.6	3.1	3.4	12	13	2.2	3	3.1	0	0	0	0	0	0
470	0	0	3.1	2.4	3.1	1	1	0	1	0	1	1	1	1	3.8	7.3	5.2	2.6	3.7	2.6	2.6	2.6	12	6.9	1.6	2.6	2.6	0	0	0	0	0
480	2.1	1	4.7	20	31	31	14	2.7	1	0	1	1	4.2	39	61	55	18	7.9	8.4	2.6	2.9	2.1	3	12	3.9	1.3	2.1	2.1	0	0	0	0
490	7.3	4.7	15	68	119	94	48	10	4.2	3.1	3.1	4.2	14	159	339	242	73	18	5.2	5.8	4.5	3.1	2.5	4.2	8.2	2	1	2.1	1.6	0	0	0
500	1	1	6.8	28	50	40	17	3.3	1.6	1	1	1	6.8	79	171	110	39	13	2.1	3.7	2.6	2.1	1.9	1.6	4.1	5.8	1	1	1.6	0	0	0
510	0	0	2.6	1.6	4.7	3.1	1.6	0	1	0	0	0	1	5.5	15	15	5.2	5.2	1.6	2.1	1.6	1	1.1	1.1	1	4.8	3.7	1	1.6	0	0	0
520	0	0	2.6	1.6	3.1	1.6	1.6	0	1	0	0	0	1	3.7	3.8	7.3	5.2	2.6	1.6	1.6	1.6	1	1	1	1	1.2	4.7	2.1	0	0	0	0
530	0	5.8	2.6	1.6	7.9	4.7	3.7	1.1	1	1	1	1	1	3.7	15	7.3	5.2	5.2	2.1	1.6	1.3	1	1	1	1	0	1.6	3.7	1	0	0	0
540	3.7	6.3	22	76	121	98	41	11	3.1	4.7	2.6	3.7	19	158	366	264	81	24	8.9	6.3	3.7	2.1	1.7	1.3	1	0	1	2.1	2.6	0	0	0
547	11	7	27	140	222	162	70	16	6.6	6.3	6.5	8.8	47	465	719	602	161	40	16	9.1	5.9	3.7	2.5	1.7	1	0	0	1	1	0	0	0
550	9.4	1	25	133	240	170	95	21	7.3	5.8	5.8	6.8	27	345	663	524	149	37	15	8.9	6.5	4.2	3	2	1	0	0	0	1	0	0	0
560	1	0	3.7	10	19	13	11	1.6	1	1	1	1	1	44	84	37	5.2	5.2	1.6	1.6	1	1	1	1	1	0	0	0	0	0	0	0
570	0	0	2.6	0	1.6	1.5	1	1.6	1	0	0	0	1	3.7	3.8	7.3	5.2	2.6	0	0	1	1	1	0	0	0	0	0	0	0	0	0
580	0	0	2.6	3.9	7.9	5.9	2.6	0	0	0	0	0	1	13	19	7.3	5.2	2.6	0	0	0	0	0	0	0	0	0	0	0	0	0	0
590	0	0	2.6	5.5	9.4	8.8	4.2	0	0	0	0	0	1.6	7.3	23	18	5.2	1	0	0	0	0	0	0	0	0	0	0	0	0	0	0

Appendix 4.2 (b) (continued...)

Raw intensity data for three dimensional emission–excitation spectrum of Tb(fod) 3

Emission	Excitation wavelength (nm)																																
Wavelength (nm)	200	210	220	230	240	250	260	270	280	290	300	310	320	330	337	340	350	360	370	380	390	400	410	420	430	440	450	460	470	480	490	500
600	0	0	1.6	1.6	1.6	2.9	1	0	0	0	0	0	1	3.7	7.6	7.3	2.6	1	0	0	0	0	0	0	0	0	0	0	0	0	0	0
610	0	0	1.6	1.6	1.6	2.9	0	0	0	0	0	0	1	3.7	3.8	7.3	2.6	1	0	0	0	0	0	0	0	0	0	0	0	0	0	0
620	0	0	1.6	1.6	1.6	1.5	0	0	0	0	0	0	0	3.7	7.6	7.3	1	1	0	0	0	0	0	0	0	0	0	0	0	0	0	0
630	0	0	1.6	1.6	1.6	1.5	0	0	0	0	0	0	0	3.7	3.8	7.3	1	1	0	0	0	0	0	0	0	0	0	0	0	0	0	0
640	0	0	1.6	1.6	1.6	1.5	0	0	0	0	0	0	0	3.7	3.8	7.3	1	1	0	0	0	0	0	0	0	0	0	0	0	0	0	0
650	0	0	1.6	1.6	1.6	1.5	0	0	0	0	0	0	0	3.7	3.8	7.3	0	1	0	0	0	0	0	0	0	0	0	0	0	0	0	0
660	0	0	2.6	2.4	1.6	2.9	1	0	0	0	0	0	0	3.7	3.8	7.3	0	1	0	0	0	0	0	0	0	0	0	0	0	0	0	0
670	0	0	5.2	6.3	3.1	2.9	1.6	0	0	0	0	0	0	3.7	3.8	7.3	0	1	0	0	0	0	0	0	0	0	0	0	0	0	0	0
680	0	0	8.4	12	4.7	2.9	3.1	0	0	0	0	0	0	3.7	1.6	7.3	0	1	0	0	0	0	0	0	0	0	0	0	0	0	0	0
690	0	0	7.3	10	4.7	4.4	2.6	0	0	0	0	0	0	3.7	1.6	7.3	0	1	0	0	0	0	0	0	0	0	0	0	0	0	0	0
700	0	0	6.3	8.6	4.7	2.9	2.1	0	0	0	0	0	0	3.7	1.6	3.7	0	1	0	0	0	0	0	0	0	0	0	0	0	0	0	0
710	0	0	5.2	6.3	3.1	2.9	1.6	0	0	0	0	0	0	1.8	1.6	3.7	0	1	0	0	0	0	0	0	0	0	0	0	0	0	0	0
720	0	0	4.2	5.5	3.1	2.9	1.6	0	0	0	0	0	0	1.8	1.6	3.7	0	1	0	0	0	0	0	0	0	0	0	0	0	0	0	0
730	0	0	3.7	3.1	3.1	1.5	1	0	0	0	0	0	0	1.8	1.6	3.7	0	1	0	0	0	0	0	0	0	0	0	0	0	0	0	0
740	0	0	2.6	2.4	3.1	1.5	1	0	0	0	0	0	0	1.8	1.6	3.7	0	1	0	0	0	0	0	0	0	0	0	0	0	0	0	0
750	0	0	2.6	1.6	1.6	1.5	1	0	0	0	0	0	0	1.8	1.6	3.7	0	1	0	0	0	0	0	0	0	0	0	0	0	0	0	0
760	0	0	2.6	1.6	0	1.5	0	0	0	0	0	0	0	1.8	1.6	3.7	0	1	0	0	0	0	0	0	0	0	0	0	0	0	0	0
770	0	0	2.6	1.6	0	0	0	0	0	0	0	0	0	1.8	1.6	3.7	0	0	0	0	0	0	0	0	0	0	0	0	0	0	0	0
780	0	0	1.6	1.6	0	0	0	0	0	0	0	0	0	1.8	1.6	3.7	0	0	0	0	0	0	0	0	0	0	0	0	0	0	0	0
790	0	0	0	1.6	0	0	0	0	0	0	0	0	0	1.8	1.6	3.7	0	0	0	0	0	0	0	0	0	0	0	0	0	0	0	0
800	0	0	0	0	0	0	0	0	0	0	0	0	0	1.8	1.6	3.7	0	0	0	0	0	0	0	0	0	0	0	0	0	0	0	0
810	0	0	0	0	0	0	0	0	0	0	0	0	0	1.8	1.6	3.7	0	0	0	0	0	0	0	0	0	0	0	0	0	0	0	0
820	0	0	0	0	0	0	0	0	0	0	0	0	0	1.8	1.6	3.7	0	0	1	0	0	0	0	0	0	0	0	0	0	0	0	0
830	0	0	0	0	0	0	0	0	0	0	0	0	0	1.8	1.6	3.7	0	0	1	0	0	0	0	0	0	0	0	0	0	0	0	0
840	0	0	0	0	0	0	0	0	0	0	0	0	0	1.8	1.6	3.7	0	0	1	0	0	0	0	0	0	0	0	0	0	0	0	0
850	0	0	0	0	0	0	0	0	0	0	0	0	0	1.8	1.6	3.7	0	0	0	0	0	0	0	0	0	0	0	0	0	0	0	0
860	0	0	0	0	0	0	0	0	0	0	0	0	0	1.8	1.6	3.7	0	0	0	0	0	0	0	0	0	0	0	0	0	0	0	0
870	0	0	0	0	0	0	0	0	0	0	0	0	0	1.8	1.6	3.7	0	0	0	0	1	0	0	0	0	0	0	0	0	0	0	0
880	0	0	0	0	0	0	0	0	0	0	0	0	0	1.8	1.6	3.7	0	0	0	0	1	0	0	0	0	0	0	0	0	0	0	0
890	0	0	0	0	0	0	0	0	0	0	0	0	0	1.8	1.6	3.7	0	0	0	0	0	0	0	0	0	0	0	0	0	0	0	0
900	0	0	0	0	0	0	0	0	0	0	0	0	0	1.8	1.6	3.7	0	0	0	0	0	0	0	0	0	0	0	0	0	0	0	0

Appendices

Chapter Five

Appendix 5.1 (synthesis of 2,3-Naphthalenedicarboxaldehyde)

2,3-Naphthalenedicarboxylic Acid

The procedure of Carlson was employed with some modifications. A mixture of α,α,α',α'-tetrabromo-*o*-xylene (4.38 g, 0.0104 mol), sodium iodide (10.43 g, 0.0696 mol), maleic anhydride (3.06 g, 0.0312 mol), and dry DMF (35 mL) was heated on a steam bath under aspirator vacuum. After approximately 1 hour the solution started to bump excessively up the condensor tube. It was decided therefore, to carry out the reflux on a hotplate/magnetic stirrer to avoid the bumping. A significant amount of reaction mixture was lost during transferal to a triple–necked flask and from the previous excessive bumping. The triple–necked flask was necessary for the monitoring of the temperature with a thermometer (temperature was kept below 100°C). The solution was refluxed smoothly for 4 hrs. The reaction mixture was poured into water (350 mL) containing sodium bisulfite (5.0 g). The pale–yellow solid obtained on filtration was dissolved in dilute NaOH and the solution decolourized with charcoal. Charcoal was removed by filtration and the filtrate cooled in an ice bath. Acidification with concentrated H_2SO_4 gave a white precipitate that was filtered, washed with cold water, and dried for 48 hrs on a freeze drier. The white precipitate which was filtered was very fine and tended to pass through standard filter paper therefore thicker filter paper was used. It was difficult however, to retrieve all the precipitate. The yield of 2,3-naphthalenedicarboxylic acid was 0.4578 g (20.38%). This sample was used in the next step without purification.

2,3-Bis(hydroxymethyl)naphthalene

A suspension of $LiAlH_4$ (0.32 g, 0.0085 mol) in 30 mL of dry ether was stirred under N_2, and a solution of 2,3-naphthalenedicarboxylic acid (0.46 g, 0.0021 mol) in 20 mL of dry THF was added dropwise at a rate that maintained a gentle reflux of the solvent. After addition was complete, the reaction mixture was heated under reflux for 5 hrs. Some loss of 2,3-naphthalenedicarboxylic acid was incurred at this step because the solid was placed in the bottom of the pressure equalizing addition funnel and then the THF poured on top of the solid. Most of the solid was wedged down the narrow part of the funnel where it was difficult for the THF to come into full contact with it therefore dissolution was excessively slow. The THF and solid was therefore swirled into a round bottomed vessel in order to encourage dissolution. This swirling, transfer procedure had to be repeated a number of times in order to retrieve all solid 2,3-naphthalenedicarboxylic acid from the addition funnel. Excess $LiAlH_4$ was destroyed by the dropwise addition of ethyl acetate. Enough ethyl acetate was added when subsequent addition of dilute aqueous HCl produced no fizzing. The clear solution was carefully decanted, and more ether was added to the residual grey precipitate. The supernatant liquid was again removed by decantation. Water was added to the residue and the mixture extracted with ether. The ether extracts were combined and washed once with brine. After drying with $MgSO_4.H_2O$, the solvent was removed using a rotary evaporator. An off white solid was removed from the round bottomed flask and filtered and washed with a mixture of ether-hexane (1:2). The washing was repeated a few times. The solid still remained an off–white colour. After drying, 102 mg (25.53%) of the diol was obtained; mp 153-155 °C (lit. mp160 °C).

2,3-Naphthalenedicarboxaldehyde

Dry dimethyl sulfoxide (1.057 mL, 0.0149 mol) in CH_2Cl_2 (3.197 mL) was added dropwise to a cold (-83.9 °C) solution of oxalyl chloride (0.13 mL, 0.0015 mol) in CH_2Cl_2 (10.833 mL). After 5 min a solution of the diol (0.102 g, 0.0005 mol) in a mixture of 3.75 mL of THF and 0.3 mL of dimethyl sulfoxide was added dropwise. The resulting white slurry was vigorously stirred for 1 hr, triethylamine (0.83 mL, 0.0060 mol) was added, and the reaction mixture allowed to warm to room temperature. After 1.5 hr, the reaction mixture was poured into water and extracted with ether. The combined ether extracts were washed with water and dried. Evaporation of the solvent gave a pale yellow solid that was recrystallized from ethyl acetate to yield 12 mg (13 %) of 2,3-naphthalenedicarboxaldehyde. It was decided that this was too small an amount to be of use, and since this was the third attempt at producing a useful amount of naphthalenedicarboxaldehyde it was decided at this point that it would be better to purchase some from Aldrich Chemical Company.

Appendix 5.2 (OPA emissions)

Emission intensity results are presented in Table 5.1(A) for a 3.3 $x10^{-5}$ mol/L solution of OPA in which no methanol was used to dissolve the OPA and no Brij® 35 was added. Intensities were recorded at various time intervals after the time of L-analine addition.

Appendix 5.2 (a)

Emission intensities for an OPA solution with no Brij® 35 and with excitation at 337 nm.

Time (mins)	Peak emission wavelength (nm)	Intensity
4	448.0	367
6	451.0	369
9	450.0	366
11	449.0	365
12	451.5	363
14	450.0	359
17	452.0	358
20	449.0	355
22	449.0	352

Emission intensity results are presented in Table 5.2(A) for a 3.3 $x10^{-5}$ mol/L solution of OPA in which 37 µL methanol was used to dissolve the OPA and 11µL 15% Brij® 35 was added. Intensities were recorded at various time intervals after the time of L-analine addition.

Appendix 5.2 (b)

Emission intensities for an OPA solution with Brij® 35 and excitation at 337 nm (1).

Time (mins)	Peak emission wavelength (nm)	Intensity
4	450.0	448
5	450.5	465
6	449.0	478
8	453.0	498
10	452.0	510
13	451.0	529
17	452.0	531
26	450.0	625
29	451.0	617
36	451.0	720
39	449.0	691
40	450.5	689
46	450.0	706
48	449.5	694
50	450.0	681
136	448.0	612
199	448.0	591

Emission intensity results are presented in Table 5.3(A) for a 3.3 $x10^{-5}$ mol/L solution of OPA as used above but with an additional 2 mL methanol added to the solution before dilution. Intensities were recorded at various time intervals after the time of L-analine addition.

Appendix 5.2 (c)

Emission intensities for an OPA solution with Brij® 35 and an additional 2 mL methanol with excitation at 337 nm.

Time (mins)	Peak emission wavelength (nm)	Intensity
21	452.0	373
23	452.0	389
25	453.0	395
31	450.5	408
33	450.5	405
35	449.0	396
41	451.0	412
43	449.5	401
45	449.5	396
137	448.0	368
139	448.5	362

Emission intensity results are presented in Table 5.4(A) for a 3.3 $x10^{-5}$ mol/L solution of OPA in which 37 µL methanol was used to dissolve the OPA and 11µL 15% Brij® 35 was added. Intensities were recorded at various time intervals after the time of L-analine addition.

Appendix 5.2 (d)
Emission intensities for an OPA solution with Brij® 35 and excitation at 337 nm (2).

Time (mins)	Peak emission wavelength (nm)	Intensity
4	450.5	648
6	450.5	650
8	450.0	652
10	451.0	652
12	448.0	648
14	450.5	645
16	449.0	638
18	449.5	629
20	449.0	621
22	449.5	611
64	450.5	629
66	450.5	612
103	448.0	596
180	449.0	565
285	447.0	519

Emission intensity results are presented in Table 5.5(A) for a 3.3 $x10^{-5}$ mol/L solution of OPA in which 100 µL methanol was used to dissolve the OPA and 300 µL 30% Brij® 35 was added. Intensities were recorded at various time intervals after the time of L-analine addition.

Appendix 5.2 (e)
Emission intensities for an OPA solution with 300 µL 30% Brij® 35 and 100 µL methanol and with excitation at 337 nm.

Time (mins)	Peak emission wavelength (nm)	Intensity
4	449.5	339
6	449.5	341
8	451.0	339
10	448.5	339
14	453.0	342
16	450.5	345
18	449.0	337
21	449.0	342
23	450.5	337
28	449.5	335
31	451.5	332
67	447.0	285
94	447.5	282

Emission intensity results are presented in Table 5.6(A) for a 3.3 $x10^{-5}$ mol/L solution of OPA in which 2 mL methanol was used to dissolve the OPA and 300 µL 30% Brij® 35 was added. Intensities were recorded at various time intervals after the time of L-analine addition.

Appendix 5.2 (f)
Emission intensities for an OPA solution with 300 µL 30% Brij® 35 and 2 mL methanol with excitation at 337 nm.

Time (mins)	Peak emission wavelength (nm)	Intensity
6	452.0	350
8	449.5	352
9	449.0	354
12	449.0	351
14	450.5	349
17	450.0	351
23	448.5	350
31	450.0	359
33	449.5	350
39	450.0	348
45	451.0	344
46	448.5	338
49	448.5	338
88	449.0	333
113	446.0	284

Emission intensity results are presented in Table 5.7(A) for a 3.3 $x10^{-5}$ mol/L solution of OPA in which 2 mL methanol was used to dissolve the OPA and 11µL 15% Brij® 35 was added. Intensities were recorded at various time intervals after the time of L-analine addition.

Appendix 5.2 (g)
Emission intensities for an OPA solution with 11 µL 15% Brij® 35 and 2 mL methanol with excitation at 337 nm.

Time (mins)	Peak emission wavelength (nm)	Intensity
4	451.0	290
5	447.5	294
6	449.5	302
9	450.0	307
15	451.0	306
18	453.5	304
20	449.0	304
30	452.0	323
32	452.0	312
42	450.5	305
60	451.0	281
62	449.5	279
75	448.0	270
96	448.5	270
120	448.0	263

Appendix 5.3 (NDA emissions)

Emission intensity results are presented in Table 5.8(A) for a 3.3 x10^{-5} mol/L solution of NDA in which 2 mL methanol was used to dissolve the NDA and no Brij® 35 was added. Intensities were recorded at various time intervals after the time of L-analine addition.

Appendix 5.3 (a)
Emission intensities for an NDA solution with no Brij® 35 and with excitation at 418 nm.

Time (mins)	Peak emission wavelength (nm)	Intensity
4	475.5	184
6	475.0	206
10	478.0	219
12	474.0	231
14	475.5	237
17	479.0	246
20	475.5	251
23	475.5	303
80	475.5	305
109	477.0	321
152	476.0	343
172	477.5	347
180	474.5	352

Emission intensity results are presented in Table 5.9(A) for a 3.3 x10^{-5} mol/L solution of NDA in which 2 mL methanol was used to dissolve the NDA and 11µL 15% Brij® 35 was added. Intensities were recorded at various time intervals after the time of L-analine addition.

Appendix 5.3 (b)
Emission intensities for an NDA solution with Brij®35 added and excitation at 418 nm.

Time (mins)	Peak emission wavelength (nm)	Intensity
3	479.0	181
5	475.5	212
9	477.5	237
11	476.5	243
14	476.5	253
15	477.0	254
16	478.5	257
18	473.5	260
20	477.5	264
22	475.5	269
25	475.5	275
30	476.5	283
39	477.0	297
121	474.5	390
129	475.0	394
167	472.0	419
177	478.0	400
180	479.5	403

Appendix 5.4 (ADA emissions)

Emission intensity results are presented in Table 5.10(A) for a 3.3 $x10^{-5}$ mol/L solution of ADA prepared in methanol before dilution in borate buffer. Intensities were recorded at various time intervals after the time of L-analine addition.

Appendix 5.4 (a)
Emission intensities for an ADA solution with excitation at 405 nm.

Time (mins)	Peak emission wavelength (nm)	Intensity
4	539.0	171
7	539.0	201
10	540.5	207
14	539.5	229
21	539.0	256
26	538.0	269
27	537.5	273
28	538.5	275
29	538.5	276
32	538.5	277
33	538.5	281
36	537.5	285
42	538.5	244
43	538.0	246
44	538.5	254
45	538.0	262
48	537.5	280
53	537.0	280
58	536.0	281
86	533.5	313
89	535.5	310
91	534.0	311
95	532.5	310
97	535.0	308
99	534.0	306
102	535.5	295
108	534.5	282
117	533.0	310
118	532.5	310
120	534.0	310
149	536.0	241
151	536.5	242